Optimization of SPME coating characteristics for metabolomics and targeted analysis with LC/MS

by

Fatemeh Mousavi

A thesis
presented to the University of Waterloo
in fulfillment of the
thesis requirement for the degree of
Doctor of Philosophy
in
Chemistry

Waterloo, Ontario, Canada, 2015

AUTHOR'S DECLARATION

This thesis consists of material all of which I authored or co-authored: see Statement of Contributions included in the thesis. This is a true copy of the thesis, including any required final revisions, as accepted by my examiners.

I understand that my thesis may be made electronically available to the public.

Statement of Contributions

I hereby declare that I am the sole author of this thesis. Materials in Chapter 2 and Chapter 3 have been already published. All of the work reported within these chapters has been performed solely by the author. The contribution of professor Janusz Pawliszyn as the co-author in both chapters was supervision of the research, and Dr. Barbara Bojko as the co-author for Chapter 3 provided comments on manuscript preparation.

Abstract

Metabolomics data provides complementary information to proteomics, genomics, and transcriptomics, in addition to enabling the tracking of the dynamic reactions in living systems. Metabolomics is widely used in various areas of study such as human diseases, drug discovery, plant analysis, and human nutrition. In metabolomics, the workflow for quantitative and comprehensive metabolic mapping of cellular metabolites can be a very challenging undertaking. Sampling and sample preparation play an important role in untargeted analysis as they influence the final composition of the analyzed extract, which can consequently influence the obtained metabolome. The choice of sample preparation method for metabolomics is based on factors such as non-selectivity, high reproducibility, integration of metabolism quenching, and extraction of a wide range of metabolite polarities. It should provide a good representation of the sample under study and obtain high sample clean-up so as to reduce matrix effects, especially when liquid chromatography coupled mass spectrometry (LC-MS) instrumentation is used for analysis. Solid phase microextraction (SPME) has already been demonstrated as a suitable technique for metabolic profiling of various biological matrices. This noninvasive and solventless extraction technique eliminates the need for metabolism quenching steps, as the coating selectively extracts metabolites, eliminating the co-extraction of interfering biomacromolecules such as proteins or enzymes.

One of the main objectives of the currently presented research was the development of a new extraction phase that is compatible with complex food matrices and that provides high extraction recovery for a wide range of metabolites. For this purpose, initial research involved the preparation of a silica-based ionic liquid coating as a stationary phase for a 96-blade SPME system for the extraction of polar metabolites from grape juice without any further sample pretreatment. The lab-made polymer demonstrated high physical and chemical stability, and results indicated that the properties of the coating could be changed by changing the functional groups during the synthesis procedure. Chapter 3 presents different SPME coating chemistries that were developed and applied to provide simultaneous extraction of a wide range of both hydrophobic and hydrophilic cellular metabolites produced by a model organism, *Escherichia coli* (*E.coli*). This research reports the first successful application of the developed 96-blade SPME method coupled to LC-MS for bacteria and plant metabolomics. Three different LC-MS methods were also evaluated for the analysis of extracted metabolites. The Orbitrap system provided a powerful platform for metabolomics due its high resolution and mass accuracy. Among different coating chemistries applied for analysis, polystyrene–divinylbenzene–weak anion exchange (PS-DVB-WAX), hydrophilic–lipophilic balance particles (HLB), and their mixtures demonstrated the highest extraction recovery and a wide range of metabolite coverage. A mixture of PS-DVB-WAX and HLB particles with 50:50 weight ratio (PS-DVB-WAX: HLB 50:50 [w/w]) was applied successfully for extraction of a wide range of metabolites, while the pentafluorophenyl Kinetex

column coupled to an Orbitrap mass spectrometer method provided the widest metabolomics coverage for the investigated system. The method separated and detected over 200 cellular metabolites with widely varying hydrophobicities, ranging from $-7 < \log P < 17$, including amino acids, peptides, nucleotides, carbohydrates, polycarboxylic acids, vitamins, phosphorylated compounds, and lipids such as hydrophobic phospholipids, as well as glycerolipids, and fatty acids at the stationary phase of the *E.coli* life cycle. Moreover, the 96-blade SPME system provided a high throughput platform, which surpassed sample throughput requirements for a typical metabolomics study whereby ~100 samples/day are processed.

Chapters 4, 5, and 6 present the obtained results of applications of the optimized method towards evaluations of environmental stresses on biological systems. Essential oils, as natural plant products with a complex mixture of constituents, are comprised of multiple antimicrobial properties related to oxygenated terpenoids, particularly phenolic terpenes, phenylpropanoids, and alcohols. This thesis presents an investigation into the mechanisms of bactericidal action of cinnamaldehyde and clove oil against *E.coli* during bacterial growth, applying 96-blade SPME in direct immersion mode coupled to ultra performance liquid chromatography-mass spectrometry (UPLC-MS). Statistical analysis demonstrated alteration in the metabolic pathway during different time points of the *E.coli* growth curve, via the up-regulation of saturated fatty acids and amino acids, as well as the down-regulation of unsaturated fatty acids, glycolysis, and TCA cycle metabolites for *E.coli* treated by cinnamaldehyde, below and above the minimum inhibitory concentration. The presented 96-blade SPME-LC/MS method was developed using multivariate design, and applied to evaluate the synergistic effect of major components of clove oil as an antibacterial agent to *E.coli*. SPME provided clear separation between different sample treatments, and valuable information regarding the mechanisms of antibacterial action of the two naturally occurring compounds, suggesting different metabolic pathways for samples treated with the active agents. As opposed to the utilization of traditional univariate optimization methods, the current study employs the application of multivariate experimental designs for optimization of extraction-influencing parameters. Based on the obtained results, eugenol, as the major component of clove oil, produced the characteristic features of an antimicrobial agent. There is no synergistic effect between the components of clove bud oil in the actual weight percent of its constituents. Evaluation of discriminating metabolites in treated samples indicated eugenol as a lead compound for the development of an active agent through the control of glycolysis in anticancer cells, as this compound demonstrated glycolysis inhibition of *E.coli* as a model organism.

The optimized SPME-LC-MS method was applied for high-throughput analysis of complex apple matrices without a sample pretreatment step. Untargeted metabolic profiling coupled with multivariate statistical analysis indicated metabolic alterations happening prior to scald development. The obtained

results could be applied towards an improvement in the nutritional stability of foodstuffs as well as allow for shelf-life expansion, in addition to increasing their potential market value.

The developed 96-blade SPME-LC-MS method is promising for global metabolomics applications, in particular in terms of extraction of unstable and short-lived metabolites in comparison to traditional techniques. SPME has also demonstrated high reproducibility and sample clean-up, which is a top requirement in metabolomics investigations.

Acknowledgements

First of all, I would like to thank God for having made everything possible by giving me strength, hope and courage to do this work, helping me to arise as a mature, responsible, stronger and wiser individual ready to face any challenge with faith and perseverance. Moreover, I would like to thank several people who have supported me to continue this journey a very rewarding and memorable experience.

My deepest gratitude to my supervisor, professor Janusz Pawliszyn for giving me the opportunity to join in his research group and such a wonderful PhD project as well as increasing my expertise and knowledge during the path of PhD. Thanks professor for the invaluable advice, guidance and encouragement!

I thank to my committee members, professor Wojciech Gabryelski, professor Scott Taylor, professor Mario Gauthier for their time and helpful advice during my studies and throughout preparation of this thesis.

I am thanking my external examiner, professor Daniel Figeys, and my internal examiner professor Ken Stark for their invaluable time on evaluation of my thesis, and their helpful feedback.

I respectfully acknowledge my colleagues, and collaborators for their support, and collaboration specially Dr. Barbara Bojko, Dr. Fatemeh Mirnaghi, Dr. Vincent Bessonneau, Dr. Angel Rodriguez Lafuente, professor Eduardo Carasek, and Mr. Dietmar Hein.

Sincere thanks to my parents Sedigheh Kazemi and Seyed Mohammad Mousavi, my brothers Mahdi, and Masoud Mousavi.

Thank you all and God bless you.

Fatemeh Mousavi, 2015

Dedication

I lovingly dedicate this thesis to my family. Your unconditional love, support, and encouragement inspire my life.

Table of Contents

List of Figures

List of Tables

List of Abbreviations and Symbols

a	Time constant
A	Surface area
AIBN	Azodiisobutyronitrile
b	Thickness of the coating
C_{18}	Octadecyl
C_f^{∞}	Equilibrium concentration of analyte on the
$C_{f\,max}$	Maximum concentration of active sites on the coating
CE	Collision energy
C_0	Initial analyte concentration
C_s	Analyte concentration in the bulk of the sample
CCD	Central composite design
CXP	Collision cell exit potential
CW	Carbowax
CFU	Colony forming units
d	Depth of the blade substrate
δ	The thickness of boundary layer
D_s	Diffusion coefficient of the analyte in the sample
DART	Direct analysis in real time
DESI	Desorption electrospray ionization
DI	Direct immersion
Diol	Diol bonded silica
DIOS	Desorption ionization on silicon
DMF	N, N-Dimethylformamide
DVB	Divinylbenzene
DP	Declustering potential
E.coli	*Escherichia coli*
EESI	Extractive electrospray ionization
EP	Entrance potential
ESI	Electrospray ionization
FP	Focusing potential
FT-ICR	Fourier transform ion cyclotron resonance
GC×GC-TOFMS	Comprehensive two dimensional gas chromatography-time of flight mass spectrometry
GALDI	Graphite-assisted laser desorption ionisation
HCl	Hydrochloric acid
HILIC	Hydrophilic interaction chromatography
HLB	Hydrophilic–lipophilic balance particles
HPLC	High pressure liquid chromatography
HS	Headspace
IL	Ionic liquid
K_{fs}	Distribution constant of the analyte between SPME coating and sample at equilibrium
l	Length of the coating
LB	Standard Luria Bertani
LC	Liquid chromatography
LLE	Liquid-liquid extraction
LOD	Limit of detection
Log P	Log of octanol/water partition coefficient
LOQ	Limit of quantitation
MALDI	Matrix assisted laser desorption ionization

MIC	Minimum inhibitory concentration
MPS	3-mercaptopropyltrimethoxysilane
MRM	Multiple reaction monitoring
MS	Mass spectrometer/spectrometry
MS/MS	Tandem mass spectrometry
n_e	Amount of analyte extracted by SPME fiber at equilibrium
NIMS	Nanostructure initiator mass spectrometry
NMR	Nucleic magnetic resonance
OPLS-DA	Orthogonal partial least squares analysis-discriminate analysis
PAN	Polyacrylonitrile
PBA	Phenylboronic acid
PCA	Principal component analysis
PDMS	Polydimethylsiloxane
ppb	Parts per billion
ppm	Parts per million
PLS	Partial least squares analysis
PS-DVB-WAX	Modified polystyrene-divinylbenzene copolymer with a weak anion exchanger
QC	Quality control
r	Radius of the support wire
R^2	Linear regression coefficient
Rpm	Revolutions per minute
RSD	Relative standard deviation
s	Second
SE	Solvent extraction
SEM	Scanning electron microscopy
SiIL	Silica based ionic liquid
SIMS	Secondary ion mass spectrometry
SLE	solid–liquid extraction
S/N	Signal-to-noise ratio
Si-RP-WCX	Silica based-reversed phase-weak cation exchange
SPE	Solid phase extraction
SPME	Solid-phase microextraction
StrataX	Surface modified styrene divinylbenzene with pyrrolidone group
t	Sampling time
TCA	Tricarboxylic acid
UV	Ultraviolet
Vf	Volume of SPME coating
Vs	Volume of sample matrix
w	Width of the coating substrate
XIC	Extracted ion chromatogram

Chapter 1

Introduction

1.1 Metabolomics and biomarker discovery

Metabolomics is the scientific study of chemical processes involving metabolites, which are defined as molecules that weight more than 1 kDa in mass [1]. The term metabolome refers to the full complement of metabolites, which are intermediates and products of metabolism present in cells, tissues, or organisms. As the end products of genomics, transcriptomics, and proteomics (Figure 1.1), metabolomics can provide an instantaneous snapshot of the physiology of the cell [2,3]. Providing a comprehensive understanding of cellular biology requires integration of all complementary data obtained using the different "omics" methodologies [4,5,6]. Genome, transcriptome, and proteome analyses are based on targeted chemical analyses of biopolymers, involving four different nucleotides in the case of genome and transcriptome analyses, and 22 amino acids in proteome analysis. These compounds are highly similar in chemical composition. The metabolome is associated with metabolism and interactions with the environment, whereas real and potential functional information of living systems is produced by genomes [7].

The concept of metabolic patterns was first introduced by Williams in 1951. He applied paper chromatography to compare urine samples of 200,000 patients from mental hospitals [8,9]. Concurrently, Horning et al. and Robinson et al. applied gas chromatography (GC) towards the analysis of urine, making their work the first research papers to be published on metabolomics in 1971 [10,11,12]. The terms used in metabolomics were coined for the first time by Oliver et al. in analogy with genomics and transcriptomics, derived from the words genome and transcriptome [7].

The metabolome is composed of a large number of metabolites with different chemical and physical properties, such as non-ionic inorganic compounds, hydrophilic carbohydrates, amino and non-amino organic acids, hydrophobic lipids, complex natural products, volatile alcohols, and ketones [13,14]. Metabolites are synthesized to complete a set of biological functions; they are the end product of a chain of chemical reactions, called a pathway. A collection of pathways is referred to as metabolism [15]. Considering all other "omics" studies, metabolomics is one of the most challenging investigations to undertake due to the unique characterization of each compound in comparison with other metabolites in a pathway. The chemical and physical properties of metabolites and the dynamics of metabolite conversion, which are connected to the environment at any time, determine the evidence of metabolites in metabolism [16]. In a living system, the metabolic network is composed of a complex multitude of related reactions. A small perturbation in the proteome, such as enzymatic alterations, may cause a significant change in the

level of metabolites present within a given system. For example, the decreased activity of a specific enzyme may cause a biological response increase in the level of its substrate. Metabolites play a very important role in connecting various biological pathways operating in living systems [17]. Metabolomics and metabonomics are often applied for unbiased global (untargeted) or holistic analyses of biological samples, such as animal/human biofluids, tissue and cell extracts, in vitro incubation media, or plant/food extracts. These techniques have the potential to discover new biomarkers by identifying differentiation patterns between metabolic profiles of test samples and matched control groups [18]. Both metabonomics and metabonomics are multidisciplinary research areas that apply various fields of expertise, including analytical chemistry, statistical analysis, biochemistry, medicine, life sciences, as well as nutritional, agricultural, or environmental sciences. Technological evolution in instrumentation has ignited a burst of research in this field towards the development of methods capable of describing whole metabolomes using a particular platform [19,20]. Biomarker discovery is the most important area within metabolomics studies for medical and life sciences, as well as for plant/food and environmental sciences [21,22]. In medical science, metabolomics/metabonomics are applied in the identification of early biomarkers of disease (diagnostic markers) or in drug efficacy prediction, biomarkers of disease progression, and drug toxicity (safety assessment). Plant and food sciences utilize metabolomics for taxonomic studies and quality or source assessment [23,24].

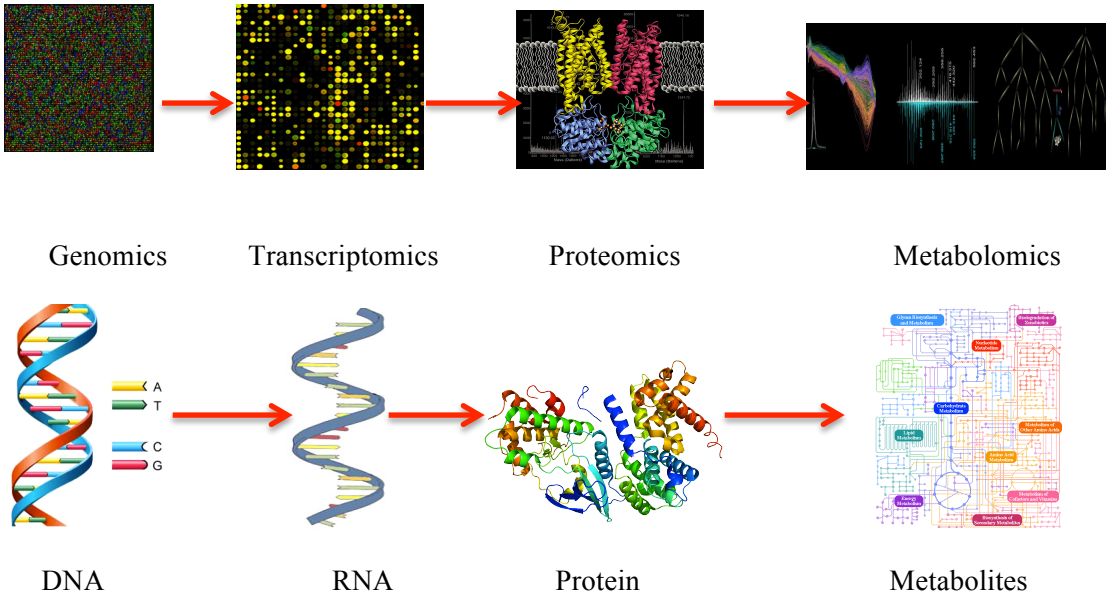

Figure 1.1 Interaction of different "omes" in a cell: Genomics conduct the exploration of all the sequences in the full genome of a distinct organism. The genome can be defined as the complete set of genes inside a cell. Transcriptomics is the study of the complete set of RNAs (transcriptome) encoded by the genome of a specific cell or organism at a specific time or under a specific set of conditions. Proteomics is defined as protein "expressiom profiling". Metabolomics can be defined to determine differences among the levels of thousands of molecules in control vs. treated samples.

Microbial metabolomics is a newly emerging field utilized to investigate changes in metabolic profiles under various environmental conditions, metabolic changes in a mutant strain or microorganism, or identification or differentiation through the generation of metabolome profiles of various microorganism species [25].

Metabolomics research can be classified as targeted or untargeted analysis. The first focuses on a specific group of metabolites in a sample that needs a high level of purification and selective extraction of metabolites, whereas untargeted metabolomics refers to identification of as many metabolites present in the sample as possible to obtain the metabolome pattern or fingerprint [26].

Metabolomics includes sample preparation, sample analysis, and data analysis; in order to obtain as much information as possible, each metabolome study requires evaluation and optimization of its sampling, sample preparation, and extraction procedures [26]. Figure 1.2 demonstrates the metabolomics workflow regularly used in scientific labs.

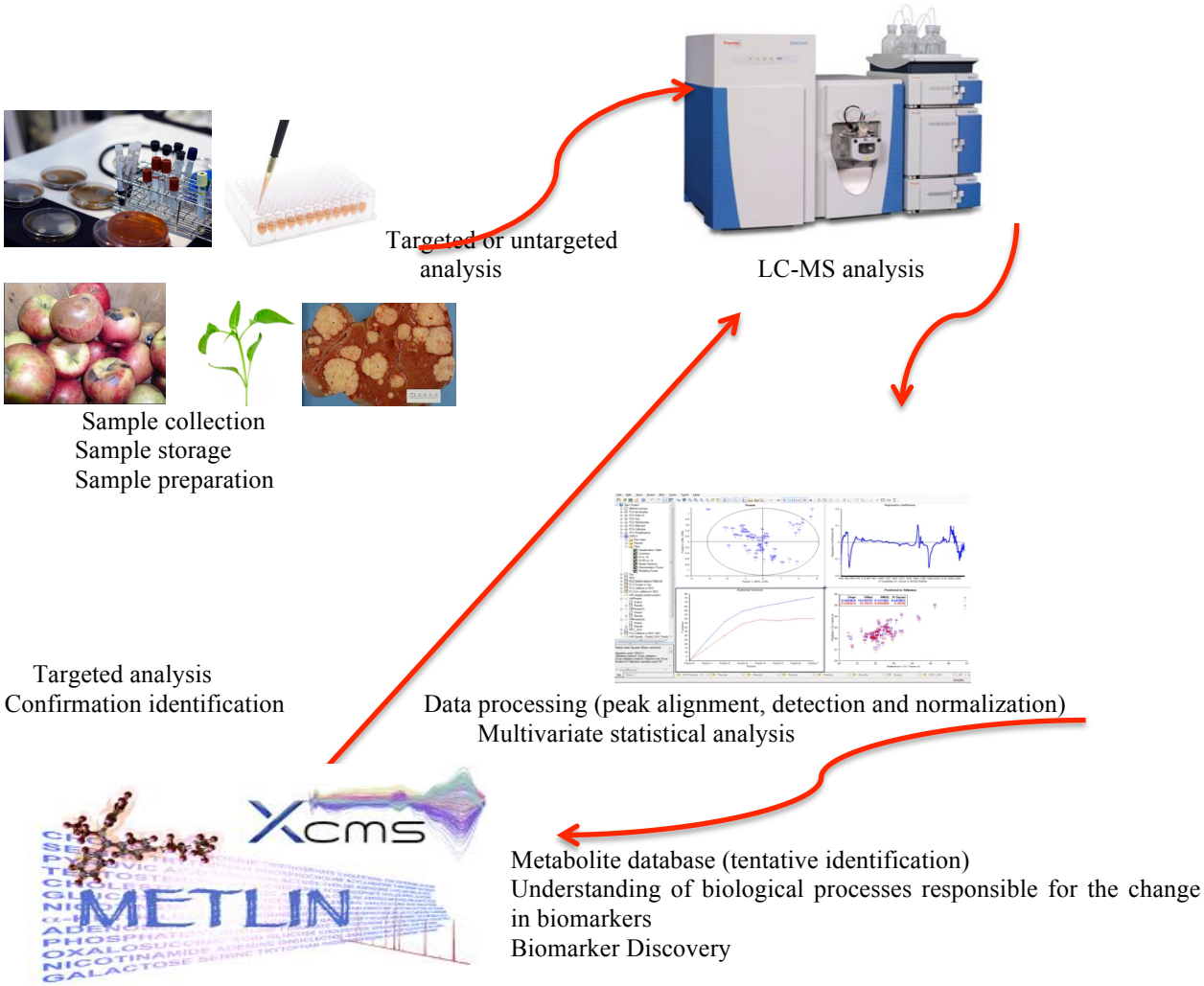

Figure 1.2 Global metabolomics workflow (targeted and untargeted analysis).

1.2 Analytical approaches for global metabolomics studies

Due to the broad range of chemical diversity that exists for metabolites, which can range from sugars to lipids, it is often challenging to perform a complete metabolome analysis with a single technique [13,14]. The two analytical techniques most widely used in metabolomics are mass spectrometry (MS) and nuclear magnetic resonance (NMR). NMR is a nondestructive, rapid, and robust technique that forgoes the need of chromatography and ionization; however, the main advantage of MS over NMR lies in the former's sensitivity and its ability to perform quantitative and targeted analyses [27-30].

Direct infusion MS has been utilized in conjunction with high-resolution instrumentation such as Fourier transform ion cyclotron resonance (FT-ICR) and Orbitrap in metabolomic determinations; however, imperfections in overcoming matrix effects and isobaric metabolite analysis limit the application of this technique [31].

Matrix-assisted laser desorption ionization (MALDI) was developed to overcome some of the weaknesses of traditional analytical techniques in regards to metabolomics determinations. The main advantages of this technique consist of the use of very small sample volumes, in addition to its suitable performance in the analysis of matrices containing salt [32-33]. As signals produced by the matrix can cause the detection of lower masses in the sample and a high relative standard deviation (RSD), other MS technologies such as graphite-assisted laser desorption ionization (GALDI), desorption ionization on silicon (DIOS), nanostructure initiator mass spectrometry (NIMS), secondary ion mass spectrometry (SIMS), direct analysis in real time (DART), desorption electrospray ionization (DESI), and extractive electrospray ionization (EESI), which can provide analyte ionization from a surface, have been developed [34-38]. However, the current number of reports in metabolomics literature involving the abovementioned approaches is limited; further research needs to be conducted to ensure the progress of these methodologies. Inspite of the progress in the metabolomics field, more efficient separation methodologies are still needed to lessen the complexity the final extract and improve the chromatographic resolutions of the overlying metabolites. Although direct infusion MS has been successful in this regard in some cases, MS is often coupled with high-resolution separation methods such as GC, liquid chromatography (LC), ultra performance liquid chromatography (UPLC), and capillary electrophoresis (CE) so as to improve these factors. These separation methods enhance the real potential of MS as well as the sensitivity of MS detection while decreasing the complexity of the samples introduced to the MS, which in turn aids in the reduction of background noise. While GC can be applied for the analysis of volatile, nonpolar, and thermally stable metabolites, most metabolites are polar and nonvolatile, and as such, must be derivatized prior to GC analysis. Derivatization, in turn, generally produces artifacts and complex chromatograms. LC offers analysis of a broader range of metabolites in varying concentrations [39-43]. As the metabolome is composed of a diverse array of compounds with various physicochemical properties, there

is no single retention mechanism that is sufficient to separate complex sample mixtures with widely varying analytes in terms of their polarity, charge, and stability [44]. In the metabolomics area, more than 90% of the published studies utilizing chromatographic methods were conducted with the use of reversed phase liquid chromatography (RPLC) [45]. However, a major limitation of RPLC lies in its poor retention of polar metabolites due to their co-elution within a void volume. One of the strategies to solve this problem is chemical derivatization; as reported by Shortreed et al. [46] and Santa et al. [47], chemical derivatization can be used to improve retention of amino acids and amines, or, as shown by Horvath et al, utilized with the application of an ion pairing reagent in the mobile phase. However, it is important to note that these reagents are not compatible with ESI interfaces [48]. Another way to increase the identification of polar metabolites involves the use of Hydrophilic interaction chromatography (HILIC) columns ranging from unmodified silica to bonded-phase particles with non-ionics such as polyol, ionics like amine, as well as zwiter ionics such as sulfoalkylbetaine fuctional groups [49,50]. In comparison to RPLC, HILIC columns are characterized by an enhancement in retention times, poor separation, and longer equilibrium times. Despite these shortcomings, HILIC is the LC-MS separation method of choice for polar metabolites [51,52]. CE is particularly applicable for polar and ionizable metabolites such as amino acids, which cannot be adapted with metabolomics approaches [53].

The high selectivity and low detection limits of mass spectrometry, alongside its compatibility with various separation techniques and applicability for quantitative analysis together function to make this technique a powerful tool for metabolomics studies [27]. In addition, efficient sample introduction and ionization of all metabolite classes assist in the attainment of superior mass spectrometry data [28,30]. LC, in comparison to direct infusion, can reduce the complexity of mass spectra as well as reduce or eliminate matrix effects produced by co-eluted compounds and interferences produced in low-resolving mass analyzers, assisting to separate isomers. Suitable MS quality of data and lower detection limits can be obtained by powerful separation techniques [45-52]. However, mass spectrometry-based techniques usually require a sample preparation step prior to analysis. Various MS-based techniques have been previously applied for metabolomics studies. Further identification and compositional analysis of metabolite species can be obtained with the use of MS/MS, while the identification of fragmentation patterns can be accomplished with CID spectra [16]. The use of ESI in both positive and negative modes can aid in adduct ion identification of different metabolites. In order to distinguish between isobars, high-resolution mass spectrometers can be applied in conjunction with empirical formula calculations towards accurate mass measurements of ion signals. In past research, the use of Fourier transform ion cyclotron mass spectrometers (FT-ICR-MS) has been reported to yield very high resolutions up to 1000000, with the highest obtained mass accuracy of 0.1-1 mamu [31]. The FT-ICR-MS instrument provides very low detection limits in the attomole to femtomole range, with an MS^n range being easily achievable with this

type of instrument [16]. In contrast, TOF-MS instruments have been reported to offer high mass resolutions of 6000-17000, with a 3-5 mamu mass accuracy in cell media samples. Hybrid instruments such as the quadrupole-TOF-MS (Q-TOF-MS) have also been applied for analysis of cell and plant extracts with high mass accuracy and resolution. High mass accuracy of spectra can assist in the identification of the fragmentation process, while allowing for spectra interpretation [16].

1.3 Sample preparation

Considering the complexity of the real sample matrices under study in terms of chemical diversity and broad dynamic range, sampling and sample preparation are generally considered as the limiting steps in metabolomics, as they induce an important source of variability. The choice of sample preparation method plays an important role in the final content of the obtained metabolome profile, as well as the quality and reliability of the final results. In addition, matrix interferences and metabolite losses are most likely to happen during these stages. Accordingly, an ideal sample preparation method for metabolomics studies should be non-selective, simple, reproducible, impartial towards metabolome coverage, and able to minimize biases for various metabolite classes without metabolite loss or degradation. It should enable high-throughput analysis, and integrate a metabolism-quenching step. In addition, the extract should be compatible for further analysis; the combination of sample preparation with a suitable chromatographic protocol provides insight into the biological system [54]. The main objective of sample preparation is the production of an extract that is well suited to the analytical technique, isolating metabolites from a complex matrix, and overcomes low sensitivity. A recent trend in sample preparation also includes the development of methods that can significantly reduce or omit the need of organic solvents, thus creating greener and environmentally friendlier techniques [55].

One of the goals of metabolomics is to connect metabolite levels with the response of biological systems to genetic or environmental variations. Therefore, the first step of sample preparation is quenching of whole biochemical processes concurrently or instantaneously [56]. The sample introduced for analysis should be a proper representative of the biological system; thus, the metabolic processes taking place in a given sample should be interrupted during sampling, allowing for a reliable snapshot of the metabolome. Quenching helps to reach this goal by stopping the metabolic processes occurring in real time through enzyme inhibition; an ideal quenching step should be able to inactivate metabolism faster than the rate of metabolic changes happening in the sample. Sample integrity should also be conserved during sampling, without any variations in the physical or chemical properties of the metabolites under study. Finally, the quenched sample should be usable for further stages of the metabolomics workflow [57].

Various quenching techniques can be used on samples from biological systems such as microbial and cell culture, plant and animal tissues, and body fluids; in such cases, quenching is accomplished through rapid

changes in temperature or pH, as these processes can cause rapid inactivation of metabolism and enzymatic activities. Quenching is usually performed by putting the biological system in a cold (-40°C) or hot (>80°C) solution, or into an acidic (pH < 2.0) or alkaline (pH > 10) solution [56]. In the case of bacterial cells, the use of organic solvents at extreme temperatures is the most commonly used quenching method. In such quenching methods, disruption of the cell envelope happens during quenching; commonly used solvents include percholric acid, trichloroacetic acid, boiling ethanol, boiling water, and liquid nitrogen. However, it is important to note that these types of disruptions can result in a reduction in the reliability of the obtained results. For example, loss of metabolites has been reported in the application of freezing procedures, while metabolite degradation, poor metabolome coverage, and lack of compatibility with MS have been reported as drawbacks of applying extreme pH conditions for quenching [56-61].

In order to analyze the metabolites by instrument without physical loss due chemical degradation or biochemical transformation, it is mandatory that metabolites are extracted from the disrupting cell envelope and consequent separation of metabolites from the biological matrix [56]. In addition to being the most time consuming step, the quenching requirement makes it so that it is practically impossible to avoid analyte loss, mainly because of the high chemical diversity present in the matrix as well as the broad dynamic range [54]. Indeed, due to the diversity and dynamic range of metabolites, most research in metabolomics has focused on a specific group or class of compounds. For example, sometimes a group of metabolites are sacrificed in favor of identification of another class with higher reproducibility. The relevant literature also reports the application of multiple extraction procedures in order to achieve wide metabolome coverage [62].

The extraction of metabolites in the metabolomics workflow is one of the most important steps to be undertaken; accordingly, optimizations need to be conducted to allow for minimal matrix interference and maximum sample recovery, which is associated with sample types and is among the aims of study. An ideal extraction method applied for metabolomics should efficiently release metabolites from the sample, eliminate interferences such as salts and proteins causing matrix effects, produce an extract compatible with the analytical technique, and concentrate metabolites for analysis [63-67]. The physical and chemical properties of each metabolite are determined by its molecular weight, molecular size, polarity, volatility, solubility, pK_a, and stability. Metabolites are small molecular weight compounds weighting less than 1000 Da, in comparison with polymers such as proteins and starch. The special volume and tridimensional structure of a given metabolite determine its molecular size. The molecular structure and the number of water molecules involved in non-covalent binding on the surface of the molecule are in turn affected by its molecular size. The polarity of the metabolites is related to the formation of polar interactions with water molecules and other polar compounds [68].

The natures of the polar and nonpolar functional groups presenting in the molecule build the polarity of the molecule. Depending on the functional groups positioned at the molecule and the pH of the environment, polarity can increase as follows: Acid > Amide > Alcohol > Ketone ≈ Aldehyde > Amine > Ester > Ether > Alkane. Based on this classification, lipids, fatty acids, waxes, terpenes, carotenoids, chlorophylls, steroids, and flavonoids are considered to be highly nonpolar metabolites; phenolics and alcohols are classified as midpolars; while amino acids, organic acids, organic amines, alkaloids, nucleosides, sugars, nucleotides, phosphates, metals, and salts are categorized as highly polar metabolites [68].

Volatility is strongly correlated with the polarity of molecules. More volatile metabolites have less polarity. The solubility of a compound is the maximum quantity of solute that can dissolve in a certain quantity of solvent or solution at a specific temperature; solubility is a function of polarity, pK_a, temperature, solvent type, and analyte size. Partition coefficient (P), the ratio of concentration of a compound in a mixture of two immiscible phases at equilibrium state, measures differences in the solubilities of compounds in these two phases. Normally, one solvent is octanol, as a hydrophobic, and the other, which is hydrophilic, is water. The stability of a compound is described by its resistance to chemical reactions, changes, or degradation, all which are affected by thermodynamics and kinetics. Temperature and light, as well as oxidative or reductive conditions can all affect metabolite stability [68]. The appropriate extraction conditions of cellular metabolites must be carefully selected in regards to all of the abovementioned factors.

Different extraction protocols are applied in metabolomics; generally, these are determined based on the type of sample matrix to be studied. For solid samples, solid-liquid extraction methods such as Soxhlet extraction, Folch extraction, supercritical fluid extraction, ultrasound-assisted extraction, and microwave-assisted extraction are used, while for liquid samples, liquid-liquid extraction (LLE), solid phase extraction (SPE), and solid phase microextraction (SPME) have been reported as the sample preparation methods of choice for metabolomics. In addition, various solvent extraction techniques have been reported in this area, such as the use of cold solvents, (50% methanol, 100% methanol, ethanol, methanol/chloroform and acetonitrile), hot solvents (80% methanol, ethanol, H_2O), alkaline solvents (KOH), and acidic solvents (perchloric acid). Each method has its own advantages and disadvantages, which will be discussed in the next sections. The choice of solvent is generally dependent on the chemical properties of the metabolites under study; in many cases, multiple solvent extractions are required to enhance metabolite extraction [69-79].

SPE is mostly applied in sample clean-up prior to chromatographic analysis. When analysis of a large number of samples is required, the use of commercialized robotics or automation devices can provide faster, superior results by reducing sample handling and increasing reproducibility. SPE is widely used in

metabolomics; however, its selectivity for just one class of compounds limits this method to targeted analysis. SPE has been applied to metabolomics investigations in various studies, such as metabolite profiling in biofluids, animal tissue, and plant samples [16]. Dilution, incomplete extraction of metabolites, chemical modification or degradation of labile metabolites, production of artifacts released during the extraction procedure such as chemical contaminants from solvents, and polymer degradation are some of the drawbacks reported for traditional extraction techniques used in metabolomics studies [16].

1.3.1 Sample preparation for cell metabolomics

Microorganisms are one of the mandatory entities of the digestive tract of humans and animals; moreover, they are used for fermentation processes in food technology and biotechnology [80]. There are more than 250 microbial pathogens that cause food-borne diseases. In this context, many cases of disease occur due to contamination of fresh and processed foods with food-born pathogens [81]. Metabolomics is one of the currently available techniques that can be applied towards the evaluation of animal and plant health and production, as well as in the tracking of food quality and safety [82]. Data obtained from genomics, proteomics, lipidomics, and metabolomics of pathogens in contaminated foods can provide reliable insights about disease outbreaks and therapeutic processes. Therefore, in vivo proteomics and metabolomics assist further functional analysis [83-85]. Currently, sensitive methods are available for the detection of bacteria and their toxins, including DNA microarray technology, GC-MS based metabolomics, LC-MS based proteomics, and lipidomics [85-88]. In order to monitor changes during food processing, 'omics' investigations of model organisms under stress conditions such as cold or heat, osmotic pressure, high pressure, nutrient availability, and antibacterial usage are essential in order to better understand their adaptation and consequent reactions to extreme conditions [89]. Antimicrobial chemicals and naturally occurring compounds are used to disinfect food contact surfaces [90].

Cell metabolomics consists of quantitative investigations into the full network of cellular metabolism; in order to further our current understanding of cell function and drug development, the properties of cells need to be further characterized [91]. In comparison to other types of metabolomics research, cell metabolomics has various advantages, such as controllable experimental conditions, minimization of individual variations, and availability of cell samples through laboratory cell cultures. In addition, investigations of drug effects on cells can be undertaken without human or animal ethical concerns. In view of these advantages, the field of cell metabolomics has experienced continuous growth, from studies on prokaryotes, especially *Escherichia coli (E.coli),* to eukaryotes such as yeast and mammalian cells [92].

The number of identified metabolites in simple microorganisms can range from the 240 in simple bacteria such as *Mycoplasma pneumonia*, to approximately 800 in *E.coli*. Since many genes in the genomes of many organisms have not been determined to date, the actual number of metabolites present in simple microorganisms may even be two or three times greater than the currently obtained numbers [93].

The metabolites present in main cellular activities, including the glycolysis pathway, TCA cycle, and intermediates in nucleotide biosynthesis, are common in all known organisms, making bacteria good model organisms for metabolomics studies. NMR and MS techniques are the most commonly utilized analytical methods for bacterial metabolomics. Various sample preparation stages need to be applied during bacteria metabolomics. Cell culture, quenching, and metabolite extraction are common pre-analytical procedures in the bacteria metabolomics workflow [94]. Organic solvents are widely used for extraction of metabolites; in order to cover all metabolites, more than one solvent is often used in extraction procedures. For example, methanol, methanol-water mixtures, or ethanol are utilized for extraction of polar metabolites, while chloroform, ethyl acetate, or hexane are applied for nonpolar extractions. In metabolomics investigations, De koning et al. applied buffered methanol-chloroform-water at low temperatures (-40°C to -20°C) for simultaneous extraction of both polar and nonpolar metabolites of bacteria, yeast, animal tissues, and filamentous fungi. High recoveries of organic acids, sugar phosphates, and sugar alcohols were achieved by this method, whereas nucleotides were not significantly extracted. On the other hand, this method is tedious and time consuming, in addition to relying on the consumption of large amounts of toxic organic solvents [95]. The utilization of boiling ethanol for cell metabolomics is another popular method for cell metabolomics investigations, although this technique has been reported to result in poor extraction recoveries of phosphorylated metabolites, nucleotides, and tricarboxylic acids. Methanol, either in pure form (100%) or in the presence of water as a polar solvent, is a very powerful organic solvent applied for extraction of intracellular metabolites from a wide range of cell cultures. Methanol was first introduced as an efficient solvent for the extraction of intracellular metabolites from bacteria and yeast by Maharjan et al. [96], and Villas-Bôas et al. [56]. Methanol is less toxic than chloroform, and applying extraction at -20°C avoids biochemical reactions and degradation of thermo labile metabolites; in addition, methanol can be easily evaporated from the final extracts. Acidic and alkaline extractions of intracellular metabolites from animal and plant tissues, filamentous fungi, and migroorganisms have been conducted through application of acidic and alkaline extraction methods. For metabolite extractions, the most commonly used acidic and alkaline solutions are perchloric acid, trichloroacetic acid, hydrochloric acid, potassium hydroxide, and sodium hydroxide. In order to eliminate the degradation of thermally labile metabolites, extractions are conducted at low temperatures (0-4°C). One of the drawbacks reported for this technique is the presence of large amounts of salts that precipitate

during pH neutralization, which cause co-precipitation of metabolites. Substantial nucleotide losses have been reported by researchers applying this method for extraction of metabolites [57].

1.3.2 Sample preparation for plant metabolomics

Plants play an important role in the cycle of nature, and are counted as a critical source of food and metabolic energy for organisms that cannot generate their own supply of food. Several thousand different metabolites are produced within the plant kingdom, with an observed diversity in concentration that ranges within six orders of magnitude. The number of metabolites found in plant species is higher due to the generation of secondary metabolites, which are more varied than primary metabolites [97]. Metabolomics applications assist in investigations of plant metabolism and phenotype analysis of various plant species following environmental and genetic perturbations. In addition, application of metabolomics investigations can aid in the discovery of novel pathways. Moreover, plant metabolomics applied to the field of nutrigenomics, in which the role of nutrition in human metabolomics and different diseases is investigated [98].

Plant metabolomics was first investigated by Twsett, who identified components in leaf extracts using chromatographic techniques. Other chromatographic techniques such as GC-MS, LC-MS, and NMR have been subsequently used in this area. The first study on plant metabolic profiling, conducted by Sauter et al., investigated different herbicides on barley plants using GC-MS [99]. Different works in this area have demonstrated that GC-MS is not applicable to cover the expanse of chemical diversity of metabolites present in plants. Accordingly, many studies have focused on LC-MS, which provides higher selectivity and impartial detection for analysis of a wide range of metabolites in plant tissue. Von Roepenack-Lahays et al. [100] reported detection of 1400 metabolites in Arabidopsis extract by quadrupole time of flight (QTOF) mass spectrometer, and Aharoni et al. [101] identified 5000 metabolites from a single plant by FT-ICR-MS. In order to increase the spatial resolution of single cell or tissue-specific investigations when only small sample sizes are available, various designation techniques have been developed, such as capillary electrophoresis coupled to laser-induced flouresence (CE-LIF) or mass spectrometer (CE-MS). Sato et al. [102] identified more than 80 metabolites related to glycolysis, an oxidative phosphate pathway in rice leaf extract. This study reported the identification of low-concentration, unstable metabolites, such as fructose-1,6-biphosphate, and ribulose-1,5-biphosphate. However, due to the complexity of plant matrices and the objective of a given investigation, different sample preparation techniques may need to be applied prior to analysis; for example, a step may need to be undertaken to extinguish plant enzyme activity at the time of sampling, while another technique may need to be applied to separate metabolites from the insoluble components of the cell, which include protein, starch, cell wall, pigments, as well as other macromolecules such as high molecular weight carbohydrates [103].

Metabolomics is affected by the type of sample preparation technique chosen. Plant metabolomics can be subdivided into the following four steps: 1) harvesting of plant materials, 2) processing prior to extraction, 3) extraction, and 4) pre-analytical sample preparation [103]. The selected analytical technique, together with physical chemical properties of the metabolites under study, determine the necessity of each step. Time or place of harvest, as well as environmental conditions, may change plant metabolome [104-106]. These changes may occur within seconds up to a few minutes; accordingly, harvesting should be carried out in a rapid fashion and any further metabolic changes should be prevented from continuing immediately after harvesting. Freezing in liquid nitrogen is the most popularly applied technique to stop metabolic changes in plant samples [105]. As cells are vulnerable during freezing, in order to remove water, freezing-drying based on lypophilisation and cryodesication can be applied [107]. Additional processing prior to extraction, such as grinding, helps improve extraction [108].

Extraction of metabolites from plant tissue is labour intensive, lacks reproducibility, and is generally not available as an automated procedure, in addition to being expensive and time-consuming. The techniques applied for metabolite extraction in the plant metabolomics workflow include solvent extraction, vapour phase extraction, steam distillation, superficial fluid extraction, and ionic liquids. To date, LLE is the most frequently used method in plant metabolomics [106,108,109,110,111]. However, the use of this technique during extraction may produce metabolite degradation, modification, or loss, as well as artifact formation [104-106]. As a large variety of metabolites is present in the plant metabolome, including nonpolars such as terpenoids, fatty acids, midpolars such as secondary metabolites, and polars such as sugars and amino acids, this highly diverse metabolome cannot be covered by single solvent use [106,109]. The ratio of solvent and plant matrix, type of solvent, extraction time, temperature, as well as the applied methods need to be determined prior to analysis. Parameters in solvent selection, summarized as its selectivity, inertness, polarity, boiling point, toxicity, in addition to environmental considerations, can interfere with the analytical techniques applied towards determinations [106]. The use of methanol coupled to a mixture of solvents, followed by applications of an acidified solution for extraction of polars and chloroform for extraction of nonpolars, is the most utilized solvent extraction procedure reported for plant metabolomics [108,109,112]. Past research has demonstrated that mixing water with organic solvents decreases the extraction of nonpolar metabolites such as chlorophyll and fatty acids, causing problems in RPLC-MS. On the other hand, water is problematic in GC-MS applications that include the extraction of both polar and nonpolar compounds. A protocol involving the use of chloroform/methanol/water (2:2:1 v/v/v) has been developed [109] and applied successfully by Yuliana et al. [112] with NMR analysis. In other work, Moritz et al. used a mixture of solvent and nonpolar solvent accompanied by shaking for extraction of polar and nonpolar metabolites from homogenized plant tissue, respectively [105]. In order to expedite the solvent extraction technique, various methods such as ultrasonic extraction, microwave, and

pressurized solvent extraction have been developed [113,108,114,115,116]. These types of extraction methods are mostly efficient for targeted analysis; an ideal method is still needed for untargeted analysis. SPE, another technique often used in plant metabolomics in order to sample clean up, offers a reduced matrix effect. C2, C8, C18, ion exchange cartridges, and polymeric adsorbents have been developed and applied in this area [108,109,117-124]. However, some of the drawbacks reported for SPE in this area are reduced metabolite coverage and metabolite loss.

Environmental stress in plants and any other organisms is defined as any change in growth conditions that interrupts the metabolic pathways. Application of metabolomics could contribute to the study of stress biology of plants and other organisms by assisting in the identification of various metabolites, such as by-products of stress metabolism, as well as stress signal transduction molecules, which are part of the acclimation response of plants. Metabolic profiling and fingerprinting, a combination of different 'omics' platforms, can assist in the capture of holistic features of plant response stress, as well as aid in the characterization of other metabolic pathways [125].

1.4 Introduction to solid phase microextraction (SPME)

Solid-phase microextraction (SPME) is a non-exhaustive sample preparation method that integrates sampling and sample preparation steps. Historically, SPME was mostly applied in combination with GC and GC-MS. However, SPME coupled to GC or GC-MS is unresponsive, and thus unable to analyze non-volatile and thermally labile compounds; therefore, scientists have tried to develop SPME in direct coupling with LC-MS. The first format of SPME to be introduced was fiber geometry, in which small amounts of extracting phases (SPE sorbents) are immobilized on a solid support (Figure 1.3). In order to improve extraction recovery, SPME was developed in other formats, such as thin film, coated stir-bars, and coated capillaries. SPME is comprised of consequent steps, which include extraction of the analytes of interested by SPME coating from the sample matrix, and desorption of the extracted analytes from the coating. Extraction of analytes can be done by setting the fiber above the sample in the case of volatile or semi-volatile analytes, or by direct immersion (DI). Desorption of extracted analytes from the surface of the coating occurs through thermal desorption for GC or solvent desorption for LC. The currently presented work is focused on the analysis of non-volatiles by LC and direct immersion SPME-LC-MS. The amount extracted by the fiber is achieved via Equation 1.1:

$$n_e = \frac{K_{fs} V_f V_s C_s^0}{K_{fs} V_f + V_s} \qquad \text{Equation 1.1}$$

Where n is the amount extracted in moles, C_0 is the initial analyte concentration in the sample, V_s is the sample volume, V_f is the fiber volume, and K_{fs} is the distribution constant between the sample matrix and SPME fiber, stated as the proportion of analyte concentration in the coating to that in the sample at

equilibrium conditions. K_{fs} (in Equation 1.2, C_f^{∞} and C_s^{∞} are the analyte concentrations in the fiber and in the sample at equilibrium time, respectively) is dependent on the type of analyte under investigation, sample matrix properties such as pH and temperature, in addition to the type an organic solvent used and the ionic strength.

$$K_{fs} = \frac{C_f^{\infty}}{C_s^{\infty}}$$ Equation 1.2

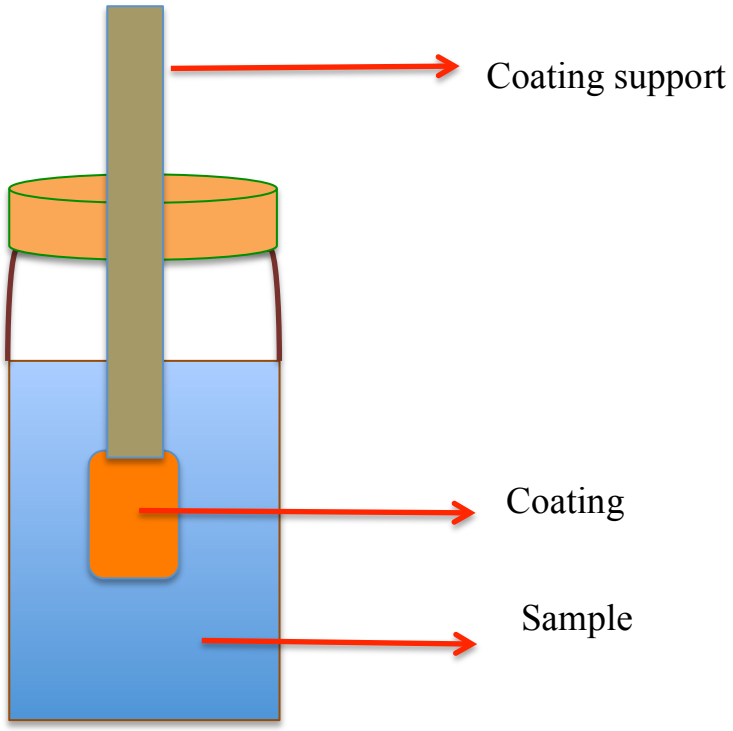

Figure 1.3 SPME procedure scheme using direct extraction mode: SPME coating is exposed directly to the sample solution, and analyte of interest is extracted into the coating. After extraction coating exposed into the desorption solvent, and after desorbing analyte into the desorption solvent, solution is ready for further analysis.

As the technique is non-exhaustive in nature, only small amounts of analyte can be extracted, as opposed to exhaustive extractions that occur in LLE and SPE applications. Coatings are classified as either solid or liquid; the choice of coating significantly impacts the performance of the method. For liquid coatings, such as polydimethylsiloxane (PDMS), analytes are absorbed by the liquid coating through a partitioning mechanism. When the coating is thinly applied, extraction will likely occur within a reasonable amount of time. However, for solid coatings with a glassy or crystalline structure, such as divinylbenzene/polydimethylsiloxane (DVB)/(PDMS), Carboxen/PDMS, and Carbowax (CW)/DVB, the extraction mechanism is based on physical interactions or adsorption; in such cases, the analytes are

adsorbed only on the pores of the coatings, not inside the coatings. Small or mid-sized analytes are retained in the pores of micropore (<20 Å) or mesopore (20–500 Å) coatings. When energy or solvents are applied, the adsorbed analytes are displaced. The mechanism of action is different for macroporore coatings (> 500 Å), which can adsorb larger analytes through hydrogen bonding, pi-pi bonding or van der Waals interactions. Long extraction times can cause analytes with poor adsorption affinity to be displaced by those that have high adsorption affinity or are high in concentration in the sample matrix. To remediate this limitation, pre-equilibrium extractions can be carried out for solid coatings. Equation 1.1 is valid for liquid coatings, while Equation 1.3 is applicable for solid coatings:

$$n_e=\frac{K_{Afs}V_fV_sC_s^0(C_{fmax}-C_f^\infty)}{V_s+K_{Afs}V_f(C_{fmax}-C_f^\infty)} \quad \text{Equation 1.3}$$

where C_{fmax} represents the maximum concentration of active sites on a solid coating, C_f^∞ represents the equilibrium concentration of a given analyte on the fiber, and K_{Afs} represents the analyte's adsorption constant at equilibrium. The adsorption constant is defined as the ratio of the surface concentration of the adsorbed analyte on a porous solid extractive phase to the concentration of the analyte in the sample at equilibrium ($K_{Afs} = S_{Af}^\infty / C_s^\infty$). Equation 1.3 demonstrates that when the equilibrium concentration of the analyte is significantly lower than the concentrations on the active sites on the coating ($C_f^\infty << C_{fmax}$), the amount of analyte extracted is linearly proportional to the initial sample concentration, while for higher concentrations, coating behavior will be nonlinear due to the saturation of active sites. Since the time required for analytes to reach equilibrium is infinite, equilibrium is expressed as the time required to extract 95% of analyte, theoretically obtained by Equation 1.4.

$$t_e = t_{95\%} = \frac{3K_{fs}b\,\delta}{D_s} \quad \text{Equation 1.4}$$

In this equation, δ represents the thickness of the boundary layer, D_s represents the diffusion coefficient of the analyte in the sample matrix, b represents the coating thickness, and K_{fs} represents the distribution constant. Based on this equation, equilibrium time is controlled by factors such as agitation conditions, which affects the thickness of the boundary layer; the distribution constant, determined by the affinity of the analytes for the coating; the thickness of the SPME coating; and the physiochemical properties of the analyte, which determines the diffusion coefficient. When time is of importance, for example, for analysis or extraction of unstable metabolites, extraction can be conducted at pre-equilibrium conditions, determined by Equation 1.5. In this equation, a is the time constant, which is determined by the mass transfer coefficients, distribution constant, sample volume, and extraction phase surface area.

$$n= (1\text{-}e^{-at})n_e= (1\text{-}e^{-at})\, n_e = \frac{K_{fs}V_fV_sC_s^0}{K_{fs}V_f+V_s} \quad \text{Equation 1.5}$$

At equilibrium conditions, Equation 1.5 can be transferred into Equation 1.1, demonstrating that equilibrium time is determined by initial concentrations. At $V_s >> V_f K_{fs}$, (large sample volumes), both equations (Equation 1.1 and 1.5) change to Equation 1.6.

$$n_e = K_{fs} V_f C_s^0 \qquad \text{Equation 1.6}$$

In this condition, the extracted amount is independent from the volume of the sample. This equation can be applied for direct on-site sampling or in vivo sampling, which is very appealing in metabolomics studies. In the case of $V_s << V_f K_{fs}$, Equation 1.1 is revised to Equation 1.7, indicating the equality of the amount extracted to the product of analyte concentration by sample volume.

$$n_e = V_s C_s^0 \qquad \text{Equation 1.7}$$

SPME calibration, a measurement of analytical signal versus analyte concentration, may be required for SPME analysis. Various calibration methods have been applied based on the type of application and instrumentation, including external, internal, standard addition, equilibrium extraction, exhaustive extraction, pre-equilibrium extraction, and diffusion-based calibration [54].

Sampling and sample preparation are the most time-consuming parts of the analytical process; indeed, studies have indicated that more than 80% of analysis time is currently spent on these steps. As in most cases, when a large number of samples need to be processed, enhancing the speed of these processes to improve sample throughput is mandatory. This can be achieved in two ways: decreasing the time of the sampling procedure, or sampling from a large number of samples simultaneously. Significant research attention has been paid to improving these steps [54]. SPME has not been excepted from these efforts, as various designs have been applied to improve sample throughput for SPME. An automation system provides numerous advantages such as speed enhancement, higher reproducibility, human error minimization, as well as a reduction in labor. Commercial autosamplers have been applied for GC applications from the 1990s, and the first coupling of SPME to an LC system was conducted through an injection tee for solvent desorption in 1995 [126,127]. In 1997, Eisert applied in-tube SPME as a proof-of-concept design for automated SPME coupled to an LC, although this system did not provide high-throughput [128]. The recent development of robotic autosamplers has effectively provided high-throughput. In 2005, the first methodology for SPME in a 96-well format was introduced [126]. The first stationary phases for the system were PDMS-DVB SPME coatings, which were used for bioanalysis [129]. Although previous designs were expensive, they provided higher accuracy and repeatability in comparison to LLE in 96-well format. In order to provide a more cost-effective design, 96 stainless steel pins coated with PDMS hollow fiber membranes were used [129]. The Concept 96 autosampler, designed

by Professional Analytical System (PAS) Technology, was first introduced for bioanalysis applications using an octadecyl silica-based 96-fiber SPME coating [130]. Following, the Concept 96-SPME system was designed with different geometries in the format of rod fibers, disks, and thin films. Different coating chemistries have since been developed for these systems, especially for biological applications [131-135]. One of the limitations of the SPME fiber is its low extraction efficiency due to the small volume of the extraction phase used as a coating. Based on Equation 1.1, the extracted amount of analyte could be increased by enhancing the volume of the extraction phase. This enhancement can be achieved in two ways: by increasing the surface area of the extraction phase, or by increasing its thickness. As previously mentioned, increasing the thickness of the coating limits the extraction speed, whereas surface area enhancement can be achieved either by increasing the diameter of the coating or through the use of thin film geometry. While fiber diameter enhancement is limited due to the format of the commercial 96-well plate, the use of thin film geometry does not suffer from the same limitations. As can be seen in Equation 1.8, extraction rates can be increased through an increase in the surface area or a decrease in coating thickness.

$$\frac{dn}{dt} = \frac{AD_s}{\delta} C_s^0 \qquad \text{Equation 1.8}$$

Previous reports indicated that the use of thin film geometry in comparison to the traditional rod fiber configuration improved extraction rates by 2-fold [136]. For this purpose, Mirnaghi et al. tried to improve the 96-SPME system using thin film geometry and a commercial 96-blade device designed by PAS technology. The Concept 96-blade SPME device is composed of eight rows with twelve flat pins coated with sorbents 2 cm from the end. In this design, the eight rows of stainless steel blades are held together by nine inter-blade holders. The robotic Concept 96-autosampler controlled by Concept software is designed to directly place the 96-blade device into the 96-well plate that contains samples or solvents for each step of preconditioning, extraction, wash, and desorption. The 96-blade SPME coatings must have high extraction recovery, reusability, reproducibility, physical and chemical stability, cost efficiency, and be easily automated. In addition, the coatings should also be biocompatible and reach equilibrium within a short period of time. Mirnaghi et al. evaluated different extraction phases for the above-mentioned system for targeted analysis of biological matrices such as blood and plasma, as well as for food samples such as wine and grape. In different works, coatings such as PBA, PS-DVB-WAX, C18, and silica gel were developed as well; however, this system had yet to be developed and applied towards extraction of a wide range of metabolites or for untargeted analysis [137,138,139]. In the current research, different coatings are evaluated and applied as the stationary phase for the 96-blade system for untargeted analysis.

1.4.1 SPME and metabolomics

SPME is a technique that assists in rapid and solvent-free sample preparation; its small sample amount requirements and automation compatibility contribute to high-throughput qualitative and quantitative determinations. Accordingly, SPME has been frequently utilized in the area of metabolomics [140-142]. This technique has the potential to acquire previously unreported information by providing metabolome snapshots at the time of sampling. SPME also provides high spatial resolution, making on-site sampling and in vivo extraction comparatively easier processes, in addition to allowing for the extraction of unstable metabolites [143].

Since SPME was originally developed for GC applications, most of its coatings were also originally designed for GC applications. PDMS, polyacryl (PA), and CARBOWAX (CW) are some of the coatings used in GC analysis, but rarely applied for targeted analysis due to their tendency to mostly extract polar metabolites, which in turn results in poor metabolome coverage [144-145]. DVB/Car/PDMS is a coating applied for the extraction of a wide variety of metabolites. This coating has been utilized for metabolic profiling of skin, pepper, cocoa, and banana [147-151]. The first reports using SPME were for extractions from the headspace (HS) of samples. The use of direct immersion SPME for analysis of complex matrices has been controversial; the adsorption of macromolecules on the surface of the coatings has been reported to produce artifacts, while non-volatiles and thermally labile extracted components were described to decompose in the injector [54]. PDMS-modified coatings have since improved solid coatings to be more biocompatible for direct immersion SPME and in vivo sampling [152]. In LC applications, fiber and thin-film SPME were utilized for bioanalysis. Vuckovic reported evaluation of 42 different SPE particles (silica, polymer, and carbon) immobilized with Loctite 349 adhesive on stainless steel fiber, and applied them for the extraction of metabolites from plasma with a wide polarity range ($-7.9 < \text{Log } P < 7.4$). The results demonstrated that mixed-mode (C18 or C8), phenylboronic acid (PBA), and polystyrene-divinylbenzene (PS-DVB) provide the widest metabolome coverage. In the same study study, SPME methodology was compared with protein precipitation and ultrafiltration, with results demonstrating that SPME could provide a complementary metabolome snapshot for the other two methods. For example, carnitine, gangaliosides, fatty acids, and lysophospholipids were successfully solely extracted by SPME, whereas application of microdialysis allowed for extraction of hydrophilic metabolites such as peptides and amino acids, which could not be extracted by SPME for in vivo sampling [153]. In addition, polyacrylonitrile, as a biocompatible binder, was shown to assist in the reduction of matrix effects for in vivo and in vitro LC applications [137-139].

Other attempts have been made to optimize the stationary phases of SPME coatings so as to provide wide metabolome coverage for different complex matrices such as biofluids, tissues, plants, microorganisms. The majority of works conducted in the plant metabolomics area using SPME were performed by GC-MS

in order to extract the volatile organic compounds originating from different biosynthesis pathways produced by plants. HS-SPME was used for pre-concentration of volatiles in bioanalysis approaches. To date, HS-SPME coupled to GC-MS has been used for comprehensive metabolic profile characterization of volatile metabolites in plant materials such as cocoa, coffee, herbs, fruits, and vegetables. Differentiation of cocoa beans related to geographical origins and storage conditions based on changes occurring in their volatile profiles was reported by Humston et al [154]. Risticevic et al. implemented direct immersion in vivo SPME in apple metabolomics, with results that demonstrated that the type of SPME coating selected for extraction affects the quality and reliability of the obtained metabolome coverage [155]. This mode of SPME provides extraction of high molecular weight metabolites as well as polar ones. In related work, volatilomics analysis was conducted by Apera et al. for four types of apple samples with application of HS-SPME-GC-TOF-MS; this analysis demonstrated the importance of sample collection and storage, as a large decrease in volatile metabolites in apple samples was observed in respect to freshly-processed samples. In addition, application of multivariate data analysis has been shown to also aid in the differentiation of samples stemming from different apple types related to their volatile alcohol and ester derivative profiles [156].

SPME has also been applied for the extraction of metabolites with a wide range of polarities from biological fluids such as blood, plasma, serum, urine, and saliva. In vivo sampling using SPME-LC-MS was successfully performed in this area; unstable metabolites such as AMP, gluthathione, and β-NAD were identified by this technique, which had not been previously reported with the use of traditional techniques [143]. DI-SPME-LC-MS was recently utilized to provide a plasma metabolome profile of patients under cardiac surgery. In this study, SPME demonstrated differentiation between metabolic pathways induced by the surgery and the applied pharmacotherapy. Lysophospholipids, triglecerols, linoleic acids, and mediators of platelet aggregation were listed as potential biomarkers in this study. Different changes in the metabolic patterns of different patients were also identified [154]. In other work, DI-SPME-LC-MS was applied for simultaneous extraction of approximately 400 metabolites in different classes with a wide range of polarities ($-3.5 < \text{Log P} < 10$) from saliva. In this study, SPME showed good discrimination between the metabolic patterns of male and female volunteers [142]. HS-SPME-GC-MS has also been applied for detection of potential cancer biomarkers through comparisons of urinary metabolic profiles. Volatile global metabolome profiling from skin in the early stages of melanoma differed from that of healthy skin and benign naevus samples, demonstrating an increase in three volatile hydrocarbons as secondary metabolites of membranes produced through lipid peroxidation or oxidation stress [157]. Silva et al. reported the presence of 82 volatile organic metabolites related to three different cancers in the headspace of urine samples. Benzene derivatives, terpenoids, and phenols have been indicated as differential metabolites in oncological samples [158].

Tissue metabolomics is another area in which SPME has been used as a noninvasive sample preparation method. In tissue sampling studies, the metabolic coverage of the mixed-mode SPME coating was shown to be comparable with results obtained from solvent extraction procedures [159]. In work conducted by Cudjo et al., in vivo SPME and microdialysis were applied for brain analysis in response to external stimuli, and results indicated that in comparison to microdialysis, SPME was more successful in providing a comprehensive metabolic pattern, in addition to yielding a higher pre-concentration of samples. In this research, Cudjo et al. reported the high affinity of SPME for the extraction of nonpolars; conversely, microdialysis was shown to extract mostly polar metabolites [160]. In other work, on-site application of in vivo SPME during lung and liver surgery towards discovery and monitoring of metabolic pathways, as well as identification of potential biomarkers, has offered potential real time data [159]. In vivo SPME in thin film format has also been reported for metabolic profiling of volatiles emitted from skin [161]. SPME has also been successfully applied for metabolic fingerprinting of the headspace of cell cultures from different tissues and cell lines, such as lung, stomach, and colon; SPME demonstrated clear separation between volatile organic compounds obtained from healthy and cancerous stomachs [162]. For example, Buszewski et al. introduced *Helicobacter* as a gastric cancer pathogen through a comparison of obtained metabolic profiles with pathogen headspace composition [163].

SPME has also been shown to be a suitable technique for identification of pathogenic contamination in foodstuffs. HS-SPME was applied for metabolic fingerprinting of volatile compounds from different bacteria species. Siripatrawan et al. reported contamination in packed food with *Salmonella typhimurium* with SPME-GC-MS with chemometrics applications in order to predict the number of bacteria in unknown samples [164]. The SPME-GC-MS metabolic platform of volatiles from *Pseudomonas aeruginosa* identified 28 new compounds [165]. In another study, Zakir et al. reported the application of the automated SPME-GC-MS method for investigations of cinnamaldehyde as an antibacterial agent against *E.coli* bacteria growth at various stages of the growth curve [166].

LC-MS plays an important role in the identification of a large number of metabolites that cannot be identified by GC-MS. In the present study, the potential of coatings developed for SPME-LC-MS targeted analysis was tested for both bacteria and plant metabolomics. To that end, evaluation of environmental stresses such as cold temperature on apple samples, as well as antibacterial agent effects on *E.coli* bacteria metabolome profiles were investigated in further applications using multivariate analysis.

1.5 Data processing tools for metabolomics

As metabolomics provide a large amount of data, the currently presented work relied on the use of statistics for data processing as well as application of multivariate analysis for concomitant processing of a large number of variables. Figure 1.4 illustrates the data analysis workflow of the presented research

work. First, raw data obtained with Xcalibur software (.raw) was converted to (mzXML) with MS conversion software. Next, the XCMS R-package (Scripps Center for Metabolomics, California, USA) was applied for data processing. The software output consisted of tables containing retention time, m/z, and intensity of features. Figure 1.5-A demonstrates the output of the software after peak detection, retention time correction, and peak alignment. The CAMERA R-package (Bioconductor Version 2.10) was applied to provide ion annotation on the list of features so as to identify detected isotopes, adducts, and in-source fragments ions. The obtained data from table 1.5 was then used for tentative identification by submitting the exact masses of the unknown metabolites obtained from chromatograms to the METLIN database using a 5 ppm mass window. Further selection of metabolites was based on the detection of at least two adducts with the same nominal mass at a given retention time; if available, authentic standards were then used towards the identification of metabolites through a comparison of accurate mass and retention time. In the next step, SIMCA-P+ software v.13.0.3 (Umetrics, NJ, USA) was used for multivariate statistical analyses. Principle component analysis (PCA) and partial least square-discriminant analysis (PLS-DA) were used in this regard. PCA is a linear transformation applied to dimensionality reduction that preserves data; it builds a new co-ordinate system describing variations within the data. Application of PCA on large tables of data obtained by R package software yielded two plots: score plots and loading plots. Score plots demonstrate patterns, trends, clusters, and outliers; it summarizes observations, and separates signals from noises. Loading plots, on the other hand, explain the position of observation in scores plot while summarizing the obtained variables. Figure 1.5 demonstrates the score and loading plots obtained for a set of data; as can be seen, the principal components are orthogonal to each other and uncorrelated. The first component is representative of the largest variance in the dataset, while consequent ones are orthogonal to the first one, demonstrating the highest remaining variance. Figure 1.5-B illustrates two clusters related to two observations in the score plot, while the loading plot (Figure 1.5-C) demonstrates how the original variables correlated to each set of clusters. In these plot scores, t_i, are new variables summarizing the original variables, ordered in a downward fashion: t_1, t_2, and so forth.

PLS is a supervised dimension reduction methodology that supervises forms of discriminant analysis, such as PLS-DA used in classification studies and biomarker identification. Figure 1.6-A demonstrates a PLS score plot that indicates the degree of separation between four sets of observations, based on treatment and incubation time. The S-plot, the output of PLS (figure 1.6-B), is a useful tool in biomarker identification; in this plot, statistically significant variables are discovered through comparisons of control and treated samples. The p_1-axis represents the magnitude of each variable on the X-axis, while the p(corr)1-axis describes the reliability of each variable in X. Variables with high magnitude and high reliability are counted as statistically significant variables; in other words, ideal biomarkers. For

metabolite confirmations, retention time and fragmentation patterns of authentic standards are then compared to those obtained from samples, and pathway analysis can be explored.

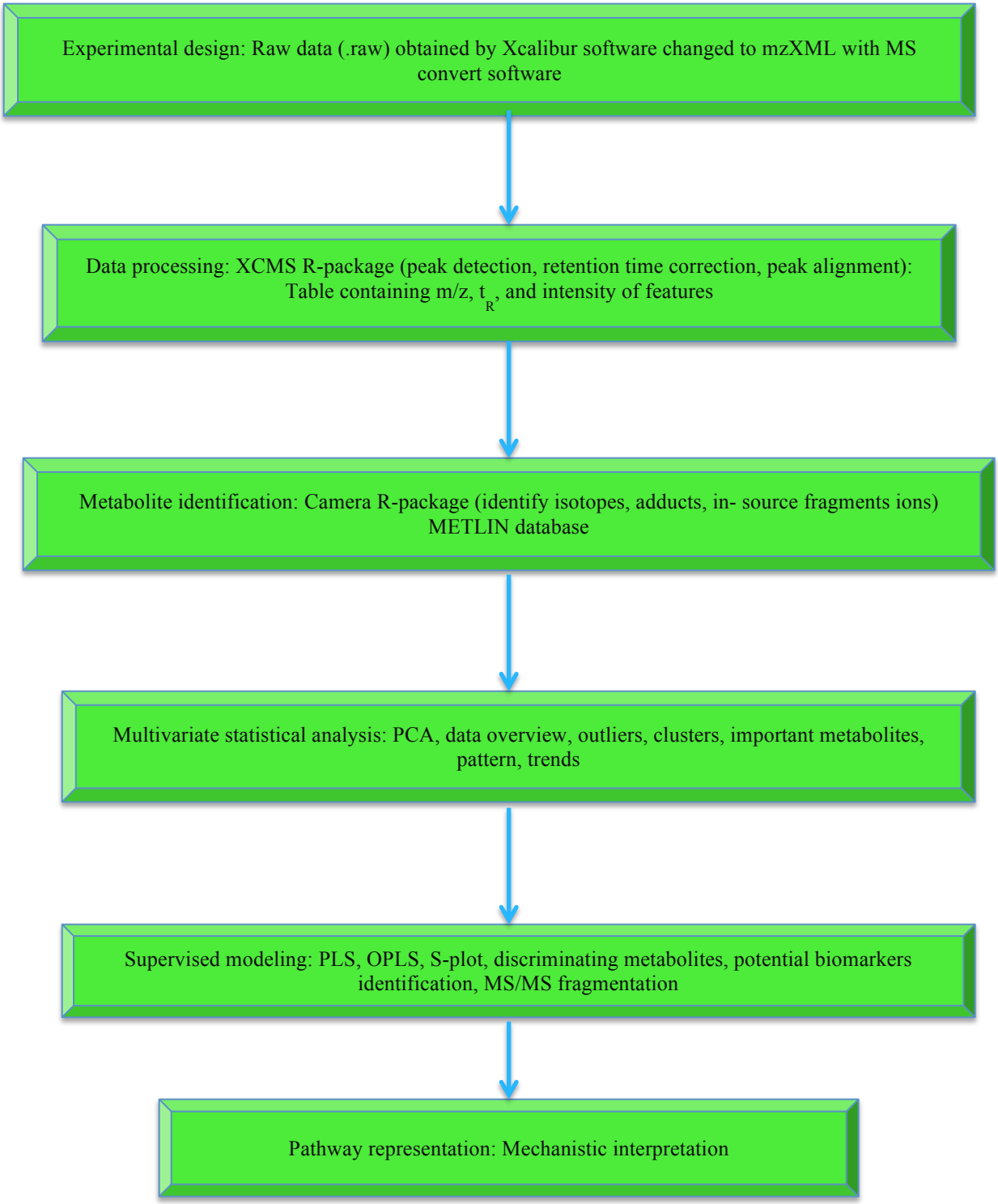

Figure 1.4 Data analysis workflow for metabolomics using R and SIMCA softwares

Figure 1.5 A) Excel file obtained from XCMS R-package and CAMERA R-package softwares, PCA converts table into score plot related to observations and loadings plot related to variables: B) observations score plot and C) variables loadings plot obtained from SIMCA-P+ software

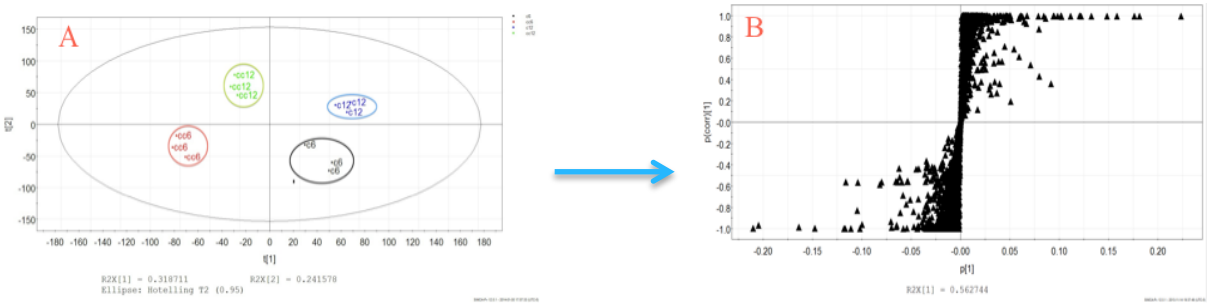

Figure 1.6 A) PLS score plot demonstrates discrimination between experimental groups (control and treated samples at two different time points), and B) S-plot (comparison of two sets of data (control and treated samples at two different incubation times: 12 hours) for extraction of putative biomarkers.

1.6 Research objective

The main objective of this body of work was the development of a 96-blade SPME-LC/MS method that can provide full metabolome coverage of biological system. Currently, there are no methods available that can provide extraction and detection of a wide variety of analytes in a single run. To this purpose, different stationary phases for the automation system were developed and evaluated, then coupled to LC-

MS analysis. Next, the developed coatings were applied for targeted analysis of *E.coli* bacteria as a model organism, and grape and apple samples as plant matrices. Accordingly, Chapter 2 focuses on the development of a silica-based ionic liquid coating suitable for the extraction of amino acids from complex matrices (grape matrix) without any further sample pretreatment. The obtained results demonstrated that changes in precursors during synthesis of the silica-based ionic liquid coating, which impact the polarity of the coating, allowed for suitable extraction coverage of metabolites from the sample under study. Chapter 3 includes an evaluation of various coating chemistries for the extraction of different classes of metabolites with different physical and chemical properties. Identified metabolites are classified as high polarity metabolites (central carbon metabolism such as the glycolytic pentose phosphate pathway and citric acid cycle intermediates, as well as biosynthetic metabolites such as amino acids, nucleotides, vitamins, and their precursors) to nonpolars, including lipids from *E.coli* culture. Chapter 4 applies the method developed in Chapter 3 for bacteria metabolomics towards an investigation of *E. coli* bacteria affected by cinnamaldehyde, both below and above the minimum inhibitory concentration (MIC) during bacterial growth. Chapter 5 includes the development of the 96-blade SPME method through application of multivariate analysis. This chapter details how the developed method was used to investigate bacteria affected by clove oil, as well as clove oil major constituents. The method successfully investigated environmental fluctuations leading to rapid adjustment of bacteria treated by different naturally occurring antibacterial agents such as cinnamaldehyde, clove oil, and other essential oils during bacteria growth, necessitating changes to the cellular network and metabolic pathway. The obtained results indicated potential biomarkers related to changes in the metabolic pathway of control samples in comparison with matched treated samples. In chapter 6, the 96-blade SPME method was evaluated for targeted and untargeted apple metabolomics studies; in this work, the developed method was applied towards further exploration into the physiological processes that lead to cell death as well as the ripening processes that affect the flavor, appearance, and overall quality of stored apple samples with superficial scald. This work used a combination of univariate and multivariate data analysis to characterize changes occurring in the metabolic profiles of “honey crisp” apples induced by cold stress, resulting in novel evidence of changes in the metabolic profile of stored apple samples in comparison with healthy ones. Finally, Chapter 7 summarizes the main research findings of this current work and proposes future directions and challenges for this field of study.

Chapter 2

Silica-based ionic liquid coating for 96-blade system for extraction of amino acids from complex matrixes

2.1 Preamble and introduction

2.1.1 Preamble

This chapter has been published as a paper: Fatemeh Mousavi, Janusz Pawliszyn, Silica-based ionic liquid coating for 96-blade system for extraction of aminoacids from complex matrixes, *J. Analytica Chimica Acta,* 2013, 803, 66-74. The materials of the current chapter are reprinted from this publication with the permission of Elsevier (Copyright Elsevier 2013). All of the work reported within this chapter has been performed solely by the author.

2.1.2 Introduction

Ionic liquids (ILs) are organic/inorganic salts with a melting point below 100°C. These compounds have some special properties, such as negligible vapor pressure, high thermal stability (~250-400°C), variable viscosity, and capability of undergoing multiple solvation interactions [167]. The popularity of ILs is due to their applications in green chemistry; however, their usage also has been extended to other research areas. ILs are also used in different areas of separation techniques, including: GC, LC, and electrophoretic methods. In LC, ILs are used as the mobile phase additives to eliminate the destructive effect of stationary phase on the retention of basic analytes. Moreover, ILs have been applied as the stationary phase for LC columns through using synthesized silica based ionic liquid (SiIL) particles [168-175].

Four various methods have been reported in the literature for synthesizing silica-based ionic liquid (SiIL). The first method begins with the attachment of bromoalkyl-1-trichlorosilane to silica; followed by the synthesized compound being endcapped with chlorotrimethyl silane. Finally, the reaction between the endcapped modified silica and ionic liquid produces SiIL [176-182]. The second method uses 3-mercaptopropyltrimethoxysilane (MPS), to modify activated silica; afterwards, the reaction of the product with the allyle group of imidazole is utilized in the presence of azodiisobutyronitrile (AIBN) as an initiator [182-186]. The third method uses a silane-coupling agent, such as 3-chloropropyltrimethoxysilane, for the modification of activated silica. The reaction is completed through the reaction of the product by imidazole [187-193]. The fourth method synthesizes ionic liquid via the reaction of 3-bromopropyl-triethoxysilane and 1-alkylimidazole. Finally, the reaction of synthesized ionic liquid with silica produces SiIL [194]. In the current work, the second method was used for synthesizing SiIL.

SPME, a popular sampling technique introduced by Pawliszyn in the early 1990s, is a simple, quick, cost effective and solventless technique, which integrates sampling and sample preparation into one step [195-197]. Automated high-throughput analysis is necessary to provide fast and precise sample preparation for analysis in various fields of clinical, pharmaceutical, food, and environmental sciences. In-house 96-coated SPME fiber using automated robotic unit was used to access high-throughput analysis via automation of SPME coupled with LC-MS/MS for parallel analysis of drugs in human blood and plasma by Pawliszyn's group in 2008 [198].

To eliminate the limitation of the previous design [198], a 96-blade system coated with thin film geometry was developed, and commercial SPE particles including C_{18}, PS-DVB-WAX, and PBA were used as the stationary phase on the stainless steel blade for 96-blade system using polyacrylonitrile (PAN) as a biocompatible binder [137,138]. These extractive phases provide high extraction recovery in the case of extraction of nonpolar compounds, but it is needed to introduce new extraction phase for extraction of polar compounds.

Based on the author's knowledge, until now ionic liquids immobilized on silica have not been applied to the stationary phase for SPME as the sample preparation technique for HPLC. According to references [199-201], molecular interactions such as strong hydrogen bonding, hydrophobic, ion-dipole, and strong ion-pairing exist in ionic liquid, which provide sufficient interaction with polar compounds. Due to these considerations, we synthesized a new stationary phase based on N-methylimidazolium cation group attached on the silica surface, and then immobilized it on the stainless steel blade with PAN glue; finally, the new extraction phase was applied for direct extraction of amino acids as a group of polar compounds from complex food matrix.

An essential active compound available in food and beverages is amino acids, which affect the food quality through taste, aroma, and color. Since these compounds are considered vital elements of human diet, their determination has an important role in food industry [202]. Most methods for analysis of this group of compounds usually require derivatization by derivatization agents to increase their detectability. However, these methods have some disadvantages, such as instability of derivatives, side reactions, reagent interferences, and significant time consumption. Thus, a reliable, rapid, and accurate method of analysis is needed for performing qualitative and quantitative analysis of amino acids to investigate food quality for nutritional and regulatory purposes and overcome the drawbacks of determined in amino acid analysis techniques based on pre- or post-column derivative methods [203].

The objective of this study is to introduce a new coating for SPME coupled with LC-MS/MS for extraction of amino acids as the high polar compounds from grape pulp without sample pretreatment. The chemical structure of understudied amino acids is shown in Figure 2.1.

2.2 Experimental

2.2.1 Chemicals and materials

1-vinylimidazole (99%), 3-mercaptopropyltrimethoxysilane, 2,2-Azobisisobutyronitrile (AIBN) (98%), and Polyacrylonitrile (PAN) were purchased from Sigma-Aldrich (MO, U.S.). 1-Bromooctadecane, (96%) was purchased from Fisher Scientific (ON, Canada). Silica gel with 60 Å average diameter was purchased from SiliCycle Inc (Quebec, Canada). Arginine, aspartic acid, glutamic acid, isoleucine, histidine, luecine, lysine, phenylalanine, proline, thereonine, tryptophan, tyrosine L-(+)-Tartaric acid and potassium-L-tartrate monobasic were purchased from Sigma-Aldrich (MO, U.S.). Acetonitrile (HPLC grade), methanol (HPLC grade), and N,N-dimethylformamide (DMF) were purchased from Caledon Laboratories (ON, Canada). Polypropylene Nunc U96 Deep Well plates were purchased from VWR International (ON, Canada).

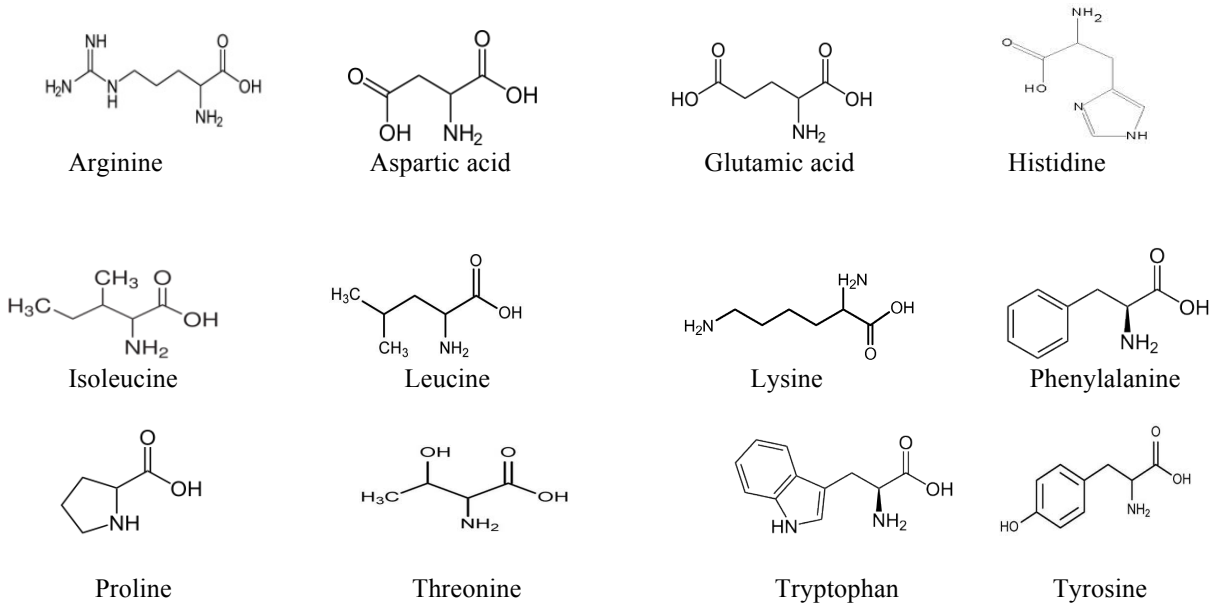

Figure 2.1 Chemical structures of understudied amino acids.

2.2.2 Liquid chromatography and mass spectrometry conditions

Chromatographic separation was performed by Discovery HS F5 column, 2.1mm×15cm, 3µm particle size (Supelco, Bellefonte, PA, USA) using gradiant condition. Flow rate was 200 µL/min, and mobile phases A and B consisted of water/formic acid (99.9/0.1, v/v) and acetonitrile/formic acid (99.9/0.1, v/v). The chromatographic elution and a 40 min gradient program was optimized for separating the model compounds as follows: 100% A (0-3 min), linear gradiant from 100 to 10% A (3-25 min), linear gradient held at 10% A from (25-34 min), the column reached to equilibrium for 6 min by applying gradient 10% A to 100% A. Quantitative analyses of compounds were performed using an API 4000 triple quadrupole

mass spectrometer (Applied Biosystems, California, U.S.) equipped with TurboIonSpray source. A CTC PAL autoinjector from Leap Technologies (CTC Analytics, NC, U.S.) was used for the injection of samples into the LC-MS/MS system (20 μL injection volume). The MS/MS analysis was performed in positive mode under multiple reaction monitoring (MRM) conditions. The summary of MS/MS parameters is given in Table 2.1, and extracted ion chromatograms of amino acids are shown in Figure 2.2.

Table 2.1 Optimized mass spectrometry condition of understudied aminoacids
Compromised ionization source values: Ion source gas 1 (GS1)= +20, curtain gas= +10, collision gas= 12, spray ionization voltage= 5000 V, and temperature= 400 °C.

Analyte	Q_1 mass (amu)	Q_3 mass (amu)	DP (V)	EP (V)	CE (V)	CXP (V)
Arginine	175.1	70.1	59	14	36	19
Aspartic acid	134.1	74.0	49	10	25	6
Glutamic acid	148.1	84.1	47	10	25	6
Histidine	156.1	110.0	47	15	25	20
Isoleucine	132.0	86.1	60	10	16	15
Luecine	132.1	86.1	47	10	25	6
Lysine	147.1	84.1	46	15	26	6
Phenylalanine	166.2	120.0	51	15	25	26
Proline	116.1	70.0	22	14	27	14
Threonine	120.1	74.0	40	14	25	15
Tryptophan	205.1	188.3	44	11	25	8
Tyrosine	182.1	136.1	61	10	20	14

2.2.3 SPME procedure using automated Concept 96-blade SPME

The Concept 96-blade SPME device and autosampler prepared by Professional Analytical System (PAS) Technology (Magdala, Germany) controlled by concept software was used to provide reproducibility and high-throughput for the analysis. The detailed description of automated 96-blade SPME system is reported in the references [137,138]. This system has 4 stations: preconditioning, extraction, wash, and desorption steps. Red seedless grapes, purchased from a local market in Waterloo (ON, Canada), were manually stemmed, washed with deionized water, dried, and crushed using a blender. The extraction was performed from 1 mL of sample for 90 min (1000 rpm agitation speed, 2.5 mm amplitude), which is the equilibrium time for all compounds. The optimized condition for wash was 10 seconds without agitation in the case of real sample analysis. Desorption was performed into 1 mL of acetonitrile/water 1:1 (v/v) as the optimized desorption solvent (1500 rpm agitation speed, 1 mm amplitude) for 60 min.

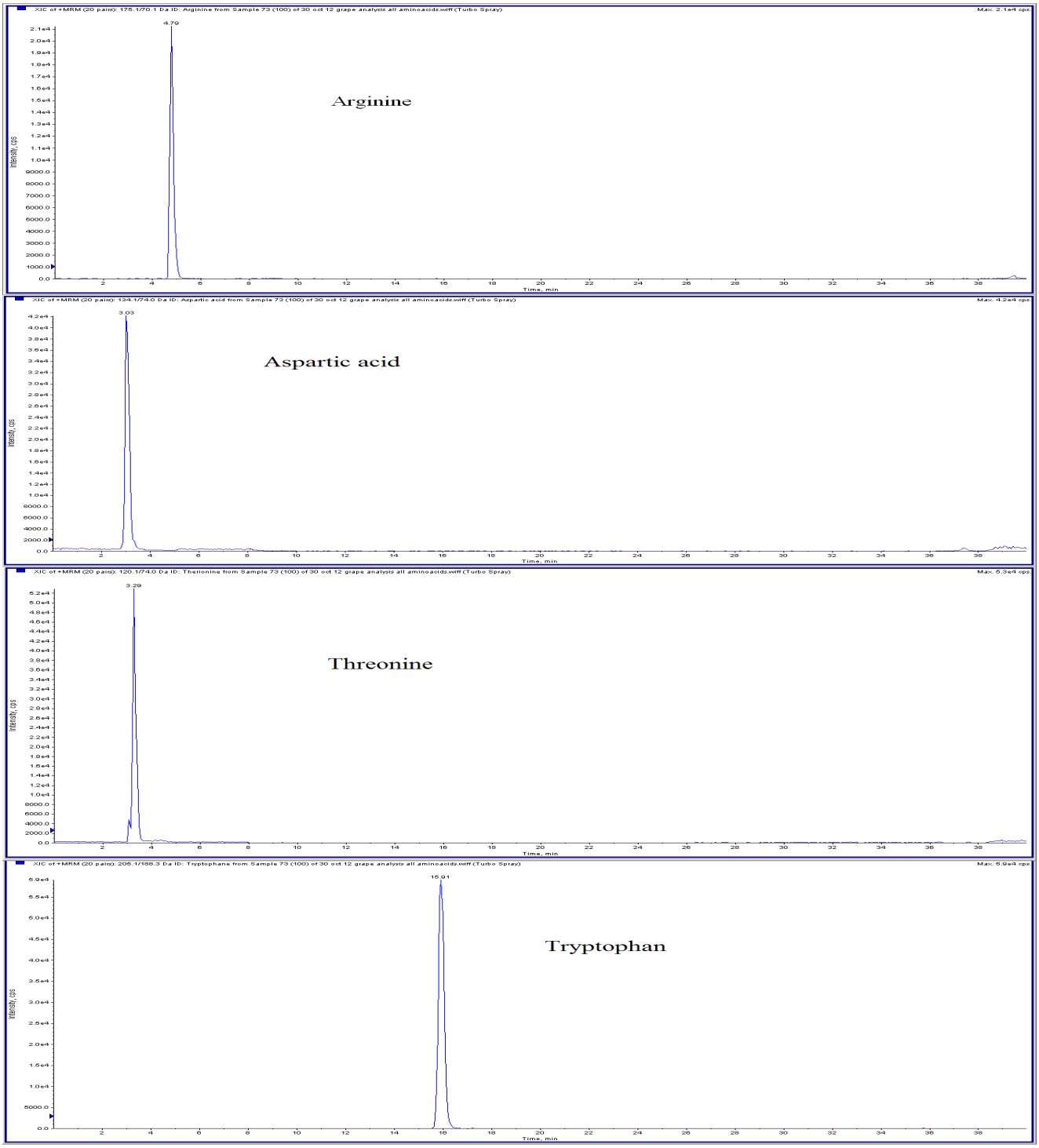
Arginine
Aspartic acid
Threonine
Tryptophan
Intensity, cps
Time, min

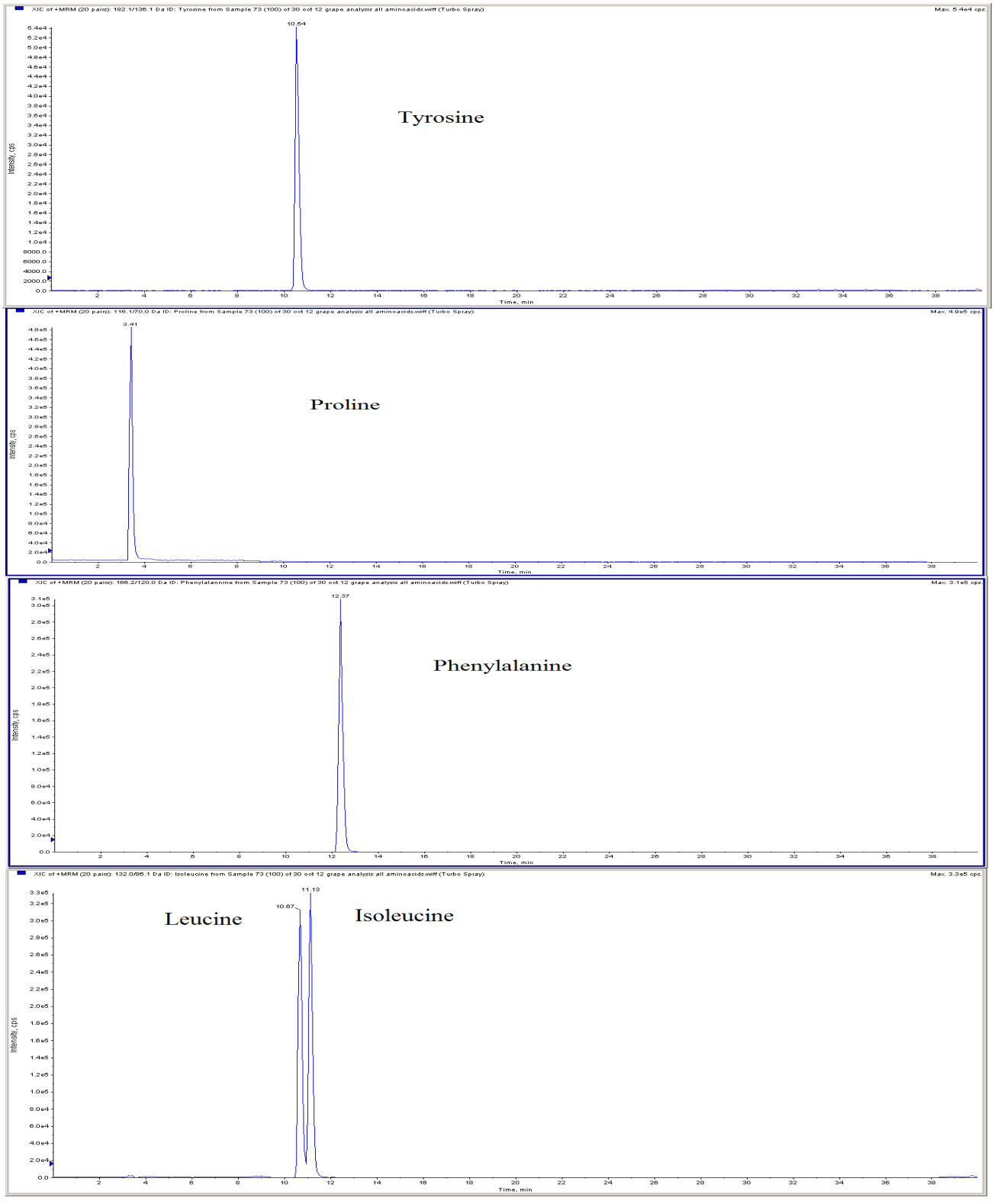
Tyrosine
10.54
Proline
3.41
Phenylalanine
12.37
Leucine
10.67
Isoleucine
11.13
Intensity, cps
Time, min

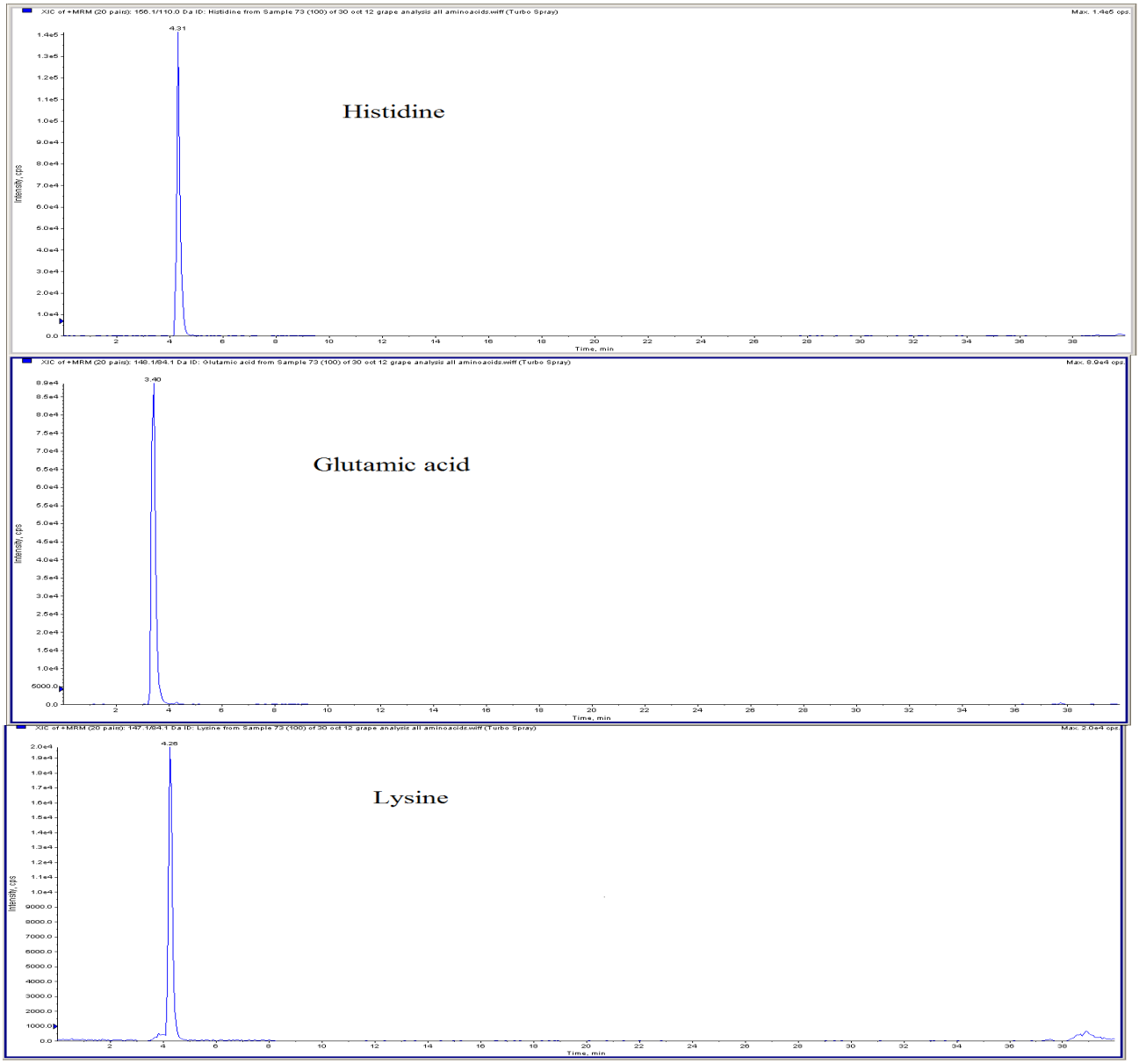

Figure 2.2 Chromatograms of aminoacids with developed LC-MS/MS method.

2.2.4 General procedure for IL synthesis

The procedure of synthesizing IL was performed based on literature [204]. In brief, 1-vinyl-3-octadecylimidazolium bromide was produced through reaction of 4.7 g 1-vinylimidazole (0.05 mol) and 18.3 g bromooctadecane (0.055 mol, 10% excess) at 60°C under agitation with a magnetic stirrer for 36 h. The IL product was separated as a precipitate through filtration process. By three consequent extractions with ethyl acetate, the remainder of liquid product was separated. After recrystallization from ethyl acetate in order to purification of the product, white solid was dried under vacuum at 60°C for 24 h.

1-Vinyl-3-octadecylimidazolium bromide was obtained as the white powder with efficiency of 75% and

73°C melting point. Avance 300 MHz Bruker (Bruker, Germany) was used to take ^{1}H NMR spectra of synthesized [C_{18}VIm]Br. ^{1}H NMR (CDCl3, ppm): δ 0.9 (t, 3H), 1.3 (m, 30H), 1.9 (qi, 2H), 4.4 (t, 2H), 5.4 (dd, 1H), 6. 0 (dd, 1H), 7.5 (dd, 1H), 7.6 (s, 1H), 7.9 (s, 1H), 10.8 (s, 1H).

2.2.5 Synthesis of the N-methylimidazolium functionalized silica

Imidazolium functionalized silica was synthesized based on the procedure in reference [205]. First, activated silica was obtained by immersion of silica in hydrochloric acid for 24 h. Next, silica was washed with deionized water until the pH of eluted water reached 5.5, and was then dried under vacuum for 8 h at 120°C. Mercaptopropyl modified silica (Si-MPS) was prepared through the reaction of activated silica (6.0g) and 3-mercaptopropyltrimethoxysilane (3.0g) in 30 mL of dry toluene under nitrogen atmosphere while stirring mechanically and refluxing for 68 h. After cooling to room temperature, the product - Si-MPS- was obtained followed by successive washing with large volumes of toluene and methanol–water. SiIL was synthesized through surface radical chain-transfer polymerization of the synthesized 1-Vinyl-3-octadecylimidazolium bromide monomers with Si-MPS based on the procedure used in reference [205]. 6.1 g of Si-MPS was added to a 100 mL three-neck round-bottomed flask. Then, the same amount of synthesized IL was dissolved in 30 mL of chloroform and added to the flask. After 20 min of bubbling N_2 through the solution, 1% AIBN was added, and the mixture was stirred at 60°C for 32 h under N_2 atmosphere. The obtained SiIL, octadecylimidazolium-modified silica ($SiImC_{18}$), was filtered and washed with chloroform, ethanol, ethanol–water, methanol, and diethyl ether, and dried under vacuum atmosphere. The structure of synthesized compound is shown in Figure 2.3.

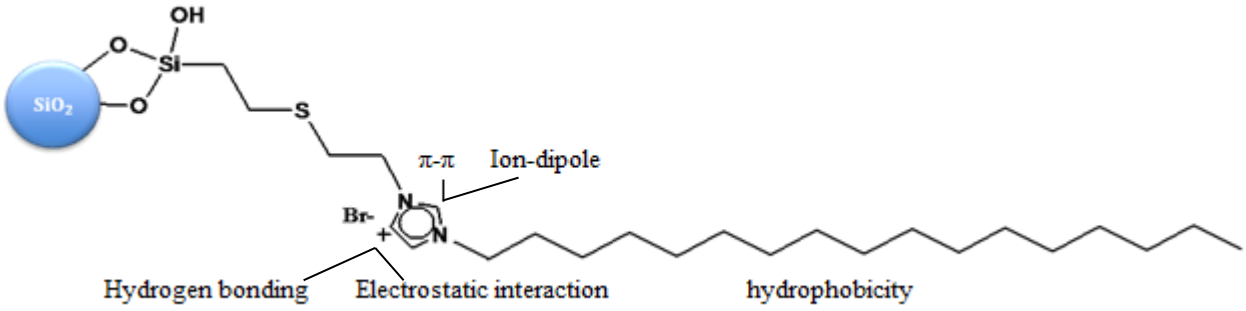

Figure 2.3 Chemical structure of silica-based 1-vinyl-3-octadecylimidazolium bromide ionic liquid and different types of possible molecular interactions.

2.2.6 Immobilization of silica based ionic liquid on the 96-blade system

Immobilization of the synthesized silica on the stainless steel blade system using PAN glue, and dipping technique was completed based on the previous works reported on commercial particles (C18, PBA, PS-DVB-WAX) [138,139]. In brief, stainless steel blades were sonicated in concentrated HCl solution for 1

hour. The blades were then washed thoroughly; and kept at 150°C for 30 min. In order to produce PAN glue solution, 0.5 g PAN was dissolved in 7.5 mL DMF; and kept at 90°C for 1 hour. 1.5 g of synthesized $SiImC_{18}$ was added in PAN glue solution and sonicated for 30 min to disperse particles homogenously. Two cm length at the ends of the stainless steel blades were dipped into the prepared suspension for 2 min, taken out, then dried for 2 min at 100°C. The dipping and drying steps were repeated 10 times until reaching the homegenous coverage of blades by the particles.

2.2.7 Preparation of standards, buffers, and spiked solution

1 mg/mL of stock solution of analytes in nanopure water was prepared and maintained at -30°C. Lower concentration standards were prepared daily from stock solution and diluted by acetonitrile/water (50:50 v/v). Tartaric buffers were formed from determined molar ratios of potassium tartarate monobasic and tartaric acid in 1 L of water, and the pH of the buffers was adjusted to pH=5.0 using hydrochloric acid or sodium hydroxide solution if needed. The concentration of organic solvents in buffers and real samples was always maintained at less than 1%. In order to achieve the equilibrium of amino acids with the sample matrix, after spiking the standard of analytes in grapes, solutions were stirred for 1 h (2400 rpm agitation) before extraction.

2.2.8 Solvent extraction (SE) procedure

To compare the performance of SPME versus traditional extraction method, SE was performed for extraction of analytes from grape pulp. 1 g of grape sample was weighed in to a 15 mL centrifuge tube with cap. 10 mL of 0.2 mM acetic acid was added to the samples. After mixing by the vortex for 2 min, the mixture was centrifuged at 5000 rpm for 10 min at -5°C. The clear supernatant was quantitatively transferred into a vial, and filtered through 0.45 μm nylon syringe filter prior to LC/MS analysis [202].

2.3 Results and discussions

2.3.1 Characterization of developed $SiImC_{18}$-PAN coating

2.3.1.1 Thermogravimetric analysis (TGA)

TA Instruments simultaneous TGA/DSC SDT Q600 (TA Instruments, IL, USA) was used for thermal geravimetric analysis. The condition of analysis was performed in static air ranging from 30°C to 800°C with a heating rate of 10°C/min. TGA, which measures the amount and rate of change in the weight of a material as a function of temperature or time in a controlled atmosphere showing thermal stability and verification of the amount of immobilized compounds, was performed for unmodified silica, synthesized Si-MPS, and $SiImC_{18}$. As presented in Figure 2.4, weight loss for MPS was between 200°C and 600°C, and mass loss was approximately 12%. For $SiImC_{18}$, weight loss was between 200°C and 600°C, and

mass loss was approximately 35%. The obtained results show that after forming covalent bonding between ionic liquid and Si-MPS, there is a higher mass loss for $SiImC_{18}$ than Si-MPS. The weight loss at the temperatures less than 100°C occurs because of elimination of physically adsorbed water. The weight loss between 250-600°C is attributed to dehydroxylation of silica surface. Enhancement of weight loss in the case of $SiImC_{18}$ compared with Si-MPS represents the higher organic content of $SiImC_{18,}$ thus verifying the attachment of synthesized $[C_{18}VIm]Br$ to the Si-MPS [194].

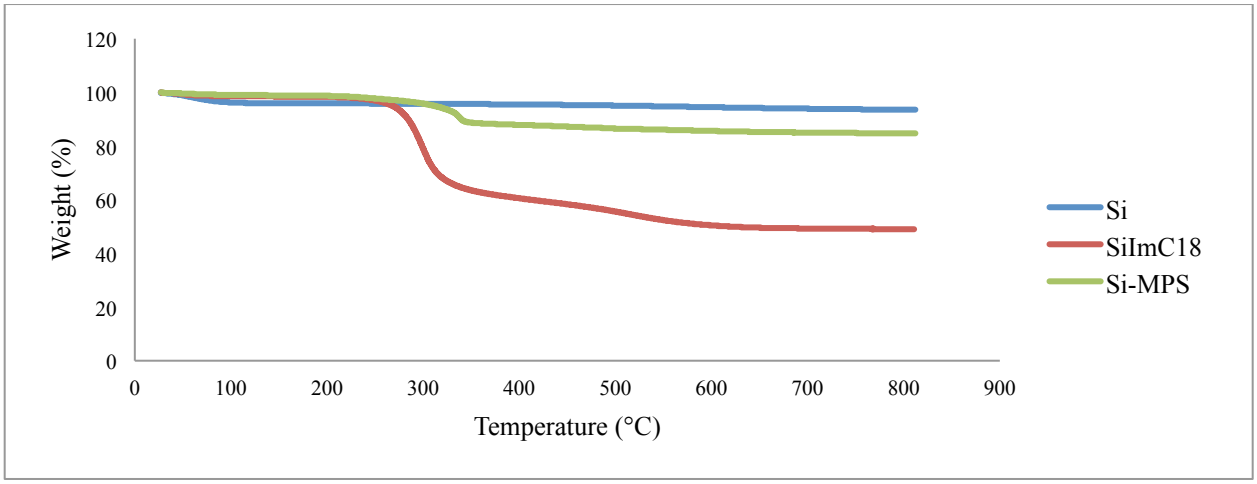

Figure 2.4 Thermogravimetric curves of silica, Si-MPS, SiImC18.

2.3.1.2 Infrared spectroscopy (IR)

Bruker Tensor 37 FTIR (Bruker, Germany) was used to take the Fourier transform infrared spectra in the range of 4000-400 cm^{-1} for identification of chemical modification of synthesized compounds. Based on IR spectra shown in Figure 2.5, differences in wave numbers and intensities of Si-MPS and $SiImC_{18}$ were evident. The peaks at 2854 and 2927 cm^{-1} are related to the C-H stretching of tetrahedral carbon, and the peaks at 1468 and 1563 cm^{-1} are related to imidazolium group, which verify the attachment of imidazolium group onto the silica surface.

2.3.1.3 NMR spectroscopy

Avance 500 MHz Bruker (Bruker, Germany) was used to take solid state ^{13}C and ^{29}Si cross-polarization/magnetic angle spinning nuclear magnetic resonance (CP/MAS NMR) spectra using 4 mm VT CP/MAS probe at 4.2 kHz to confirm the attachment of IL to the silica particle surface. Figure 2.6 demonstrates the ^{13}C NMR and ^{29}Si NMR of the synthesized $SiImC_{18}$ which provides valuable structural information. As shown in Figure 2.6 (a), the signals at -50 and -57 ppm are related to the monofunctional Si-O-Si and more stable bifunctional Si-O-Si linkages, respectively. The signals at -95 and -108 ppm are related to Si atoms with geminal and free hydroxyl groups, respectively. The signal at -115 ppm is related to Si atoms at siloxan network [205]. The signals related to carbons of mercaptopropyl, imidazolium and

alkyl groups of [C_{18}VIm]Br are represented in Figure 2.6 (b) investigated by ^{13}C NMR.

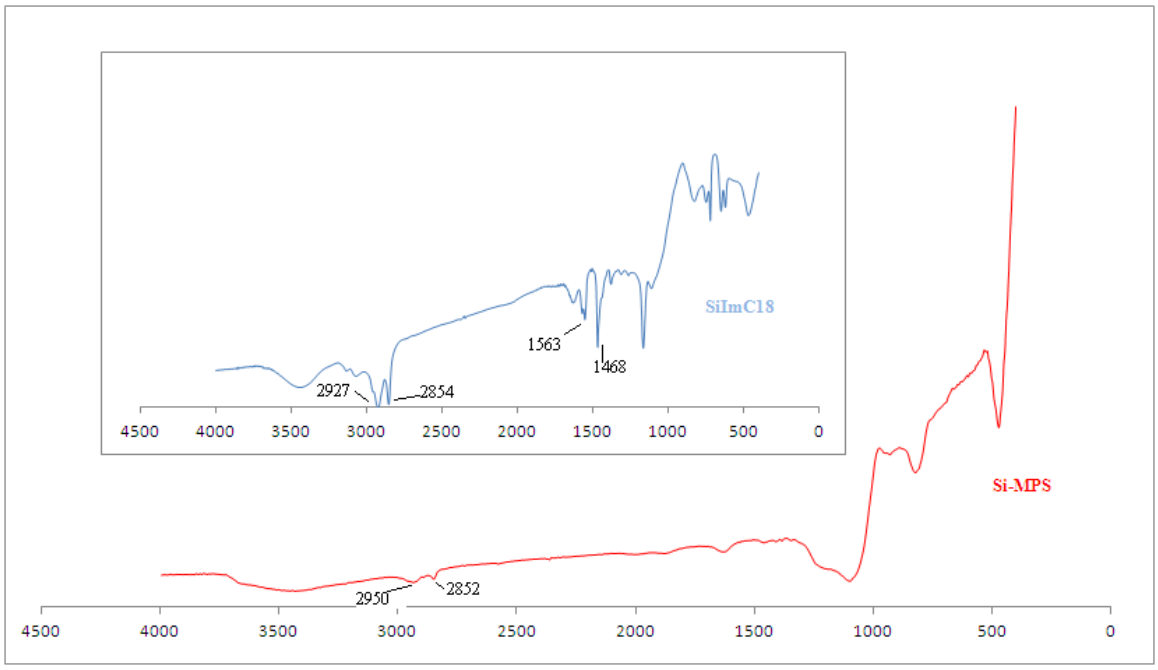

Figure 2.5 FTIR spectra of Si-MPS and SiImC18.

2.3.1.4 Characterization of SiImC$_{18}$-PAN SPME coating immobilized on the stainless steel blade and scanning electron microscopy

The topography and morphology of the coated blades was prepared by scanning electron microscopy (SEM). SEM images were recorded using an Ultrapure1530 field emission scanning electron microscopy (Zeiss NTS GmbH, Germany). Figure 2.7 shows the SEM images of the coating after being sputtered with 10 nm of gold on the surface. The SEM was also used to estimate the average thickness of the coating, which was approximately 20 µm. The distribution coefficients (K_{fs}) of the analytes between the fiber coating and sample matrix were calculated by Equation 1.1.

V_f for thin film geometry coatings can be calculated from Equation 2.1, in which (l) is the coating length, (w) is the width of the blades, (d) is the depth of the blades, and (b) is the coating thickness [138].

$$V_f = 2[lb(w + 2b)] + 2[lb(d + 2b)] + [b(d + 2b)] \qquad \text{Equation 2.1}$$

The new extraction phase not only has an octadecyl chain to provide nonpolar interactions, but also has functionalized imidazolium groups, which provide additional interactions such as π-π and hydrogen bonding to the polar analytes. The information about V_f, K_{fs}, fiber constant, $K_{fs}.V_f$, and absolute extraction recovery, % AER, and intra- and inter-blade reproducibility for extraction of analytes from

tartaric buffer are summarized in Table 2.2.

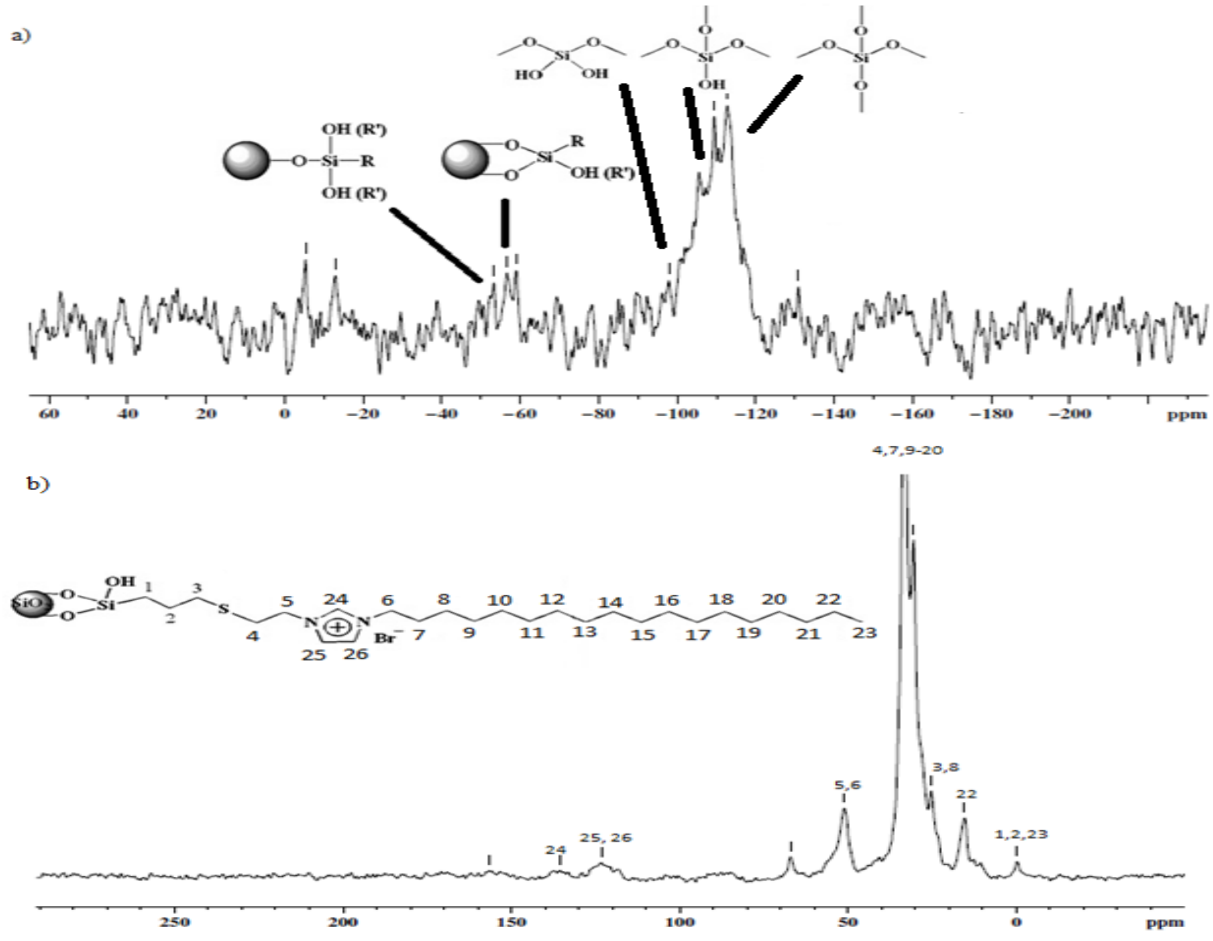

Figure 2.6 a) ^{29} Si CP/MAS NMR and b) ^{13}CNMR spectra of SiImC$_{18}$.

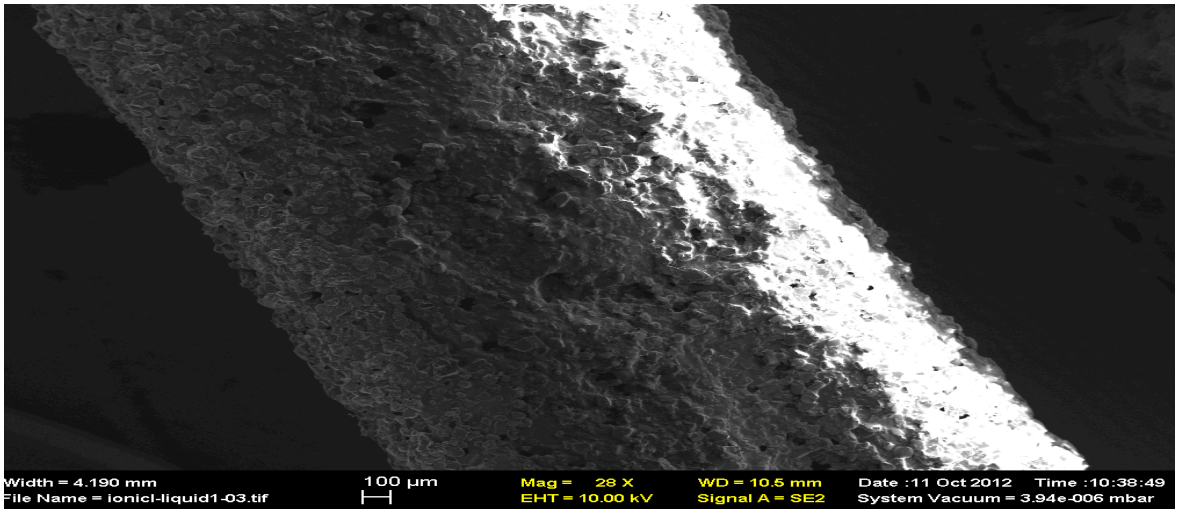

Figure 2.7 SEM image of SiImC18 -PAN coating using- 28× magnification for surface morphology.

2.3.2 SPME method development

2.3.2.1 Preconditioning

To investigate the effect of preconditioning step on the extraction of amino acids as the model compounds, experiments were performed for extraction of analytes from tartaric buffer for 60 min. In one experiment, extraction was performed without any application of preconditioning step. For two other experiments, 1 mL methanol:water 1:1 (v/v) was applied to wet the coating for 30 and 60 min before extraction step for the assessment of the effect of preconditioning step as the mixture of the two aqueous and organic solvents (methanol and water) wet and activate the surface of the coating with different functional groups for extraction. Extraction of amino acids was done from 1 mL tartaric buffer (pH=5.0). As the understudied grape matrix had the pH=5.0, all the extraction steps for the SPME method development were done at pH=5.0 to simulate a similar conditions for pH and ionic strengths in regards to real sample analysis. Based on the results (Figure 2.8), applying 30 min preconditioning before extraction could provide better extraction efficiency compared with no preconditioning step; however, there is no noticeable difference between using 30 min and 60 min time for preconditioning step in the range of experimental error, so there was no need for evaluation of this step in higher times. Finally, 60 min preconditioning in 1 mL methanol:water 1:1 (v/v) was applied for all experiments before extraction.

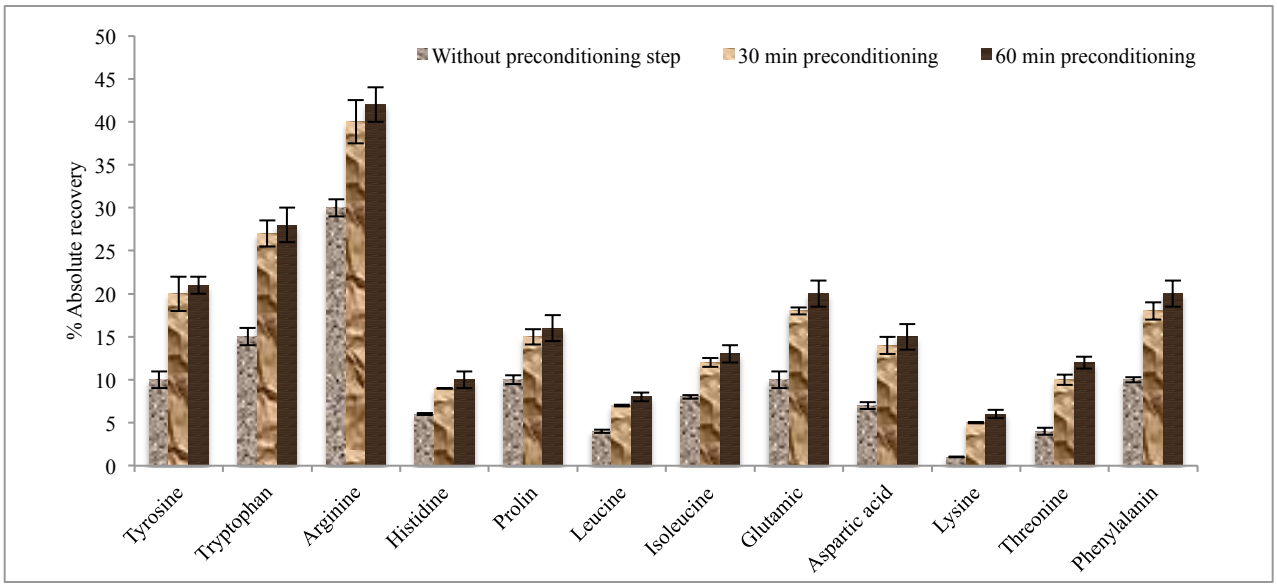

Figure 2.8 Investigation of the effect of preconditioning on the extraction recovery of aminoacids, extraction from 100 ppb of amino acids in tartaric buffer (pH=5.0).

2.3.2.2 Extraction

When the change in the amount extracted is less than the experimental error during extraction, the system reaches equilibrium, which provides extraction of 95% of an analyte from sample matrix. At equilibrium time, the highest sensitivity and extraction efficiency is achieved [54]. Extraction time profile of amino

acids was evaluated for 30, 60, 90 and 120 min of extraction from 1 mL tartaric buffer and grape pulp in different experiments. The concept 96-autosampler system provided 1000 rpm agitation speed. The results are shown in Figure 2.9. Based on the extraction time profile, the minimum time required for all the analytes to reach equilibrium with the coating was approximately 90 min for both matrixes; consequently, 90 min extraction time was used for the entire study.

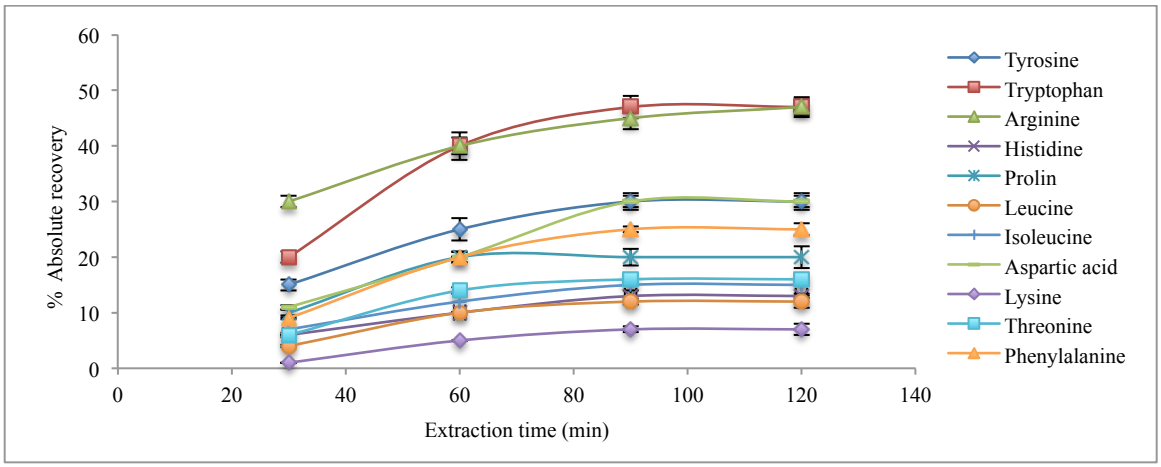

Figure 2.9 Extraction time profile for understudied analytes, extraction from 100 ppb of amino acids in tartaric buffer (pH=5.0)

3.2.2.3 Wash

In the case of real sample analysis, the complexity of the grape matrix is due to high sugar and proteins content; therefore interferences must be removed before introduction of coatings into desorption solvent. To decrease matrix effect (ion suppression/ ion enhancement) because of co-elution of interferences and deterioration of coating, a wash step was needed. Using wash step provides removal of interferences caused matrix effect of amino acids; on the other hand, analytes removal should be noticed in this step. The optimization of wash step showed that immersing the coatings in 1 mL nanopure water for 20 s without agitation after extraction step could remove the analytes during this stage. However, 10 s immersion in water under the same conditions could also be effective. The loss of analytes during this step was under 1%. Also matrix effect (ion suppression/ ion enhancement) evaluation showed that application of this step could help prevention of transferring interferences in to the final extract.

2.3.2.4 Desorption

To optimize desorption condition, the optimal desorption solvent must be identified to desorb the highest amount of analytes from the coating during shortest time while eliminating or decreasing the potential of carry over. Two mixtures as desorption solvents at the maximum agitation speed of concept 96-autosampler system were evaluated: methanol:water 1:1 (v/v) and acetonitrile:water 1:1 (v/v). Based on the results shown in Figure 2.10, acetonitrile:water 1:1 (v/v) provided higher extraction recovery and the

least carry over for all amino acids. Desorption time profile was also investigated for all the model compounds. As is clear from Figure 2.11, approximately 60 min could provide complete desorption of all analytes from the coating. Evaluation of carryover as the second desorption step for 60 min using acetonitrile:water 1:1 (v/v) showed that the amount of analytes remained on the coating after first desorption was negligible (less than 3%). Thus, 1 mL acetonitrile:water 1:1 (v/v) for 60 min was used as the optimized desorption solvent and desorption time for the entire study.

2.3.2.5 Reusability and reproducibility of SilmC$_{18}$-PAN coating

Performance of the SiImC$_{18}$ coatings was evaluated through assessment of physical stability and extraction recovery of aminoacids from tartaric buffer (pH=5.0) and grape pulp under optimized conditions for 4 sets of coated blades each with 12 coatings. In the case of tartaric buffer, the extraction efficiency dropped after 50 times extraction; in the case of grape sample the extraction efficiency dropped approximately 30% for all analytes after 20 times extraction. The results of the evaluation of reusability and physical stability of the new coating for extraction from tartaric buffer (pH=5.0) and grape pulp are shown in Figures 2.12 and 2.13 respectively. This study demonstrated that the washing step after the extraction from complex real sample is needed to increase the coating stability. Because of the complexity of matrix, some physical changes were observed on the surface of coatings after increasing the number of extractions. It seems that lower stability of coating by repetition in the case of extraction from grape pulp matrix is because of adsorption of particulates to the unreacted silanol sites of the synthesized compound.

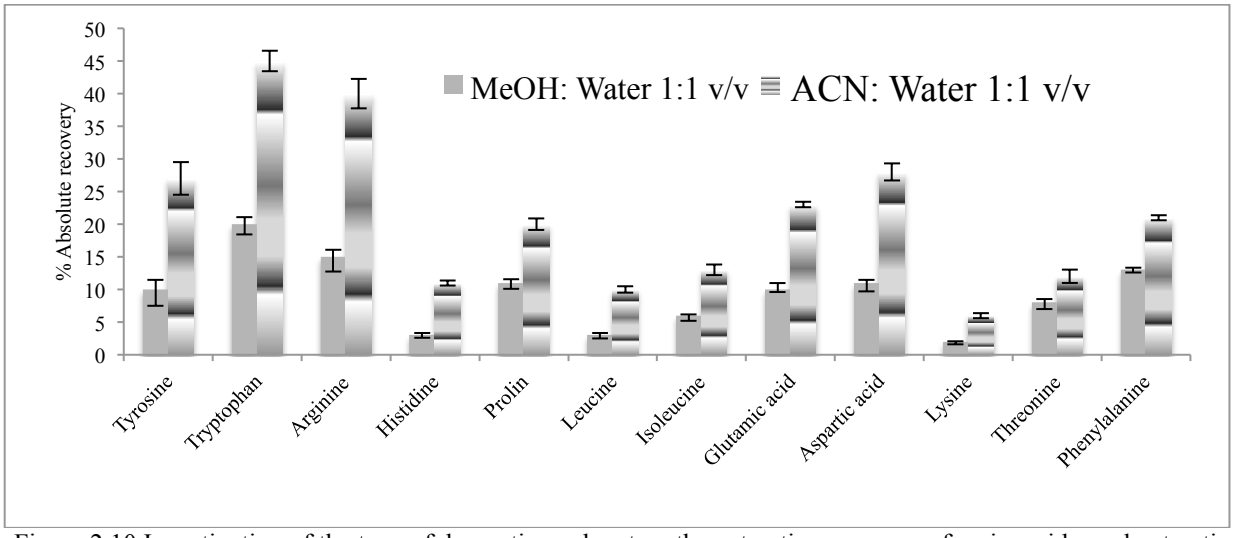

Figure 2.10 Investigation of the type of desorption solvent on the extraction recovery of aminoacids, and extraction from 100 ppb of aminoacids in tartaric buffer (pH=5.0).

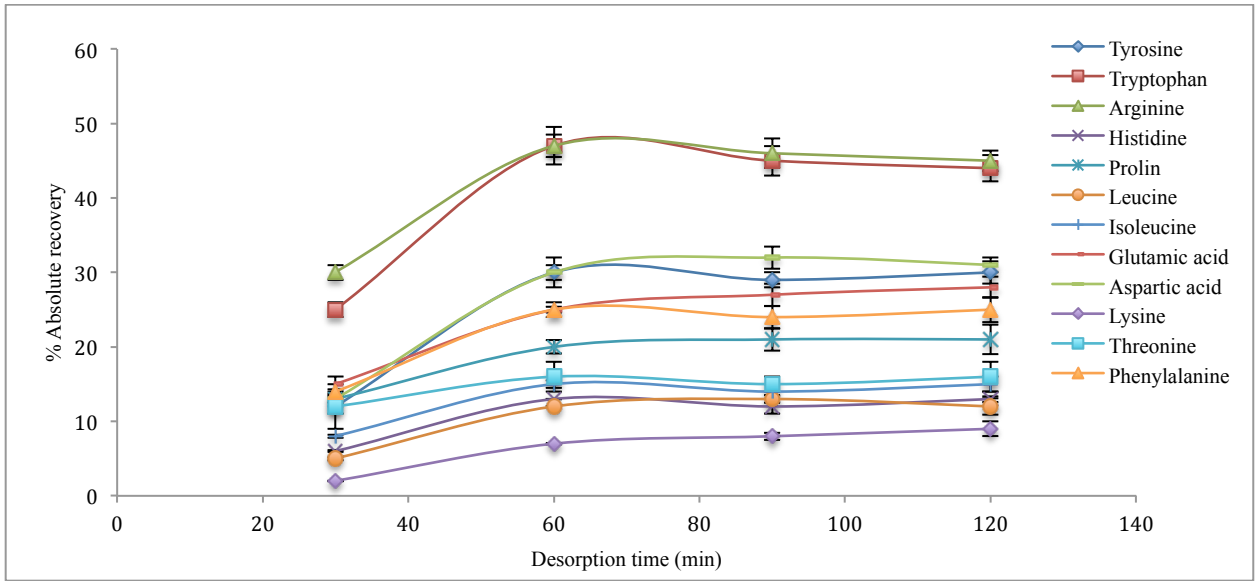

Figure 2.11 Desorption time profile for understudied aminoacids, extraction from 100 ppb of aminoacids in tartaric buffer (pH=5.0)

2.3.3 Silica based ionic liquid 96-blade SPME-LC-MS/MS method validation

Evaluation of figures of merit was performed to ensure data quality and reliability. The linear range, limit of detection (LOD) and limit of quantitation (LOQ) were investigated for the extraction from tartaric buffer (pH=5.0) and grape matrix with the developed SiIL coating. The linear calibration model was achieved by performing least square regression of the instrument response versus the concentration of analytes. The range of linearity, linear regression coefficient (R^2), LOD and LOQ for SPME-LC/MS/MS analysis of all amino acids from tartaric buffer (pH=5.0) and grape pulp are presented in Table 2.3. A signal-to-noise ratio (S/N) of three is generally accepted for estimating LOD and signal-to-noise ratio of ten is used for estimating LOQ. The obtained LOD and LOQ levels for tartaric buffer ranged from 0.1-0.5 µg/L and 0.3-1.0 µg/L, respectively; and in the case of grape pulp, LOD and LOQ levels were 0.3-2.0 µg/L and 0.5-3.0 µg/L, respectively. In addition, R^2 values were found in the range of 0.9901-0.9962 for the understudied analytes with the linearity in the concentration ranges of 1.0-200 µg/L for arginine, aspartic acid, lysine, and tyrosine, 0.5-200 µg/L for phenylalanine and tryptophan, 1.5-200 µg/L for glutamic acid, histidine, isoleucine, leucine, and threonine, and 3.0-200 µg/L for proline in the case of extraction from tartaric buffer, and in the case of extraction from grape pulp, linearity was in the ranges of 1.0-150 µg/L for arginine, aspartic acid and lysine, and tyrosine, 0.5-150 µg/L for phenylalanine and tryptophan, 1.5-150 µg/L for glutamic acid, histidine, isoleucine, leucine and threonine, and 3.0-150 µg/L for proline. The new developed SPME-LC-MS/MS showed high sensitivity and reproducibility for grape analysis.

2.3.4 Evaluation of matrix effect

Co-elution of sample matrix can decrease or increase ionization efficiency of analytes. Reduction or elimination of matrix effects is possible through optimization of chromatographic conditions and use of suitable sample clean-up prior to injection to LC-MS/MS regarding the type of matrix. In the present study, using a biocompatible SPME coating and wash step after extraction provide selective extraction and improved clean-up of the sample which prevented introduction of polysaccharides, proteins, and other interferences to analytical instrument. Furthermore, standard addition calibration was used for compensating any possible matrix effects. The new proposed SPME coating was capable of extracting polar analytes from complex matrix with the cleaner final extraction in comparison to extraction obtained by SE. To evaluate absolute matrix effect for SPME, the signals obtained for the post extraction of tartaric buffer extract spiked with the analytes (S_A) were compared with those of the standard with the same concentration (S_B) using ($S_A/S_B \times 100\%$). A percentage of absolute matrix effect between 80-120% is acceptable; however, the higher amount shows ion enhancement, and the lower amount indicates ion suppression [206]. As there is no blank grape matrix for the absolute matrix effect evaluation, tartaric buffer was used as the blank solution. Table 2.4 displays the results related to this study. No significant matrix effect (ion suppression/ion enhancement) was detected for the analysis of amino acids from tartaric buffer in this work. In the case of real sample analysis, sample extract dilution was done for both extracts obtained from SPME and SE. The final sample extract for both SPME and SE were diluted with different dilution factors. Comparison between results demonstrated that in the case of SPME, there was no need for extra dilution of sample extract; however, the extract of SE needed high dilution levels to reduce matrix effect (ion suppression/ ion enhancement) of amino acids. The obtained results showed presence of interferences in the sample extract and inefficient separation of analytes from sample matrix in the case of SE in compared with SPME. However, using biocompatible coating and removal of interferences during wash step helped decrease of matrix effect occurrence for SPME.

Table 2.2 $SiImC_{18}$ –PAN coating parameters, %AER (absolute extraction recovery), % inter- intra-blade RSD in tartaric buffer and grape pulp matrixes.

Analyte	LogP	V_f (mL)	K_{fs}	K_{fs}. V_f (mL)	% AER	Tartaric buffer % intra-blade RSD (n=12)	Tartaric buffer % inter-blade RSD (n=4)	Grape pulp % intra-blade RSD (n=12)	Grape pulp % inter-blade RSD (n=4)
Arginine	-4.20	2.6×10^{-3}	381	1.00	50	4	9	6	8
Aspartic acid	-3.89	2.6×10^{-3}	42	0.11	10	5	8	8	8
Glutamic acid	-3.83	2.6×10^{-3}	33	0.09	8	4	7	7	9
Histidine	-3.32	2.6×10^{-3}	57	0.15	13	10	13	12	14
Isoleucine	-1.59	2.6×10^{-3}	67	017	15	6	11	9	10
Luecine	-1.52	2.6×10^{-3}	52	0.14	12	7	10	13	13
Lysine	-2.99	2.6×10^{-3}	29	0.08	7	5	7	6	7
Phenylalanine	-1.38	2.6×10^{-3}	127	0.33	25	4	8	8	10
Proline	-2.15	2.6×10^{-3}	96	0.25	20	7	10	10	12
Threonine	-2.94	2.6×10^{-3}	73	0.19	16	10	12	10	14
Tryptophan	-1.06	2.6×10^{-3}	338	0.88	47	4	8	8	10
Tyrosine	-2.26	2.6×10^{-3}	163	0.42	30	4	12	9	11

2.3.5 Quantitation of amino acid compounds in grape samples

Standard addition was used for quantitative analysis of amino acids applied to 9 different concentration points. To achieve better precision, each point was done three times. Plots of response of instrument to concentration for each analyte were investigated, and by the extrapolation of the response to zero, the original concentration of analytes in the sample can be obtained. Before LC-MS/MS analysis, final extracts were diluted whenever needed to fit the response of instrument in the linear range of calibration curves and prevention of matrix effect. Table 2.5 displays presented amount of amino acids in grape pulp sample through SPME-LC-MS/MS and SE-LC-MS/MS analysis. In some cases, the results are matched in respect to the standard deviation ranges; however, in most cases, the obtained results for SE are higher than those of SPME. The reason for this observation is discussed in the following paragraph. SPME can provide free and active concentration of analytes; on the other hand, SE is an exhaustive method able to extract total concentration of analytes. The understudied analytes have some bindings towards macromolecules such as proteins and polysaccharides in grape matrix, which could be released under severe conditions of using acidic or basic conditions. In the case of SE, grape sample and all concentration points of standard addition calibration were centrifuged (5000 rpm for 10 min). Thus, the bonded fraction of analytes in the sample was precipitated. In this case, free amount of analytes in the supernatant could be separated by SE, and after required dilution to fit the linear response of instrument also prevention of matrix effect be injected to LC–MS/MS for analysis. The extract obtained from SE was not as clean as desorbed solution of SPME, which indicates the stronger capability of SPME to produce cleaner sample extract. Otherwise, in some cases, the extracted amount obtained by SE was higher than that of obtained by SPME, which is probably due to the presence of a part of the bounded analytes as there were some tiny colorful particulates, which could be seen in the supernatant and final extract used for analysis; also, high matrix effect was resulted in the case of SE compared to SPME. In fruit samples, there are interactions and bindings between the analytes and macromolecules and particulates of the sample matrix. These adsorption and conjugation of analytes is variable for different analytes based on different binding sites and analyte interaction with the matrix surfaces. SPME can extract the free concentration of analytes in the sample matrix. In order to extract the total (free and unbound) concentration of analytes, it is needed for enzymatic, acidic or basic hydrolysis to release the binding part of analytes before extraction.

Table 2.3 Figure of merits evaluation for the SiImC$_{18}$–PAN SPME-LC-MS/MS.

	Tartaric buffer				Grape pulp			
Analyte	LOD (µg/L)	LOQ (µg/L)	R^2	Linear range (µg/L)	LOD (µgL)	LOQ (µg/L)	R^2	Linear range (µg/L)
Arginine	0.1	0.3	0.9911	1.0-200	0.3	1.0	0.9924	1.0-150
Aspartic acid	0.1	0.3	0.9907	1.0-200	0.3	1.0	0.9907	1.0-150
Glutamic acid	0.2	0.7	0.9932	1.5-200	0.4	1.5	0.9912	1.5-150
Histidine	0.1	0.3	0.9946	1.5-200	0.4	1.5	0.9961	1.5-150
Isoleucine	0.2	0.7	0.9953	1.5-200	0.4	1.5	0.9933	1.5-150
Leucine	0.2	0.7	0.9918	1.5-200	0.4	1.5	0.9902	1.5-150
Lysine	0.1	0.3	0.9910	1.0-200	0.3	1.0	0.9905	1.0-150
Phenylalanine	0.1	0.3	0.9913	0.5-200	0.1	0.5	0.9915	0.5-150
Proline	0.5	2.0	0.9962	3.0-200	1.0	3.0	0.9913	3.0-150
Threonine	0.3	1.0	0.9953	1.5-200	0.5	1.5	0.9932	1.5-150
Tryptophan	0.1	0.3	0.9942	0.5-200	0.1	0.5	0.9901	0.5-150
Tyrosine	0.1	0.3	0.9948	1.0-200	0.3	1.0	0.9921	1.0-150

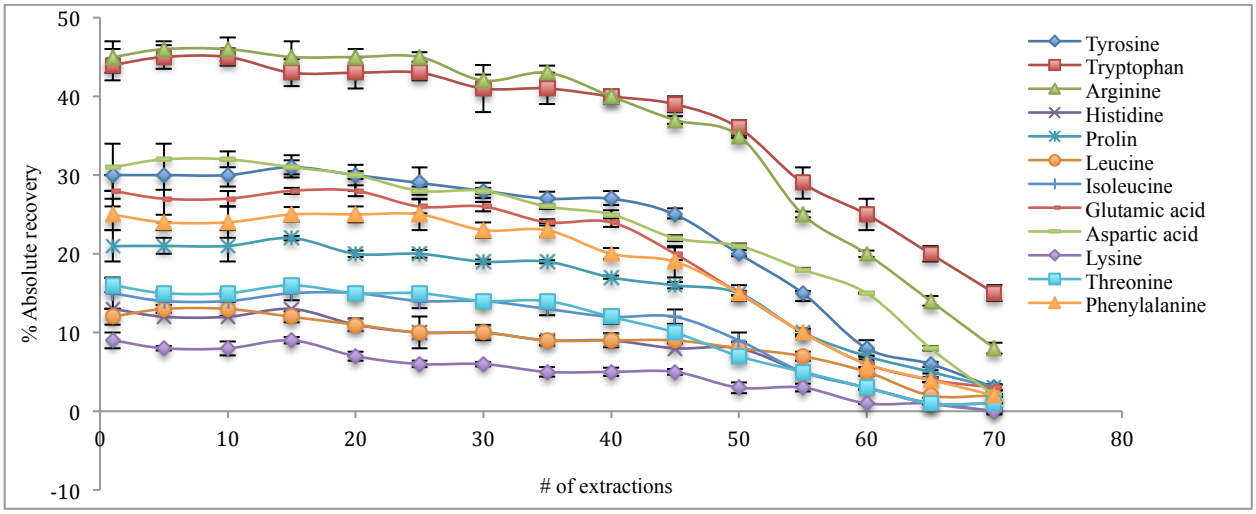

Figure 2.12 Evaluation of reusability of SiImC$_{18}$-PAN, and extraction from 100 ppb of amino acids in tartaric buffer (pH=5.0).

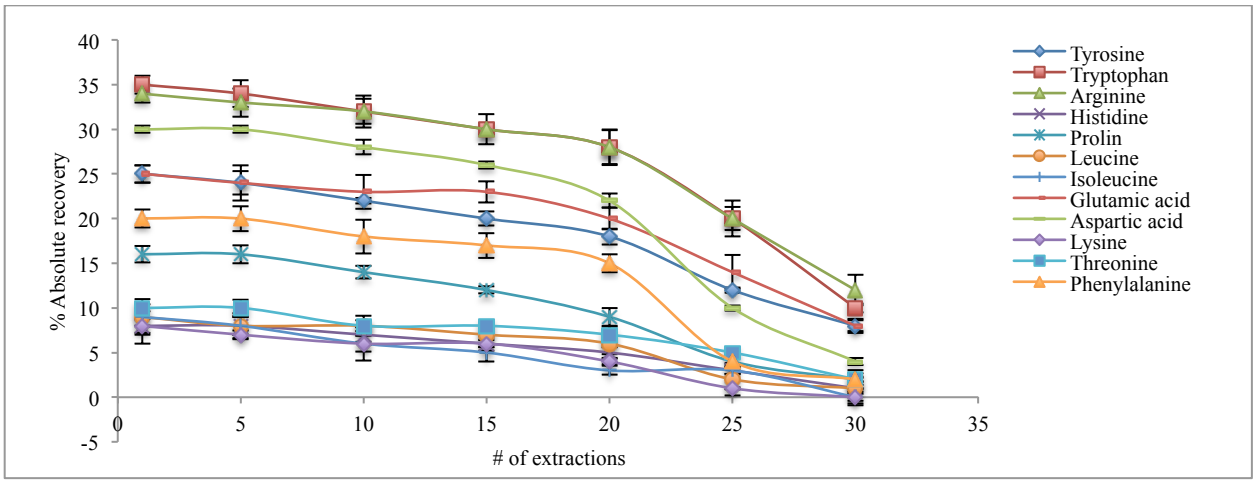

Figure 2.13 Evaluation of reusability of SiImC$_{18}$-PAN, and extraction from 100 ppb of amino acids in grape pulp (pH=5.0).

Table 2.4 Evaluation of % absolute matrix effect

Analyte	% Absolute matrix effect (±SD)
Arginine	115 (±4)
Aspartic acid	100 (±8)
Glutamic acid	81(±2)
Histidine	83 (±6)
Isoleucine	101 (±7)
Leucine	102 (±7)
Lysine	105 (±10)
Phenylalanine	106(±9)
Proline	89 (±6)
Threonine	99 (±8)
Tryptophan	117 (±4)
Tyrosine	85 (±7)

Table 2.5 Concentrations of aminoacids using SPME (standard addition calibration method) and the comparison with that of solvent extraction

Analyte	Concentration with SPME µg/g (±SD)	Concentration with SE µg/g (±SD)
Arginine	18 (±2)	42 (±8)
Aspartic acid	19 (±1)	25 (±2)
Glutamic acid	25 (±1)	77 (±8)
Histidine	41 (±3)	62 (±7)
Isoleucine	18 (±2)	22 (±4)
Leucine	20 (±3)	23 (±5)
Lysine	87 (±10)	127 (±13)
Phenylalanine	15 (±1)	61 (±7)
Proline	13 (±1)	61 (±5)
Threonine	24 (±4)	31 (±3)
Tryptophan	13 (±1)	44 (±5)
Tyrosine	28 (±2)	43 (±3)

2.4 Conclusions and future directions

One of the challenges SPME faced with is the lack of potential extractive phase for extraction of high polar compounds from complex matrixes. The current work introduces a new type of polymer as an extraction phase for 96-blade thin film SPME providing hydrophobic, π-π, electrostatic, hydrogen bonding and ion dipole interactions. Precursor selection during synthesis can determine the type of interaction between analytes and metabolites under study. The new developed coating was successfully used for the direct analysis of amino acids in grape pulp with significant reduced matrix effect compared to solvent extraction. Silica based ionic liquid is a promising coating for extraction of polar amino acids, sugars, vitamins and other polar compounds. Moreover, the application of $SiImC_{18}$–PAN 96-blade SPME system provides high throughput analysis of up to 96 samples simultaneously without any extra needs to sample pretreatment. Consequently, this system could be applicable for the highly automated analysis of unprocessed samples in the areas of food, biological, pharmaceutical, environmental, clinical and metabolomics studies through changing functional groups in synthesized silica based ionic liquid polymers.

Chapter 3

Development of high throughput 96-blade Solid Phase Microextraction-Liquid Chromatrography-Mass Spectrometry protocol for metabolomics

3.1 Preamble and introduction

3.1.1 Preamble

This chapter has been published as a paper: Fatemeh Mousavi, Barbara Bojko Janusz Pawliszyn, Development of high throughput 96-blade solid phase microextraction-liquid chromatrography-mass spectrometry protocol for metabolomics, Journal of **Analytica Chimica Acta, In press**. (doi:10.1016/j.aca.2015.08.016). The materials of the current chapter are reprinted from this publication with the permission of Elsevier (Copyright Elsevier 2015). All of the work reported within this chapter has been performed by the author. Co-author Barbara Bojko provided comments on the manuscript.

I, Barbara Bojko, authorize Fatemeh Mousavi to use the material for her thesis.

3.1.2 Introduction

Metabolomics is the comprehensive measurement of the end products of biological mechanisms at the cellular level [207]. Quenching, metabolite extraction, instrumental analysis of extracted metabolites, statistical analysis, and data interpretation are different steps often applied in untargeted metabolomics. Currently, no single method is able to detect a whole metabolome, as metabolomes are comprised of a wide variety of metabolites with various chemistries, polarities, solubilities, and chemical stabilities, as well as with differing ranges of concentration [208,209].

One of the most important analytical methods widely used in metabolomics is LC-MS equipped with an electrospray ionization (ESI) mode. Previously, different LC columns were used for separation of metabolites extracted from bacteria, with results indicating the need for both RP and HILIC columns to separate a wide range of metabolites [207-213]. One of the probable issues in LC-MS analysis is change in the signal intensity of the metabolites in the presence of complex matrix because of ionization enhancement or ionization suppression called matrix effect. Choice of sample preparation and chromatographic separation before ESI-MS plays an important role in matrix effect reduction resulting in more reliable outcomes [207].

Investigations of different methods have shown that the method of sampling and sample preparation can affect the metabolic profile of a system under study [214]. As such, an ideal sample preparation technique for metabolomics should be nonselective, reproducible, nondestructive, and provides extraction of a wide variety of metabolites without metabolite loss, degradation, or transformation and integrated well with metabolism quenching step [215]. In metabolomics, quenching is applied to inactivate the metabolism and preserve sample integrity through rapid interruption of enzymes. This is accomplished by modifying sample conditions such as its pH or temperature [216]. Cold methanol, liquid nitrogen (-196°C), as well as acidic and alkali solvents have been commonly used for quenching, causing metabolite and enzyme leakages through the cellular membrane and reduced recoveries [217-219]. An extraction step, often used in metabolome workflows, should provide efficient separation of metabolites from interferences such as salts and proteins, thus making the extract compatible and representative of the sample prior to introduction to appropriate analytical instrument. In most cases, solvent extraction is used at very low or high temperatures, although changes in temperature result in significant drawbacks, especially for unstable metabolites [159,211,220]. There is a need for a sample preparation technique that provides efficient separation of broad range of metabolites from interfering matrix components, thus facilitating good chromatographic resolution and mass spectrometric quantification and identification.

SPME, a solventless extraction technique frequently used in a wide range of applications including on site sampling and *in vivo* analysis, was recently applied for global metabolomics studies [142,143,159,166]. Using SPME eliminates the need for a separate quenching step, as only small molecular weight species are extracted by the coating. Bio-macromolecules such as proteins including enzymes, which could cause course conversion of metabolites, are separated from remaining metabolites in the matrix. Therefore there is no need for further sample pretreatment to eliminate their activity. In essence the extraction into sorbent eliminates need for several steps used in traditional procedures such as quenching, clean up and pre-concentration steps. In comparison to traditional extraction techniques, SPME provides much cleaner sample extract thus decreasing matrix effect [159].

A few studies have used SPME coupled with GC-MS to study bacteria metabolomics; however, to the authors' best knowledge, bacterial metabolomics by SPME-LC-MS has not been explored to date. Hossain et al. applied automated headspace solid phase microextraction (HS-SPME) for quantitative and semi-quantitative analysis of *E.coli* affected by cinnamaldehyde as an antibacterial agent [166]. In other work, Bean et al. used SPME in combination with GC×GC-TOFMS to identify volatile metabolites in the HS of *Pseudomonas aeruginosa* PA14 [221]. These methods are able to cover compounds characterized by high Henry constant, but a comprehensive LC-MS method is needed to cover determination of widest range of chemical property compounds.

In the present study, the development of a high throughput 96-blade SPME-LC-MS approach for *in vivo* global metabolic profiling of *E.coli* as a model organism was evaluated. At first, nine different types of polymer and silica-based particles were evaluated for targeted metabolomics. Then, the ones showing high stability and reusability, and uppermost extraction recovery, for both polar and nonpolar metabolites were applied to *in vivo* determination. SPME method optimization was performed considering efficient enrichment of extracted metabolites into different coatings. The isolated bacterial metabolites were characterized using three different chromatographic columns. Finally, the optimum protocol providing the identification of a maximum number of metabolites with highest peak intensity was determined. Also, the stability test was performed to determine how long coatings could be stored after *in vivo* sampling in addition to matrix effect investigations to propose the optimum protocol. Previously, Vuckovic et al. [28] evaluated number of biocompatible SPME coatings for untargeted metabolomics profiling of metabolites with a wide range of polarities in biological fluids by LC-MS. The current study provided a wider polarity range with higher sensitivity due to the higher amount of sorbent in the 96-blade system in comparison to the previously utilized commercially available SPME fibers. Moreover, concept 96 autosampler provided advantages such as reduced analysis time, sample high-throughput, and good reproducibility.

3.2 Experimental section

3.2.1 Chemical and materials

LC-MS grade solvents and LC-MS grade formic acid (1 mL glass ampules) were obtained from Fisher Scientific (Ottawa, Canada). N,N-dimethylformamide (DMF) was purchased from Caledon Labs (Georgetown, Canada). Polypropylenes deep 96-well plates (Nunc) and easily modified polystyrene–divinylbenzene (Macherey-Nagel) particles were purchased from VWR International (Mississauga, Canada). Phenylboronic acid particles were purchased from Varian Inc. Discovery silica-based-C18 particles, silica-based weak cation exchange, and Diol bonded silica particles were obtained from Supelco (PA), and StrataX was provided by Phenomenex. All metabolites, peptone, yeast extract, and NaCl were purchased from Sigma–Aldrich. The *E. coli* BL21 was obtained from Professor John Brennan's lab at McMaster University (Hamilton, Ontario, Canada) as a gift. The Concept 96-SPME-blade unit and robotic Concept 96 autosampler were purchased from Professional Analytical Systems (PAS) Technology (Magdala, Germany) for SPME sample preparation.

3.2.2 Bacterial strain and culture condition

E.coli BL21 was used as non-pathogenic bacteria for a microbial metabolomics study in the present work. Standard Luria Bertani (LB) media (10 g trypton, 5 g yeast extract, and 5 g NaCl in 1 L nanopure water) was used as the media for growth of bacteria, and LB agar media (10 g trypton, 5 g yeast extract, and 5 g

NaCl; 15 g Agar in 1 L nanopure water) was used to count the number of colony forming units per mL (CFU mL^{-1}) in bacterial suspensions. Cells were grown in nutrient media at 37°C and 125 rpm for 24 hours. To provide the countable number of colonies on the agar media, cultures were serially diluted with sterile media. Next, 100 µL of diluted media were distributed on the warm agar plate, and incubated at 37°C for 24 hours. The growth curve of *E.coli* culture was obtained by counting the CFU mL^{-1} from the first moment of adding bacteria to the LB media up until 18 hours. Sampling of the whole study with all coatings were conducted from a culture containing 2×10^5 CFU mL^{-1} at the stationary phase of bacterial growth (after 14 hours incubation).

3.2.3 Coating preparation

The main objective of this research was the development of a coating for the 96-blade SPME system with thin film geometry that provided the best coverage for a wide variety of metabolites. For this purpose, different polymer chemistries were selected for testing. These include the commercially available SPE particles: C18, polystyrene-divinylbenzene-weak anion exchange (PS-DVB-WAX), hydrophilic-lipophilic balance (HLB), phenylboronic acid (PBA), silica based-reversed phase-weak cation exchange (Si-RP-WCX), surface modified styrene divinylbenzene with pyrrolidone group (StrataX), as well as the lab made silica based ionic liquid (Si-IL), and tris-amide functionalized porous silica (HILIC) particles. All particles were immobilized on the stainless steel blade surfaces of the 96-blade system by spraying method, using polyacrylonitrile as a biocompatible binder. All coatings were prepared with approximately the same thickness (120 µm). Both the coating preparation procedure, as well as information pertaining to the 96-blade SPME system, have been reported in previous works [138,139,222]. In brief, polymer particles (20% of total volume) were added in 10% w/w PAN in DMF (heated in the oven at 90°C for 60 min) solution. A flask type sprayed was used for spraying the slurry on the thin film steel surface using nitrogen gas flow. After spraying, in the case of each layer the coatings were immediately cured in the oven at 150°C for 5 min. This process was continued until reaching an appropriate thickness and robustness. In the current study, the new coatings were prepared by mixing various particles with different weight ratios (PS-DVB-WAX:HLB 50:50 [w/w], PS-DVB-WAX:HLB 80:20 [w/w], PS-DVB-WAX:Si-IL 80:20 [w/w]) to determine the interaction effect of multi-particle coatings on metabolome coverage. Figure 3.1 shows the structure of the particles used as stationary phases for the 96-blade SPME system.

3.2.4 Preparation of targeted metabolites mixtures

A SPME sample preparation method using different commercially available SPE particles and lab made polymers was developed for extraction of different classes of targeted metabolites having various

chemical properties, such as: amino acids (tyrosine, valine, asparagine, histidine, arginine, isoleucine, citrulline, cysthationine, S-adenosyl-L-methionine, and taurine); nucleotides (adenosine, cytidine); vitamins (nicotinamide and riboflavin); carboxylic acids (citric acid and Fumaric acid); carbohydrates (allantion, D-ribose-5-phosphate, and D-glucose-6-phosphate); redox-electron carries and precursors (FAD and NAD); nucleosides phosphates (CMP, AMP, dUMP, and ADP), and CoA's (CoA hydrates). Stock standard solutions were prepared in water/methanol, stored at a temperature of -20°C, and left unexposed to the light. For instrument calibration, working standard solutions with a known concentration of metabolites were prepared by diluting stock standards with a desorption solvent. The extraction solution was prepared by spiking the 1µg/mL stock standard solution in sterilized LB media. The concentration of organic solvents in samples was always kept at less than 1%.

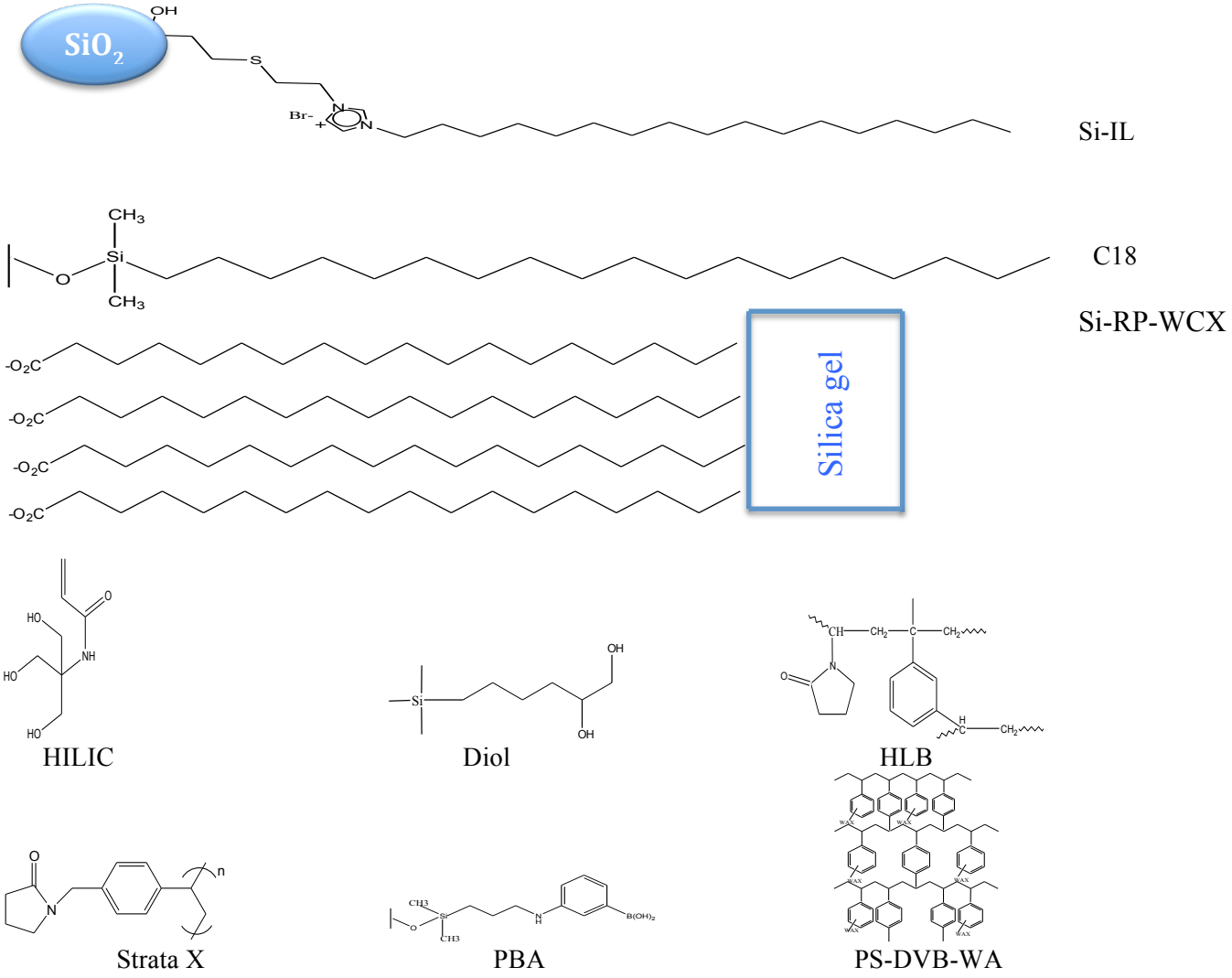

Figure 3.1 Chemical structure of evaluated particles for 96-blade system.

3.2.5 Targeted analysis using SPME-LC-MS/MS

SPME method development was conducted for different coatings by optimizing the preconditioning, extraction, washing, and desorption steps using the concept 96-blade SPME device and the robotic concept 96-autosampler. The coatings were conditioned prior to extraction for 30, 60, 90, and 120 min in 1 mL ethanol:water 70:30 (v/v) mixture in 96-well plate along with agitation at 850 rpm to prepare the surface of the coatings for extraction. After preconditioning, extractions were carried out for 30, 60, 90, and 120 min at an extraction agitation speed of 1000 rpm (2.5 mm amplitude) and direct immersion mode from 1 mL 200 mg/mL spiked metabolites in Standard Luria Bertani (LB) media to determine equilibrium time. After the extraction, coatings were washed for 10, 20, 30, 40, and 60 s in 1 mL water +0.1% formic acid under agitation at 850 rpm in order to remove particulates and salt from the surface of the coatings. The experiment was conducted without a washing step as well to evaluate the effect of using wash step after extraction. Desorption was performed in 1 mL acetonitrile:water 50:50 (v/v), acetonitrile:water 80:20 (v/v), and methanol:water 50:50 (v/v) at an optimal 1500 rpm speed for 30, 60, 90, and 120 min. Next, the desorption solution was transferred to the LC–MS/MS autoinjector for separation and quantitation. In this part of the study, chromatographic separation was performed by a Discovery HS F5 column, 150×2.1mm, 3µm particle size (Supelco, Bellefonte, PA, USA) along with Luna HILIC Si, using gradient elution. For the RP column, flow rate was 200 µL/min, and mobile phases A and B consisted of water/formic acid (99.9/0.1,v/v) and acetonitrile/formic acid (99.9/0.1,v/v), respectively. The 40 min gradient program was optimized for separation of the model compounds as follows: 100% A (0-3 min), linear gradient from 100 to 10% A (3-25 min), linear gradient held at 10% A (25-34 min), and column equilibration for 6 minutes by applying gradient 10% A to 100% A. Chromatographic conditions for the HILIC column are explained in the following section. Quantitative analyses of compounds were performed using an API 4000 triple quadrupole mass spectrometer **(**Applied Biosystems, California, USA) equipped with a TurboIonSpray source. A CTC PAL autoinjector from Leap Technologies (CTC Analytics, NC, USA) was used for the injection of samples into the LC-MS/MS system (20 µL injection volume). The MS/MS analysis was performed in positive and negative ionization modes under multiple reaction monitoring (MRM) conditions. A summary of the MS/MS parameters is presented in Tables 3.1 and 3.2.

3.2.6 Untargeted cell metabolomics analysis

The coatings that provided the highest extraction recoveries in the targeted analysis study (PS-DVB-WAX, HLB, Si-RP-WCX, PBA, and Si-IL) were applied for an untargeted *in-vivo* metabolomics study. Moreover, PS-DVB-WAX, HLB and Si-IL were mixed together with different weight ratios of individual particles to produce mixed coatings (PS-DVB-WAX:HLB 50:50 [w/w], PS-DVB-WAX:HLB 80:20

[w/w], and PS-DVB-WAX:Si-IL 80:20 [w/w]]) so as to evaluate the interaction of different particles in terms of peak intensity and metabolite coverage. Optimized conditions obtained from the targeted analysis study were applied for the untargeted microbial metabolomics study (Section S1 to Section S5). After preconditioning and sterilizing of the coatings with ethanol:water 70:30 (v/v), extraction was conducted from a 1 mL culture containing 2×10^5 colony forming units per mL (CFU mL^{-1}) of *E.coli* at stationary phase in direct immersion mode inside 96-well plate. Next, washing was conducted for 30 s with agitation to remove particulate and macromolecules from the coating surface. Then, extracted metabolites were desorbed in an optimized desorption solvent for 120 min, and the desorption solution was preserved at -80°C for LC-MS analysis using three different LC-MS methods. An LC-MS system consisting of a Thermo Accela autosampler, pumps, and an Exactive benchtop Orbitrap system (Thermo, San Jose, California, USA) was used for LC-MS analyses. The extracted analytes using the diverse aforementioned SPME coatings were analyzed by three different LC columns to ensure that all extracted analytes were retained and detected: Kinetex pentaflourophenyl (PFP), HILIC, and XBridge C18. A Kinetex PFP column [100×2.1mm, 1.7µm] (Phenomenex, Torrance, CA, USA) with a guard filter (SecurityGuard ULTRA Cartridges UHPLC PFP for 2.1 mm) was applied with a flow rate of 300 µl/min, using mobile phase A containing water: formic acid 99.9:0.1%, and mobile phase B composed of acetonitrile: formic acid 99.9:0.1%. The starting mobile phase conditions for Kinetex PFP were 90% A from 0 to 1.0 min, followed by a linear gradient to 10% A from 1.0 to 9.0 min, and an isocratic hold at 10% A until 12.0 min. The total run time was 16 min per sample, including a 4 min column re-equilibration period. A Luna HILIC Si, 100×2mm, 3µm particle size was used with a flow of 400µL/min. Mobile phase A consisted of acetonitrile/ammonium acetate buffer (9/1, v/v, effective salt concentration 20mM), and mobile phase B consisted of acetonitrile/ammonium acetate buffer (1/1, v/v, effective salt concentration 20mM). The starting mobile phase composition was 100% A held for 3.0 min, with ramp to 100% B in 5.0 min. 100% B was held for 4.0 min. The column was re-equilibrated for 8 min prior to the next injection, thus making the total run time 20 min per sample. For XBridge C18 (150×4.6 mm, 3.5µm), mobile phase A consisted of acetonitrile: water 90:10 with 15mM effective concentration of ammonium acetate, and mobile phase B consisted of 0.5% acetic acid in isopropanol with a flow rate of 200µL/min. The starting mobile phase conditions for the XBridge C18 column were 90% A from 0 to 6.0 min, followed by a linear gradient to 40% A from 6.0 to 8.0 min, then another linear gradient to 30% from 8.0 to 18.0 min, and finally a linear gradient to 90% from 18 to 18:30 min. An isocratic hold was set at 90% A until 22.0 min. The total run time was 22 min per sample. Analyses were performed in both positive and negative ESI modes for all three LC methods. The injection volume for all methods was 10 µL. Samples were stored and refrigerated (4°C) on the autosampler while waiting for injection. Samples were run in randomized order, and a QC sample was run periodically to verify instrument performance.

Table 3.1 Optimized mass spectrometry condition of investigated targeted metabolites in positive mode. Compromised ionization source values: Ion source gas 1 (GS1)= +20, curtain gas= +10, collision gas= 12, spray ionization voltage= 4500 V, and temperature= 350 °C.

Analyte	Q_1 mass (amu)	Q_3 mass (amu)	DP (V)	EP (V)	CE (V)	CXP (V)
Tyrosine	182.1	136.1	61	10	20	8
Allantion	159.0	116.1	75	8	10	20
Cytidine	244.0	112.1	56	10	17	21
Isoleucine/leucine	132.0	86.1	60	10	16	15
Riboflavin	377.2	243.0	131	10	34	24
Methionine	150.0	60.9	22	10	30	9
Taurine	147.1	60.9	81	12	15	10
Histidine	155.9	110.2	78	15	26	12
Cysteine	121.9	107.1	104	13	30	16
Arginine	175.1	70.1	59	14	36	19
Valine	117.9	72.1	65	15	17	14
Asparagine	133.0	74.0	59	10	22	14

Table 3.2 Optimized mass spectrometry condition of investigated metabolites in negative mode. Compromised ionization source values: Ion source gas 1 (GS1)= +12, Ion source gas 2 (GS2)=10 curtain gas= +10, Ion spray voltage= -4500 V, and temperature= 325 °C.

Analyte	Q_1 mass (amu)	Q_3 mass (amu)	DP (V)	EP (V)	CE (V)	CXP (V)
FAD	784.3	437.1	-111	-15	-40	-15
D-Ribose-5-Phosphate	228.9	96.9	-101	-9	-22	-6
Guanosine-5-monophosphate	361.9	79.0	-128	-5	-56	-14
Coenzyme A hydrate	356.9	79.0	-180	-9	-65	-15
Thiamine hydrate	336.9	147.0	-68	-10	-38	-11
D-Glucose-6-phosphate	258.7	96.9	-106	-10	-20	-6
Cystathionine	220.9	133.9	-92	-9	-20	-10
Biotin	243.0	166.0	-123	-10	-23	-11
Citrulline	173.9	131.0	-98	-5	-20	-9
2-deoxy-uridine-5-phosphate	306.9	79.0	-122	-10	-55	-14
D-trihalose dihydrate	376.0	341.1	-91	-10	-29	-12
Cytidine-5-monophosphate	321.9	79.0	-138	-10	-60	-14
Beta-Nicotinamide	662.1	602.1	-211	-10	-46	-10
Adenosine diphosphate	426.0	158.9	-132	-10	-35	-11
Adenosine-5-monophosphate	345.9	79.0	-135	-10	-57	-15
Fumaric acid	114.8	97.9	-74	-5	-30	-5
Citric acid	190.7	110.9	-75	-5	-27	-7

This QC sample was prepared by mixing 10 µL part of each sample as one sample. MS acquisitions were performed using AGC = balanced (1.000.000 ions), 100.000 resolution at m/z of 200, with an injection time into the C-trap of 100, and 250 ms for the two RP and HILIC methods, respectively. Sheath gas (arbitrary units), auxiliary gas (arbitrary units), ESI voltage (kV), capillary voltage (V), capillary temperature (°C), and tube lens voltage (V) were (i) 40, 25, 4.0, 27.5, 275, and 100 for positive ESI RP LC-MS; (ii) 50, 25, -2.7, -67.5, 325, and -85 for negative ESI RP LC-MS; (iii) 60, 30, 2.8, 90, 325, and 155 for positive ESI HILIC LC-MS; and (iv) 50, 25, -2.5, -55, 275, and 100 for negative ESI HILIC LC-MS. External instrument mass calibrations were performed every 24 h, and found to be within 2 ppm for all ions. Separated metabolites were analyzed using Xcalibur software version 2.1 (Thermo) by isolating the extracted ion chromatograms (XIC), using a 5 ppm window around the accurate mass of a given compound.

3.2.7 Data processing, metabolite identification, and data analysis

The raw data obtained with Xcalibur software (.raw) was converted to (mzXML) with the MS conversion software. The converted data was then processed with the XCMS R-package (Scripps Center for Metabolomics, California, USA). The output is a table containing retention time, m/z, and intensity of features [142]. Table 3.3 shows the optimum parameters used for peak detection, retention time correction, and peak alignment [223]. The CAMERA R-package (Bioconductor Version 2.10) was applied to provide ion annotation on the list of features to identify detected isotopes, adducts, and in-source fragments ions. An Exactive Orbitrap detector was used in this study, providing high mass resolution and sensitivity.

The first step of tentative identification was done by submitting the exact mass of unknown metabolites obtained from chromatograms to the METLIN database with a 5 ppm mass window. Further selection of metabolites was based on the detection of at least two adducts with the same nominal mass at given retention time; in the case of availability of authentic standard identity of the metabolite was confirmed based on comparison of accurate mass and retention time [142,223]. According to the analytical conditions, for the RP chromatographic column, polar compounds eluted at the beginning of the run, while nonpolar compounds eluted later. However, for the HILIC chromatographic column, the separation condition was reversed. Th Log P of the metabolites and the retention times of the peaks were also taken into account in order to minimize false positive identifications of the compounds when no authentic standard was available. SIMCA-P+ software v.13.0.3 (Umetrics, NJ, USA) was used for statistical analyses. Principle component analysis (PCA) and partial least square-discriminant analysis (PLS-DA) were used to assess the performance of different coating chemistries as the stationary phases for the 96-

blade SPME system through the identification of the metabolites impacted and the discrimination of the metabolomics patterns of *E.coli*.

Table 3.3 Parameters settings used for data processing with XCMS R-package

Method	p.p.m	Peak width	Bw	mzwid	Prefilter
Kinetex PFP-Orbitrap	2.5	C(5,20)	2	0.015	C(3,5000)
Luna HILIC Si-Orbitrap	2.5	C(10,60)	5	0.015	C(3,5000)
XBridge C18-Orbitrap	2.5	C(10,60)	5	0.105	C(3,5000)

3.3 Results and discussion

3.3.1 SPME method development for targeted analysis

Extraction phase optimization was performed by targeted determination of a mixture of amino acids, nucleotides, vitamins, carboxylic acids, carbohydrates, redox-electron carriers and precursors, nucleosides phosphates, and CoA's. Nine different silica and polymer-based particles with different functional groups (commercially available SPE particles and lab made synthesized polymers) were used in evaluation. Samples were extracted from LB broth (pH=6.5) spiked with known concentrations of targeted metabolites used to simulate the nutritional media for bacterial growth in the *in vivo* study. The 96-blade development of SPME microbial metabolomics methodology includes optimization of four steps: preconditioning, extraction, wash, and desorption. In such investigations important parameters related to each step were optimized for all coatings to reach the maximum extraction recovery. Prior to extraction of analytes, the surfaces of the coatings were prepared for extraction. The more hydrophilic coatings (HILIC, Diol, Si-IL, and PBA) needed a longer preconditioning time in comparison to hydrophobic sorbents. Results indicate that application of ethanol:water 70:30 (v/v) solution to the surfaces of the coatings for 120 min as a preconditioning step prepared the coatings for extraction better than preconditioning with lower preconditioning times, or merely applying the dried SPME surface directly for extraction. In addition to preconditioning, ethanol also served to sterilize the surface of the coatings. The evaluation of the extraction time profiles for the targeted analytes showed that 120 min extraction of targeted metabolites from LB broth at 1000 rpm reached sorption equilibrium for all analytes. Optimization of the washing step after the extraction step is important for removal of salts, large macromolecules, and other particulates; this produces a cleaner extract and reduces matrix effects related to ion suppression or ion enhancement, as well as extending the reusability of the coating. Results showed that washing the coating surfaces for 30 s with water + 0.1% formic acid accompanied by agitation directly after extraction decreased matrix effects; however, it should be noted that the wash time period needs to be limited, as increasing the wash time by more than 30 s may cause a significant loss of polar analytes. When washing times were kept at 30 s, metabolite losses were kept at below 20% within three replicates for the most polar analytes for all coatings. Percentage of wash loss during 30 s wash step using

PS-DVB-WAX:HLB 50:50 [w:w] coupled to Kinetex PFP column is visualized in Figure 3.2. After the wash step, extracted metabolites were desorbed through immersion of the coatings in a desorption solvent. Desorption solvents and desorption times were optimized for different 96-blade SPME coatings. The desorption solution was chosen to perform well in desorption and dissolution of both extracted polar and nonpolar metabolites as well as to be compatible with RP and HILIC columns. The obtained results showed that a combination of acetonitrile:water 50:50 (v/v) at 1500 rpm vortex agitation for 2 hours provided the highest extraction recovery for all target compounds and coatings under study, with less than 5% carryover as demonstrating during the second desorption.

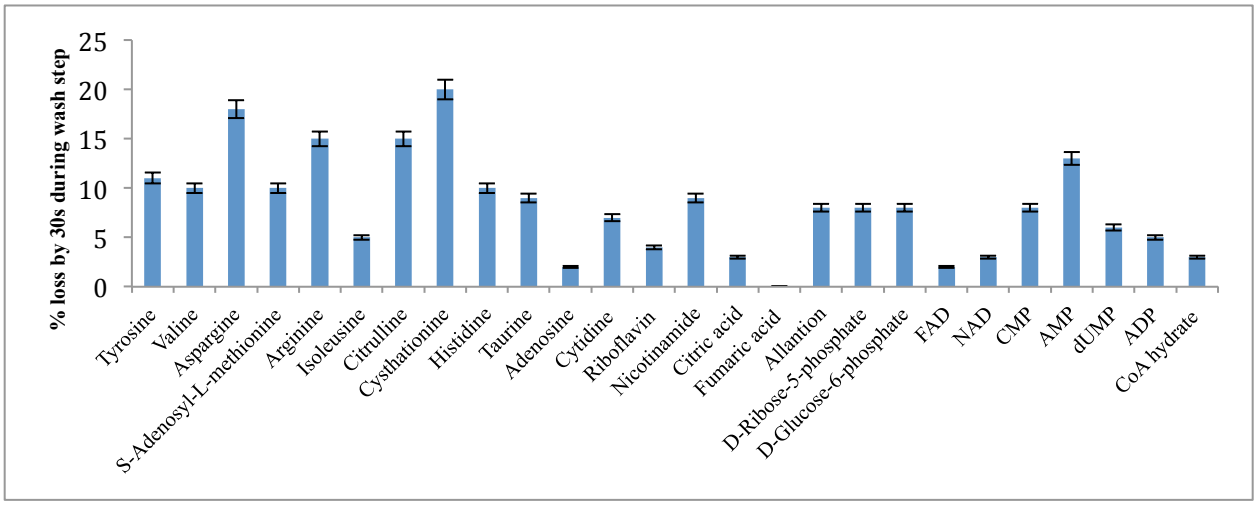

Figure 3.2 Percentage of wash loss during 30 s wash step using PS-DVB-WAX:HLB 50:50 [w:w] coupled to Kinetex PFP column.

The coatings under investigations were evaluated based on extraction recovery, stability, and reproducibility. Results demonstrated that among all nine evaluated coatings, PS-DVB-WAX, HLB, C18, Si-RP-WCX, PBA, and Si-IL had good stability, while Diol, HILIC, and strata X coatings showed very low stability; particles were detached from the surface of stainless steel blades after 10 extractions, consequently causing low reproducibility and unreliable results. Therefore, these coatings were not evaluated for further untargeted metabolomics studies. Figure 3.3 shows a comparison of percent absolute extraction recoveries (ratio of amount extracted to total spiked metabolites × 100%) of the chosen targeted metabolites from LB broth with different 96-blade SPME coatings at optimized SPME conditions for each coating. Metabolites with different polarities and functional groups were extracted with different absolute extraction recoveries using various SPME coatings. Among the mentioned coatings, C18 did not show high extraction recoveries for the polar metabolites under study, while PBA, Si-IL, Si-RP-WCX, HLB, and PS-DVB-WAX indicated high extraction recoveries. As the primary

objective of this study was to identify the coatings providing high extraction recoveries for both polar and nonpolar metabolites, C18 was eliminated from further studies. Comparison results between the absolute extraction recoveries of different coatings showed that HLB and PS-DVB-WAX yielded the highest extraction recoveries for both polar and nonpolar metabolites. HLB demonstrated higher extraction recovery for more nonpolar metabolites while PS-DVB-WAX indicated higher extraction recovery for more polar metabolites. In order to investigate interaction effect of SPME made from different stationary phases, particles were mixed together in different weight ratios, and SPME method development was done for the three developed mixed coatings: PS-DVB-WAX:HLB 50:50 [w/w], PS-DVB-WAX:HLB 80:20 [w/w], and PS-DVB-WAX:Si-IL 80:20 [w/w)].

The optimization of important parameters in SPME method development (desorption solvent type, preconditioning time, extraction time profile, and desorption time profile) for PS-DVB-WAX:HLB 50:50 [w/w] for extraction of targeted metabolites from LB broth is shown in Figure 3.4. The %RSDs for three replicates in all experiments were below 13%. Based on the obtained results, 2 hours preconditioning of the coatings in ethanol:water 70:30 (v/v) was sufficient to prepare the surface of the coating for extraction (Figure 3.4-B). Acetonitrile:water 50:50 (v/v) provided the highest absolute extraction recovery (Figure 3.4-A). As showed in Figure 3.4-C, after 2 hours of extraction, all metabolites reached equilibrium with the surface of the coatings, and a period of 120 min of desorption (Figure 3.4-D) in the acetonitrile:water 50:50 (v/v) solution was sufficient to desorb all extracted analytes with less than 3% carryover for the second desorption.

3.3.2 SPME-LC-MS method development for bacterial cell metabolomics studies

3.2.2.1 SPME method development

Eight different SPME coating chemistries (Figure 3.1) under optimized conditions obtained from targeted analysis were applied to extract metabolites from the *E.coli* metabolism life cycle from the same batch culture. Metabolite separation was achieved using three different LC columns (Kinetex PFP, HILIC, and XBridge C18) to ensure separation and detection of all metabolites extracted using different SPME coatings and evaluate the best combination of SPME-LC-MS method for detection of the highest number of metabolites. Results showed that the evaluated coatings provided extraction of different metabolites varying in chemical functional groups and polarities with different peak intensities. A metabolic profile comparison using different SPME coatings was conducted through multivariate data analysis. Clear separation in the scattered plots was observed based on thousands of extracted features separated by various stationary phases for the 96-blade system and analyzed by three different LC-MS methods. As demonstrated by Figure 3.5, there are eight groups of specific clusters related to each developed SPME coating, with three microbial replicates for each coating. Data analysis demonstrated that SPME coating

type has direct influence on metabolic profiling and metabolite recovery; extraction phases that act similarly in terms of features extracted have closer data points. Differentiation between various types of coatings is represented both by differences in number of metabolites extracted and peak intensities. Different SPME-LC-MS methods demonstrated different recovery yields for various classes of metabolites because of various functional groups in evaluated coatings. Table 3.4 demonstrated the number of extracted features by each SPME coatings coupled to different chromatographic methods.

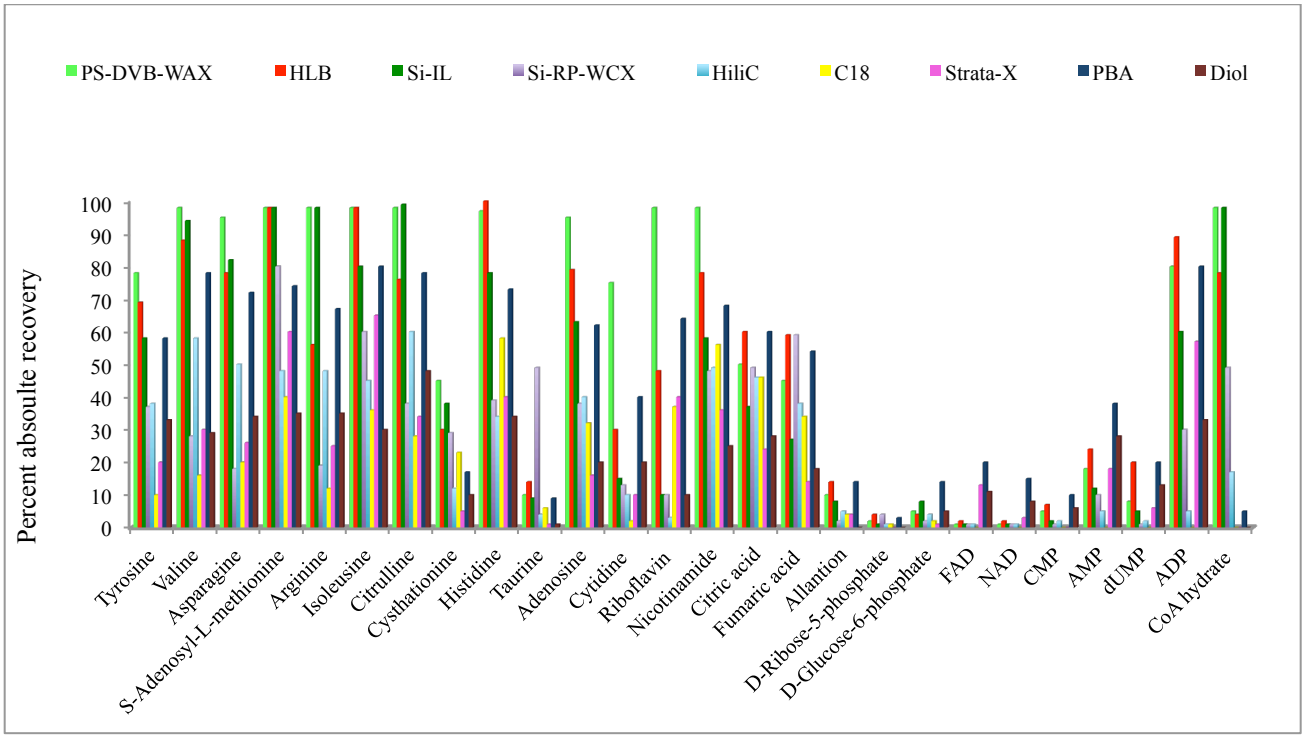

Figure 3.3 Comparison of the percent absolute recoveries of targeted metabolites for different 96-blade SPME coatings.

An evaluation of the obtained results indicated that PBA, Si-IL, and Si-RP-WCX had similar extraction behaviors, as all three coatings showed approximately the same extraction recoveries for the same class of metabolites especially polar ones; however, these three coatings did not provide high extraction recoveries for nonpolar metabolites. Polar metabolites ($-4 < \log P < 4$) such as amino acids, peptides, carboxylic acids, monosaccharides, and sugar acids were extracted better with these types of coatings, rather than hydrophobic compounds such as prenol lipids, glycerolipids, glycerophospholpids, fatty acids. The diol-containing group in PBA provided covalent bonds and better interaction with hydrophilic compounds. Si-IL synthesized in our laboratory acted as a mixed mode type of coating containing an alkyl group with an anion exchange group in its structure. The imidazolium group in this coating provided extraction of hydrophilic compounds from the sample. Carboxylic acid functional groups attached to the alkyl groups in the structure of the Si-RP-WCX coating provided extraction of polar metabolites.

Therefore, these types of coatings that are particularly suitable to extract hydrophilic metabolites are classified as polar coatings.

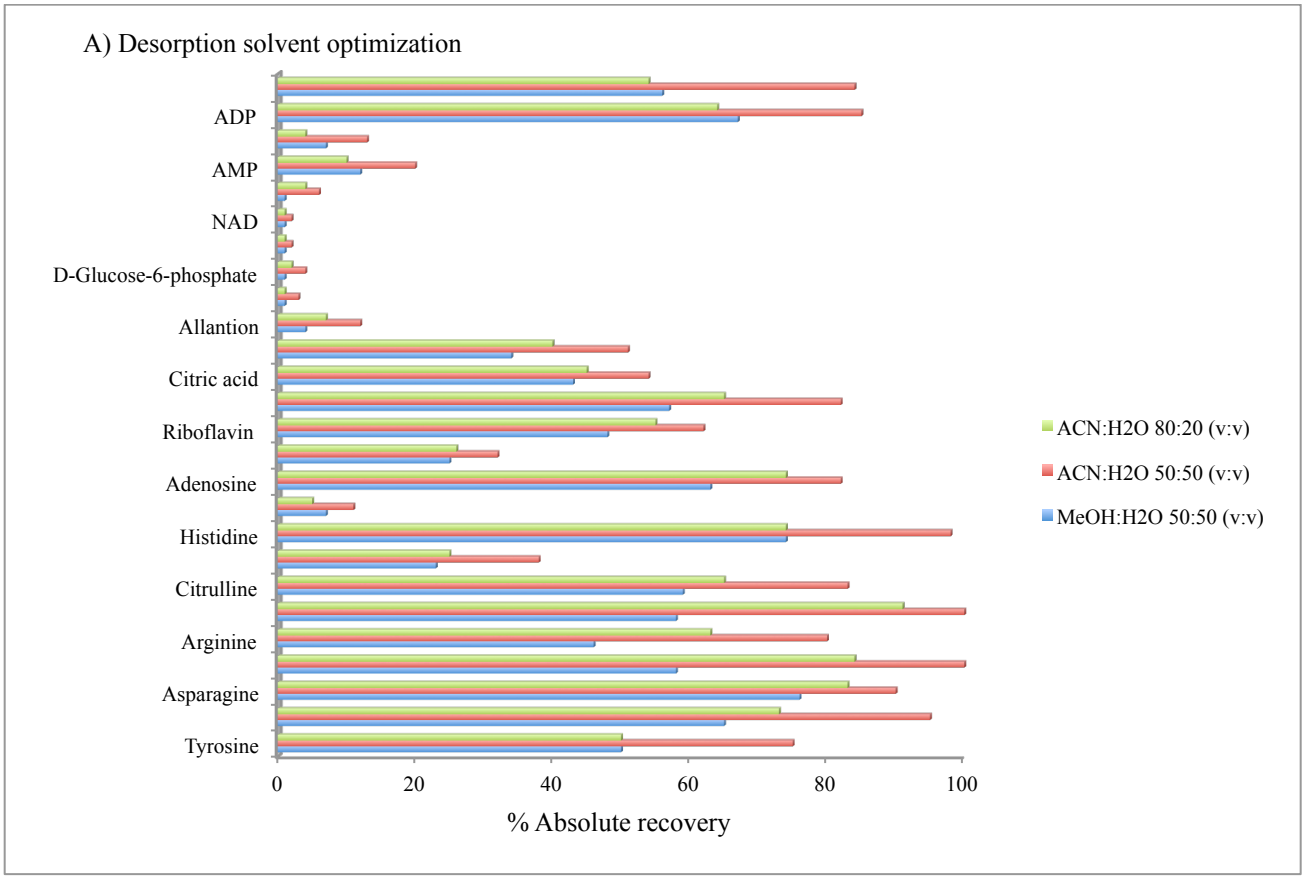

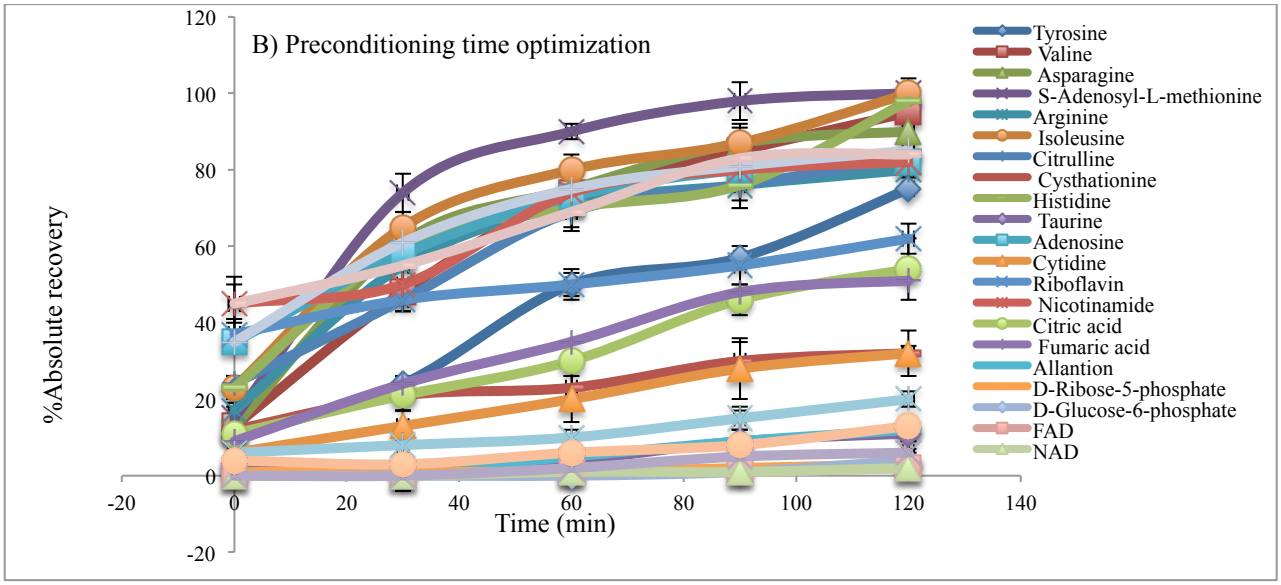

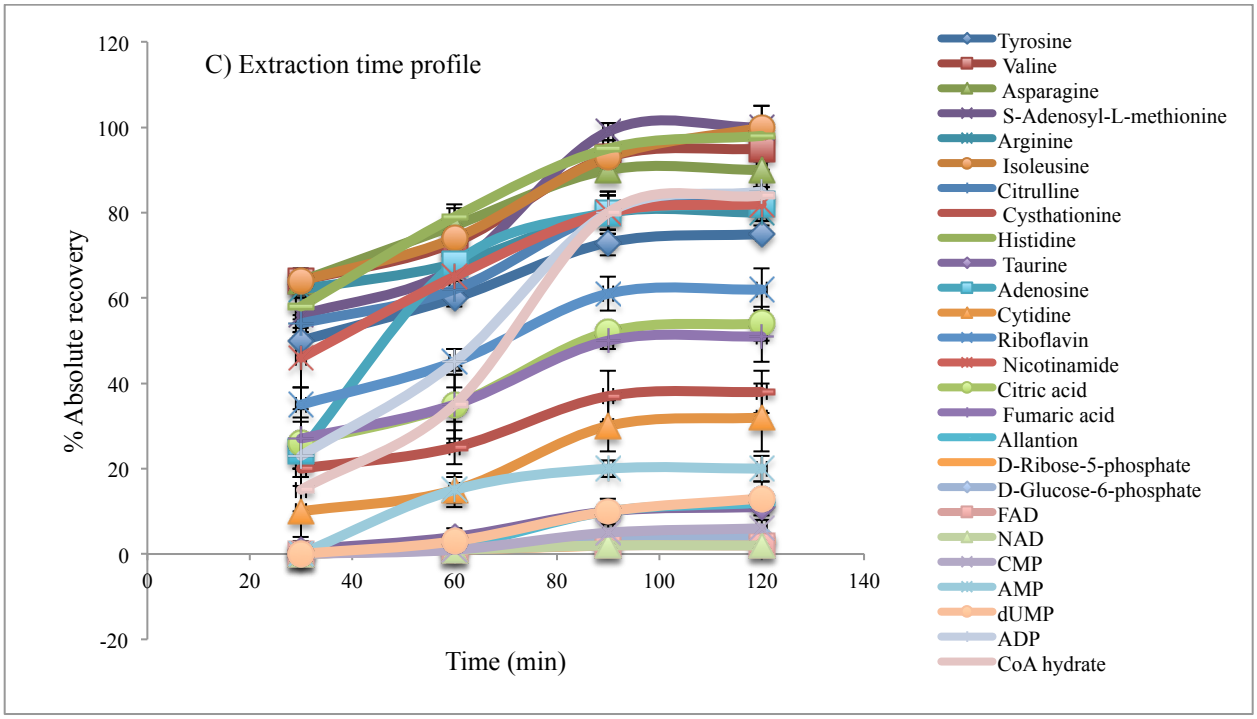

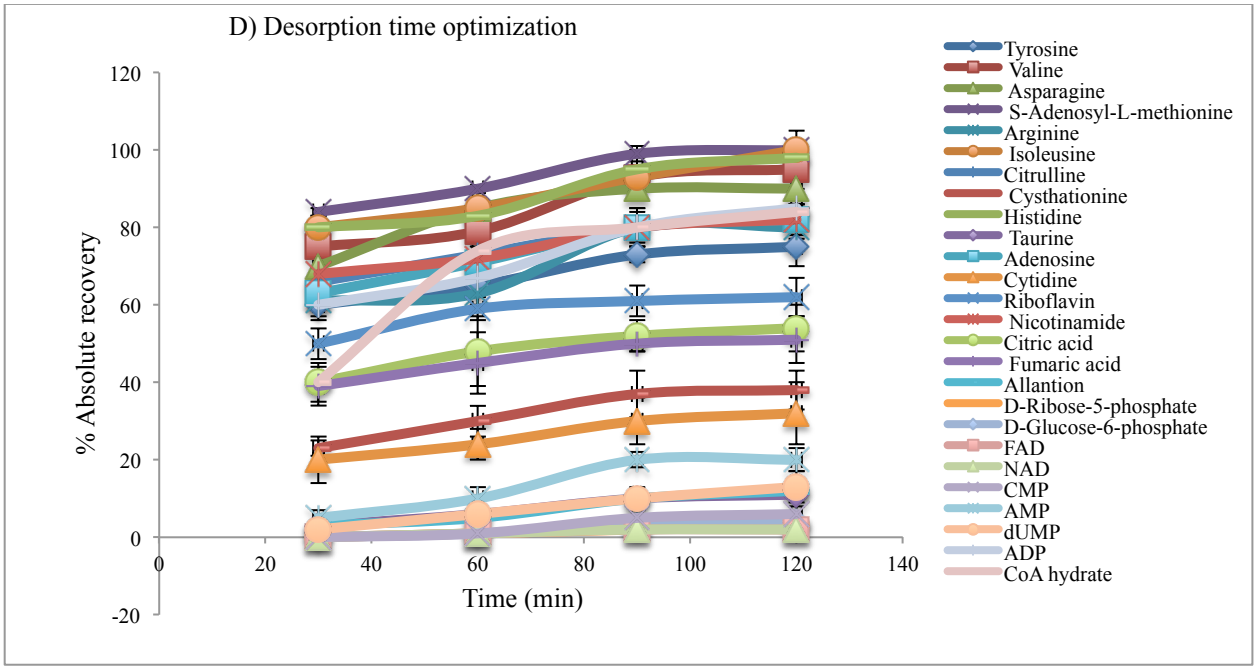

Figure 3.4 SPME method development for PS-DVB-WAX:HLB 50:50 [w:w] and Kinetex PFP column A) Desorption solvent optimization, B) Preconditioning time optimization, C) Extraction time profile, and D) Desorption time optimization.

Table 3.4 Number of features extracted by different 96-blade SPME coatings from 2×10^5 CFU/mL bacteria at stationary phase grown in LB broth and separated by three different LC columns.

LC column	Kinetex PFP	Kinetex PFP	Luna HILIC Si	Luna HILIC Si	XBridge C18	XBridge C18
Ionization mode	ESI (+)	ESI (-)	ESI (+)	ESI (-)	ESI (+)	ESI (-)
Coating	**Number of features**					
Si-IL	4003	4009	4696	1244	1837	1850
PBA	3273	3274	1633	1243	2163	1678
Si-RP-WCX	5065	5065	1684	1088	2856	2398
PS-DVB-WAX	10625	10625	2903	2285	3466	3414
HLB	10420	10420	4232	1791	3956	4204
PS-DVB-WAX:HLB 50:50 [w:w]	13205	12029	4851	2285	4583	4579
PS-DVB-WAX:HLB 80:20 [w:w]	12289	12289	5113	2630	3547	3972
PS-DVB-WAX:IL 80:20 [w:w]	8071	8019	3676	2158	4583	4854

HLB and PS-DVB-WAX demonstrated higher extraction recovery for both polar and nonpolar metabolites compared to PBA, Si-IL, and Si-RP-WCX. Polar modified PS-DVB copolymer with weak anion exchange provided high extraction efficiency for both polar and nonpolar metabolites ($-7 < \log P < 7$). The Oasis HLB particle is a macroporous copolymer made from a balanced ratio of two monomers: lipophilic divinyl benzene and hydrophilic N-vinylpyrolidone. The HLB coating was shown to exhibit mostly nonpolar characteristics ($-4 < \log P < 15$), as the results indicated that it mostly extracted nonpolar metabolites with higher peak intensity; however, this coating can also extract polar metabolites as well, but with lower extraction recoveries than that of nonpolar metabolites. On the other hand, PS-DVB-WAX yielded exactly the opposite result. This coating extracted polar metabolites with higher extraction recoveries than nonpolar metabolites. As these two coatings (HLB and PS-DVB-WAX) provided metabolite coverage for both polar and nonpolar metabolites, the 96-blade SPME coatings composed of a mixture of particles were evaluated. To investigate the effect of interaction of particles, PS-DVB-WAX:Si-IL 80:20 [w/w], PS-DVB-WAX:HLB 50:50 [w/w], and PS-DVB-WAX:HLB 80:20 [w/w] coatings were prepared. As multidimensional scaling plot demonstrated (Figure 1), adjacent clusters in PCA score plots indicated correlations and similarities between the mixed coatings (PS-DVB-WAX:Si-IL 80:20 [w/w], PS-DVB-WAX:HLB 50:50 [w/w], and PS-DVB-WAX:HLB 80:20 [w/w]) and individual coatings (PS-DVB-WAX, HLB, and Si-IL) in terms of similarities in extracted metabolites and their peak intensities. Data analysis of the obtained results from LC-MS showed that the single extraction method using PS-DVB-WAX: HLB 50:50 (w:w) coupled to different chromatographic techniques assists to provide broad metabolite coverage which develop untargeted metabolome profiling for both highly polar

and nonpolar metabolites. The degree of simultaneous extraction of both polar and nonpolar metabolites based on increasing peak intensities using various coatings is ordered as follows: PS-DVB-WAX:HLB 50:50 [w/w] > PS-DVB-WAX:HLB 80:20 [w/w] > PS-DVB-WAX:SiIL 80:20 [w/w] > PS-DVB-WAX > HLB > Si-IL > Si-RP > PBA. As it can be seen, in untargeted metabolomics studies, the number of peaks and their intensity corresponding to the extracted features is dependent on the selected SPME coating and method of analysis. A S-plot was used for identification of discriminating features between different coatings, with PS-DVB-WAX:HLB 50:50 [w/w] used as a reference coating. Results showed that the highest overlap of clusters were related to mixed coatings (PS-DVB-WAX:Si-IL 80:20 [w/w]), PS-DVB-WAX:HLB 50:50 [w/w]), PS-DVB-WAX:HLB 80:20 [w/w]) and coatings prepared with individual particles (PS-DVB-WAX, HLB, Si-IL) in comparison with other coatings (PBA, Si-RP-WCX) for both positive and negative ionization modes and for all three columns in terms of number of features, extracted metabolites, and peak intensities. PS-DVB-WAX: HLB 50:50 (w:w) as the best candidate of 96-blade system for untargeted analysis is able to extract a wide variety of metabolites in terms of polarities characterized by $-7 < \log P < 15$, and $100 < MW < 1000$ such as metabolites related to central carbon metabolism (glycolytic, and pentose phosphate pathway like glucose, ribulose-5-phosphate, glucose-6-phosphate, and intermediates of citric acid cycle such as aconitic acid, succinic acid, malic acid), and biosynthetic metabolites (amino acids such as S-adenosyl-L-methionine, asparagine, cystathionine, betaine, homoserine, etc, and nucleotides including cytidine 3'-triphosphate, nicotinic acid mononucleotide, adenosine diphosphate ribose, adenosine 3',5'-bisphosphate, adenosine triphosphate) classified as polar metabolites to hydrophobic metabolites such as lipids linolenic acid, hexacosanoic acid, and stearic acid, PG(22:0/19:0), PG(16:0/16:0), PC(P-20:0/12:0), which are widely distributed within *E.coli* membrane separated with three different LC columns combined. Tables 3.5 display the list of identified metabolites using PS-DVB-WAX: HLB 50:50 (w:w) coupled to three different columns in both ionization modes after removal of the parts of the chromatograms related to void volume and re-equilibration time confirmed with authentic standards. Figure S5 demonstrates Heatmap of metabolites extracted by different 96-blade SPME coating (Metabolite levels correspond to the color intensity). The lower color intensity indicates reduced levels of the respective metabolites and vice versa. The each box color represents the data after calculating the mean of three replicates.

The obtained results demonstrated that different stationary phases for the 96-blade system could provide different metabolites profiles; therefore, the coating should be carefully selected based on the focus of study on different classes of metabolites. Using SPME sorbents composed of a mixture of particles with different polarities is similar to using a mixture of different solvents for extraction in order to achieve wider metabolite coverage. The developed 96-blade SPME technique is more successful for untargeted metabolomics in comparison to other extraction techniques such as SPE and LLE. One of the drawbacks

of SPE in comparison to SPME is its limitation because of breakthrough volume. Using the same extraction phase for both, SPME and SPE experiments, Mirnaghi et al. [224] proved the suitability of SPME for untargeted analysis of metabolites in broad range of polarity where the breakthrough volume cannot be determined prior to extraction. Additionally, due to its open bed format SPME does not suffer from the clogging that is an issue with SPE cartridges.

Hye Shin et al. [220] evaluated different solvents for extraction of metabolites from bacterial cells, and they found that a mixture of acetonitrile:methanol:water (2:2:1) and water:isopropanol:methanol (2:2:5) provided the highest peak intensity, number of extracted metabolites, and reproducibility in comparison to pure methanol and acetonitrile:water (1:1). However, as the type of extraction solvent could affect the metabolomics profiling, the solvent must be carefully selected in regards to the purpose of the metabolic profiling under investigation. Polyamines, amino acids, organic acids, sugar phosphates, and fatty acids were detected by the best-nominated solvent.

In the current study, global metabolomics profiling using PS-DVB-WAX:HLB 50:50 [w/w] provided a wider range of metabolite coverage than acetonitrile:methanol:water (2:2:1) and water:isopropanol:methanol (2:2:5) evaluated by Hye Shin et al. [220]. The PS-DVB-WAX:HLB 50:50 [w/w] coating provided wide metabolome coverage (Table 3.5), from highly polar and ionic metabolites such as peptides, nucleotides, mono/di/tri/tetrasaccharides, sugar acids, and glycosyl compounds, to nonpolar metabolites such as linoleic acid and derivatives, fatty acids, glycerophospholipids, and prenol lipids which is comparable with identified metabolites using commercial SPME fibers as well as previously developed traditional solvent extraction techniques. Based on the present observation, saccharides (mono/di/tri/tetrasaccharides), nucleotides (purine nucleotides, pyrimidine nucleotides), imidazole nucleosides, peptides, and diazins are the main class of compounds extracted by SPME, which were not reported in extraction with LLE. Moreover, the SPME technique provided no risk of chemical modification, contamination, and analyte loss while in solvent extraction technique consumption of large volumes of organic solvent and emulsion formation result in metabolite loss [28]. One of the other advantages of SPME is capability of this technique for characterization of short-lived or unstable species or biotransformation reaction intermediates [225-230]. Vuckovic et al. applied *in vivo* SPME procedure for direct sampling of the circulating blood of mice and demonstrated that in comparison to ultrafiltration and solvent precipitation techniques, SPME has capability of capturing unstable energy metabolites displaying an important development in metabolomics [143]. In the present study, the results demonstrated that SPME extracted adenosine, adenosine monophosphate, adenosine triphosphate, and glutathione as unstable metabolites from *E.coli* metablome. This technique is also less invasive over traditional extraction methodologies [231].

3.3.2.2 LC-MS method development for bacterial cell metabolomics studies

Most works in the area of nontargeted metabolomics have been conducted with the use of RP C18 columns, as they have shown to be the columns that provide the highest number of features. However, RP C18 columns provide poor separation of polar metabolites eluted in the void volume, which may result in ion suppression and low metabolomic coverage [213]. To obtain reliable results in profiling thousands of features, it is necessary to optimize chromatographic separation and reduce matrix effects. Detection of as many metabolites as possible enhance the chance of capturing up regulated or down regulated metabolites in the metabolome.

In the present work, three different LC columns (HILIC, XBridge C18, and Kinetex PFP) were selected to ensure analyte retention and provide metabolome coverage for extracted metabolites with different SPME coatings. HILIC columns operate based on hydrophilic interaction chromatography, and are mostly used for separation of polar metabolites. XBridge C18 and Kinetex PFP columns were selected as RP columns. The XBridge C18 column is modified to retain polar as well as nonpolar metabolites, and the Kinetex PFP column acted as a mid-polar stationary phase. Table 3.4 demonstrates the number of features extracted using different coatings separated by different investigated columns in both polarization modes. The highest number of features represents overall metabolome coverage, and peak intensity of features indicates the threshold required for quantification [211].

The Kinetex PFP column separated the highest number of features and identified metabolites ranged between $-7 < \log P < 15$, and the highest number of identified metabolites were related to carboxylic acid and derivatives, peptides, amino acids and derivatives, prenol lipids, glycosyl compounds, mono/di/trisaccharides, glycerophospholipids, fatty acids and conjugates. In the case of Kinetex PFP column, pentafluorophennyl bonded phase incorporates fluorine atoms on the periphery of the phenyl ring, applying multiple retention mechanisms for separation of challenging compounds. These interactions include hydrophobic, π-π, dipole-dipole, H-bonding, and shape selectivity. Both polar and aromatic compounds can be retained with a PFP column as there are electronegative fluorine atoms producing an electron deficient phenyl ring. This highly polar phenyl ring enables highly polar analytes and their stereoisomers to also be retained by dipole-dipole and H-bonding interactions. This wide separation coverage was not achieved by the amino-based HILIC and the XBridge C18 columns. The Kinetex PFP stationary phase with gradient elution provided a higher resolution, decreased run time and improved sensitivity compared to regular HPLC. Figure 3.6 shows the chromatogram of the separated metabolites using Kinetex PFP extracted by PS-DVB-WAX:HLB 50:50 [w/w] using an Orbitrap mass spectrometer in both positive and negative ESI modes. The identified metabolites separated by HILIC column were ranged between $-8.0 < \log P < 9.0$, and the majority of the separated metabolites were related to glycosyl compounds, peptides, phenols and derivatives, amino acids and derivatives, and

mono/disaccharides. The HILIC column with amino bonded functional groups demonstrated good retention of highly polar compounds. However, these types of columns need longer equilibration times than RP columns, and produce broader peak shapes. According to comprehensive metabolomics studies, while the HILIC column does not provide much additional information for global metabolomics profiling, it can provide more resolution of polar compounds, which might be useful in some applications [215].

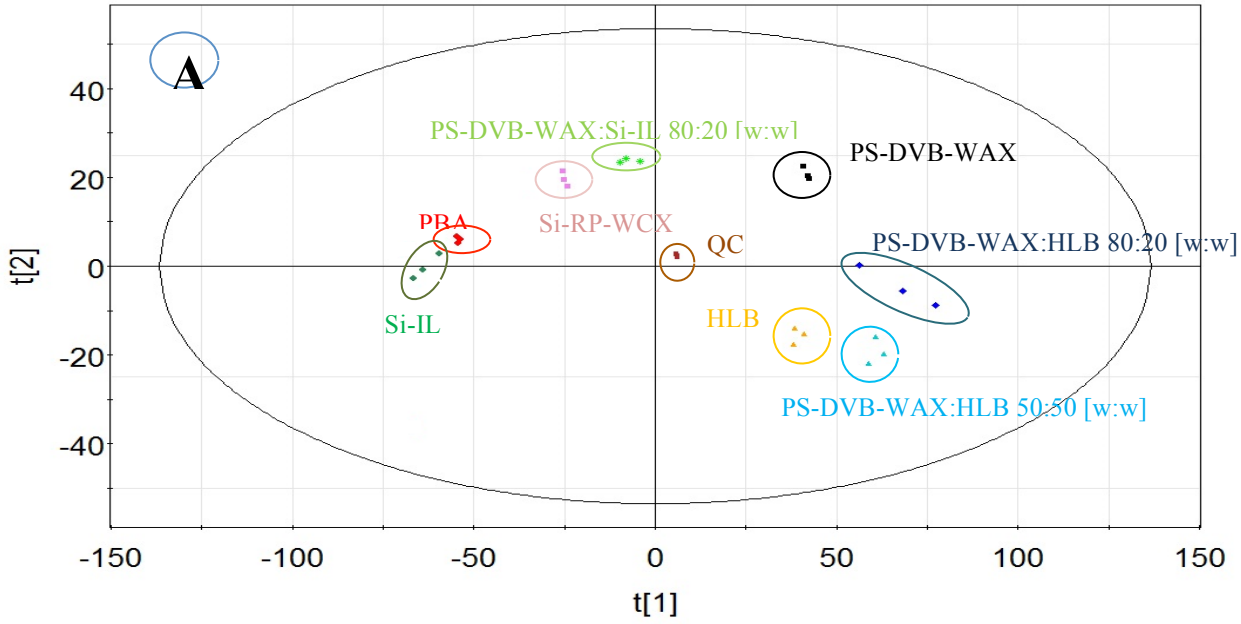

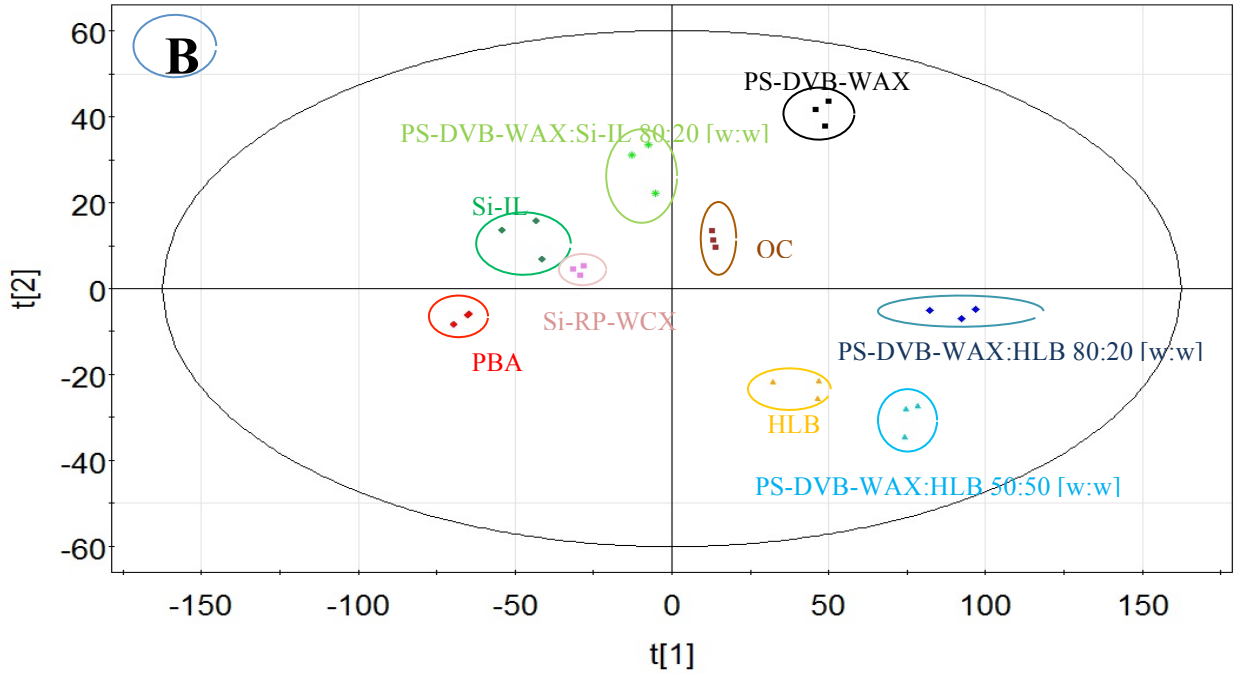

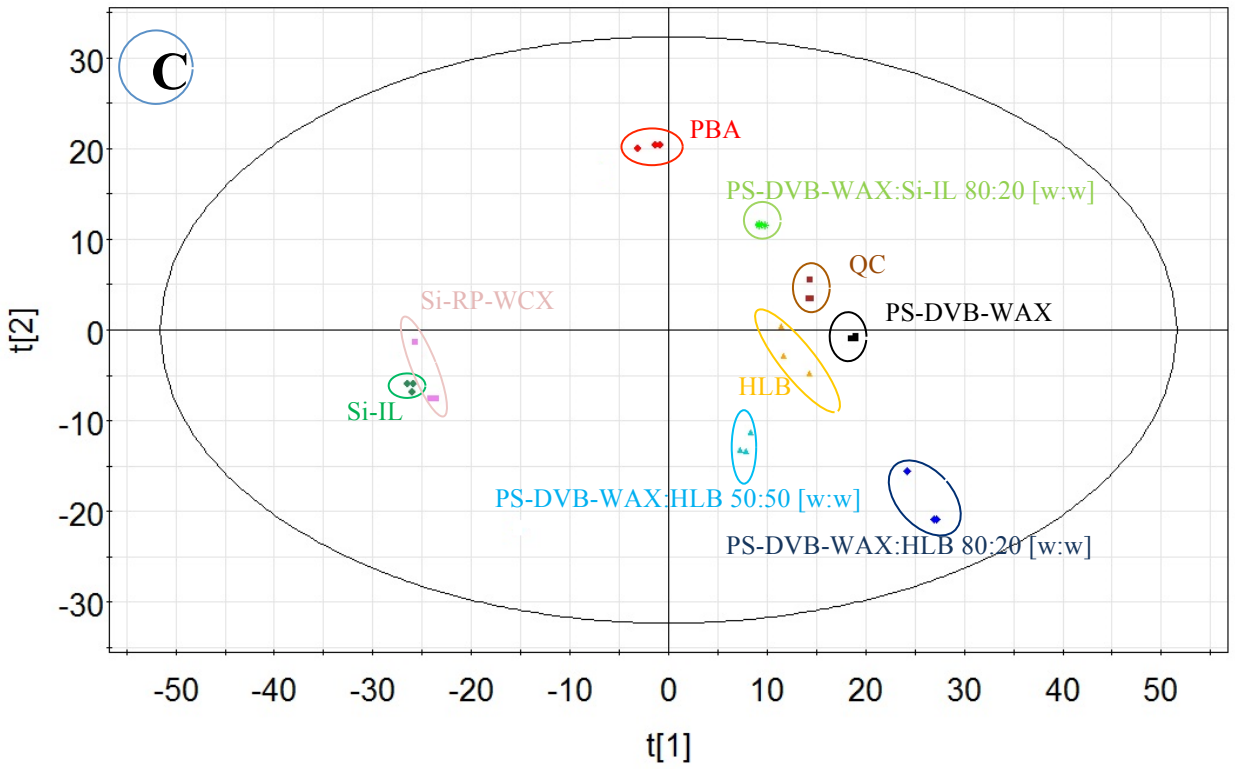
C
PBA
PS-DVB-WAX:Si-IL 80:20 [w:w]
QC
Si-RP-WCX
PS-DVB-WAX
HLB
Si-IL
PS-DVB-WAX:HLB 50:50 [w:w]
PS-DVB-WAX:HLB 80:20 [w:w]
t[2]
t[1]

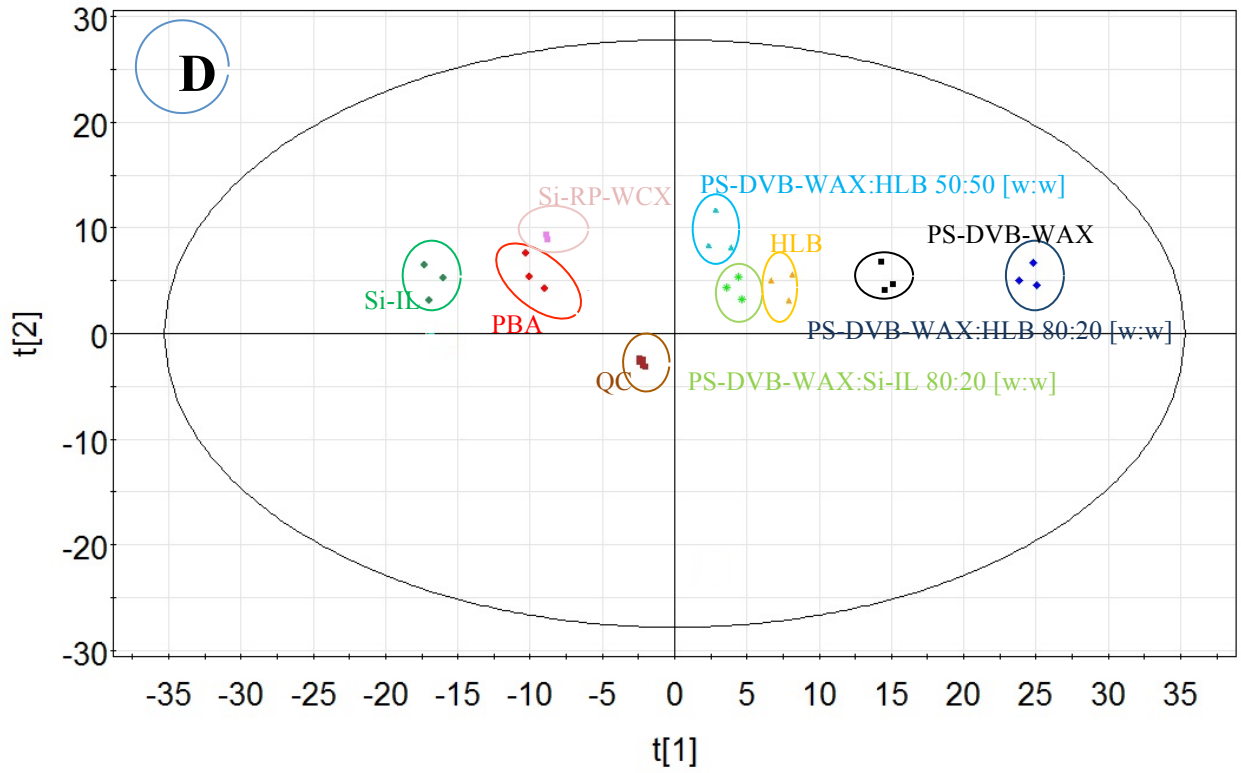
D
Si-RP-WCX
PS-DVB-WAX:HLB 50:50 [w:w]
HLB
PS-DVB-WAX
Si-IL
PBA
PS-DVB-WAX:HLB 80:20 [w:w]
QC
PS-DVB-WAX:Si-IL 80:20 [w:w]
t[2]
t[1]

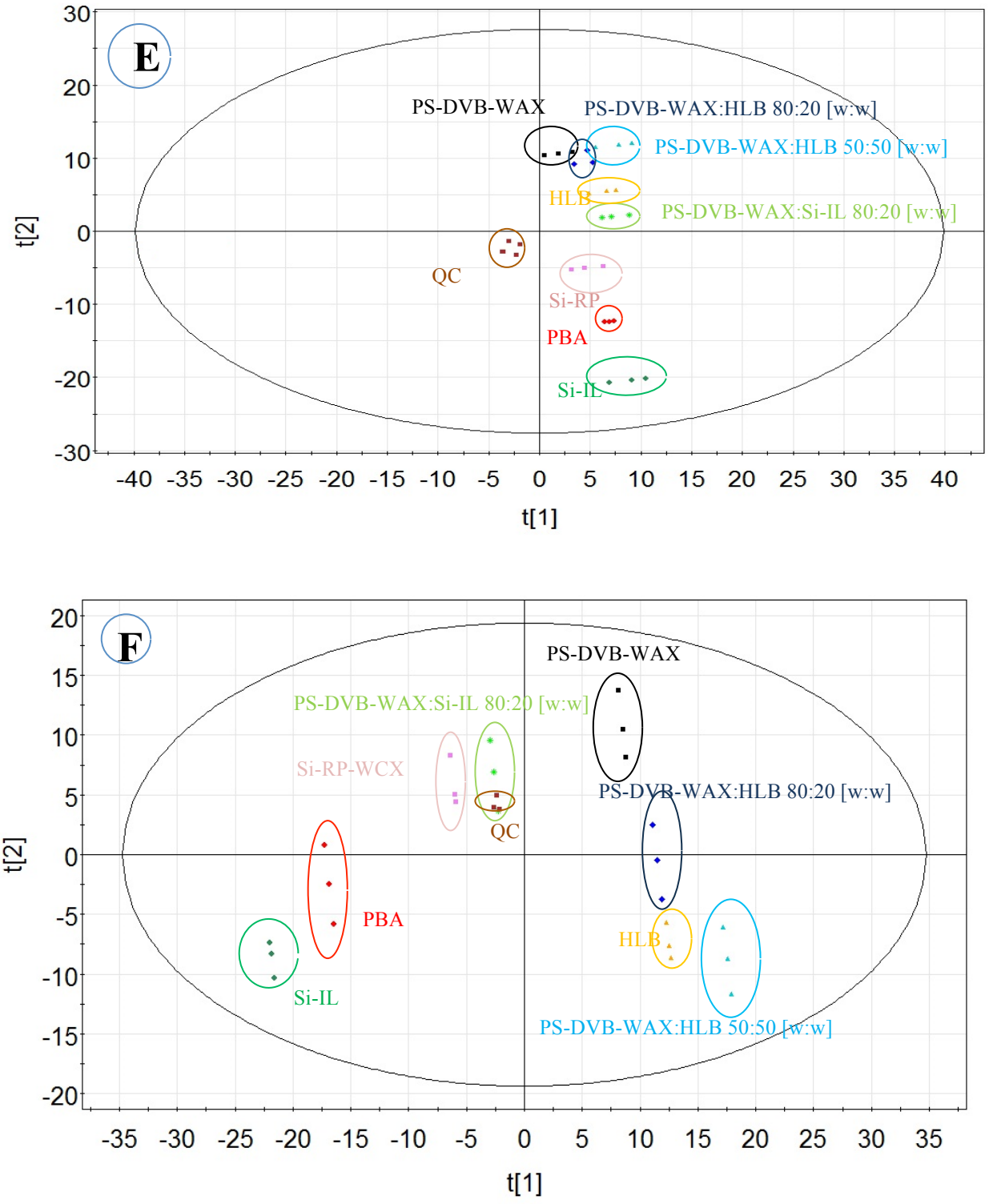

Figure 3.5 PCA score plot using Kinetex PFP column in positive ionization mode (A), PCA score plot for Kinetex PFP using negative ionization mode (B), PCA score plot using Luna HILIC Si column in positive ionization mode (C), PCA score plot using Luna HILIC Si column in negative ionization mode (D), PCA score plot using XBridge C18 in positive ionization mode (E), PCA score plot using XBridge C18 in negative ionization mode (F).

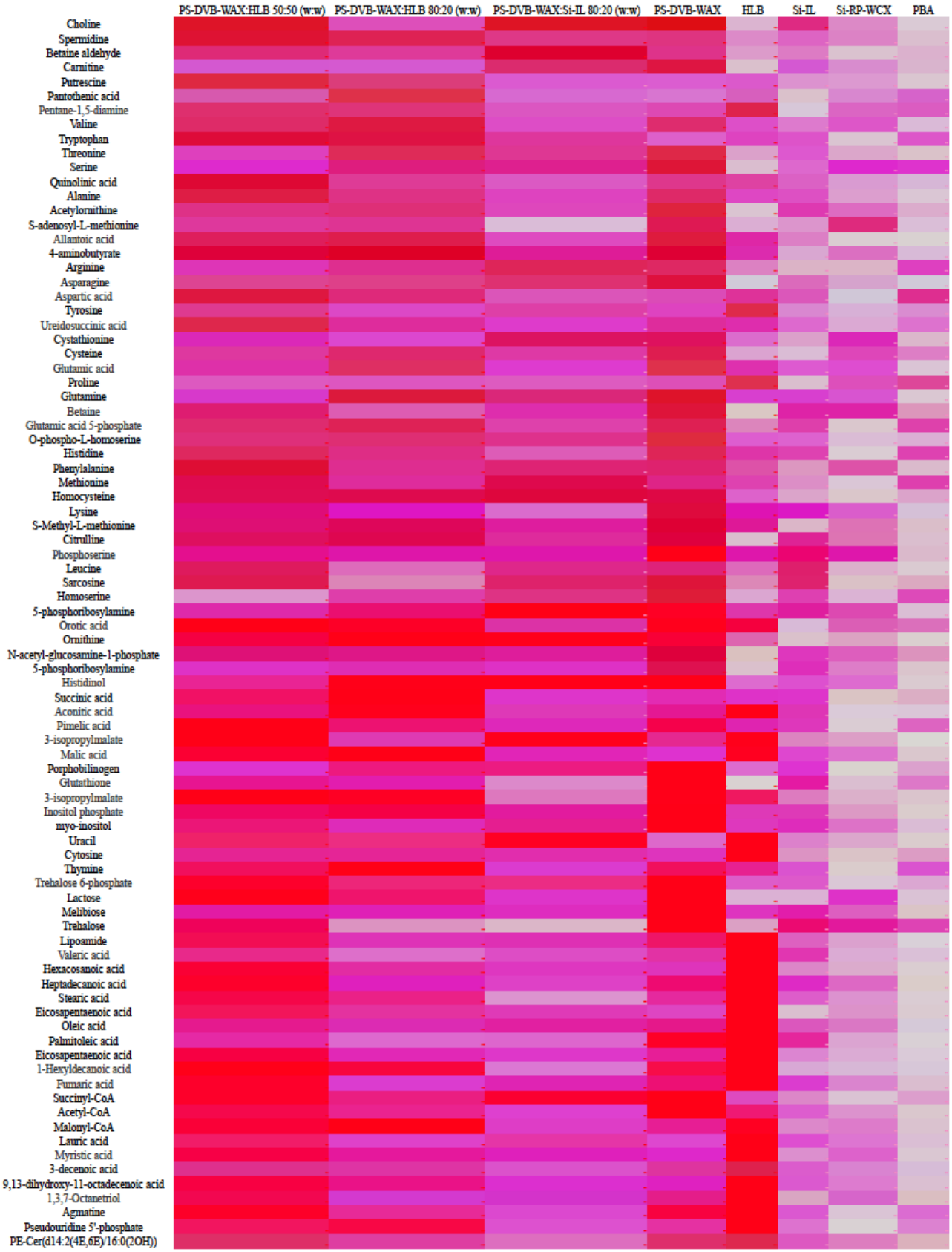
PS-DVB-WAX:HLB 50:50 (w:w)
PS-DVB-WAX:HLB 80:20 (w:w)
PS-DVB-WAX:Si-IL 80:20 (w:w)
PS-DVB-WAX
HLB
Si-IL
Si-RP-WCX
PBA
Choline
Spermidine
Betaine aldehyde
Carnitine
Putrescine
Pantothenic acid
Pentane-1,5-diamine
Valine
Tryptophan
Threonine
Serine
Quinolinic acid
Alanine
Acetylornithine
S-adenosyl-L-methionine
Allantoic acid
4-aminobutyrate
Arginine
Asparagine
Aspartic acid
Tyrosine
Ureidosuccinic acid
Cystathionine
Cysteine
Glutamic acid
Proline
Glutamine
Betaine
Glutamic acid 5-phosphate
O-phospho-L-homoserine
Histidine
Phenylalanine
Methionine
Homocysteine
Lysine
S-Methyl-L-methionine
Citrulline
Phosphoserine
Leucine
Sarcosine
Homoserine
5-phosphoribosylamine
Orotic acid
Ornithine
N-acetyl-glucosamine-1-phosphate
5-phosphoribosylamine
Histidinol
Succinic acid
Aconitic acid
Pimelic acid
3-isopropylmalate
Malic acid
Porphobilinogen
Glutathione
3-isopropylmalate
Inositol phosphate
myo-inositol
Uracil
Cytosine
Thymine
Trehalose 6-phosphate
Lactose
Melibiose
Trehalose
Lipoamide
Valeric acid
Hexacosanoic acid
Heptadecanoic acid
Stearic acid
Eicospentaenoic acid
Oleic acid
Palmitoleic acid
Eicosapentaenoic acid
1-Hexyldecanoic acid
Fumaric acid
Succinyl-CoA
Acetyl-CoA
Malonyl-CoA
Lauric acid
Myristic acid
3-decenoic acid
9,13-dihydroxy-11-octadecenoic acid
1,3,7-Octanetriol
Agmatine
Pseudouridine 5'-phosphate
PE-Cer(d14:2(4E,6E)/16:0(2OH))

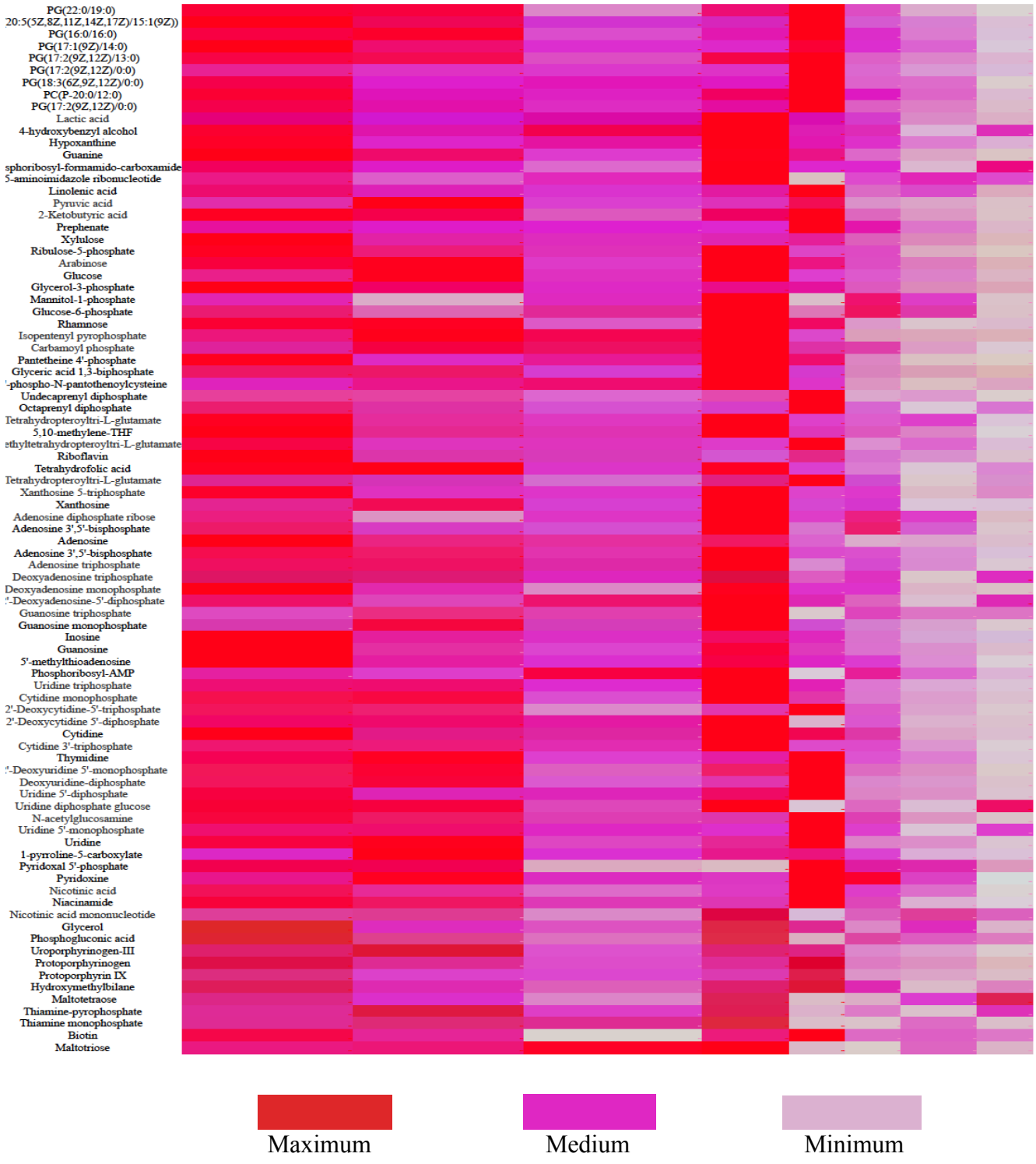

Figure 3.6 Heatmap of metabolites extracted by different 96-blade SPME coatings (Metabolite levels correspond to the color intensity). The lower color intensity indicates reduced levels of the respective metabolites and vice versa. The each box color represents the data after calculating the mean of three replicates.

Nucleoside di/triphosphate is one of the most important metabolites identified using the HILIC column, and the XBridge C18 columns could not separate it. Alternatively, the XBridge C18 column could separate mostly prenol lipids, glycerophospholipids. This column used as an RP column in this research demonstrated good separation of nonpolar compounds ranged between $-3 < \log P < 17$; however, in terms of retaining highly polar and ionic metabolites, this column did not provide high efficiency.

The metabolome coverage among different evaluated columns HILIC, Kinetex PFP, and XBridge C18 chromatographic modes was evaluated by using the ion features defined by their exact mass corresponding to detected adduct ions. These analyses indicated that the highest number of unique features were detected by Kinetex PFP in both ESI modes. Figure 3.8 demonstrated the difference between metabolic coverage of different evaluated columns. The difference between Kinetex PFP column and HILIC ($5 \pm 12\%$) is related to separation of highly polar purine nucleotides with HILIC column while $5 \pm 10\%$ difference between XBridge C18 with Kinetex PFP is related to separation of highly nonpolar glycerolipids with XBridge C18. The results obtained in this study are promising for the Kinetex PFP in terms of separation of a wide variety of metabolites in one single run; however, for a group of highly polar and nonpolar metabolites, there is a need for the HILIC and C18 columns, respectively. Serially applying multiple dimension chromatographic methods by using HILIC and XBridge C18 columns in parallel could be the solution for retaining and resolving peaks related to highly polar metabolites such as phosphorylated nucleotides by HILIC column, and highly nonpolar glycerolipids by XBridge C18 columns. Ivanisevic et al. reported integration of RP and HILIC chromatography for metabolomics coverage of hydrophobic, lipids, hydrophilic, and central carbon metabolites [207]. In this work, the authors reported 56,000 features extracted from *E.coli* for both positive and negative ESI modes using HILIC (Luna Aminopropyl) and RP (XBridge C18) columns, and in cases where time and sample sizes are limited, the RP in positive mode and HILIC in negative mode can be combined to yield a maximum amount of biological information [207].

The outcome of the obtained results shows that in order to have comprehensive metabolite coverage, it is better to do coupling of RP and HILIC columns. This can be achieved in two ways: off-line coupling called heart-cutting or on-line coupling called comprehensive LC×LC. These configurations provide advantages such as increase in peak capacity, improvement in separation, especially for co-eluted peaks, and decrease in signal suppression [212,232,233]. Edwards et al. [212] applied two-dimensional (2D) separation combining SAX and RPLC columns for a complex *E.coli* cell matrix, providing a metabolomic profile with increased peak capacity, resolution and sensitivity. In this study authors addressed that compared to RPLC with the same gradient of 2D, 74 more compounds (within experimental error) were separated. This study is mostly focused on polar compounds such as glycolysis and TCA cycle metabolites, and there is no report about extraction of nonpolars.

3.3.3 Matrix effect

To reduce matrix effect, which is a significant issue in complex sample analyses by ESI-MS, the chosen sample preparation technique needs to provide high quality sample clean up. In this study, the use of biocompatible coatings and a washing step helped to decrease possible matrix effects. The absolute matrix effect for targeted metabolites was calculated based on the procedure developed by Matuszewski et al. [206]. Bacteria extract prepared using the optimized SPME protocol was spiked with a known concentration of targeted metabolites. The obtained results from the SPME-LC-MS analysis of spiked bacteria extract were compared with the results of neat standards at the same concentration. Ion suppression and ion enhancement are defined for results less than 80% and more than 120%, respectively [206,234]. Figure 3.9 shows that no matrix effects were found for the targeted metabolites characterized by wide range of physicochemical properties with the optimized SPME method. For the untargeted metabolomics study, the stability of the QC following injection of a large number of samples represented by QC clusters in PCA score plots (Figure 3.5, and Figure 3.10) demonstrated good stability of instrument function because of the excellent clean up of sample extracts, thereby yielding reliable results and minimizing instrument maintenance.

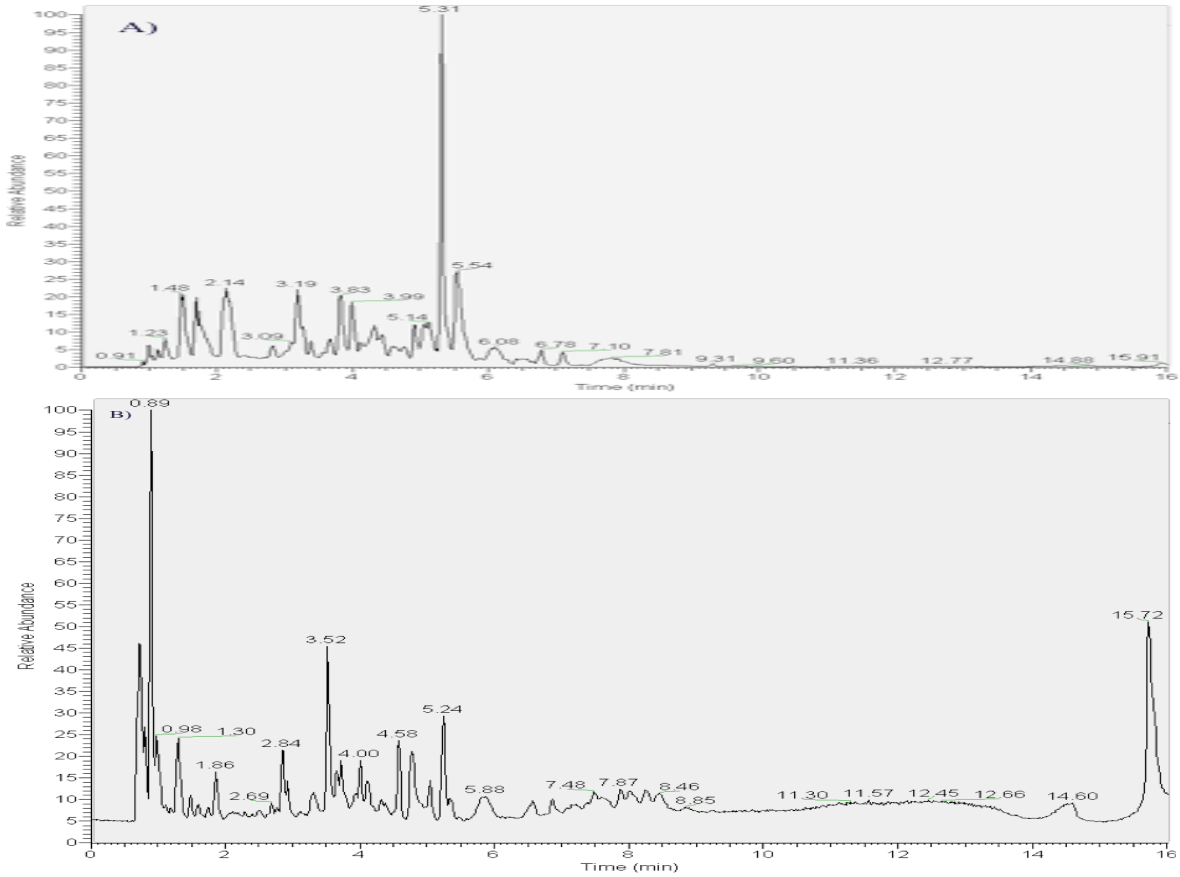

Figure 3.7 Chromatogram related to separation of extracted metabolites from bacteria using PS-DVB-WAX:HLB 50:50 (w/w) 96-SPME blade coupled to Kinetex PFP and Orbitrap mass spectrometer A) positive ESI B) negative ESI mode.

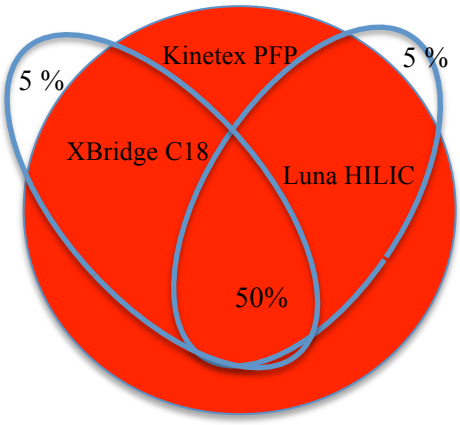

Figure 3.8 Metabolome coverage by three different columns based on accurate mass.

Table 3.5 Classes of all identified metabolites extracted and analysed by the optimized PS-DVB-WAX:HLB 50:50 (w:w) coupled to three different columns for in vivo sampling from bacterial media containing 2×10^5 CFU/mL cells at stationary phase of growth curve at both ionization modes (*: separated by Kinetex PFP, +: separated by HILIC column, #: separated by XBridge C18 column). Masses are theoretical mass for the chemical formula and experimentally measured masses of hydrogen adduct ions in both positive and negative ESI.

Alcohols and Polyols					
Metabolite	**Theoretical mass (molecule)**	**Exp. mass $[M+H]^+$**	**Exp. Mass $[M-H]^-$**	**Formula**	**Log P**
Choline * + #	104.1075	105.1147	103.0997	$C_5H_{14}NO$	-3.6
Alkylamines					
Metabolite	**Theoretical mass (molecule)**	**Exp. mass $[M+H]^+$**	**Exp. Mass $[M-H]^-$**	**Formula**	**Log P**
Spermidine * + #	145.1578	146.1657	144.1500	$C_7H_{19}N_3$	-1.1
Betaine aldehyde * +	102.0918	103.0997	101.0840	$C_5H_{12}NO$	-4.7
Carnitine * +	161.1052	162.1130	160.0973	$C_7H_{15}NO_3$	-4.9
Pantothenic acid * + #	219.1106	220.1184	218.1028	$C_9H_{17}NO_5$	-1.4
Pentane-1,5-diamine * + #	102.1156	103.1235	101.1078	$C_5H_{14}N_2$	-0.4
Amino acids					
Metabolite	**Theoretical mass (molecule)**	**Exp. Mass $[M+H]^+$**	**Exp. Mass $[M-H]^-$**	**Formula**	**Log P**
Valine * + #	117.0789	118.0868	116.0711	$C_5H_{11}NO_2$	-2.3
Tryptophan * + #	204.0898	205.0977	203.0820	$C_{11}H_{12}N_2O_2$	-1.1
Threonine * +	119.0582	120.0660	118.0504	$C_4H_9NO_3$	-3.5
Serine * + #	105.0425	106.0504	104.0347	$C_3H_7NO_3$	-3.9
Quinolinic acid * + #	167.0218	168.0296	166.0140	$C_7H_5NO_4$	-0.54
Acetylornithine * + #	174.1004	175.1082	173.0926	$C_7H_{14}N_2O_3$	-3.6

S-adenosyl-L-methionine * +	399.1450	400.1528	398.1372	$C_{15}H_{23}N_6O_5S$	-5.3
Allantoic acid * + #	176.0545	177.0623	175.0467	$C_4H_8N_4O_4$	-2.6
4-aminobutyrate * + #	103.0633	104.0711	102.0555	$C_4H_9NO_2$	-3
Arginine * +	174.1116	175.1195	173.1038	$C_6H_{14}N_4O_2$	-3.9
Asparagine * +	132.0535	133.0613	131.0456	$C_4H_8N_2O_3$	-4.3
Aspartic acid * +	133.0375	134.0453	132.0296	$C_4H_7NO_4$	-3.5
Tyrosine * + #	181.0738	182.0817	180.0660	$C_9H_{11}NO_3$	-2.4
Ureidosuccinic acid * + #	176.0433	177.0511	175.0354	$C_5H_8N_2O_5$	-1.7
Cystathionine * +	222.0674	223.0752	221.0596	$C_7H_{14}N_2O_4S$	-5.8
Cysteine * + #	121.0197	122.0275	120.0119	$C_3H_7NO_2S$	-2.8
Glutamic acid * +	147.0531	148.0609	146.0453	$C_5H_9NO_4$	-3.5
Proline * + #	115.0633	116.0711	114.0555	$C_5H_9NO_2$	-2.7
Glutamine * +	146.0691	147.0769	145.0613	$C_5H_{10}N_2O_3$	-4
Betaine * +	117.0789	118.0868	116.0711	$C_5H_{11}NO_2$	-4.5
Glutamic acid 5-phosphate * +	227.0194	228.0273	226.0116	$C_5H_{10}NO_7P$	-3
O-phospho-L-homoserine * +	199.0245	200.0324	198.0167	$C_4H_{10}NO_6P$	-3.2
Histidine * +	155.0691	156.0773	154.0616	$C_6H_9N_3O_2$	-3.3
Phenylalanine * +	165.0789	166.0868	164.0711	$C_9H_{11}NO_2$	-1.4
Methionine * + #	149.0510	150.0588	148.0432	$C_5H_{11}NO_2S$	-2.2
Homocysteine * + #	135.0354	136.0432	134.0275	$C_4H_9NO_2S$	-2.6
Lysine * +	146.1055	147.1133	145.0977	$C_6H_{14}N_2O_2$	-3.8
S-Methyl-L-methionine * +	164.0745	165.0823	163.0667	$C_6H_{14}NO_2S$	-3.3
Citrulline * +	175.0956	176.1035	174.0878	$C_6H_{13}N_3O_3$	-3.9
Phosphoserine * +	185.0089	186.0167	184.0011	$C_3H_8NO_6P$	-3.2
Leucine * + #	131.0946	132.1024	130.0868	$C_6H_{13}NO_2$	-1.8
Homoserine * +	119.0582	120.0660	118.0504	$C_4H_9NO_3$	-3.8
Amino sugars					
Metabolite	**Theoretical mass**	**$[M+H]^+$**	**Exp. Mass**	**Formula**	**Log P**

	(molecule)		$[M-H]^-$		
5-phosphoribosylamine * +	229.0351	230.0429	228.0273	$C_5H_{12}NO_7P$	-3.5
Orotic acid * + #	156.0171	157.0249	155.0092	$C_5H_4N_2O_4$	-1.2
Ornithine * +	132.0898	133.0977	131.0820	$C_5H_{12}N_2O_2$	-3.3
N-acetyl-glucosamine-1-phosphate * +	301.0562	302.0640	300.0484	$C_8H_{16}NO_9P$	-3.3
5-phosphoribosylamine * +	229.0351	230.0429	228.0273	$C_5H_{12}NO_7P$	-3.5
Azoles					
Metabolite	**Theoretical mass (molecule)**	**Exp. Mass $[M+H]^+$**	**Exp. Mass $[M-H]^-$**	**Formula**	**Log P**
Histidinol * + #	141.0902	142.0980	140.0823	$C_6H_{11}N_3O$	-1.7
Carboxylic acids and derivatives					
Metabolite	**Theoretical mass (molecule)**	**Exp. Mass $[M+H]^+$**	**Exp. Mass $[M-H]^-$**	**Formula**	**Log P**
Succinic acid * + #	118.0266	119.0344	117.0187	$C_4H_6O_4$	-0.4
Aconitic acid * + #	174.0164	175.0242	173.0086	$C_6H_6O_6$	-0.52
Pimelic acid * + #	160.0735	161.0813	159.0657	$C_7H_{12}O_4$	0.94
3-isopropylmalate * + #	176.0684	177.0763	175.0609	$C_7H_{12}O_5$	0.16
Malic acid * + #	134.0215	135.0293	133.0137	$C_4H_6O_5$	-1.1
Porphobilinogen * + #	226.0953	227.1031	225.0875	$C_{10}H_{14}N_2O_4$	-2.7
Glutathione	306.0759	307.0818	305.0673	$C_{10}H_{16}N_3O_6S$	-4.9
3-isopropylmalate * + #	176.0684	177.0763	175.0606	$C_7H_{12}O_5$	0.16
Cyclic alcohols and derivatives					
Metabolite	**Theoretical mass (molecule)**	**Exp. Mass $[M+H]^+$**	**Exp. Mass $[M-H]^-$**	**Formula**	**Log P**
Inositol phosphate * +	260.0297	261.0375	259.0218	$C_6H_{13}O_9P$	-3.9
myo-inositol * +	180.0633	181.0712	179.0555	$C_6H_{12}O_6$	-3.8
Diazins					
Metabolite	**Theoretical mass (molecule)**	**Exp. Mass $[M+H]^+$**	**Exp. Mass $[M-H]^-$**	**Formula**	**Log P**
Uracil * + #	112.0272	113.0351	111.0194	$C_4H_4N_2O_2$	-0.86
Cytosine * + #	111.0433	112.0510	110.0358	$C_4H_5N_3O$	-1.1
Thymine * + #	126.0429	127.0507	125.0351	$C_5H_6N_2O_2$	-0.46
Disaccharides					
Metabolite	**Theoretical mass (molecule)**	**Exp. Mass $[M+H]^+$**	**Exp. Mass $[M-H]^-$**	**Formula**	**Log P**
Trehalose 6-phosphate * +	422.0825	423.0903	421.0747	$C_{12}H_{23}O_{14}P$	-4.8

Lactose * +	342.1162	343.1240	341.1083	$C_{12}H_{22}O_{11}$	-4.7
Melibiose * +	342.1162	343.1240	341.1083	$C_{12}H_{22}O_{11}$	-4.7
Trehalose * +	342.1162	343.1240	341.1083	$C_{12}H_{22}O_{11}$	-4.7
Dithiolanes					
Metabolite	**Theoretical mass (molecule)**	**Exp. Mass $[M+H]^+$**	**Exp. Mass $[M-H]^-$**	**Formula**	**Log P**
Lipoamide * + #	205.0595	206.0673	204.0516	$C_8H_{15}NOS_2$	1.31
Fatty acids and conjugates					
Metabolite	**Theoretical mass (molecule)**	**Exp. Mass $[M+H]^+$**	**Exp. Mass $[M-H]^-$**	**Formula**	**Log P**
Valeric acid * + #	102.0680	103.0759	101.0602	$C_5H_{10}O_2$	1.37
Hexacosanoic acid * #	396.3967	397.4045	395.3889	$C_{26}H_{52}O_2$	10.7
Heptadecanoic acid * #	270.2558	271.2637	269.2480	$C_{17}H_{34}O_2$	6.7
Stearic acid * #	284.2715	285.2793	283.2637	$C_{18}H_{36}O_2$	7.15
Eicosapentaenoic acid * #	302.2245	303.2324	301.2167	$C_{20}H_{30}O_2$	6.23
Oleic acid * #	282.2558	283.2637	281.2480	$C_{18}H_{34}O_2$	6.78
Palmitoleic acid * #	254.2245	255.2324	253.2167	$C_{16}H_{30}O_2$	5.89
Eicosapentaenoic acid * #	302.2245	303.2324	301.2167	$C_{20}H_{30}O_2$	6.23
1-Hexyldecanoic acid * #	256.2402	257.2480	255.2324	$C_{16}H_{32}O_2$	6.26
Fumaric acid * + #	116.0109	117.0187	115.0031	$C_4H_4O_4$	-0.041
Fatty acid esters					
Metabolite	**Theoretical mass (molecule)**	**Exp. Mass $[M+H]^+$**	**Exp. Mass $[M-H]^-$**	**Formula**	**Log P**
Succinyl-CoA * + #	867.1313	868.1390	866.1234	$C_{25}H_{40}N_7O_{19}P_3S$	-0.61
Acetyl-CoA * + #	809.1257	810.1336	808.1179	$C_{23}H_{38}N_7O_{17}P_3S$	-0.58
Malonyl-CoA * + #	853.1156	854.1234	852.1077	$C_{24}H_{38}N_7O_{19}P_3S$	1.39
Fatty acids and conjugates					
Metabolite	**Theoretical mass (molecule)**	**Exp. Mass $[M+H]^+$**	**Exp. Mass $[M-H]^-$**	**Formula**	**Log P**
Lauric acid * + #	200.1776	201.1854	199.1698	$C_{12}H_{24}O_2$	4.48
Myristic acid * + #	228.2089	229.2165	227.2020	$C_{14}H_{28}O_2$	4.77
3-decenoic acid * + #	170.1306	171.1385	169.1228	$C_{10}H_{18}O_2$	2.99

Fatty acyls					
Metabolite	**Theoretical mass (molecule)**	**Exp. Mass $[M+H]^+$**	**Exp. Mass $[M-H]^-$**	**Formula**	**Log P**
9,13-dihydroxy-11-octadecenoic acid * + #	314.2457	315.2535	313.2378	$C_{18}H_{34}O_4$	4.62
Fatty alcohols					
Metabolite	**Theoretical mass (molecule)**	**Exp. Mass $[M+H]^+$**	**Exp. Mass $[M-H]^-$**	**Formula**	**Log P**
1,3,7-Octanetriol * + #	162.1255	163.1334	161.1177	$C_8H_{18}O_3$	-0.34
Guanidines					
Metabolite	**Theoretical mass (molecule)**	**Exp. Mass $[M+H]^+$**	**Exp. Mass $[M-H]^-$**	**Formula**	**Log P**
Agmatine * + #	130.1218	131.1296	129.1140	$C_5H_{14}N_4$	-1.2
Glycosyl compounds					
Metabolite	**Theoretical mass (molecule)**	**Exp. Mass $[M+H]^+$**	**Exp. Mass $[M-H]^-$**	**Formula**	**Log P**
Pseudouridine 5'-phosphate * + #	324.0358	325.0436	323.0280	$C_9H_{13}N_2O_9P$	-3.2
Glycerophospholipids					
Metabolite	**Theoretical mass (molecule)**	**Exp. Mass $[M+H]^+$**	**Exp. Mass $[M-H]^-$**	**Formula**	**Log P**
PE-Cer(d14:2(4E,6E)/16:0(2OH)) * #	618.4372	619.4451	617.4294	$C_{32}H_{63}N_2O_7P$	8.73
PG(22:0/19:0) #	848.6506	849.6584	847.6428	$C_{47}H_{93}O_{10}P$	15.28
PG(20:5(5Z,8Z,11Z,14Z,17Z)/15:1(9Z)) * #	752.4628	753.4706	751.4550	$C_{41}H_{69}O_{10}P$	11.60
PG(16:0/16:0) * #	722.5097	723.5176	721.5019	$C_{38}H_{75}O_{10}P$	11.77
PG(17:1(9Z)/14:0) * #	706.4784	707.4863	705.4706	$C_{37}H_{71}O_{10}P$	11.16
PG(17:2(9Z,12Z)/13:0) * #	690.4472	691.4550	689.4393	$C_{36}H_{67}O_{10}P$	10.55
PG(17:2(9Z,12Z)/0:0) * #	494.2644	495.2722	493.2566	$C_{23}H_{43}O_9P$	5.68
PG(18:3(6Z,9Z,12Z)/0:0) * #	506.2644	507.2722	505.2566	$C_{24}H_{43}O_9P$	5.68
PC(P-20:0/12:0) * #	717.5672	718.5750	716.5594	$C_{40}H_{80}NO_7P$	12.63
PG(17:2(9Z,12Z)/0:0) * #	494.2644	495.2722	493.2566	$C_{23}H_{43}O_9P$	5.68
Hydroxy acids and derivatives					
Metabolite	**Theoretical mass (molecule)**	**Exp. Mass $[M+H]^+$**	**Exp. Mass $[M-H]^-$**	**Formula**	**Log P**
4-hydroxybenzyl alcohol * + #	124.0524	125.0602	123.0446	$C_7H_8O_2$	0.9
Imidazopyrimidines					
Metabolite	**Theoretical mass (molecule)**	**Exp. Mass $[M+H]^+$**	**Exp. Mass $[M-H]^-$**	**Formula**	**Log P**
Hypoxanthine * + #	136.0385	137.0463	135.0306	$C_5H_4N_4O$	0.048

Guanine * + #	151.0494	152.0572	150.0415	$C_5H_5N_5O$	-0.59
Imidazole nucleosides and nucleotides					
Metabolite	**Theoretical mass (molecule)**	**Exp. Mass $[M+H]^+$**	**Exp. Mass $[M-H]^-$**	**Formula**	**Log P**
Phosphoribosyl-formamido-carboxamide * +	366.0576	367.0654	365.0498	$C_{10}H_{15}N_4O_9P$	-4.1
5-aminoimidazole ribonucleotide * +	295.0569	296.0647	294.0491	$C_8H_{14}N_3O_7P$	-4.3
Lineolic acids and derivatives					
Metabolite	**Theoretical mass (molecule)**	**Exp. Mass $[M+H]^+$**	**Exp. Mass $[M-H]^-$**	**Formula**	**Log P**
Linolenic acid * + #	278.2245	279.2324	277.2167	$C_{18}H_{30}O_2$	6.06
Keto-acids and derivatives					
Metabolite	**Theoretical mass (molecule)**	**Exp. Mass $[M+H]^+$**	**Exp. Mass $[M-H]^-$**	**Formula**	**Log P**
2-Ketobutyric acid * + #	102.0316	103.0395	101.0238	$C_4H_6O_3$	0.77
Prephenate * + #	226.0477	227.0555	225.0399	$C_{10}H_{10}O_6$	0.061
Monosaccharides					
Metabolite	**Theoretical mass (molecule)**	**Exp. Mass $[M+H]^+$**	**Exp. Mass $[M-H]^-$**	**Formula**	**Log P**
Xylulose * + #	150.0528	151.0606	149.0450	$C_5H_{10}O_5$	-2.6
Ribulose-5-phosphate * + #	230.0192	231.0269	229.0113	$C_5H_{11}O_8P$	-2.4
Arabinose * + #	150.0528	151.0606	149.0450	$C_5H_{10}O_5$	-2.9
Glucose * + #	180.0633	181.0712	179.0555	$C_6H_{12}O_6$	-2.9
Glycerol-3-phosphate * + #	172.0137	173.0215	171.0058	$C_3H_9O_6P$	-2
Mannitol-1-phosphate * +	262.0453	263.0531	261.0375	$C_6H_{15}O_9P$	-3.9
Glucose-6-phosphate * + #	260.0297	261.0375	259.0218	$C_6H_{13}O_9P$	-3.1
Rhamnose * + #	164.0684	165.0763	163.0606	$C_6H_{12}O_5$	-1.9
Organic oxoanionic compounds					
Metabolite	**Theoretical mass (molecule)**	**Exp. Mass $[M+H]^+$**	**Exp. Mass $[M-H]^-$**	**Formula**	**Log P**
Isopentenyl pyrophosphate * + #	246.0058	247.0136	244.9980	$C_5H_{12}O_7P_2$	0.2
Carbamoyl phosphate * + #	140.9827	141.9905	139.9748	CH_4NO_5P	-1.2
Organic phosphoric acids and derivatives					
Metabolite	**Theoretical mass (molecule)**	**Exp. Mass $[M+H]^+$**	**Exp. Mass $[M-H]^-$**	**Formula**	**Log P**
Pantetheine 4'-phosphate * + #	358.0963	359.1041	357.0885	$C_{11}H_{23}N_2O_7PS$	-1.7

Glyceric acid 1,3-biphosphate * + #	265.9592	266.9671	264.9514	$C_3H_8O_{10}P_2$	-2.3
Peptidomimetics					
Metabolite	**Theoretical mass (molecule)**	**Exp. Mass $[M+H]^+$**	**Exp. Mass $[M-H]^-$**	**Formula**	**Log P**
4'-phospho-N-pantothenoylcysteine * + #	402.0861	403.0940	401.0783	$C_{12}H_{23}N_2O_9PS$	-2
Prenol lipids					
Metabolite	**Theoretical mass (molecule)**	**Exp. Mass $[M+H]^+$**	**Exp. Mass $[M-H]^-$**	**Formula**	**Log P**
Undecaprenyl diphosphate #	926.6318	927.6396	925.6240	$C_{55}H_{92}O_7P_2$	16.89
Octaprenyl diphosphate * #	722.4440	723.4518	721.4362	$C_{40}H_{68}O_7P_2$	11.92
Pteridines and derivatives					
Metabolite	**Theoretical mass (molecule)**	**Exp. Mass $[M+H]^+$**	**Exp. Mass $[M-H]^-$**	**Formula**	**Log P**
Tetrahydropteroyltri-L-glutamate * + #	703.2561	704.2639	702.2483	$C_{29}H_{37}N_9O_{12}$	-6.1
5,10-methylene-THF * + #	457.1709	458.1788	456.1631	$C_{20}H_{23}N_7O_6$	-2
5-Methyltetrahydropteroyltri-L-glutamate * +	717.2718	718.2796	716.2639	$C_{30}H_{39}N_9O_{12}$	-5.7
Riboflavin * + #	376.1382	377.1461	375.1304	$C_{17}H_{20}N_4O_6$	-0.92
Tetrahydrofolic acid * + #	445.1709	446.1788	444.1631	$C_{19}H_{23}N_7O_6$	-2.8
Tetrahydropteroyltri-L-glutamate * +	703.2561	704.2639	702.2483	$C_{29}H_{37}N_9O_{12}$	-6.1
Purine nucleotides					
Metabolite	**Theoretical mass (molecule)**	**Exp. Mass $[M+H]^+$**	**Exp. Mass $[M-H]^-$**	**Formula**	**Log P**
Xanthosine 5-triphosphate * +	523.9746	524.9825	522.9668	$C_{10}H_{15}N_4O_{15}P_3$	-4.1
Xanthosine * + #	284.0756	285.0835	283.0678	$C_{10}H_{12}N_4O_6$	-1.2
Adenosine diphosphate ribose +	559.0716	560.0795	558.0638	$C_{15}H_{23}N_5O_{14}P_2$	-6.7
Adenosine 3',5'-bisphosphate +	427.0294	428.0372	426.0215	$C_{10}H_{15}N_5O_{10}P_2$	-6.1
Adenosine * + #	267.0967	268.1045	266.0889	$C_{10}H_{13}N_5O_4$	-2.1
Adenosine 3',5'-bisphosphate * +	427.0294	428.0372	426.0215	$C_{10}H_{15}N_5O_{10}P_2$	-6.1
Adenosine triphosphate +	506.9957	508.0035	505.9879	$C_{10}H_{16}N_5O_{13}P_3$	-6.2
Deoxyadenosine triphosphate * +	491.0008	492.0086	489.9930	$C_{10}H_{16}N_5O_{12}P_3$	-5.3
Deoxyadenosine monophosphate * +	331.0681	332.0759	330.0603	$C_{10}H_{14}N_5O_6P$	-3.9
2'-Deoxyadenosine-5'-diphosphate * +	331.0682	332.0759	330.0603	$C_{10}H_{14}N_5O_6P$	-4.4
Guanosine triphosphate * +	522.9907	523.9971	521.9828	$C_{10}H_{16}N_5O_{14}P_3$	-3.6
Guanosine monophosphate *	363.0580	364.0658	362.0501	$C_{10}H_{14}N_5O_8P$	-2.9

+ #					
Inosine * + #	268.0807	269.0885	267.0729	$C_{10}H_{12}N_4O_5$	-2.5
Guanosine * + #	283.0916	284.0994	282.0838	$C_{10}H_{13}N_5O_5$	-2.7
5'-methylthioadenosine * + #	297.0895	298.0973	296.0817	$C_{11}H_{15}N_5O_3S$	-0.61
Phosphoribosyl-AMP * +	559.0716	560.0795	558.0638	$C_{15}H_{23}N_5O_{14}P_2$	-4.1
Pyrimidine nucleotides					
Metabolite	**Theoretical mass (molecule)**	**Exp. Mass $[M+H]^+$**	**Exp. Mass $[M-H]^-$**	**Formula**	**Log P**
Uridine triphosphate * +	483.9685	484.9763	482.9607	$C_9H_{15}N_2O_{15}P_3$	-3.4
Cytidine monophosphate * +	323.0518	324.0596	322.0440	$C_9H_{14}N_3O_8P$	-3.3
2'-Deoxycytidine-5'-triphosphate * +	466.9896	467.9974	465.9817	$C_9H_{16}N_3O_{13}P_3$	-3.6
2'-Deoxycytidine 5'-diphosphate * + #	387.0232	388.0310	386.0154	$C_9H_{15}N_3O_{10}P_2$	-3
Cytidine * + #	243.0855	244.0933	242.0776	$C_9H_{13}N_3O_5$	-2.8
Cytidine 3'-triphosphate * +	482.9845	483.9911	481.9775	$C_9H_{16}N_3O_{14}P_3$	-4.3
Thymidine * + #	242.0902	243.0980	241.0824	$C_{10}H_{14}N_2O_5$	-1.1
2'-Deoxyuridine 5'-monophosphate * + #	308.0409	309.0487	307.0331	$C_9H_{13}N_2O_8P$	-1.6
Deoxyuridine-diphosphate * + #	388.0072	389.0151	386.9994	$C_9H_{14}N_2O_{11}P_2$	-2.1
Uridine 5'-diphosphate * + #	404.0022	405.0100	402.9943	$C_9H_{14}N_2O_{12}P_2$	-3
Uridine diphosphate glucose * +	566.0550	567.0628	565.0472	$C_{15}H_{24}N_2O_{17}P_2$	-5
N-acetylglucosamine * +	221.0899	222.0977	220.0821	$C_8H_{15}NO_6$	-3.2
Uridine 5'-monophosphate * + #	324.0358	325.0436	323.0280	$C_9H_{13}N_2O_9P$	-2.5
Uridine * + #	244.0695	245.0773	243.0617	$C_9H_{12}N_2O_6$	-2.4
Pyrrolines					
Metabolite	**Theoretical mass (molecule)**	**Exp. Mass $[M+H]^+$**	**Exp. Mass $[M-H]^-$**	**Formula**	**Log P**
1-pyrroline-5-carboxylate * + #	113.0476	114.0555	112.0398	$C_5H_7NO_2$	-2.3
Pyridines and derivatives					
Metabolite	**Theoretical mass (molecule)**	**Exp. Mass $[M+H]^+$**	**Exp. Mass $[M-H]^-$**	**Formula**	**Log P**
Pyridoxal 5'-phosphate * + #	247.0245	248.0324	246.0167	$C_8H_{10}NO_6P$	-2.1
Pyridoxine * + #	169.0738	170.0817	168.0660	$C_8H_{11}NO_3$	-0.95
Nicotinic acid * + #	123.0320	124.0398	122.0242	$C_6H_5NO_2$	-0.17
Niacinamide * + #	122.0480	123.0558	121.0401	$C_6H_6N_2O$	-0.39

Pyridine nucleotides					
Metabolite	**Theoretical mass (molecule)**	**Exp. Mass $[M+H]^+$**	**Exp. Mass $[M-H]^-$**	**Formula**	**Log P**
Nicotinic acid mononucleotide * +	337.0562	338.0640	336.0484	$C_{11}H_{16}NO_9P$	-5.5
Sugar acids and derivatives					
Metabolite	**Theoretical mass (molecule)**	**Exp. Mass $[M+H]^+$**	**Exp. Mass $[M-H]^-$**	**Formula**	**Log P**
Phosphogluconic acid * +	276.0246	277.0402	275.0171	$C_6H_{13}O_{10}P$	-3.5
Tetrapyrroles and derivatives					
Metabolite	**Theoretical mass (molecule)**	**Exp. Mass $[M+H]^+$**	**Exp. Mass $[M-H]^-$**	**Formula**	**Log P**
Uroporphyrinogen-III * + #	836.2752	837.2830	835.2674	$C_{40}H_{44}N_4O_{16}$	1.39
Protoporphyrinogen * + #	568.3049	569.3127	567.2971	$C_{34}H_{40}N_4O_4$	6.2
Protoporphyrin IX * + #	562.2580	563.2658	561.2501	$C_{34}H_{34}N_4O_4$	6.78
Hydroxymethylbilane * + #	854.2858	855.2936	853.2779	$C_{40}H_{46}N_4O_{17}$	0.53
Tetrasaccharides					
Metabolite	**Theoretical mass (molecule)**	**Exp. Mass $[M+H]^+$**	**Exp. Mass $[M-H]^-$**	**Formula**	**Log P**
Maltotetraose * +	666.2218	667.2296	665.2140	$C_{24}H_{42}O_{21}$	-8.2
Thiamine pyrophosphate					
Metabolite	**Theoretical mass (molecule)**	**Exp. Mass $[M+H]^+$**	**Exp. Mass $[M-H]^-$**	**Formula**	**Log P**
Thiamine-pyrophosphate * +	425.0449	426.0527	424.0371	$C_{12}H_{19}N_4O_7P_2S$	-5.8
Thiamine monophosphate * +	344.0708	345.0786	343.0629	$C_{12}H_{17}N_4O_4PS$	-5.7
Thienoimidazolidines					
Metabolite	**Theoretical mass (molecule)**	**Exp. Mass $[M+H]^+$**	**Exp. Mass $[M-H]^-$**	**Formula**	**Log P**
Biotin * + #	244.0881	245.0959	243.0803	$C_{10}H_{16}N_2O_3S$	0.17
Trisaccharides					
Metabolite	**Theoretical mass (molecule)**	**Exp. Mass $[M+H]^+$**	**Exp. Mass $[M-H]^-$**	**Formula**	**Log P**
Maltotriose * +	504.1690	505.1768	503.1612	$C_{18}H_{32}O_{16}$	-6.5

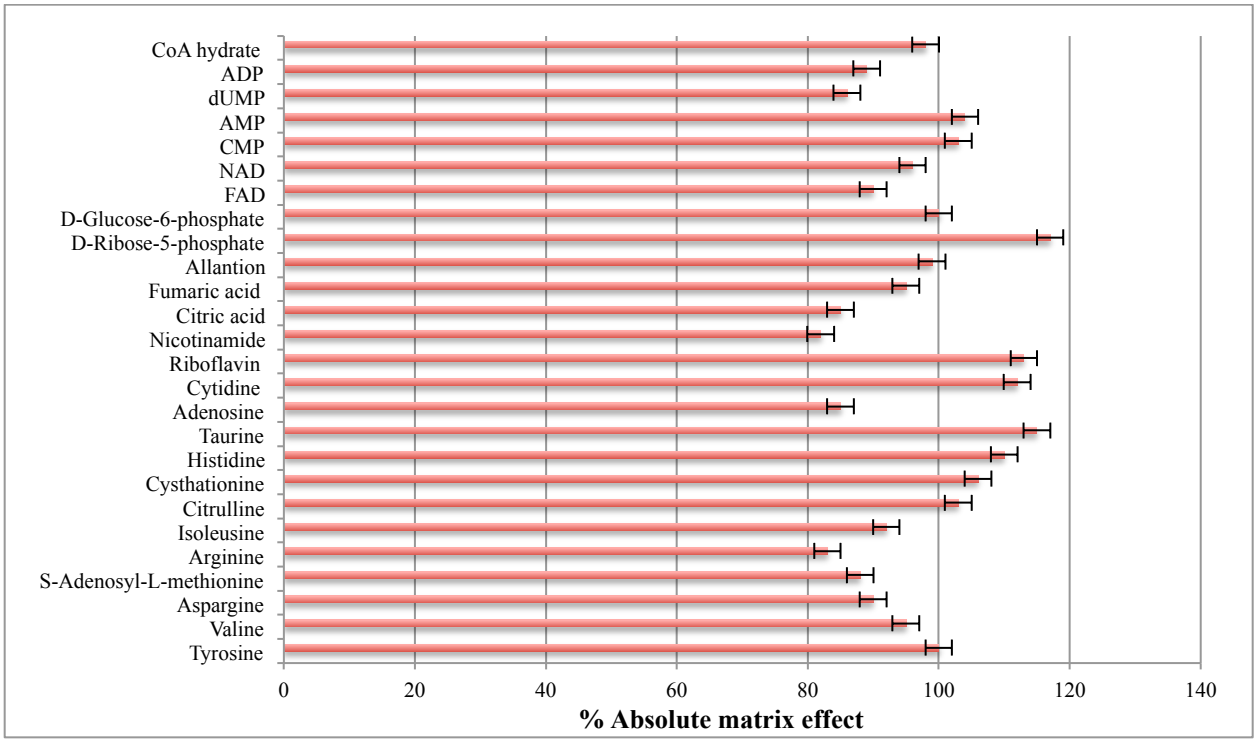

Figure 3.9 Absolute matrix effect for targeted analysis using PS-DVB-WAX: HLB 50:50 [w:w] and Kinetex PFP column.

3.3.4 Stability of metabolites on the coating and preservation before analysis

The stability of the metabolites after extraction on the surface of coating was investigated to determine how long the SPME coatings could be stored after sampling in case there is a need to preserve the coatings before analysis. An evaluation was conducted using a PS-DVB-WAX: HLB 50:50 [w/w] coating at optimized conditions and the Kinetex PFP as the column for separation. Desorption was completed at three time points: immediately after extraction, 5 hours and 10 hours after extraction when stored at room temperature. Coatings were also stored for 20 hours after extraction at -80°C. Results were compared with those obtained from desorptions performed immediately after extraction. The PCA score plot in Figure 3.10 shows the differentiation between various clusters related to desorption immediately after extraction (0h), 5 hours after extraction (5h), and 10 hours after extraction (10h) while storing at room temperature, and desorption after storing coatings for 20 hours at -80°C. A slight difference was observed between 5h and 10h clusters. Low differentiation was also observed between clusters related to stored coatings at -80°C and immediately desorbed coatings. However, differentiation was noted between 5h and 10h clusters with respect to immediate desorption and 20h storage at -80^{o}C. This would indicate that metabolite profile changed over time on the surface of the coatings when the coatings were not kept at very low temperatures. Thus, storage under low freezing conditions could prevent the change and degradation of the extracted metabolites. The identification of the metabolites that altered over time

demonstrated that lipids and amino acids are two classes of metabolites that can undergo changes after extraction on the surface of coatings if the coating is not preserved at a low temperature immediately after extraction. This change can be related to oxidation or degradation of compounds. Unstable lipid metabolites that were noted to decrease when coatings were stored at room temperature before desorption include fatty acids and conjugates such as 3-decenoic acid, tetradecanoic acid; fatty acyls such as 9,13-dihydroxy-11-octadecenoic acid, prenol lipids such as undecaprenyl diphosphate; fatty alcohols such as 1,3,7-octanetriol; glycerophospholipids such as PG(17:1(9Z)/14:0), PG(17:2(9Z,12Z)/0:0). Autoxidation of unsaturated fatty acids exposed to air led to formation of hydroperoxides that degraded to secondary oxidation products such as ketones and aldehydes. This lipid oxidation is widely detected in the food industry, in which the flavor, odour, colour, and nutritional value of foods are negatively affected during storage. The lipid oxidation process is initiated under heat or light stress and increases with the degree of unsaturation [235]. Amino acids and peptides are other examples of unstable metabolites. Tyrosine, glutamine, methionine, proline, aspartic acid, threonine**,** asparagine, and proline betaine were found to be unstable metabolites that decreased by storage at room temperature. Hydrolysis, deamination, oxidation, diketopiperazine and pyroglutamic acid formation, and racemization are potential degradation pathways for peptides and amino acids. For example, dehydration of aspartic acid to form cyclic imide intermediate or deamination of amino acids into aspartic acid or glycine can occur. Oxidation can also occur to amino acids by both chemical and photochemical pathways.

Diketopiperazine and pyroglutamic acid formation can occur to the peptide by cleavage of the first two amino acids in the form of diketopiperazine if proline or glycine is in positions 1 or 2. This conversion can occur in peptides containing asparagine in the N terminal. Chiral integrity of amino acids and peptides can happen as well [236]. In the present study, 2,5-Dioxopiperazine and pyroglutamic acid are two differentiate metabolites increased in 10h samples versus 0h ones.

A decrease in metabolite peak intensities was also indicated for extracted semi-volatiles and volatile organic compounds such as volatile aldehydes, alcohols and indols. Time elapsed in storage allows these compounds to escape from the surface of the coatings. As such, if coatings need to be transferred/transported for further analysis, it suggested that coatings be stored at -80°C and covered with aluminum foil so as to protect the extracted metabolites on the surface of the coatings from photo degradation.

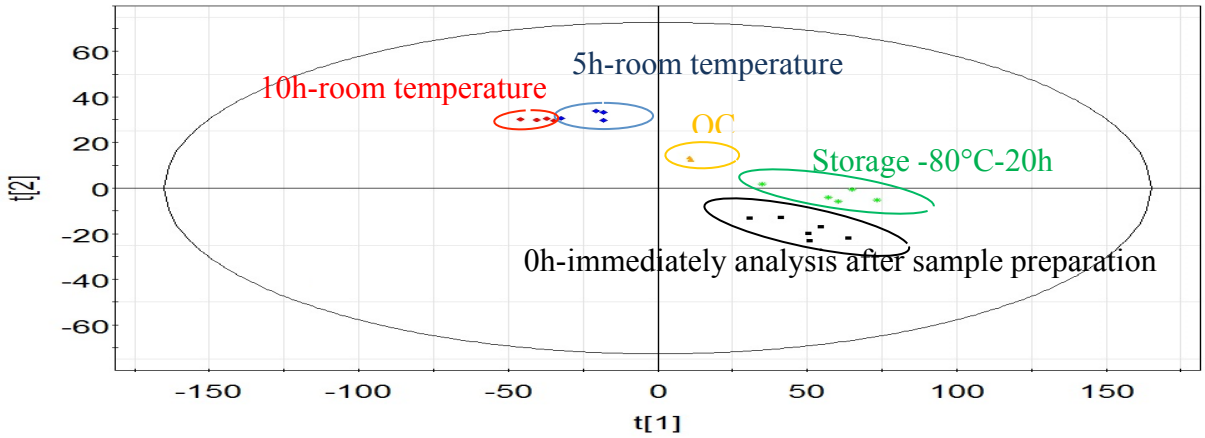

Figure 3.10 PCA sore plot using PS-DVB:HLB 50:50 [w:w] and Kinetex PFP column to evaluate metabolite stability on the surface of coating during storage (positive ionization mode).

3.4 Conclusions and future directions

The objective of this study was to develop a systematic high-throughput metabolomics platform to analyze a broad coverage of metabolites from various samples, including cell, body fluids, and tissue. This is the first study to comprehensively optimize different coating chemistries for the 96-blade SPME system for direct extraction mode of untargeted metabolite profiling studies in combination with LC-MS. As previous studies in this area have concluded, different methods are needed to provide a metabolic profile for a broad coverage of metabolites. Different types of HPLC columns and SPME coating chemistries were applied to identify the best combination of SPME-LC-MS method for metabolomics profiling of bacterial cells with relatively high metabolome coverage. This consisted of accurately measuring wide ranges of classes of compounds in terms of polarities in untargeted metabolic profiling. The proposed and evaluated PS-DVB-WAX:HLB 50:50 [w/w] coating was able to extract the highest number of metabolites with a broader log P range than other previously developed coatings. Moreover, the obtained results demonstrated that each type of SPME coating Chemistry has selectivity towards a specific class of metabolites. Therefore, an individual coating can be selected in order to focus on the specific class of metabolites and do targeted analysis without interferences from other metabolites. The investigation of metabolite stabilities indicate that SPME is able to extract unstable compounds; however, it is important to either immediately proceed with subsequent steps of the analysis or to preserve the coatings with extracted analytes at -80°C freezer in dark. This facilitates to obtain accurate representation of the metabolite composition in the living system. The Kinetex PFP column separated the highest number of features compared with other investigated columns. Based on the results, 2D-LC by using HILIC and RP columns could provide a broader metabolic profile. In the next chapters, the application of the optimized SPME-LC-MS method with widest metabolome coverage described above will be applied towards discovery of potential biomarkers of bacteria/cells under stress conditions.

Chapter 4

Effect of cinnamaldehyde as an antibacterial agent on *E.coli* growth using 96-blade Solid Phase Microextraction coupled to Liquid Chromatography-Mass Spectrometry

4.1 Introduction

In recent times, transcriptomics, proteomics, and metabolomics, as functional genomics techniques, have burgeoned investigative fields in different areas of research; however, their challenging methodologies, particularly for in vivo analysis, have abated further progress in various areas of research [237]. Metabolomics, the newest "omics" science, involves the detection and semi-quantification of low molecular weight (<1000 Da) species in biological systems, referred to as metabolites, which result as end products of cellular reactions corresponding to direct effects on the cell phenotype. Contrastingly, transcriptomics and proteomics are mostly applied to provide extensive information related to genotype [238,239]. Metabolites are the building blocks of proteins, RNA, DNA, and cell membranes. They play important roles in system metabolism, signaling, and regulation with provision of vital components for life. The goal of metabolomics is to investigate the metabolic profiles of biological systems at a specified time and under specific environmental conditions. As metabolomics has the closest proximity to the phenotype of a given biological system, any environmental perturbation in a given biological system is reflected rapidly in its metabolome. For example, studies on stress responses of *E.coli* as a model organism have demonstrated that changes in its metabolic profile are higher than transcript changes. Also, in comparison to other 'omics' approaches, the high-throughput approach available for metabolic analyses of large numbers of samples provides a more cost effective alternative for determinations of changes in biological systems [240].

Recently, microbial metabolomics has received a lot of scientific attention due to its potential applications in a wide range of research areas, for instance, drug discovery and development, food metabolomics, and metabolic engineering [25]. Biofilm formation on food as well as exposure of food contact surfaces to human pathogens enhances their ability to survive in harsh environments, as well as their resistance in response to antibacterial treatments. Biofilm growth inhibition may retard spoilage of edible goods, consequently making them safer for human consumption, which in turn benefits both the food production industry as well as consumers [241]. In this regard, one of the most important areas of research in microbial metabolomics involves investigations into the bactericidal modes of action of antibacterial agents against different bacterial strains.

Plants, as a rich source of biologically active components, have been prominently used as a basis for drug development, contributing to human health [242]. Essential oils, as secondary metabolites produced by aromatic plants, are volatile compounds that are characterized by a strong odor, and used as food preservers due to their antiseptic, bactericidal, virucidal, fungicidal, and medicinal properties. The cytotoxic nature of these compounds is attributed to the presence of phenol, aldehyde, and alcohol functional groups in their structures, which have a pro-oxidant effect on proteins and DNA through the generation of reactive oxygen species [243-245].

The addition of essential oils such as linalool, thymol, eugenol, carvone, cinnamaldehyde, vanillin, carvacrol, citral, and limonene in food products has been accepted by the European Commission and the United States Food and Drug Administration (FDA). To this extent, essential oils have been used as flavors and microorganism growth inhibitors in food products to increase food shelf-life [246].

Previous studies have shown that various biologically active components exhibit differing effects on bacterial growth, as these compounds have unique functional groups that work through different pathways to stop bacterial metabolism. In past work, cluster discrimination between different antibacterial components was observed, as each compound was shown to exhibit stress specificity providing various metabolic patterns [247]. However, in order to introduce a new active component as an antibacterial component, its bacterial resistance mechanism needs to first be characterized.

Cinnamon is one of the oldest herbal medicines used as a spice and traditional medicine. Cinnamaldehyde, as the main component of cinnamon bark extract, produces its distinct cinnamon odor and flavor. This compound has been proven to be active against pathogenic bacteria, fungi, and viruses [248-250]. The target action of cinnamon is introduced either on cell structure and membrane functionality, proteins and enzymes, or other essential processes involved in biosynthesis or energy generation [246]. Cinnamaldehyde is also capable of altering the lipid profile of the microbial cell membrane [251]. Consequently, tracking biochemical alterations during treatment of the biological system by this antibacterial agent could be used to find specific biomarkers or pathway mechanisms [159].

Metabolomics can been conducted through the use of a variety of analytical platforms, although MS coupled to LC or GC has been most regularly applied. Due to the complexity of the biological matrix under study, in this case, bacteria media, appropriate sample preparation steps need to be taken prior to analysis so as to reduce possible matrix effects [240]. To this extent, different sample preparation techniques have been introduced for bacterial metabolomics, each with its own set of advantages and disadvantages. In recent times, SPME has been successfully shown as a feasible technique for global metabolomics determinations. The use of SPME towards metabolomics applications includes several advantages, such as its applicability for in vivo analysis, reduced matrix effects, extraction of a wide

variety of metabolites, extraction of unstable or short-lived metabolites, and circumvention of chemical modification [252].

Recently, qualitative and semi-quantitative analyses of metabolic responses of *E.coli* to cinnamaldehyde were conducted through the use of headspace solid phase microextraction (HS-SPME). This research showed that the metabolic profile of *E.coli* treated by cinamaldehyde changed in comparison to control samples. In this research, 25 volatile and semivolatile metabolites were identified in the HS of complex biological samples [166]. The most important goal in untargeted analysis is to detect as many metabolites as possible so as to enhance the chances of detecting dysregulated metabolites in a biological system, which can indicate the metabolic pathways affected by the stimuli. This chapter presents a comprehensive study of *E.coli* bacteria affected by cinnamaldehyde, performed with the recently developed SPME-LC/MS protocol (Chapter 3) to evaluate potential biomarkers related to the microorganism's response to stress induced by the biologically active component.

In metabolomics investigations, the method chosen for extraction and separation of metabolites must be able provide a comprehensive metabolic profile that reflects the large number of metabolites present in biological systems [253]. The developed 96-blade SPME-UPLC-MS method described in Chapter 3 provides a comprehensive as well as unbiased metabolic profile, ranging from polar metabolites such as amino acids and nucleotides, to nonpolar metabolites such as lipids. The method is simple, fast, reproducible, and incorporates a metabolism-quenching step while providing high-throughput analysis. With the proposed protocol, the extraction of both hydrophilic and hydrophobic metabolites can be performed in one experiment, making this method a time-efficient alternative as compared to solvent-based sample preparation methods. For this series of experiments, The UPLC-MS method was coupled to Orbitrap with high mass resolution, excellent analytical sensitivity, signal stability, and mass accuracy over long analysis time was applied for comparative global metabolomics profiling.

The optimized protocol was applied to sets of samples of *E.coli* harvested at different growth phase time points. The samples were treated with cinnamaldehyde at concentrations ranging from lower to higher than minimum inhibitory concentration (MIC). Different trends in metabolite concentrations were observed over time for each set of experiments, and multivariate analysis was applied towards determinations of statistically significant discriminating features between control and test groups. The observed changes reflected perturbations in the regular metabolic pathways of *E.coli* induced by the bactericidal effect of cinnamaldehyde. The findings were supported by results previously obtained from transcriptomics and proteomics studies.

4.2 Material and methods

4.2.1 Chemical and materials

LC-MS grade solvents and LC-MS grade formic acid (1 mL glass ampules) were obtained from Fisher Scientific (Ottawa, Canada). Polypropylenes deep 96-well plates (Nunc) and easily modified polystyrene–divinylbenzene (Macherey-Nagel) particles were purchased from VWR International (Mississauga, Canada). All metabolites, peptone, yeast extract, NaCl, and cinnamaldehyde were purchased from Sigma–Aldrich. *E.coli* BL21 samples were donated from the laboratory of Professor John Brennan at McMaster University (Hamilton, Ontario, Canada). The Concept 96-SPME-blade unit and robotic Concept 96 autosampler were purchased from Professional Analytical Systems (PAS) Technology (Magdala, Germany) for SPME sample preparation.

4.2.2 Bacterial strain, culture condition, and cinnamaldehyde effect on bacterial strain growth

E.coli BL21 was used as non-pathogenic bacteria for the currently presented microbial metabolomics study. Standard Luria Bertani (LB) media (10 g trypton, 5 g yeast extract, and 5 g NaCl in 1 L nanopure water) was used as media for growth of bacteria, while LB agar media (10 g trypton, 5 g yeast extract, and 5 g NaCl; 15 g Agar in 1 L nanopure water) was used to count the number of colonies forming in units per mL (CFU mL^{-1}) in bacterial suspensions. Cells were grown in nutrient media at 37°C and 125 rpm for 24 hours. To provide countable numbers of colonies present in agar media, cultures were serially diluted with sterile media. Next, 100 µL of diluted media were distributed on the warm agar plate, and incubated at 37°C for a 24-hour period. The growth curve of *E.coli* culture was obtained by counting the CFU mL^{-1} from the first moment of bacteria addition to LB media up until 24 hours had elapsed.

Different concentrations of cinnamaldehyde in methanol (0-2000 mg L^{-1}) were added into the 96-well plate containing a suspension of bacterial cells grown in different cell tubes with an initial concentration of 10^5 CFU mL^{-1}. Subsequently, growth curves were obtained for each of the *E.coli* cultures grown on the plate with agar gel incubated at 37°C for 24 hours in the presence of cinnamaldehyde. Final and initial CFU mL^{-1} figures were obtained for control cultures and cinnamaldehyde-treated cultures grown under the same conditions, and used to obtain a MIC value for cinnamaldehyde.

4.2.3 Metabolite extraction, and metabolic profiling using 96-blade-SPME-UPLC-MS

In the present study, for each set of samples, bacteria were cultivated in sterile 96-well plates. Subsequently, the 96-thin film (blades) SPME system operated by the robotic Concept 96-autosampler was applied for in vivo metabolite extractions. The stainless steel blades were coated with PS-DVB-WAX:HLB 50:50 [w/w]. The coating preparation procedure as well as information related to the concept

autosampler have been reported in previous works [138]. The experimental design consisted of two approaches: in the first case, bacteria was treated with cinnamaldehyde (below and above MIC) at the beginning of incubation, and extraction was performed at 0, 3, 6, 9, 12, and 15 hours from 1 mL of *E.coli* culture in sterile LB media (initial concentration 5.0 log CFU mL^{-1}). As a control, a sample obtained from the same batch of *E. coli* culture was extracted under identical conditions with no cinnamaldehyde addition. In the second case, cinnamaldehyde (above minimum inhibitory concentration) was added every three hours after *E. coli* incubation up to the 15th hour. For each time point, metabolic profiling data was obtained in triplicate.

The SPME procedure conditions for all experiments were as follows: coatings were conditioned for 120 min in 1 mL ethanol:water 70:30 (v/v) mixture in the 96-well plate with orbital agitation set at 850 rpm. Next, extraction from 1 mL 5.0 log CFU mL^{-1} *E.coli* (initial concentration) in sterile LB media was carried out in direct immersion mode for 60 min with agitation speed set at 1000 rpm (2.5 mm amplitude). After extraction, coatings were washed for 30 seconds in 1 mL of distilled water with 0.1% formic acid under agitation at 850 rpm in order to remove loosely attached particulates and salt from the surface of the sorbent. Desorption was performed in 1 mL acetonitrile:water 50:50 (v/v), at 1500 rpm speed for 60 min. Next, the desorption solution was transferred to the autosampler of the LC–MS system for separation and quantitation. Optimization of the SPME protocol is described in Chapter 3.

Chromatographic separation was performed with a Kinetex PFP column [100 × 2.1mm, 1.7µm] (Phenomenex, Torrance, CA, USA) with a guard filter (SecurityGuard ULTRA Cartridges UHPLC PFP for 2.1 mm). The column temperature was maintained at 25°C, and gradient mobile phase conditions were composed of phase A (water containing 0.1% formic acid) and phase B (acetonitrile with 0.1% formic acid) with the following set conditions: 0-1 min 90% A; 1-9 min 90-10% A; 9-12 min 10% A; 12-16 min 10-90% A. All extracts were injected randomly, while blank and QC samples were injected throughout the sequence between every 15 extract injections so as to avoid cross contamination, as well as verify instrument performance. The QC sample was prepared by mixing 10 µL aliquots of each extract. The injection volume was 10 µL. Autosampler temperature was set at 4°C, and extracts were kept at 4°C.

The high-resolution orbitrap Exactive mass spectrometer (Thermo, San Jose, California, USA) was operated in both negative and positive electrospray ionization (ESI) modes and at 100-1000 m/z mass range. Optimum sheath gas (arbitrary units), auxiliary gas (arbitrary units), ESI voltage (kV), capillary voltage (V), capillary temperature (°C), and tube lens voltage (V) were set at 40, 25, 4.0, 27.5, 275, and 100 for positive ESI mode, and 50, 25, -2.7, -67.5, 325, and -85 for negative ESI mode. External instrument mass calibration was performed every 24 h, resulting in 2 ppm mass accuracy. Compound identification was confirmed for discriminant features using a Q-Exactive mass spectrometer (Thermo Fisher Scientific, CA, USA) operating in positive and negative ionization modes with the same

chromatographic conditions as the primary analysis. Collision energy ranging from 50-100 V was applied for MS/MS fragmentation of target ions.

4.2.4 Metabolite identification, data mining, and statistical analysis

The raw data (.raw) obtained with Xcalibur software version 2.1 (Thermo) was converted to (mzXML) with the MS conversion software. The converted data was then processed with the XCMS R-package (Scripps Center for Metabolomics, California, USA). The output is a table containing retention times, m/z, and intensity of features [142]. Alignment, framing, peak picking, and feature detection were done with R software. The CAMERA R-package (Bioconductor Version 2.10) was applied to provide ion annotation on the list of features so as to identify detected isotopes, adducts, and in-source fragment ions.

Putative identification of discriminant compounds was based on comparisons of their accurate masses with METLIN online database queries, using a 5 ppm tolerance window. Data from MS/MS METLIN and MassBank databases as well as literature surveys were subsequently applied to confirm the identification of putative candidates. Moreover, commercially available chemical standards were analyzed by UPLC-MS and MS/MS to confirm metabolite identities by retention time and mass spectral matching. Ions were targeted by collision energy and the MS/MS fragmentation and retention time of discriminant features were compared by those of commercially available chemical standards. Calculations and comparisons between expected m/z values of common adducts for common adduct species and observed experimental values were done from peaks within spectra.

Multivariate data analysis was performed with the use of SIMCA-P+ software (Umetrics, NJ, USA) for statistical analyses. PCA and PLS-DA were used to assess information regarding variances in metabolic phenotypes corresponding to bacteria cultures treated with antibacterial agents at different time points in comparison to control samples at the same time intervals. Potential biomarkers for distinguishing treated *E.coli* by cinnamaldehyde from control *E.coli* cultures were acquired by analysis of S-plots obtained from OPLS score plots. The KEGG database was used in the identification of important metabolic pathways and subsequent biological interpretations. For this data processing step, abundant dysregulated features were filtered according to the following criteria: p-value < 0.01, fold change >1.5, and MS peak intensity >10000 ion counts, representing the threshold required to generate high-quality MS spectra on an Orbitrap instrument.

4.3 Results and discussion

4.3.1 E.coli and effect of cinnamaldehyde on *E.coli* growth

In order to investigate the influence of cinnamaldehyde on *E. coli* growth, the minimum concentration of cinnamaldehyde needed for inhibition of *E.coli* growth was obtained via addition of different

concentrations of cinnamaldehyde to media containing the same *E.coli* concentration (Figure 4.1). As can be seen, concentrations of cinnamaldehyde above the 500 mg L^{-1} threshold resulted in total inhibition of *E.coli* at an initial concentration of 10^5 CFU mL^{-1} in LB media.

The influence of sub-lethal doses of cinnamaldehyde (100 mg L^{-1}) on bacteria growth was also studied and compared with control samples. Bacterial growth was observed through lag phase, exponential phase, and stationary phase. For the system under study, a slow growth of *E.coli* was observed for 3 hours after incubation. The bacteria then proceeded to enter its exponential phase for a subsequent 12 hour period. Lastly, exponential growth was observed to stop in batch cultures, indicating the bacteria reached its stationary stage. Figure 4.2 demonstrates the growth curve of *E.coli* at control conditions in comparison to samples where cinnamaldehyde was added in sub-lethal concentrations. At sub-lethal concentrations of cinnamaldehyde, the rate of bacterial growth was observed to decrease during the lag phase, which was prolonged for 6 hours in comparison to the control culture; following this period, bacteria cultures were observed to achieve stable growth after adaptation to the new environment.

As described in the Experimental section, cinnamaldehyde was also added to bacteria culture at different incubation time points. In the case of bacteria treated with cinnamaldehyde at lethal concentrations (above MIC), immediately after cell incubation, no bacteria were observed to appear on the agar gel plating during growth, indicating that at the established concentrations, cinnamaldehyde completely inhibited bacterial growth. Cinnamaldehyde, as an antibacterial agent containing an aldehyde group in its structure conjugated to a carbon double bond with a highly electronegative arrangement, interferes with biological processes involving electron transfers. It covalently binds with nitrogen-containing structures such as DNA and proteins via their amine groups, thus extinguishing the metabolic functions of *E.coli* [251]. The polarity of this bond makes the carbon atom electrophilic and reactive to nucleophiles such as primary amines; it also reacts with oxygen-, sulfur-, or nitrogen-centered nucleophiles, resulting in carbamates, thiocarbamates, or thiourea derivatives, respectively, under mild conditions. To monitor the metabolic stress response of *E.coli* exposed to cinnamaldehyde, samples treated with different conditions were taken from different stages of the growth curve for analysis, followed by subsequent analysis of changes in metabolic profiling between treated and control *E.coli* samples.

4.3.2 E.coli metabolic profiling (different phases)

Metabolite profiling of *E.coli* during different growth stages was performed using untargeted LC-MS analysis. According to the obtained results, the highest numbers of features were obtained during the exponential phase of the control samples: 83722 and 77382 features in positive and negative modes, respectively. The features of all chromatographic peaks were extracted for the discovery of discriminative metabolites during bacteria growth. A total of 500 unique metabolites were detected after a comparison of

features against metabolite candidates available from the METLIN database. As multiple hits were observed for some metabolites, a final list of 300 metabolites was proposed.

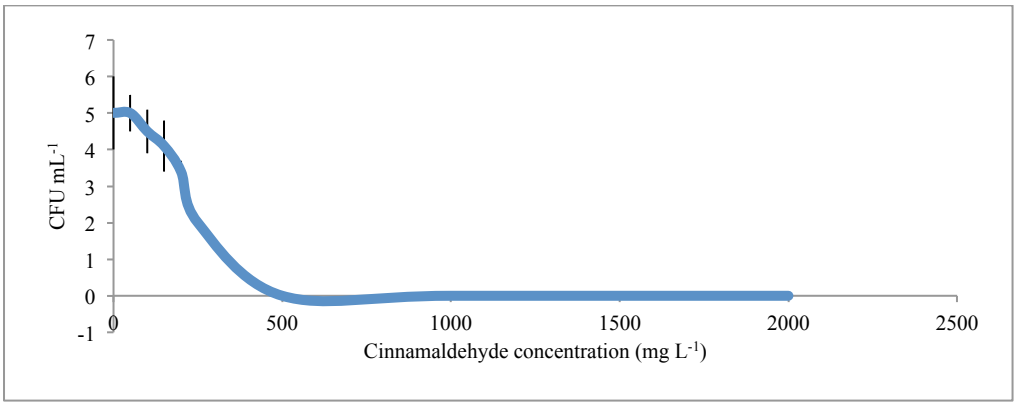

Figure 4.1 Investigation of MIC of cinnamaldehyde on *E.coli* (10^5 CFU ml^{-1}) growth. E.coli growth stopped for the 10^5 CFU ml^{-1} via treating the system by cinnamaldehyde above 500 mg L^{-1}-biological replicates 3 times for each point.

The trends in the obtained metabolite profiles were observed to change at different growth phases, as shown in Figure 4.3. For instance, levels of amino acids such as phenylalanine or serine were observed to increase during the lag phase, and then decrease during the log phase, while for other amino acids, such as threonine, isoleucine, and valine, values were observed to increase gradually during all phases. Increased levels of most amino acids during the stationary phase may suggest an enhancement in enzymatic activity related to protein degradation. Changes in the lipid composition of bacteria were also observed during *E.coli* growth, especially for fatty acids and phospholipids; throughout the *E. coli* growth cycle, levels of saturated fatty acids such as myristic acid and palmitic acid were observed to increase, while levels of unsaturated fatty acids such as palmitoleic acid were observed to decrease. Moreover, increases in cyclopropane fatty acids such as cis-9,10 methylene hexadecanoic acid, and 11-R 12-S methylene octadecanoic acid were observed to occur during the *E.coli* growth cycle; further validating previous findings by Kates et al. reported the accumulation of cyclopropane fatty acids as a result of microorganism growth such as *Serratia marcescens, Lactobacillus* sp., and *E.coli* [254].

In the present work, levels of phospholipids such as phosphatydil glycerol (PGs) were also observed to decrease, while phosphatidylethanolamine acid (PEs) levels correspondingly decreased. Previous work has indicated that the observed decrease in unsaturated fatty acids during the growth cycle of *E.coli* could be attributed to their conversion to cyclopropane fatty acids, while the observed decrease in PGs levels may be connected to their conversion to cardiolipin. Cardiolipin is involved in the transfer of phosphatidyl functional groups from one PG to the hydroxyl group of another PG [255]. It is likely that the observed metabolic alterations are linked to bacteria adaptation to new media conditions due to the increase in bacteria numbers during growth.

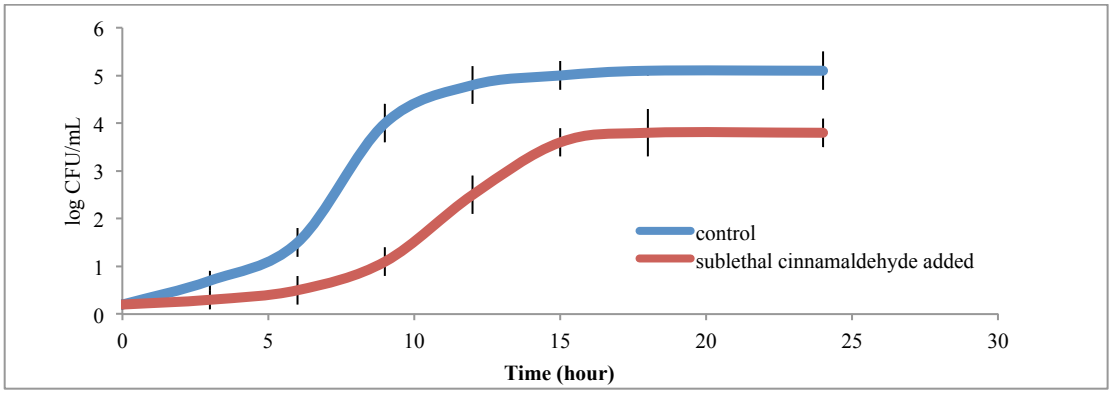

Figure 4.2 *E.coli* growth curves for control sample, and cinnmaldehyde treated bacteria at sublethal concentration. Comparison between two curves demonstrates delay in lag phase and exponential phase of *E.coli* growth.

4.3.3 Identification of discriminant metabolites in cinnamaldehyde treated bacteria during *E.coli* growth

To characterize the metabolic response of *E.coli* to cinnamaldehyde as an antibacterial agent, comparisons of signal abundance in control versus treated groups were conducted for cinnamaldehyde at two different concentrations, below and above the minimum inhibitory concentration (MIC=500 mg L^{-1}), 100 mg L^{-1} and 2000 mg L^{-1}, respectively. For this purpose, different types of experiments were designed so as to evaluate results in terms of different errors (biological or nonbiological), as well as explain significant biological differences with higher confidence. Biological replicates were prepared for *E.coli* samples grown and treated under the same conditions in different 96-well plates and in different days so as to monitor possible biological variability. Moreover, technical replicates were performed in order to determine experimental error attributed to the analytical techniques employed (SPME, MS, and LC methods). The obtained results indicated a variation of less than 10% RSD for the technical analytical approach, while PCA score plots were used to demonstrate variability in biological replicates. PCA score plots showed clear separation between extractions performed for treated *E.coli* groups and controls, as well as extractions conducted between different incubation times, in addition to good clustering of QC samples for both positive and negative ionization modes. Two principal components explain 64% of the variance; PC1 51% and PC2 13% for positive ESI, and PC1 45% and PC2 12% for a total negative ESI of 57%.

Further characterization of the differences between groups was performed using the PLS model. For PCA, the PLS plot demonstrated clear separation between treated and control bacteria at different growth time points. S-plots obtained from OPLS analysis provided retention times, exact masses, and fragmentation patterns that were used for identification of discriminating metabolites.

Trends in time-dependent metabolite profiles were observed for both concentrations of cinnamaldehyde. Metabolic variations for both immediate cinnamaldehyde addition, and cinnamaldehyde addition to growing cultures at different time intervals were also investigated.

Figure 4.4 presents metabolic profiles of bacteria affected by cinnamaldehyde at 100 mg L^{-1}, while Figure 4.5 presents a list of metabolite changes after 12 hours of bacteria incubation in the presence of cinnamaldehyde (added to growing media immediately after incubation, concentration below MIC) as compared with control results (non-treated *E. coli*). Results showed an increase in levels of amino acids for samples treated with cinnamaldehyde at MIC, while levels of metabolites related to the TCA cycle such as fumaric acid, malic acid, and glucose 6-phosphate were observed to decrease, indicating down-regulation of TCA cycle metabolism. Levels of saturated fatty acids were observed to increase while unsaturated fatty acid levels were observed to decrease, resulting in prolonged bacteria life time likely attributed to increasing cell membrane fluidity in stress conditions. An increase in levels of cyclopropane fatty acids such as cis-9,10 methylene hexadecanoic acid, and 11-R 12-S methylene octadecanoic acid was observed to occur in relation to cinnamaldehyde addition. Karkas et al. reported that at severe environmental conditions, small amounts of cyclopropane fatty acids were produced to protect the double bound of fatty acids from oxidation [256]. Other studies have also shown an increase in these metabolites as a function of bacteria growth at high temperature conditions [257,258]. In the present work, the observed increase in cyclopropane fatty acids by cinnamaldehyde addition could support the evidence of bacteria adaptation to newly introduced harsh conditions.

In addition, increases in levels of N-methylated amino acids such as proline were observed to occur. *E.coli* responds to cinnamaldehyde addition as a stress factor by adjusting its membrane composition through the production of N-methylated amino acids such as proline, which function to maintain cell turgor by osmotic regulation and redox metabolism to eliminate excess amounts of reactive oxygen species (Figure 4,5). N-methylated amino acids produced by a new class of genes called *osm* (osmotic tolerance) were introduced as potent osmoprotectants and anti-stress activity regulators against dehydration in bacteria by Le Rudulier et al [259]. The potential of these metabolites in the presence of naturally occurring compounds in bacteria environment was confirmed through the introduction of cinnamaldehyde in growing bacteria. The cell membrane is the first target of cinnamaldhyde, as this compound can change membrane permeability as well as protein functions embedded inside the membrane. Lambert et al. and Burt et al. reported that in the presence of sub-lethal concentrations of naturally occurring antibacterial agents, bacteria reacts by overexpressing stress-response proteins to repair damaged proteins; however, at lethal concentrations, this response is unable to prevent cell death [260,261].

4.3.4 Potential biomarkers in the case of *E.coli* treated by cinnamaldehyde above MIC

No bacteria growth was observed for bacteria cultures treated with cinnamaldehyde above MIC immediately after incubation (t=0). Growing bacteria cultures treated with cinnamaldehyde above MIC every 3 hours after inoculation were sampled every 60 minutes following cinnamaldehyde addition. PCA score plots (Figure 4.6 and Figure 4.7) showed clear separation between treated *E.coli* groups and controls, as well as good clustering of QC samples for both positive and negative ionization modes. Pooled quality control (QC) samples were analyzed following introduction of every set of 15 samples. In the PCA score plots, the QC samples are tightly located in the middle, demonstrating good reproducibility of analysis for this metabolomics study. Metabolic profiling of *E.coli* before perturbation at different time points demonstrated significant metabolic changes. Furthermore, the metabolic profiles of bacteria treated by cinnamaldehyde under MIC showed significant differentiation from samples treated with sequential addition of cinnamaldehyde levels above MIC threshold. Individual clusters were found to contain samples corresponding to different time points and different cinnamaldehyde dosing regimens, demonstrating that different pathways of bacterial metabolome are affected by application of cinnamaldehyde at different stages of *E. coli* growth.

A total of 32 up- and 27 down-regulated metabolites were detected (p-value < 0.0001) for samples dosed with cinnamaldehyde above MIC treatment levels. The list of identified compounds is provided in Table 4.1. Data analysis demonstrated that cinnamaldehyde addition above MIC inhibited the metabolism of *E.coli* via different mechanisms, such as inhibition of enzyme-catalyzed reactions, inhibition of cell membrane synthesis following cell lysis and cell death, inhibition of protein synthesis, and protein disruption, which cause disruption of essential enzymatic synthesis, as well as interaction with plasma membranes, consequently affecting membrane permeability as well as metabolism inhibition. Comparisons of profiles yielded significant differentiation in the metabolic pathways of bacteria treated with cinnamaldehyde. Based on the obtained results, it can be concluded that introduction of lethal doses of cinnamaldehyde disrupts different metabolic pathways such as fatty acids, phospholipids, amino acids, peptides, glycolysis, as well as the TCA cycle, which is discussed in the following section. To the best of this author's knowledge, this is the first time that some of the observed changes in the metabolic pathway of *E.coli* as a function of cinnamaldehyde dosing are reported in the literature.

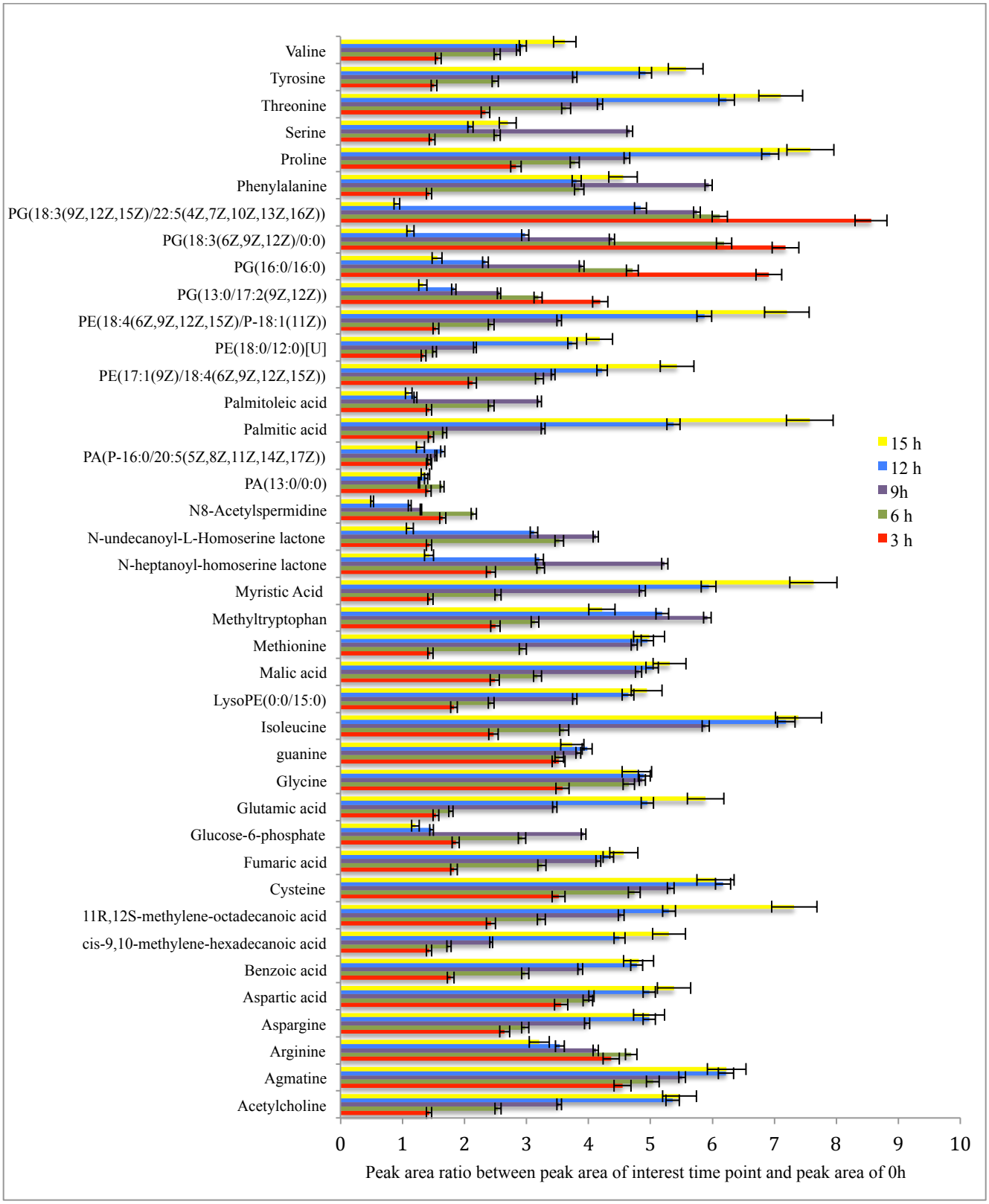

Figure 4.3 Statistically significant changed metabolites ($p<0.001$) during *E.coli* growth (control samples) as a ratio of peak area of interest time point and peak area of 0h. Error bars are related to biological replicates.

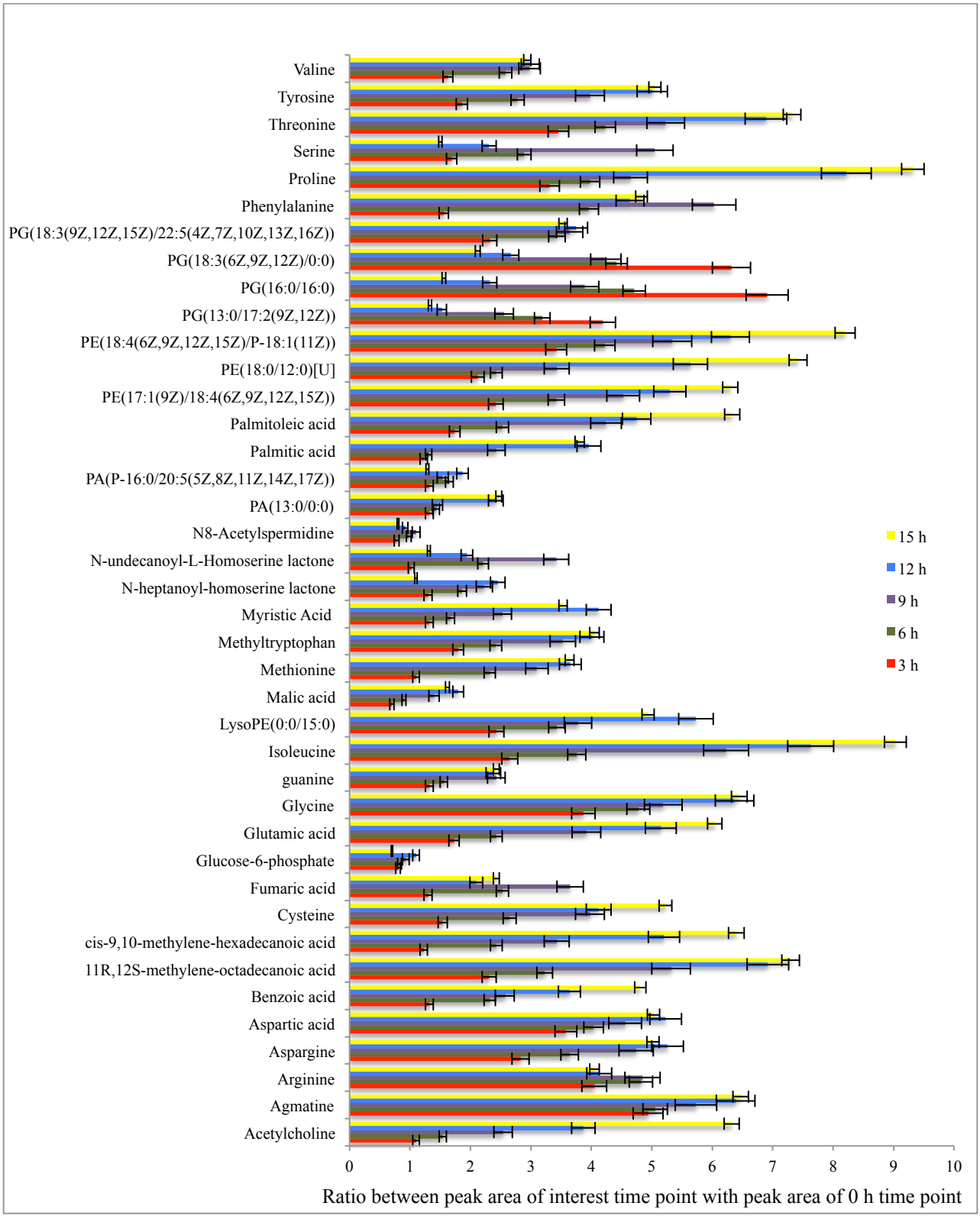

Figure 4.4 Statistically significant metabolite changes ($p<0.001$) during *E.coli* growth curve as a ratio of peak area of interest time point and peak area of 0h for cinnamaldehyde treated *E.coli* (under MIC). Error bars are related to biological replicates.

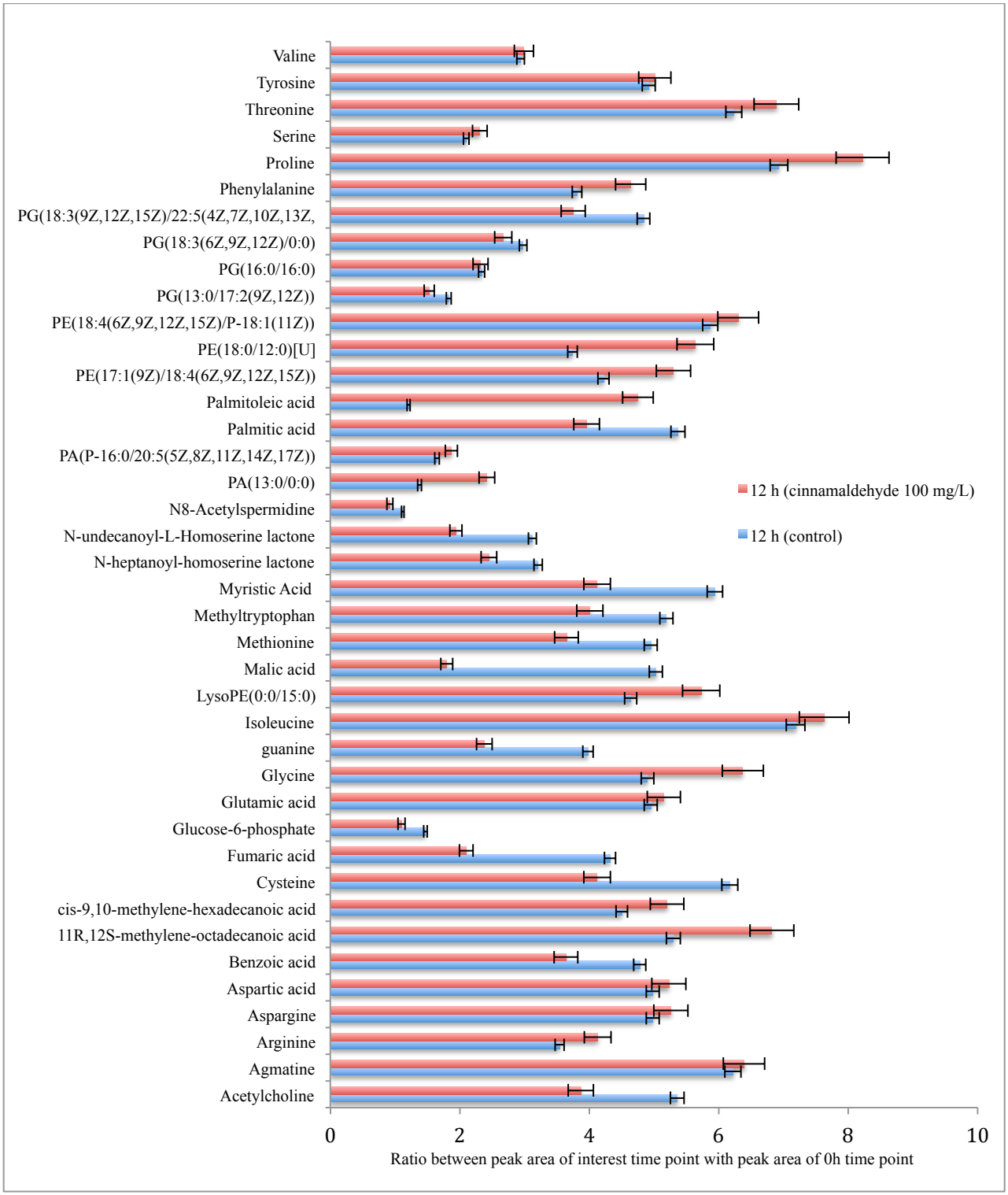

Figure 4.5 Comparison of statistically significant metabolic change ($p<0.001$) between control *E.coli*, and cinnamaldehyde (under MIC) treated *E.coli* at t=12 hours after incubation, error bars are related to biological replicates.

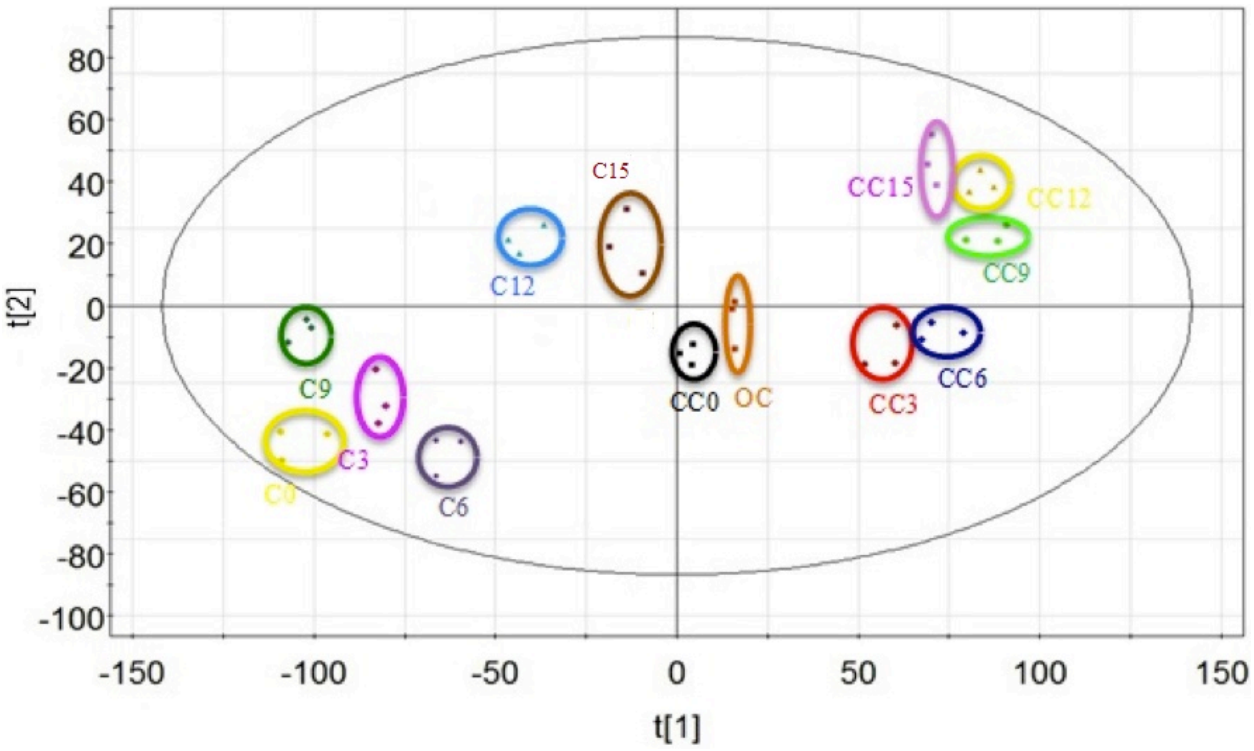

Figure 4.6 PCA score plot_positive ESI mode: *E.coli* bacteria during growth curve at # hours after bacteria incubation in meida and treatment by cinnamaldehyde above MIC at # hours: CC#, control bacteria during growth curve at # hours after incubation: C#. (Experimental points are related to biological replicates).

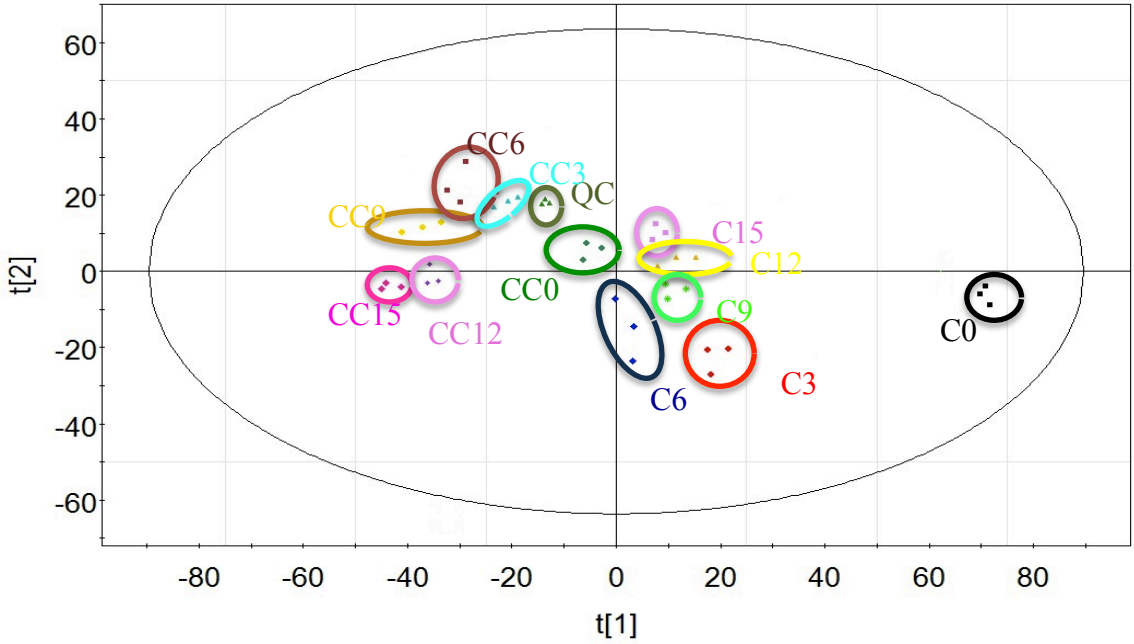

Figure 4.7 PCA score plot_negative ESI mode: *E.coli* bacteria during growth curve at # hours after bacteria incubation in meida and treatment by cinnamaldehyde above MIC at # hours: CC#, control bacteria during growth curve at # hours after incubation: C#. (Experimental points are related to biological replicates).

Table 4.1 Statistically significant differentiated metabolites between cinnamadehyde treated bacteria above MIC added every 3 hours after incubation and control *E.coli* sample (metabolites confirmed by retention time and fragmentation pattern matching with commercially available standards are highlighted in bold font)
(Regulation:↑↓; Up-regulated:↑; Down-regulated: ↓)

Metabolite	Chemical formula	METLIN ID	Class	P value	mz	↑↓	Adduct	ppm
Betaine aldehyde	$C_5H_{11}NO$	278	Alkylamines	0.00062	102.0910	↓	M+ H	-2.9
Carnitine	$C_7H_{15}NO_3$	63461	Alkylamines	4.45447e-6	162.1131	↑	M+ H	4.3
Indole-3-acetaldehyde oxime	$C_{10}H_{10}N_2O$	63562	Amino Acids and Derivatives	2.36999e-8	175.0871	↓	M+H	3.4
N(6)-[(Indol-3-yl)acetyl]-L-lysine	$C_{16}H_{21}N_3O_3$	66141	Amino Acids and Derivatives	5.95920e-7	304.1660	↓	M+H	1.6
Glycine betaine	$C_5H_{11}NO_2$	287	Amino Acids and Derivatives	7.81195e-7	118.0866	↓	M+H	3.3
2-hydroxymethylserine	$C_4H_9NO_4$	65894	Amino Acids and Derivatives	2.15173e-7	136.0610	↑	M+ H	4.4
N2-(D-1-Carboxyethyl)-L-lysine	$C_9H_{18}N_2O_4$	63467	Amino Acids and Derivatives	9.61847e-6	219.1331	↑	M+H	-3.6
Phenylacetylglycine	$C_{10}H_{11}NO_3$	4237	Amino Acids and Derivatives	6.60221e-7	194.0815	↑	M+H	1.7
5-methoxytryptophan	$C_{12}H_{14}N_2O_3$	103475	Amino Acids and Derivatives	2.47692e-6	257.0901	↑	M+Na	1.9
Phenylalanylproline	$C_{14}H_{18}N_2O_3$	23997	Amino Acids and Derivatives	0.00002	263.1393	↑	M+H	1.1
3-(Phosphoacetylamido) alanine	$C_5H_{11}N_2O_7P$	66116	Amino Acids and Derivatives	0.00001	280.9932	↑	M+K	-1.1
Proline	$C_5H_9NO_2$	29	Amino acids and derivatives	0.00003	116.0710	↑	M+H	3.4
Aspartic acid	$C_4H_7NO_4$	15	Amino acids and derivatives	0.00001	134.0448	↑	M+H	0
Glutamic acid	$C_5H_9NO_4$	19	Amino acids and derivatives	1.4215e-6	148.0604	↑	M+H	0
Phenylalanine	$C_9H_{11}NO_2$	28	Amino acids and derivatives	2.2586e-7	166.0868	↑	M+H	3.6
Histidine	$C_6H_9N_3O_2$	21	Amino acids and derivatives	0.00005	156.0769	↑	M+H	1.2
Arginine	$C_6H_{14}N_4O_2$	13	Amino acids and derivatives	5.0953e-7	175.1189	↑	M+H	0
Tryptophan	$C_{11}H_{12}N_2O_2$	33	Amino acids and derivatives	0.000014	205.0972	↑	M+H	0
Methionine	$C_5H_{11}NO_2S$	26	Amino acids and derivatives	1.16363e-6	150.0584	↓	M+H	0
Valine	$C_5H_{11}NO_2$	35	Amino acids and derivatives	0.000036	118.0864	↑	M+H	1.7
Isoleucine	$C_6H_{13}NO_2$	23	Amino acids and derivatives	6.53741e-8	132.1020	↑	M+H	0.7
Cysteine	$C_3H_7NO_2S$	3757	Amino acids and derivatives	0.000071	122.0275	↑	M+H	4.1
Threonine	$C_4H_9NO_3$	32	Amino acids and derivatives	0.000033	120.0656	↑	M+H	0.8
Glutamine	$C_5H_{10}N_2O_3$	18	Amino acids and derivatives	4.66183e-6	147.0771	↑	M+H	4.7
Lysine	$C_6H_{14}N_2O_2$	71200	Amino Acids and Derivatives	3.52559e-9	147.1129	↑	M+H	0.7
Galactosyl 4-hydroxyproline	$C_{10}H_{16}O$	86214	Carboxylic acid and derivatives	1.457687e-6	153.1281	↑	M+H	4.6
Phytic acid	$C_6H_{18}O_{24}P_6$	4238	Cyclic alcohols and derivatives	0.00047	698.8250	↓	M+K	0.8
myo-inositol 3-triphosphate	$C_6H_{13}O_9P$	359	Cyclic alcohols and derivatives	3.83342e-6	261.0372	↓	M+ H	1
8-Methylnonenoate	$C_{10}H_{17}O_2$	62842	Fatty Acids and Conjugates	1.55983e-10	170.1304	↓	M+H	1.8
7-oxo-11E-Tetradecenoic acid	$C_{14}H_{24}O_3$	45868	Fatty Acids and Conjugates	1.65801e-6	241.1804	↓	M+H	2.5
Fumarylacetic acid	$C_6H_6O_5$	45910	Fatty Acids and Conjugates	1.27344e-6	181.0101	↓	M+Na	-3.3

6,8,10,12-pentadecatetraenal	$C_{15}H_{22}O$	91269	Fatty Acids and Conjugates	6.71761e-6	241.1563	↓	M+ Na	0
9,10-dihydroxy-12-octadecenoic acid	$C_{18}H_{34}O_4$	35501	Fatty Acids and Conjugates	9.52547e-7	337.2351	↓	M+Na	0.6
3,5,7-Trimethyl-undecatetraene	$C_{14}H_{22}$	97470	Fatty Acids and Conjugates	0.00024	191.1793	↓	M+H	-0.5
Hexadecatetraenoic acid	$C_{16}H_{24}O_2$	34835	Fatty Acids and Conjugates	0.00055	249.1845	↓	M+H	-1.6
13-Hexadecenoic acid	$C_{16}H_{30}O_2$	34927	Fatty Acids and Conjugates	6.3251e-6	277.2145	↓	M+Na	2.8
Dodecadienoic acid	$C_{12}H_{20}O_2$	34896	Fatty Acids and Conjugates	0.00160	197.1534	↓	M+H	-1.0
α-hydroxy myristic acid	$C_{14}H_{28}O_3$	35391	Fatty Acids and Conjugates	3.27691e-7	267.1955	↓	M+Na	9.3
Myristoyl-EA	$C_{16}H_{33}NO_2$	46563	Fatty Acids and Conjugates	0.00001	310.2136	↓	M+K	-1.9
2-hydroxy capric acid	$C_{10}H_{20}O_3$	35411	Fatty Acids and Conjugates	0.00071	187.1338	↓	M-H	-0.7
9,12-hexadecadienoic acid	$C_{16}H_{28}O_2$	34787	Fatty acids and conjugates	0.00086	251.2010	↓	M-H	2
6-Tridecene	$C_{13}H_{26}$	97873	Fatty Acids and Conjugates	7.33244e-7	181.1955	↓	M-H	-3.3
4-keto lauric acid	$C_{12}H_{22}O_3$	35733	Fatty Acids and Conjugates	0.00038	215.1644	↑	M+H	1.4
2-keto palmitic acid	$C_{16}H_{30}O_3$	35744	Fatty Acids and Conjugates	0.00005	269.2117	↑	M-H	-1.8
2,6 dimethylheptanoyl carnitine	$C_{16}H_{31}NO_4$	58391	Fatty Acid Esters	5.44908e-6	324.2151	↓	M+ Na	1.8
9,12-hexadecadienoic acid	$C_{16}H_{28}O_2$	34787	Fatty acyls	0.00086	251.2012	↓	M-H	-1.6
Hexadecanoic acid	$C_{16}H_{32}O_2$	187	Fatty acyls	0.00086	255.2324	↑	M-H	-1.9
Pentadecatetraenal	$C_{15}H_{22}O$	91269	Fatty aldehydes	6.71761e-6	217.1591	↓	M-H	-2.7
Dodecanamide	$C_{12}H_{25}NO$	36671	Fatty amides	0.00029	200.2013	↑	M+ H	2.4
1-nonaDecanol	$C_{19}H_{40}O$	26349	Fatty alcohols	5.83294e-7	283.2999	↓	M-H	-2.4
PA(13:0/0:0)	$C_{16}H_{33}O_7P$	3886	Glycerophospholipids	1.36265e-8	367.1884	↑	M-H	-1.9
PA(P-16:0/20:5(5Z,8Z,11Z,14Z,17Z))	$C_{39}H_{67}O_7P$	82262	Glycerophospholipids	6.21982e-7	717.4254	↑	M+K	-2.8
PE(18:0/12:0)[U]	$C_{35}H_{70}NO_8P$	40423	Glycerophospholipids	0.00027	664.4898	↑	M+H	-1.9
LysoPE(0:0/15:0)	$C_{20}H_{42}NO_7P$	62289	Glycerophospholipids	0.00018	440.2765	↑	M+H	-1.4
Lysophosphatidylserine	$C_{24}H_{48}NO_9P$	34531	Glycerophospholipids	0.00005	525.3062	↑	M+	-0.8
Agmatine	$C_5H_{14}N_4$	3523	Guanidines	3.88392e-6	131.1286	↓	M+H	-3.8
2-Hydroxydecanedioic acid	$C_{10}H_{18}O_5$	5413	Hydroxy acids and derivatives	1.6437e-7	257.0792	↑	M+K	-3.2
4-hydroxyindole	C_8H_7NO	34514	Indols	2.36999e-8	134.0605	↓	M+ H	-3.7
Methylindole	C_9H_9N	5453	Indols	0.00009	132.0806	↓	M+H	-1.5
Guanine	$C_5H_5N_5O$	315	Imizopyrimidines	2.11405e-9	152.0572	↓	M+Na	3.9
Creatinine	$C_4H_7N_3O$	8	Lactams	0.00234	114.0662	↓	M+H	0
Glucose	$C_6H_{12}O_6$	3755	Monosaccharides	6.07467e-6	203.0531	↑	M+Na	2.4
Glutamyl-hydroxyproline	$C_{10}H_{11}N_5O_5$	69076	Peptides	6.80448e-8	282.0821	↑	M+H	-3.8
Prolylhydroxyproline	$C_{10}H_{16}N_2O_4$	58518	Peptides	6.76841e-6	229.1190	↑	M+H	3.4
Tyrosyl-alanine	$C_{12}H_{16}N_2O_4$	85991	Peptides	1.67676e-9	253.1174	↑	M+H	-3.1
Riboflavin (Vitamin B2)	$C_{17}H_{20}N_4O_6$	233	Pteridines and derivatievs	0.00008	377.1460	↑	M+H	1.3
Cyclic CMP	$C_9H_{12}N_3O_7P$	3436	Pyrimidine nucleotides	7.08504e-6	306.0481	↑	M+H	1.3
Hexylglutathione	$C_{16}H_{29}N_3O_6S$	24067	----------	0.00060	392.1854	↑	M+H	1.2

N-decanoyl-L-Homoserine lactone	$C_{14}H_{25}NO_3$	45310	----------	9.41730e-7	256.1923	🡻	M+H	-6.2
N-tetradecanoyl-L-homoserine lactone	$C_{18}H_{33}NO_3$	64716	----------	9.46201e-7	310.2375	🡻	M-H	-3.9

4.3.4.1 Changes in membrane lipids

Results related to comparisons of extractions conducted at different time points of the *E.coli* growth curve using two concentration levels of cinnamaldehyde indicated significant differences between the growth curve course and the obtained metabolite profiles. Of note, the metabolic profile of lipids has been observed to significantly differ under different stress conditions. The cytoplasmic membrane of *E.coli* consists of phospholipids containing three fatty acids: palmitic (hexadecanoic) acid as a saturated fatty acid, as well palmitoleic (hexadecenoic) acid and cis-vaccenic (cis-11-octadecenoic) acid as unsaturated fatty acids [262]. The concurrent changes in unsaturated fatty acid concentration levels, in conjunction with the observed decrease in saturated fatty acid levels in under-MIC cinnamaldehyde-treated cultures, can be attributed as principal factors related to changes in the obtained lipid profile; levels of palmitic acid and docosanoic acid, saturated fatty acids, were observed to decrease, while an increase in the level of palmitoleic acid, an unsaturated fatty acid, was observed to occur. A metabolic pathway investigation indicated that at sub-lethal concentrations of cinnamaldehyde, the enzyme desaturase caused an increase in membrane fluidity by promoting changes in saturated fatty acids to unsaturated fatty acids. In the presence of stress conditions, cells maintain membrane fluidity by recruiting unsaturated fatty acids as membrane phospholipids. Desaturase enzyme produces saturated fatty acids by transferring two hydrogen atoms to oxygen, allowing microorganisms to remain alive longer through the maintenance of membrane structure and function [263]. The consequent increase in bacteria resistance due to this adaptation can be clearly observed through a comparison between the growth curves of *E.coli* treated with sub-lethal cinnamaldehyde concentrations and *E.coli* control groups. However, *E.coli* response to cinnamaldehyde was noted to differ at lethal cinnamaldehyde concentrations. In this condition, levels and the chain length of metabolites such as unsaturated fatty acids 8-methylnonenoate, 7-oxo-11E-tetradecenoic acid, 7-oxo-11E-tetradecenoic acid, fumarylacetic acid, 6,8,10,12-pentadecatetraenal, 9,10-dihydroxy-12-octadecenoic acid, 3,5,7-Trimethyl-undecatetraene, hexadecatetraenoic acid, dodecadienoic acid and their chain length, in addition to hydroxyl fatty acids such as α-hydroxy myristic acid, Myristoyl-EA, and 2-hydroxy capric acid were observed to decrease, while saturated fatty acid concentration of 2-keto palmitic acid were observed to increase concurrently. The observed phenomenon can be attributed to the effect of cinnamaldehyde on enzymes involved in fatty acid synthesis, such as fatty acid enzymes that cause an increase in cis isomers, and multicomponent membrane desaturase enzymes, which produce unsaturated fatty acids by creating double bonds in saturated acyl chains through the elimination and subsequent

transfer of hydrogen atoms to oxygen. According to scanning electron microscopy (SEM) observations conducted by Pasqua et al., damage to the cell membrane due to cinnamaldehyde treatment is accompanied by alterations in fatty acid profiles. The decrease in membrane fluidity caused by changes in metabolic lipid profiles through the enhancement of unsaturated fatty acids is one of the literature-reported effects of cinnamaldehyde applications on bacterial cultures [262]. Damage to the cell membrane causes leakage of macromolecules and cell lysis as well [264-266]. Under these conditions, the membrane does not function properly due to reduced fluidity, and the reduced flexibility of proteins causes improper functions. Previous studies reported a decrease in respiratory activity as well as cytoplasmic material coagulation accompanied by increasing cell membrane rigidity [263,267,268]. In addition, the newly determined change in the metabolic pathway of cinnamaldehyde-treated *E.coli*, observed by significant up-regulation in lysophosphatidylserine, could be related to phospholipase or carboxylic ester hydrolase inactivation, which could be attributed to the interaction of cinnamaldehyde by the above-mentioned enzymes. The chromatogram and corresponding masses assigned as adducts of some lipids are presented in Figure 4.8.

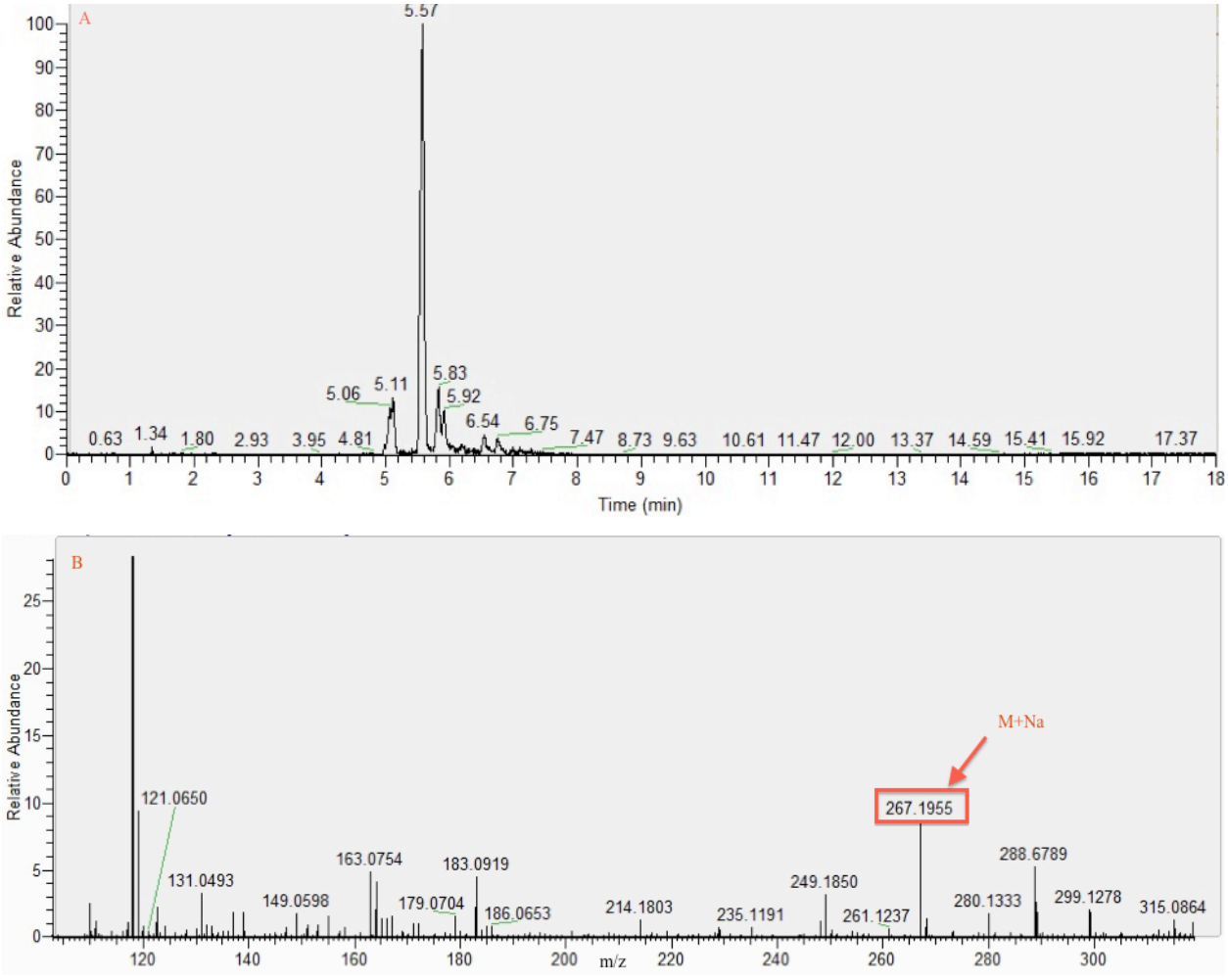

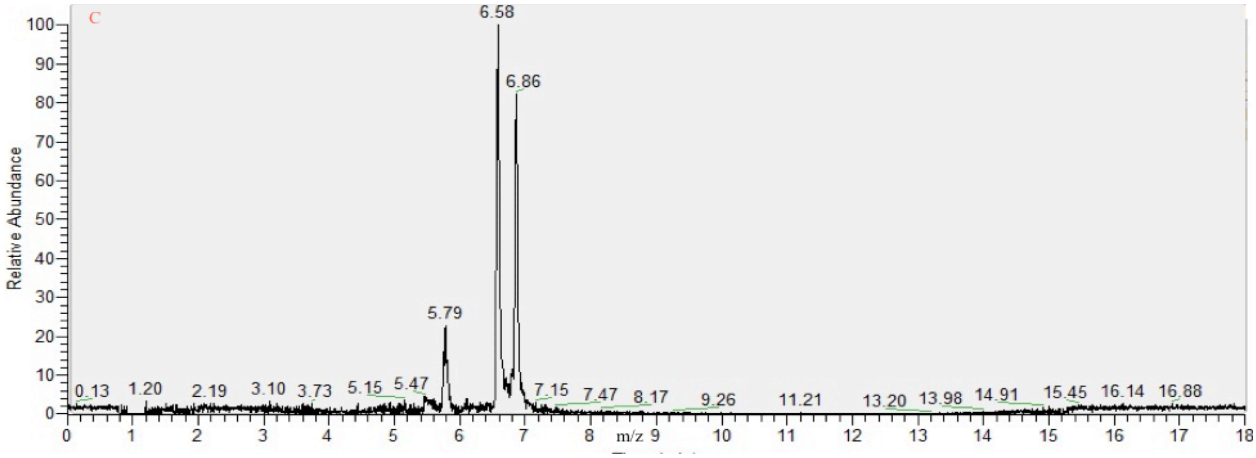
C
Relative Abundance
m/z
6.58
6.86
5.79
0.13
1.20
2.19
3.10
3.73
5.15
5.47
7.15
7.47
8.17
9.26
11.21
13.20
13.98
14.91
15.45
16.14
16.88

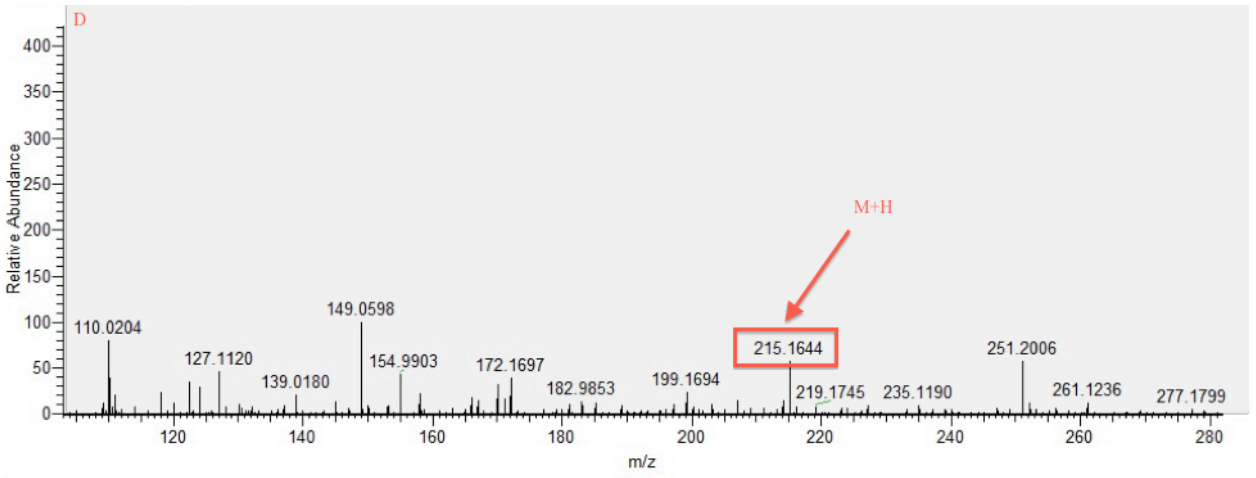
D
Relative Abundance
m/z
M+H
110.0204
127.1120
139.0180
149.0598
154.9903
172.1697
182.9853
199.1694
215.1644
219.1745
235.1190
251.2006
261.1236
277.1799

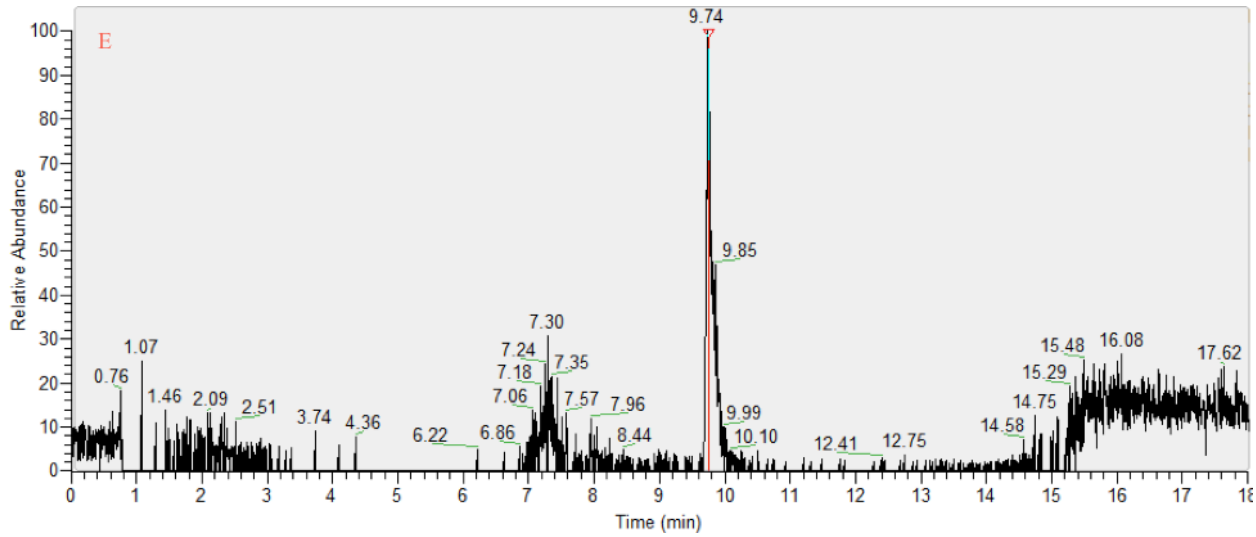
E
Relative Abundance
Time (min)
9.74
9.85
7.30
7.24
7.35
7.18
7.06
7.57
7.96
8.44
6.22
6.86
9.99
10.10
12.41
12.75
14.58
14.75
15.29
15.48
16.08
17.62
1.07
0.76
1.46
2.09
2.51
3.74
4.36

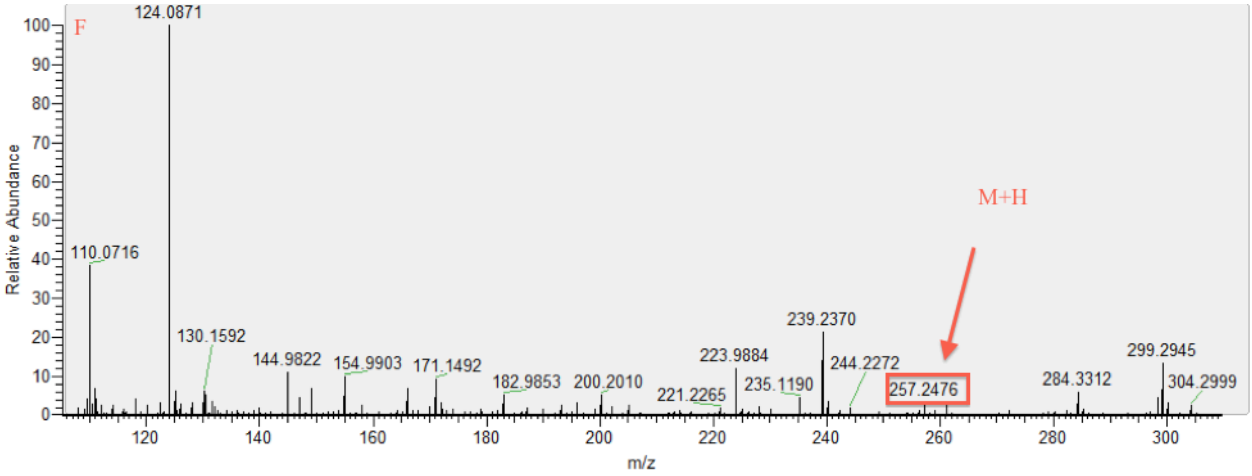

Figure 4.8 Chromatograms and corresponding mass spectra indicating masses assigned as adducts of α-hydroxy myristic acid (A, B), 4-keto lauric acid (C, D), palmitic acid (E,F)

4.3.4.2 Changes in amino acids

The observed increase in levels of amino acids and peptides such as lysine, tyrosyl-alanine, glutamyl-hydroxyproline, 2-hydroxymethylserine, N(6)-[(Indol-3-yl)acetyl] lysine, phenylacetylglycine, lysopine, histidine, 5-methoxytryptophan, phenylalanylproline, 3-(Phosphoacetylamido)alanine, threonine, glutamine, and prolylhydroxyproline could be attributed to protein denaturing and inhibition of protein synthesis, which is caused by a halt in the synthesis of essential enzymes as a result of the addition of cinnamaldehyde. On the other hand, a comparison of changes in metabolite levels between cinnamaldehyde-treated bacteria and control bacteria demonstrated that this compound can perturb enzyme-catalyzed reactions such as glutathione, arginine decarboxylase, and histidine decarboxylase. For example, increases in riboflavin and histidine could be attributed to the interruption of histidine decarboxylase action. Conversely, a decrease in the agmatine metabolite may be caused by the inhibition of arginine decarboxylase by cinnamaldehyde. Cinnamaldehyde has been reported as an inhibitor for enzymes such as histidine decarboxylase by Wendakoon et al [269], while Auger et al. reported that arginine is decarboxylated by arginine decarboxylase to agmatine [270]. For the presently introduced work, the obtained results demonstrated that this blockage in the abovementioned pathway can be achieved with the addition of cinnamaldehyde. The chromatogram and corresponding masses assigned as adducts of some amino acids are presented in Figure 4.9.

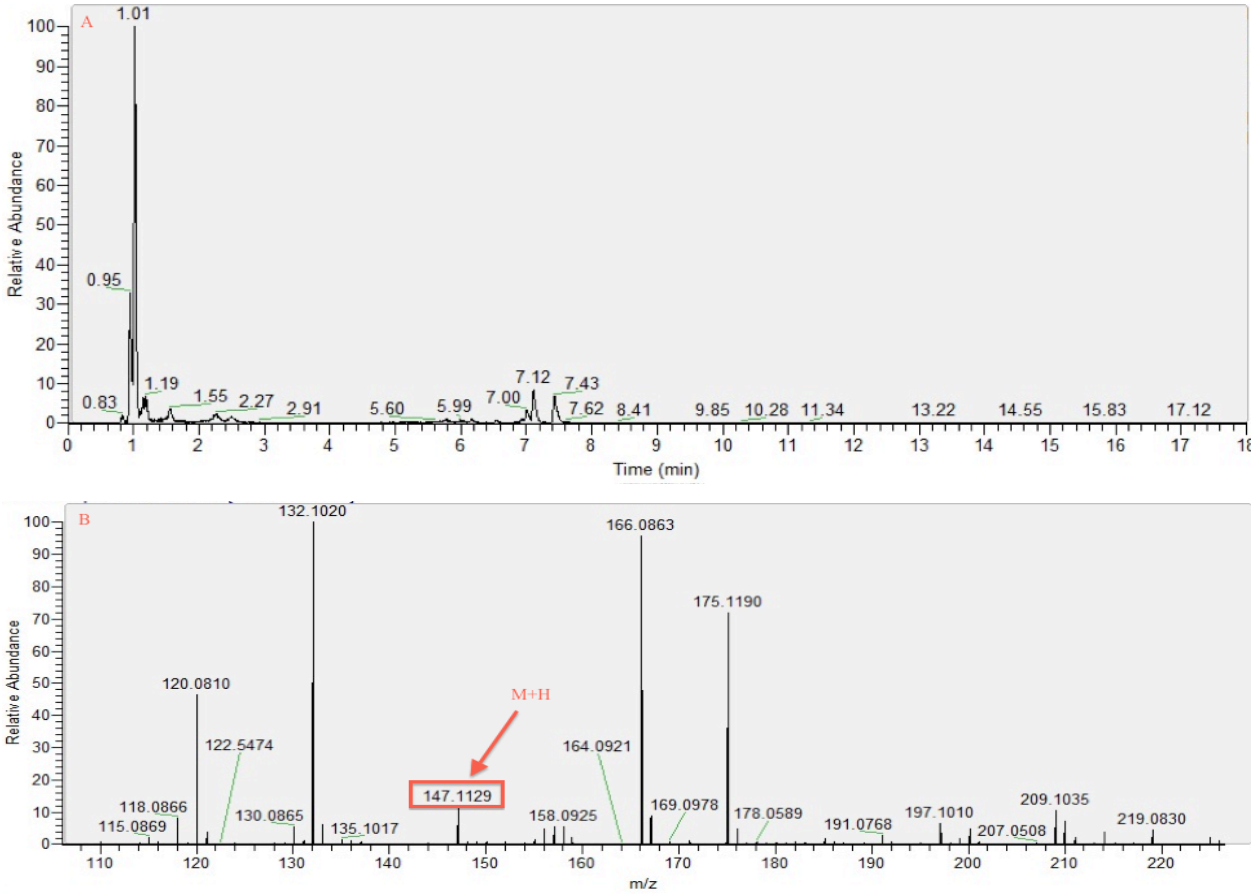
A
1.01
0.95
0.83
1.19
1.55
2.27
2.91
5.60
5.99
7.00
7.12
7.43
7.62
8.41
9.85
10.28
11.34
13.22
14.55
15.83
17.12
Relative Abundance
Time (min)
B
132.1020
166.0863
175.1190
120.0810
M+H
122.5474
164.0921
147.1129
118.0866
115.0869
130.0865
135.1017
158.0925
169.0978
178.0589
191.0768
197.1010
209.1035
207.0508
219.0830
Relative Abundance
m/z

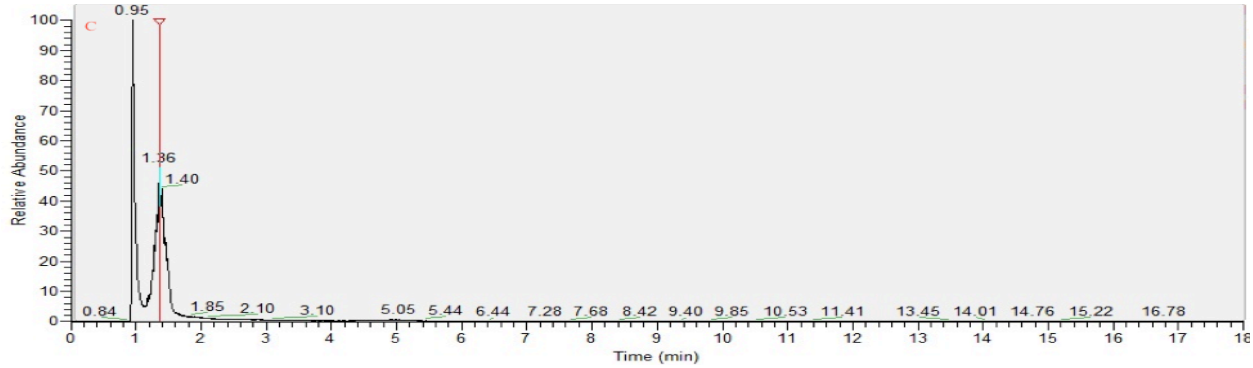
C
0.95
1.36
1.40
0.84
1.85
2.10
3.10
5.05
5.44
6.44
7.28
7.68
8.42
9.40
9.85
10.53
11.41
13.45
14.01
14.76
15.22
16.78
Relative Abundance
Time (min)

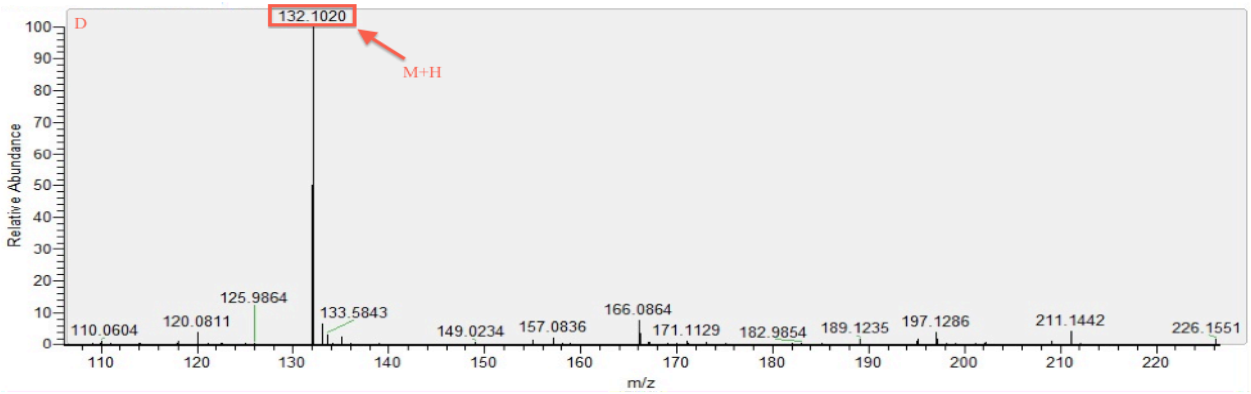
D
132.1020
M+H
125.9864
133.5843
110.0604
120.0811
149.0234
157.0836
166.0864
171.1129
182.9854
189.1235
197.1286
211.1442
226.1551
Relative Abundance
m/z

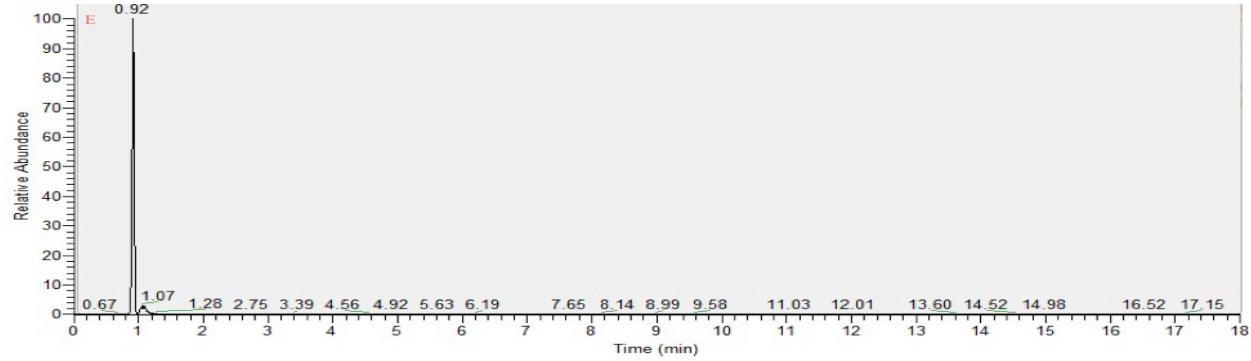
E
0.92
1.07
0.67
1.28
2.75
3.39
4.56
4.92
5.63
6.19
7.65
8.14
8.99
9.58
11.03
12.01
13.60
14.52
14.98
16.52
17.15
Relative Abundance
Time (min)

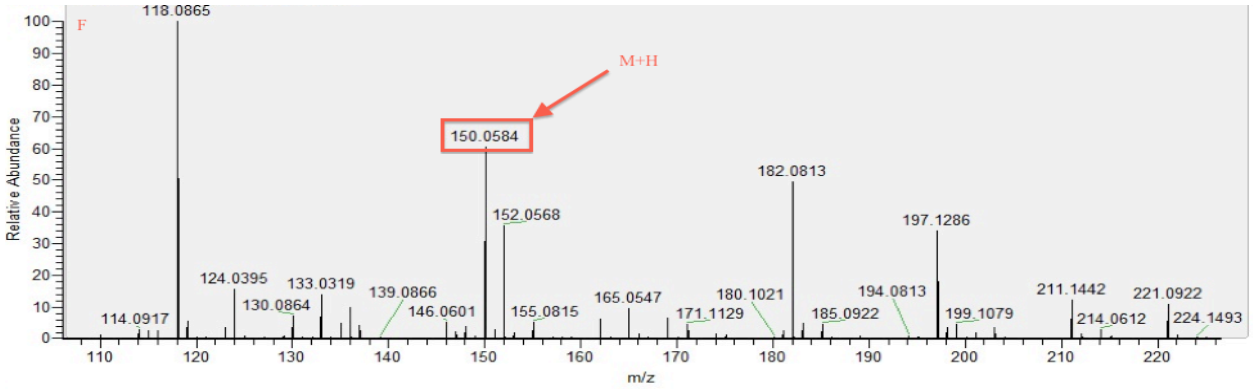
F
118.0865
M+H
150.0584
182.0813
152.0568
197.1286
124.0395
133.0319
139.0866
130.0864
146.0601
155.0815
165.0547
180.1021
171.1129
194.0813
185.0922
199.1079
211.1442
221.0922
214.0612
224.1493
114.0917
Relative Abundance
m/z

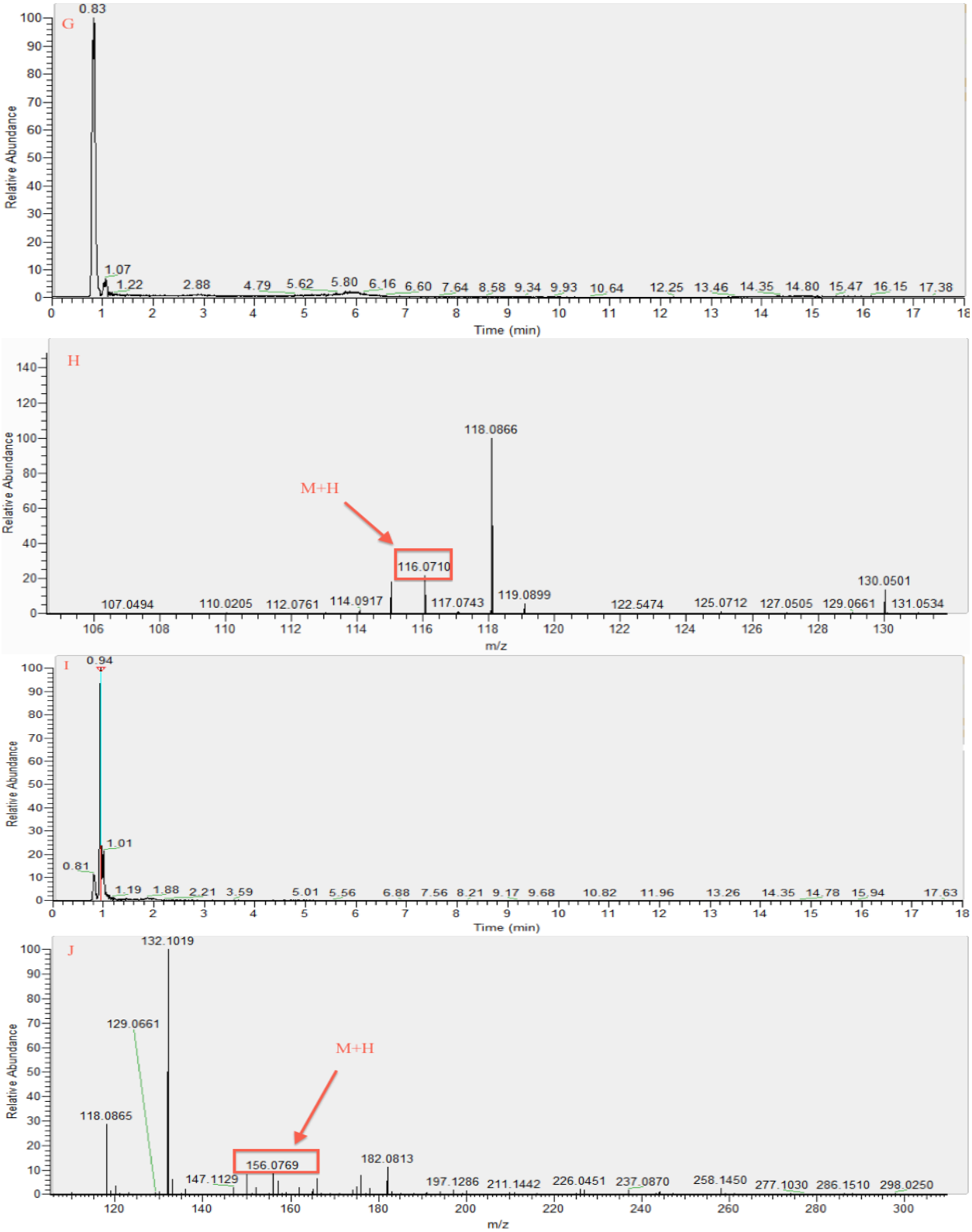

Figure 4.9 Chromatograms and corresponding mass spectra indicating masses assigned as adducts of lysine (A, B), isoleucine (C, D), methionine (E, F), proline (G, H), histidine (I, J)

4.3.4.3 Inhibition of glycolysis pathway

The obtained results indicated that cinnamaldehyde can act to perturb the citrate metabolic pathway, consequently influencing enzymes involved in ATP synthesis. Accumulation of glucose indicates disruption of this metabolic pathway in bacteria affected by cinnamaldehyde. Moreover, the observed increase in glucose, which is an initial metabolite in the glycolysis pathway, indicates an interruption in the action of the enzymes involved in this pathway or decrease in ATP as the source of energy. In support of findings presented by Gill et al., which indicate that cinnamaldehyde diffusion to the cell periplasm induces a decrease in ATPase activity in the cell membrane [271,272], the currently presented results related to down-regulated and up-regulated metabolites in pathways involved in ATPase confirm the effect of cinnamaldehyde on the activity of this enzyme. Picone et al. observed that the inability of cells to metabolize glucose leads to loss of their viability [273]. The observed up-regulation of glucose, which is assigned to inhibit the glycolysis pathway, in cinnamaldehyde-treated samples indicates that this naturally-occurring agent has potential as a possible candidate for cancer treatments. Most cancer cells uptake glucose in the glycolysis pathway in order to use ATP generation as an energy source; accordingly, the development of compounds as glycolytic inhibitors could be introduced as a new class of anticancer agents and therapeutic applications [274].

4.3.4.4 Changes in other metabolites

It seems that cinnamaldehyde affects CMP kinase activity through interruption of the phosphorylation mechanism due to cyclic CMP enhancement. Accumulation of carnitine accompanied by down-regulation of glycine betaine could be directly linked to inhibition of various catabolic enzymes such as carnitine dehydrogenase. The carnitine pathway may play more than one role in cell function; in addition to generation of an osmoprotectant (glycine betaine), carnitine may play a role in the generation of an external electron acceptor in anaerobic respiration. Moreover, glycine betaine levels were observed to decrease in *E.coli* under administration of above-MIC cinnamaldehyde levels, suggesting that cinnamaldehyde may impair the glycine betaine pathway in which choline dehydrogenase is involved. Strϕm et al. introduced glycine betaine as an osmoprotectant in *E.coli* under stress conditions induced by addition of salt and exposure to cold [275]. In the present study, the observed results indicated that under administration of cinnamaldehyde above MIC levels, this metabolite was unable to preserve cell turgor.

Other down-regulated metabolites such as myo-inositol 3-triphosphate and phytic acid were also indicated as discriminant compounds for the present study. Phytase (myo-inositol hexakisphosphate phosphohydrolase) is classified as a phosphatase enzyme that catalyzes phytic acid hydrolysis as a source of phosphorous [276,277]. This type of change in metabolome profile infers inhibition of phytase activity in cinnamaldehyde-treated sample. This study indicated that cinnamaldehyde could stop enzymatic activity while concurrently blocking the nitrogen or carbonyl terminal of proteins through covalent bonds.

Another enzyme inferred to be inhibited due to cinnamaldehyde addition in growing bacteria media is glutathione S-transferase, known to catalyze the addition of glutathione thiol groups to suitable electrophilic species. This enzyme is responsible for producing reduced glutathione by catalyzing the conjugation of electrophilic compounds. Up-regulation of hexylglutathione due to cinnamaldehyde addition to bacteria media inhibits S-hexyl glutathione activity as an inhibitor for the glutathione S-transferase function. Kanai et al. reported three distinct types of glutathione S-transferase from *E.coli* with defensive characteristics against oxidative stress (hydrogen peroxide) [278]. The presented research work demonstrated that cinnamaldehyde influences glutathione S-transferase activity; the same observation has been previously reported in the literature for *E.coli* treated by hydrogen peroxide, showing that cinnamaldehyde acts as an oxidative agent. The chromatogram and corresponding masses assigned as adducts of some of differenciate metabolites between control and treated samples are presented in Figure 4.10.

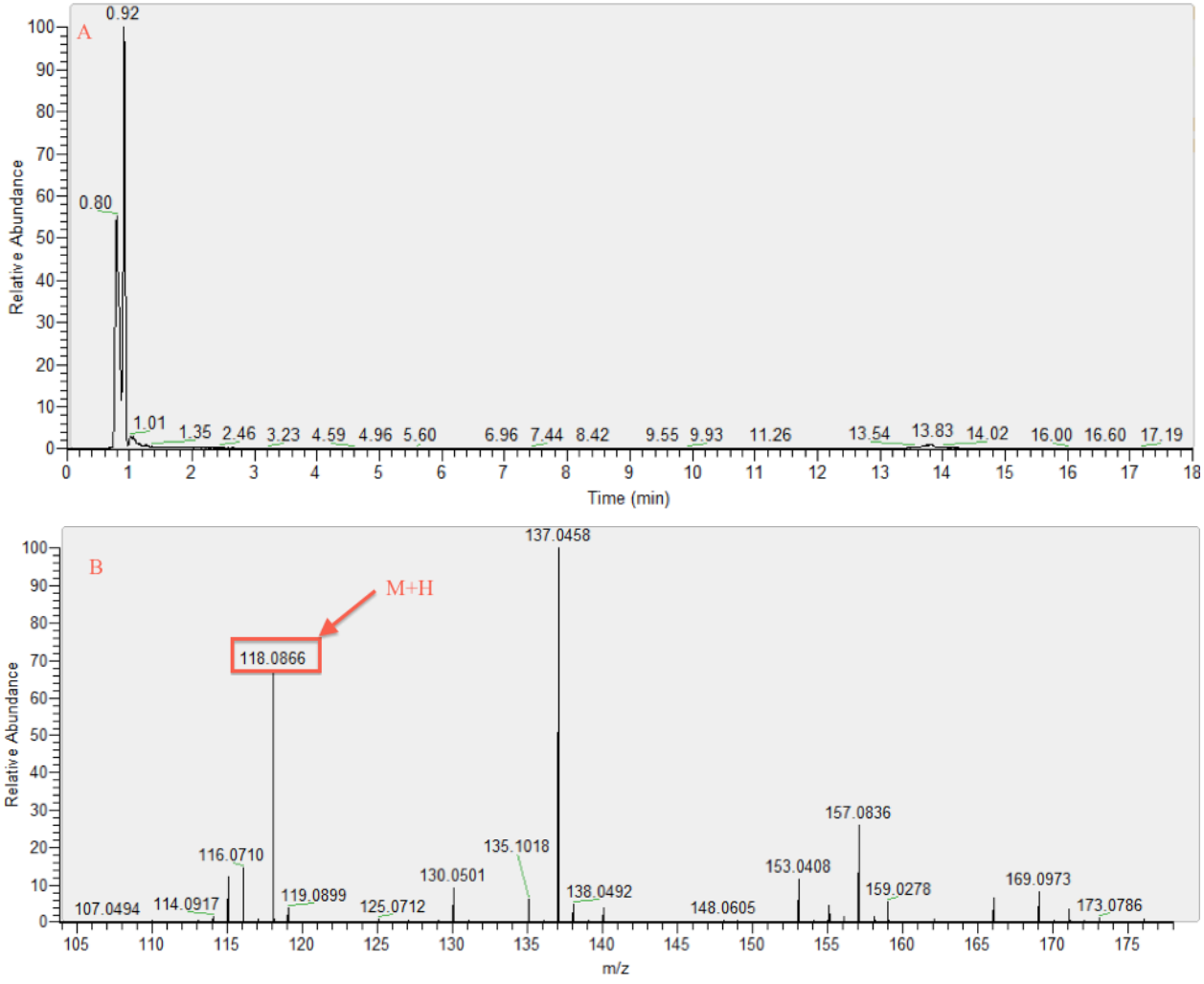

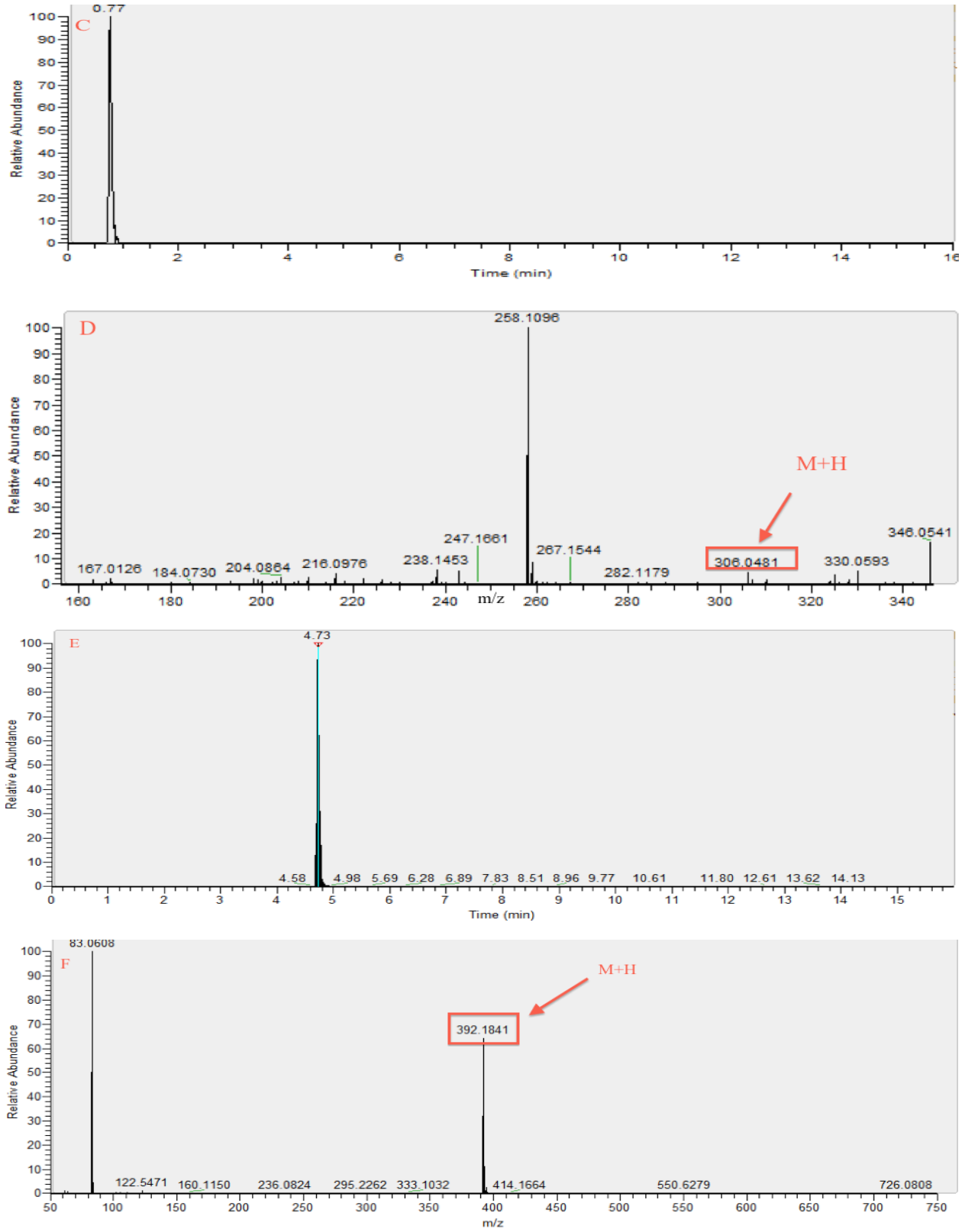

Figure 4.10 Chromatograms and corresponding mass spectra indicating masses assigned as adducts of Glycine betaine (A, B), cyclic CMP (C, D), hexylglutathione (E, F).

4.3.4.5 Anti-quorum sensing activity

Quorum sensing, defined as cell to cell signaling, is the phenomena in which bacteria secrets auto-inducers; when these compounds reach their threshold level, their interaction with transcriptional regulators affects gene expression [279]. Enzymatic degradation of signaling molecules inhibits biofilm formation in systematic and local infections, pathogenicity, and antibiotic resistance. In this study, the significant down-regulation observed in N-decanoyl-L-Homoserine lactone and N-tetradecanoyl-L-Homoserine lactone levels can be attributed to an inhibition in the ability of *E.coli* to form biofilms in cinnamaldehyde-treated media. Accordingly, cinnamaldehyde can be considered as a potential agent that interrupts biofilm generation by decreasing production of homoserine lactone as an auto-inducer; consequently, the inhibition of quorum sensing signals reduces the problem of resistance and virulance. Urbanowski et al. previously suggested cinnamaldehyde or one of its metabolites as an antagonist to auto-inducer receptor binding [280]; the observed changes in the metabolic profile of *E.coli* obtained in the currently presented work further support their results.

The abovementioned changes in metabolic pathways as a function of cinnamaldehyde administration on *E.coli* bacteria cultures provide concrete evidence to support the potential of cinnamaldehyde as a potent antibacterial agent. The chromatogram and corresponding masses assigned as adducts of metabolites between control and treated samples are presented in Figure 4.11.

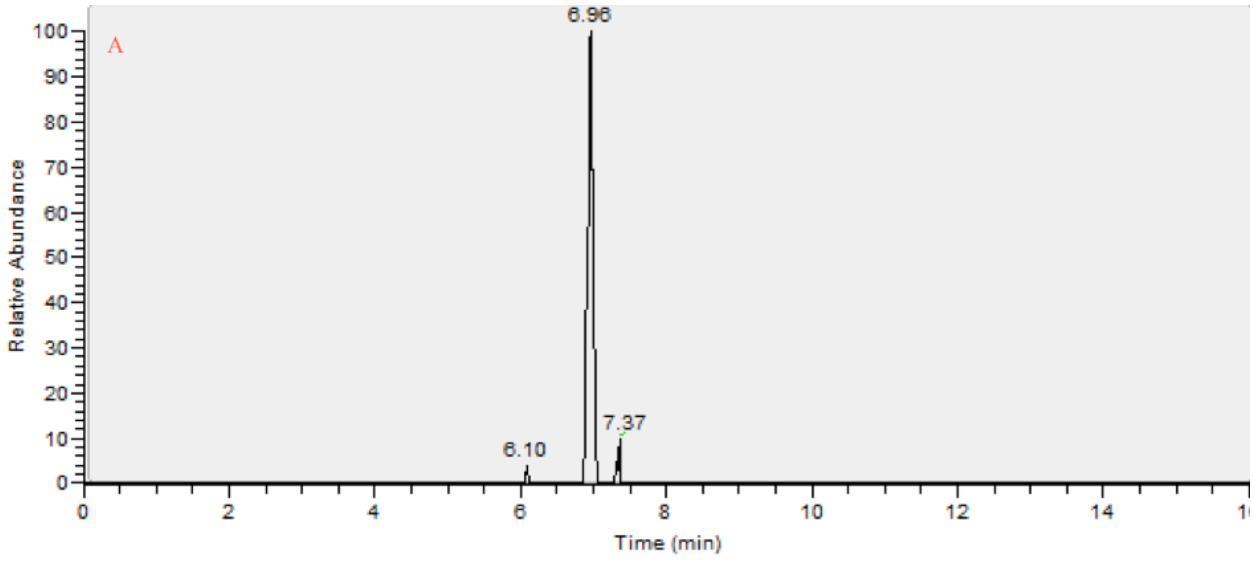

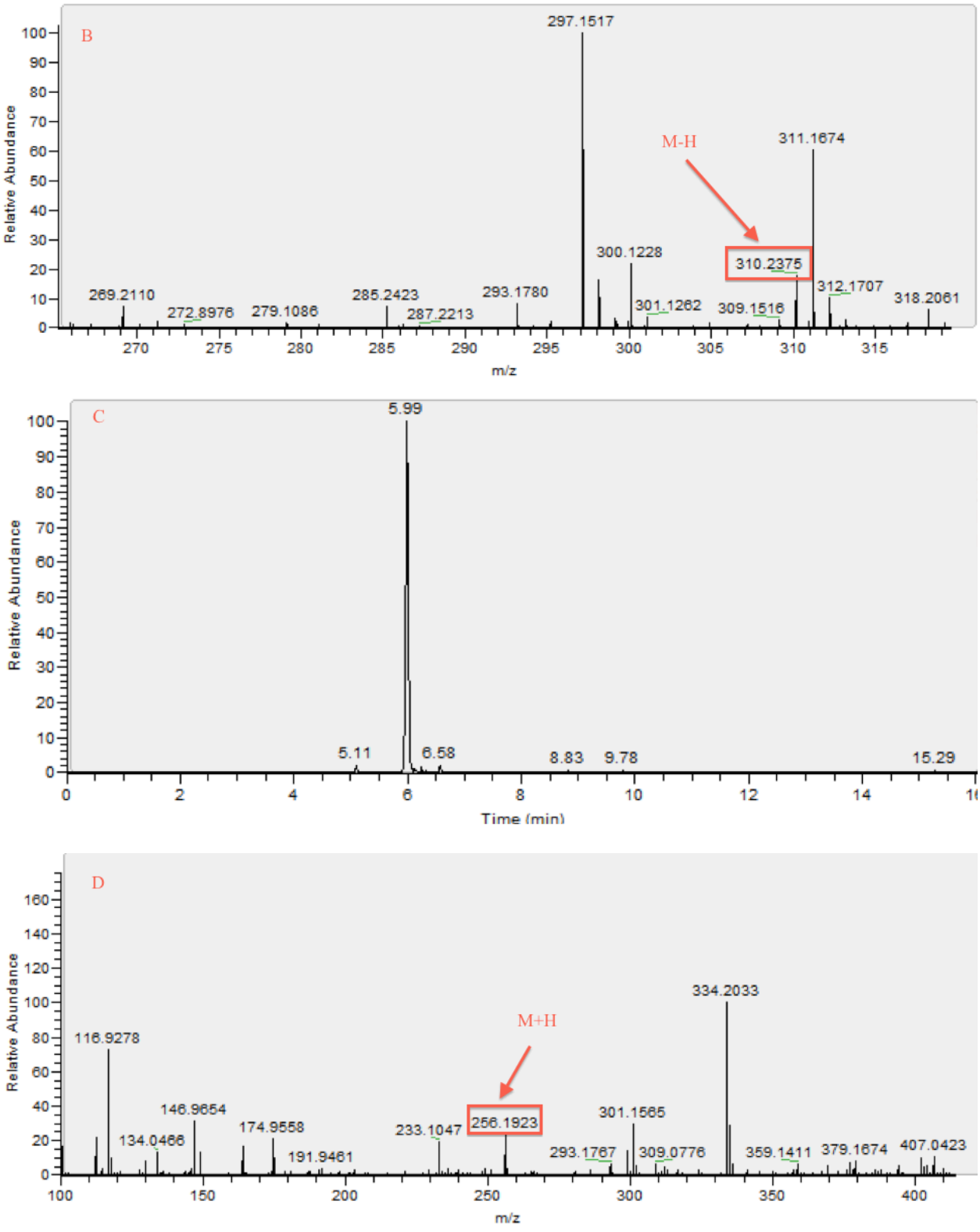

Figure 4. 11 Chromatograms and corresponding mass spectra indicating masses assigned as adducts of N-tetradecanoyl-L-homoserine lactone (A, B), N-decanoyl-L-Homoserine lactone (C, D).

4.4 Conclusions and future directions

In this research, the developed SPME-UPLC-MS based metabolomics coupled with statistical analysis presented in Chapter 3 was successfully applied for in vivo bacteria metabolomics. Metabolites with a wide variety of chemical and physical properties were extracted directly from *E.coli* culture using a newly developed extractive phase without the need of prior sample preparation steps. The presented procedure helps provide a comprehensive platform for determination of statistically significant differentiated metabolites between *E.coli* treated with cinnamaldehyde as a model antibacterial agent and matched control samples, detection of potential biomarkers involved in metabolic pathways, and time-resolved analysis. Satisfactory separation was observed between samples extracted prior and during different *E.coli* growth curve time points, and differentiation was noted between modes of treatment of cinnamaldehyde. Metabolic profile variations in different stages of the *E.coli* growth curve were investigated, demonstrating that the developed method was able to provide clear metabolic profile separations between various time points of *E.coli* growth. Metabolic stress response profiles of *E.coli* demonstrated different metabolic profiles as a function of administrated cinnamaldehyde levels. Potential biomarkers were identified for bacteria treated by cinnamaldehyde, which was further confirmed to affect metabolic pathways related to TCA cycle, fatty acids, glycolysis, amino acid metabolism, cell membrane, and protein synthesis. In addition, new biochemical pathways, which disrupt metabolism in bacteria treated by cinnamaldehyde, were introduced. The proposed approach may offer additional opportunities to food microbiologists for evaluation of metabolic pathways involved in growth and survival of pathogens in foods, food processing environments, as well as humans.

Chapter 5

Use of SPME-LC/MS with chemometrics and multivariate analysis towards metabolome characterization of clove oil as an antibacterial agent on *E.coli*

5.1 Introduction

Essential oils, biosynthesized and extracted from aromatic plants, are widely used in medicine, as well as in the food and fragrance industries due to their antimicrobial characteristics. Their defensive properties stem from their antibacterial, antiviral, insecticidal, antiparasitic, antifungal, and antioxidant activities [281-286]. Among the essential oils, terpenes, terpenoids, phenol-derived aromatic components, and aliphatic constituents have been shown to obstruct or deter the growth of bacteria, yeast, and mould through membrane and cytoplasm disruption [287-289].

Three thousands essential oils are currently known; of these, approximately 300 are applied commercially in the fragrance industry [281]. Among these naturally-occurring compounds, oxygenated terpenoids such as alcohols and phenolic terpenes have demonstrated the highest antimicrobial potential [281,290,291]. In related work, Smith-Palmer et al. applied 21 plant essential oils as antibacterial agents against five food-borne pathogens (*Campylobacter jejuni, Salmonella enteridis, E.coli, Staphylococcus aureus and Listeria monocytogenes*); their findings indicated that oils derived from bay, cinnamon, clove, and thyme yielded the highest bactericidal effect [292]. These oils have various constituents; for instance, clove bud oil is composed of eugenol (76.8%), eugenyl acetate (9.5%) and β-caryophyllene (6.0%) [293]. The interactions between these different constituents lead to synergistic, antagonistic, indifference, or additive effects [294,295]. Due to these properties, essential oils are utilized in food and drug discovery industries to control the proliferation of food-borne bacteria and pathogenic microorganisms [296,297]. When the sum of individual effects related to individual components is equal to the combined effect, an additive effect will be observed, whereas an antagonistic effect is observed when the effect of each constituent is lower than the effect of a mixture of them. When the effect of a mixture is more than that of each component, it is defined as a synergistic effect, and when no interactions take place between constituents, this property is called indifference [298-300].

The mechanisms of action of these naturally-occurring compounds against pathogens are still vague, especially at the metabolic level. As the metabolism of living systems alters in response to environmental stress, metabolomics aims to provide complementary information to genomics, transcriptomics, and proteomics [301]. In studies of mechanisms of action of living systems, scientists seek to determine specific reactions that occur as responses to specific stimuli. To do so, scientists must study variations

between two samples under different conditions; for this purpose, global analysis of all metabolites in a given system is employed to discover potential biomarkers of specific reactions [302]. The global metabolomics platform includes different steps: sample preparation, instrumental analysis, and data analysis. Determinations of significant metabolite changes are attainable using bioinformatics software. Analytical instrumentation platforms such as LC/MS, GC/MS, and NMR are widely used in global metabolomics studies. Of these, NMR is a nondestructive method with relatively low intensity; even in cases where this method is coupled to LC in order to reduce matrix complexity and increase metabolic coverage, NMR is unable to determine more than approximately 100 metabolites [231]. LC/MS provides the most comprehensive metabolomics coverage in comparison to GC/MS and NMR. In order to increase sensitivity for LC/MS and provide wider metabolome coverage, as well as eliminate ion suppression and ion enhancement effects, a wide range of research has been focused on sample preparation techniques. In metabolomics, an ideal sample preparation technique should be nonselective, reproducible, simple, and fast, in addition to allowing for high-through applications and the integration of a metabolism-quenching step [303]. SPME, as one of the recently emerging techniques utilized in sample preparation for metabolomics studies, covers all of the abovementioned characteristics needed in an ideal sample preparation method [28,143,159].

In the current study, an experimental design was applied to optimize effective factors for SPME method development. The experimental design was employed to extract the highest amount of information within the lowest number of experimental run-throughs. This allowed for the identification of optimum values related to each factor while decreasing analysis time and expenses [304,305]. In most previous works done with SPME, univariate optimization methods were applied to study important variables influencing extraction; variables were examined individually and in sequence, with all other factors kept constant. In this traditional method, after the completion of univariate SPME method development, some SPME parameters required double-checking, followed by repetition of corresponding optimization experiments. In contrast, multivariate designs offer simultaneous variation of several control variables, consequently decreasing the number of experiments needed for method development. Moreover, multivariate designs indicate probable variable interactions that are not detectable by classical experimental designs [305].

In the current study, a multivariate experimental design was applied to identify the following influential variables: desorption solvent type, extraction time, wash time, and desorption time in the 96-blade SPME system. The optimized method was then applied to assess the effect of clove bud oil and its major constituents on growing *E.coli* metabolome under the same experimental conditions, using a two-level full factorial design. Next, the metabolic profile of antibacterial agent-treated cells and control cells were generated by optimized SPME-LC/MS and subjected to multivariate data analysis. These metabolic patterns produced clear separations on a PLS-DA analysis that are related to up-regulated and down-

regulated metabolites. This multivariate experimental design at optimized SPME conditions was also applied to investigate the interaction effect of different major components of clove bud oil on *E.coli* growth.

5.2 Experimental part

5.2.1 Chemical and materials

LC-MS grade solvents and LC-MS grade formic acid (1 mL glass ampules) were obtained from Fisher Scientific (Ottawa, Canada). Polypropylene deep 96-well plates (Nunc) and easily modified polystyrene–divinylbenzene (Macherey-Nagel) particles were purchased from VWR International (Mississauga, Canada). All metabolites, peptone, yeast extract, NaCl, clove bud oil, eugenol, eugenyl acetate, and caryophyllene were purchased from Sigma–Aldrich. *E.coli* BL21 strain was kindly donated by Professor John Brennan's lab at McMaster University (Hamilton, Ontario, Canada). The Concept 96-SPME-blade unit and robotic Concept 96 autosampler were purchased from Professional Analytical Systems (PAS) Technology (Magdala, Germany) for SPME sample preparation.

5.2.2 Metabolite Standard Mixture Preparation

A standard mixture of metabolites with a wide range of polarities, such as amino acids, amines, organic acids, sugars, nucleosides, and small peptides (Table 5.1) was prepared for optimization of SPME conditions using multivariate analysis. Stock standard solutions were prepared in water/methanol/ethanol, kept frozen (-30°C), protected from light, and prepared fresh weekly. Extractions were conducted from a spiked standard 1 μg/mL stock solution and added to LB media. Organic solvent content for all extraction standards was maintained at 1% (v/v). For instrument calibration, working standard solutions with known concentrations of metabolites were prepared by dilution of the stock standard with a desorption solvent.

5.2.3 Bacterial strain and antibacterial activity evaluation

Frozen cultures of *E.coli* BL12 were streaked on an LB agar media plate (10 g trypton; 5 g yeast extract; 5 g NaCl; 15 g Agar in 1 L nanopure water), and incubated overnight at 37°C. One isolated colony was re-streaked on LB Agar media and incubated at 37°C for 24 h. Following, one isolated colony was inoculated into 5 mL of LB media (10 g trypton; 5 g yeast extract; 5 g NaCl in 1 L nanopure water), then incubated at 37°C for 24 h under agitation at 125 rpm. The microbial broth was then serially diluted in fresh media. The resulting 10^7 colony-forming units (CFU/mL) were utilized for the whole study.

Using GC/MS, the major components of clove bud oil were identified as eugenol (76.8%), eugenyl acetate (9.5%) and β-caryophyllene (6.0%). The MIC threshold for clove oil was identified through addition of different amounts of clove oil to the same *E.coli* culture, followed by incubation at 37°C for 16 hours; results indicated that 10 μL was the MIC for clove oil for a 10^7 CFU/mL *E.coli* culture.

To evaluate the antibacterial activity of each constituent of clove oil against *E.coli*, different amounts of eugenol (8 μL), eugenyl acetate (1 μL) and β-caryophyllene (0.6 μL) were separately added to the same concentration of bacteria in different cell tubes, and bacteria growth was encouraged by incubating at 37°C for 16 hours at 125 rpm. Next, 100μL of each grown culture were streaked on separate agar plates, and then incubated at 37°C overnight. In the case of eugenol, no bacteria growth occurred, but growth did occur for cultures treated with eugenyl acetate and caryophyllene.

The two-level full factorial design, developed to be compatible with Statistica software, was applied to evaluate the effect of different constituents of clove bud oil on *E.coli*'s metabolic profile as well as to investigate the synergistic effect of the clove oil constituents. In this part of the currently presented study, all experiments were done in triplicate apart from the central points, which were replicated four times.

5.2.4 Coating preparation for 96-blade SPME and automated SPME procedure for high throughput analysis

In the present study, extraction was done using a 96-blade SPME system coated by PS-DVB-WAX:HLB 50:50 [w/w] as stationary phase for a stainless steel blade conducted by the robotic concept 96-autosampler provided by PAS Technology. Coating preparation procedures as well as information related to the concept 96-autosampler are reported in Chapter 3, which also provides a comprehensive study related to the suitability of the abovementioned coating for metabolomics.

The 96-blade SPME platform is comprised of four different steps: preconditioning, extraction, wash, and desorption. A triangular design and a central composite design (CCD) were applied for variable optimization. This triangular design was used for desorption solvent optimization, while CCD was used for optimum extraction and desorption time, as well as for optimization of wash time for each step of the 96-blade SPME method. The sums, geometric means, and averages of peak areas were investigated as responses for optimization. The Statistica computer program was used for this experimental design.

Fibres were pre-conditioned for 1 hour in 1 mL ethanol:water 70:30 (v/v). Next, extractions were conducted from 1 mL culture (control and antibacterial agent treated) set in sterile 96-well plates for 2 h (1000 rpm agitation speed, 2.5 mm amplitude). A 20s wash step in water was performed after the extraction step so as to remove proteins, salt, and particulates from the coating surfaces. Afterwards, desorption was carried out for 90 min in 1 mL of acetonitrile/water 1:1 (v/v) as the optimized desorption solvent obtained by CCD. Final extracts were kept in -80°C until analysis.

Table 5.1 Physicochemical properties of metabolites included in standard metabolite mixture.

Analyte	Formula	Molecular Weight	pKa	Log P
3-hydroxybutyric acid (HBA)	$C_4H_8O_3$	104.1	4.41	-0.47
Adenine	$C_5H_5N_5$	135.1	4.15	-0.09
Adenosine	$C_{10}H_{13}N_5O_4$	267.2	NA	-1.05
Adenosine diphosphate (ADP)	$C_{10}H_{15}N_5O_{10}P_2$	427.2	NA	-2.64
Adenosine monophosphate (AMP)	$C_{10}H_{14}N_5O_7P$	347.2	NA	-1.68
Adenosine triphosphate (ATP)	$C_{10}H_{16}N_5O_{13}P_3$	507.2	NA	-3.61
β-Estradiol	$C_{18}H_{24}O_2$	272.4	NA	4.01
β-NAD	$C_{21}H_{27}N_7O_{14}P_2$	663.4	NA	-3.68
Cholic acid	$C_{24}H_{40}O_5$	408.6	4.98	2.02
Choline	$C_5H_{14}NO^+$	104.1	NA	-5.16
Citric acid	$C_6H_8O_7$	192.1	2.79	-1.64
Fructose	$C_6H_{12}O_6$	180.2	12.1	-1.55
Fumaric acid	$C_4H_4O_4$	116.1	3.03	0.46
Glucose	$C_6H_{12}O_6$	180.2	12.9	-3.24
Glucose 6-phosphate	$C_6H_{13}O_9P$	260.1	1.11	-3.79
Glutamic acid	$C_5H_9NO_4$	147.1	2.23	-3.69
Glutathione (oxidized)	$C_{20}H_{32}N_6O_{12}S_2$	612.6	NA	-7.89
Glutathione (reduced)	$C_{10}H_{17}N_3O_6S$	307.3	NA	-5.41
Histamine	$C_5H_9N_3$	111.1	9.8	-0.7
Histidine	$C_6H_9N_3O_2$	155.2	2.76	-3.32
Linoleic acid	$C_{18}H_{32}O_2$	280.4	4.77	7.05
Lysine	$C_6H_{14}N_2O_2$	146.2	3.12	-3.05
Maleic acid	$C_4H_4O_4$	116.1	1.83	-0.48
Nicotinamide	$C_6H_6N_2O$	122.1	3.35	-0.37
Phenylalanine	$C_9H_{11}NO_2$	165.2	1.24	-1.38
Protoporphyrin IX	$C_{34}H_{34}N_4O_4$	562.7	NA	7.43
Pyruvic acid	$C_3H_4O_3$	88.1	2.45	-1.24
Riboflavin	$C_{17}H_{20}N_4O_6$	376.4	10.2	-1.46
Ribose-5-phosphate	$C_5H_{11}O_8P$	230.1	NA	-2.65
Sucrose	$C_{12}H_{22}O_{11}$	342.3	12.6	-3.7
Taurocholic acid	$C_{26}H_{45}NO_7S$	515.7	NA	0.01
Tryptophan	C11H12N2O2	204.2	7.38	-1.06
Uridine diphosphate glucose (UDPG)	C15H24N2O17P2	566.3	NA	-5.8

5.2.5 Metabolic profile for bacteria affected by clove oil and its major constituents UHPLC-ESI-MS analysis

Separation was carried out on a Kinetex pentafluorophenyl coreshell column (1.7 μm, 2.1 mm × 10 mm) (Phenomenex, Torrance, CA, USA) with a guard filter (SecurityGuard ULTRA Cartridges UHPLC PFP for 2.1 mm). The column temperature was maintained at 25°C, and gradient mobile phase conditions were composed of phase A (water containing 0.1% formic acid) and phase B (acetonitrile with 0.1% formic acid) set to the following conditions: 0-1 min 90% A; 1-9 min 90-10% A; 9-12 min 10% A; 12-16 min 10-90% A. Total run time was 16 min per sample. The injection volume for this method was 10 μL. Samples were stored under refrigeration (4°C) in the autosampler while waiting for injection, and injected in a randomized fashion. A QC sample was run periodically to verify instrument performance. Injection

of control samples and antibacterial-treated samples was done alternatively. Blank and QC samples were injected after every set of 15 injections so as to avoid cross contamination as well as verify instrument performance. The used QC sample was prepared by mixing 10 μL of each sample into one combined sample.

The MS system was operated using an accurate mass Exactive benchtop Orbitrap system (Thermo, San Jose, California, USA) in both negative and positive electrospray ionization (ESI) modes and 100-1000 m/z mass range. Optimum values for sheath gas (arbitrary units), auxiliary gas (arbitrary units), ESI voltage (kV), capillary voltage (V), capillary temperature (°C), and tube lens voltage (V) were set at 40, 25, 4.0, 27.5, 275, and 100 for positive ESI mode, and 50, 25, -2.7, -67.5, 325, and -85 for negative ESI mode, respectively. External instrument mass calibrations were performed every 24 h, and found to be within 2 ppm for all ions. Separated metabolites were analyzed using Xcalibur software version 2.1 (Thermo) by isolating the extracted ion chromatograms (XIC), using a 5 ppm window around the accurate mass.

5.2.6 Metabolite identification, data mining, and statistical analysis

An Exactive Orbitrap detector was used, providing high mass resolution and sensitivity. Raw data obtained with Xcalibur software (.raw) was converted to (mzXML) with MS conversion software. The converted data was then processed with a web-based platform called XCMS online (Scripps Center for Metabolomics, California, USA). The processing of metabolomics data by XCMS Online is divided into three stages: data upload, parameter selection, and result interpretation. Samples for each group to be compared in mzXML format were uploaded through Java applet. Parameters related to UPLC/Orbitrap were set, and data processing was conducted after job submission. The output is a table containing retention times, m/z values, and intensity of features, accompanied by some statistical values as well as some graphical features. XCMS identifies features whose relative intensity differs between sample groups, determining p-values as well as fold changes. The software carried out mass spectral peak deconvolution, alignment, peak picking (feature detection), and ion annotation on the list of features in order to identify the detected isotopes, adducts, and in-source fragment ions. Multivariate data analysis was used by SIMCA-P+ software (Umetrics, NJ, USA) for statistical analyses. Log transformation and pareto scales prior to PCA were done to differentiate between control samples and treated ones. Orthogonal Projections to Latent Structures Data analysis (OPLS-DA) was performed on obtained data, and the resulting S-plots were applied towards further modeling to investigate biomarkers produced in bacteria culture treated by antibacterial agents. Metabolite identities were specified based on their accurate mass, retention time, comparison of fragmentation data with authentic standards, and METLIN

databases within 5 ppm. In order to identify important metabolic pathways, and biological interpretation, the KEGG database was used.

5.3 Results and discussion

5.3.1 Optimization of SPME parameters

When utilizing the 96-blade SPME-LC/MS, the SPME method development procedure needs to be conducted efficiently, as the effectiveness of the resulting analyte pre-concentration depends on many parameters, such as coating type, choice of stationary phase for the 96-blade system, extraction conditions, desorption conditions, and wash conditions.

In order to achieve the most efficient desorption of analytes with a wide range of polarities and physical-chemical properties from the surface of the coating, the optimum desorption solvent was investigated. A triangular design was carried out to determine the influence of different desorption solvents and their interactions on the recovery of the 96-blade SPME method. Acetonitrile, water, methanol, and their combination (100% acetonitrile, 100% water, 100% methanol, acetonitrile:water 1:1 (v/v), acetonitrile:methanol 1:1 (v/v), methanol:water 1:1 (v/v), , and acetonitrile:methanol:water 1:1:1 (v/v/v)) were applied using the triangular design. The sum, average, and geometric mean of peak areas obtained from the computer program were then compared to identify the optimum responses. Figure 5.1 demonstrates the results of this triangular design process.

An evaluation of results indicated that based on the average and sum of the detector responses to each metabolite, acetonitrile:water 1:1 (v/v) was the optimum desorption solvent composition for the study, while based on plots obtained versus the geometric mean, acetonitrile:water:methanol 5:4:1 (v/v/v) was the optimum desorption solvent composition. The central tendency of a set of measurement results is typically found by calculating the arithmetic mean ($\bar{X}$) and, less commonly, the median or geometric mean. The mean is an estimate of the true value as long as there is no systematic error. In the absence of systematic error, the mean approaches the true value (μ) as the number of measurements (n) increases. Finally, 1 mL of acetonitrile:water 1:1 (v/ v) at 1500 rpm was chosen as the optimized desorption solvent in this study for the extraction of targeted metabolites with logP from -7 to +7 spiked in LB media. The response, based on the sum of the peak areas, is one of the most useful parameters for the optimization of SPME conditions, and therefore was used as the endpoint in this study to evaluate the significance of each of the aforementioned factors.

To optimize the time for each stage of the 96-blade SPME procedure, CCD was applied to obtain the optimum time that provided the highest extraction recovery. Minimum and maximum values of time for each step were arbitrarily selected to cover the wide range of experimental conditions. Plots were

evaluated based on three statistical definitions; however, the optimum condition was chosen based on results obtained from the sum of peak areas.

The experimental variables that were evaluated included extraction time (15–120 min), wash time (0–120 s) and desorption time (15–120 min), all using the optimized desorption solvent.

A CCD with a central point (17 runs in total) was performed to determine the optimized time for each step of the extraction, wash, and desorption, and their interactions on the 96-blade SPME system. The CCD matrix and the surface response are presented in Table 5.2 and Figure 5.2, respectively. The sensitivity of the method was significantly improved by applying the method at optimum times for each step. The optimized conditions obtained from utilization of the CCD matrix and response surface methodology indicated that a 120 min extraction time, 30 seconds as wash time, and 90 min desorption time provided the highest extraction recovery for all targeted metabolites.

Table 5.2 Central composite design matrix used to obtain optimum extraction, wash, and desorption time for a set of targeted metabolites using PS-DVB-WAX:HLB 50:50 (w:w).

Experiment #	Extraction time (min)	Wash time (second)	Desorption time (min)
1	36.3	24.3	36.3
2	36.3	95.7	98.8
3	98.8	95.7	36.3
4	98.8	24.3	98.8
5	67.5	60.0	67.5
6	36.3	96.7	36.3
7	36.3	24.3	98.8
8	98.8	24.3	36.3
9	98.8	95.7	98.8
10	67.5	60.0	67.5
11	15.2	60.0	67.5
12	119.7	60.0	67.5
13	67.5	60.0	15.2
14	67.5	60.0	119.7
15	67.5	0	67.5
16	67.5	119.7	67.5
17	67.5	60.0	67.5

5.3.2 Interaction between clove oil components using full factorial design

After the evaluation of optimum conditions for the 96-blade SPME system, a full factorial design was applied to identify the most important constituent of clove bud oil in stopping *E.coli* metabolism, as well as potential interactions between its major components. Based on observations done to evaluate the inhibitory effect of clove oil, its antibacterial activity is due to the major components eugenol, eugenyl acetate, and caryophyllene. To determine the effect of the most important constituent of clove bud oil in terms of antibacterial activity and potential variable interactions, a two-level full factorial design, 2^3, was

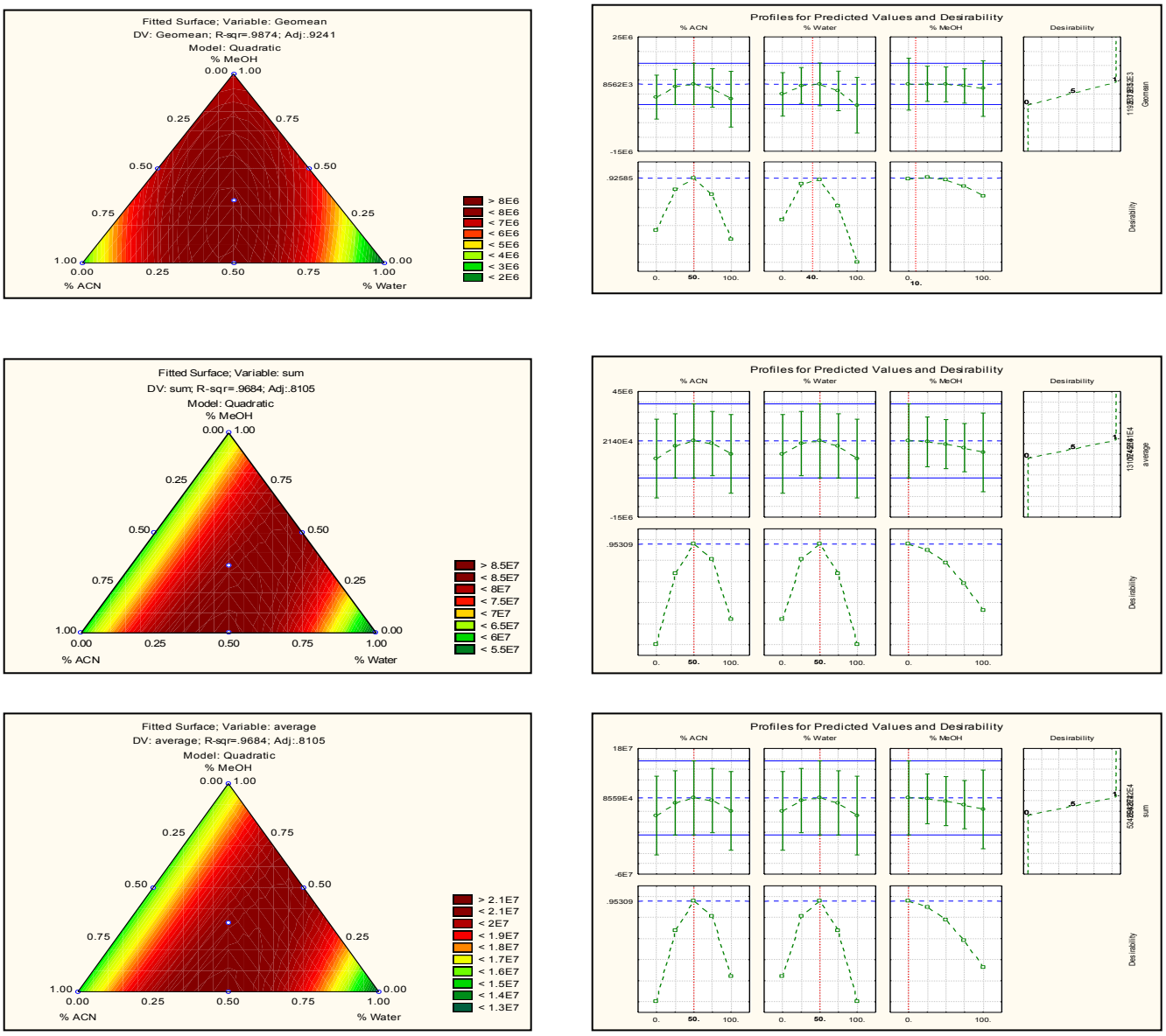

Figure 5.1 Triangular design and desirability plots for desorption solvent optimization applying geometric mean (geomean), sum, and average of analytical signal vs. desorption solvents. Each angle is related to one desorption solvent, the middle of triangle side is the mixtre of desorption solvent at the angle of each side. The mixture of all three solvents represents the center of triangles.

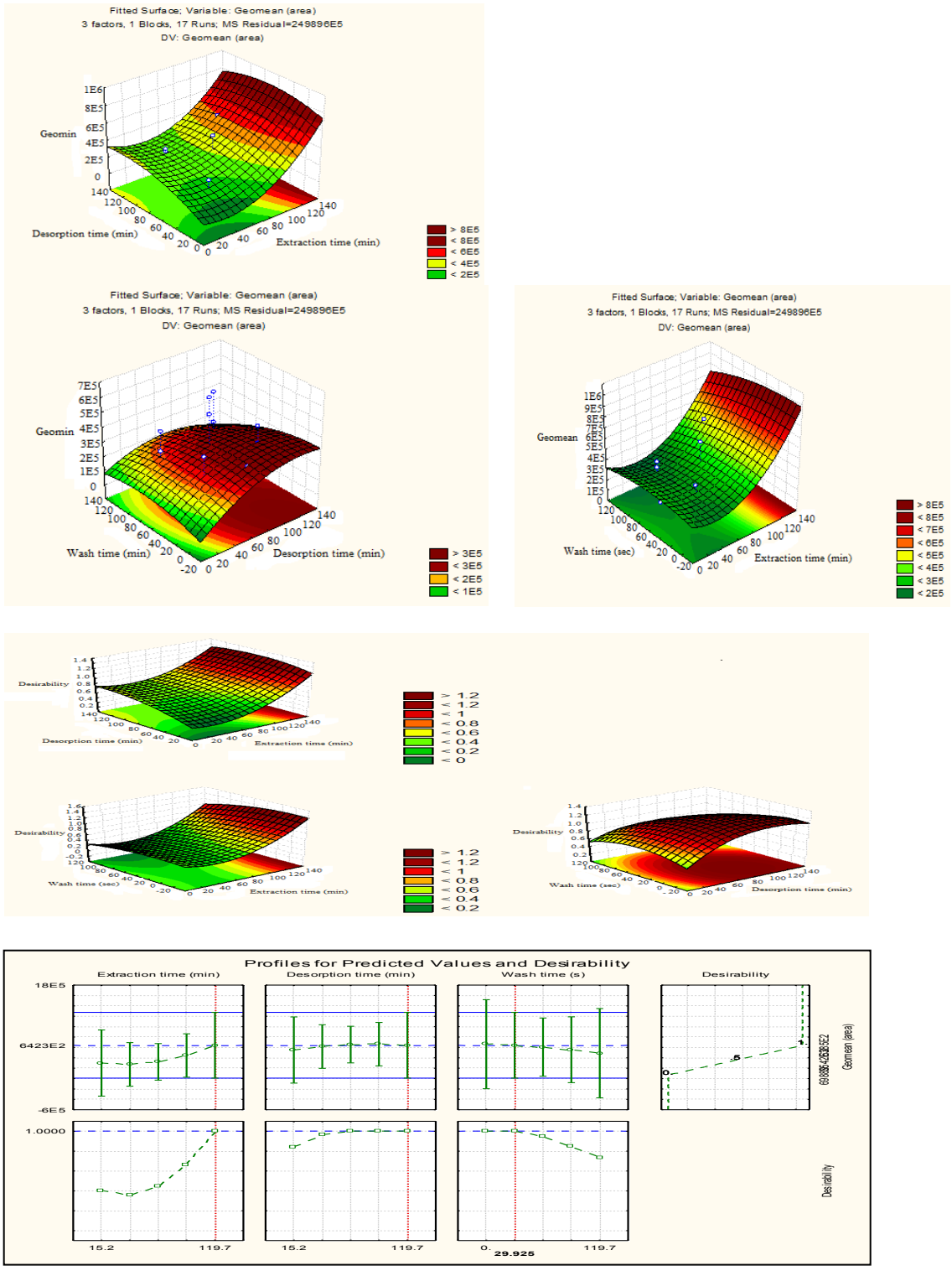

Figure 5.2 Response surface plot for analytical signal vs. extraction time, desorption time and wash time (min) for extraction from spiked analytes in LB media (100 µg mL^{-1}) resulted from central composite design in order to obtain optimum time for extraction, wash, and desorption steps in 96-blade SPME.

Table 5.3 Full factorial design matrix for investigation of the effects of different clove oil constituents on *E.coli* metabolic profile (Eugenol: 8 µL, eugenyl acetate: 1 µL and β-caryophyllene: 0.6 µL Carryophelene).

Exp#	Eugenol	Eugenyl acetate	**β**-Caryophyllene
1	-1	-1	-1
2	+1	-1	-1
3	-1	+1	-1
4	+1	+1	-1
5	-1	-1	+1
6	+1	-1	+1
7	-1	+1	+1
8	+1	+1	+1

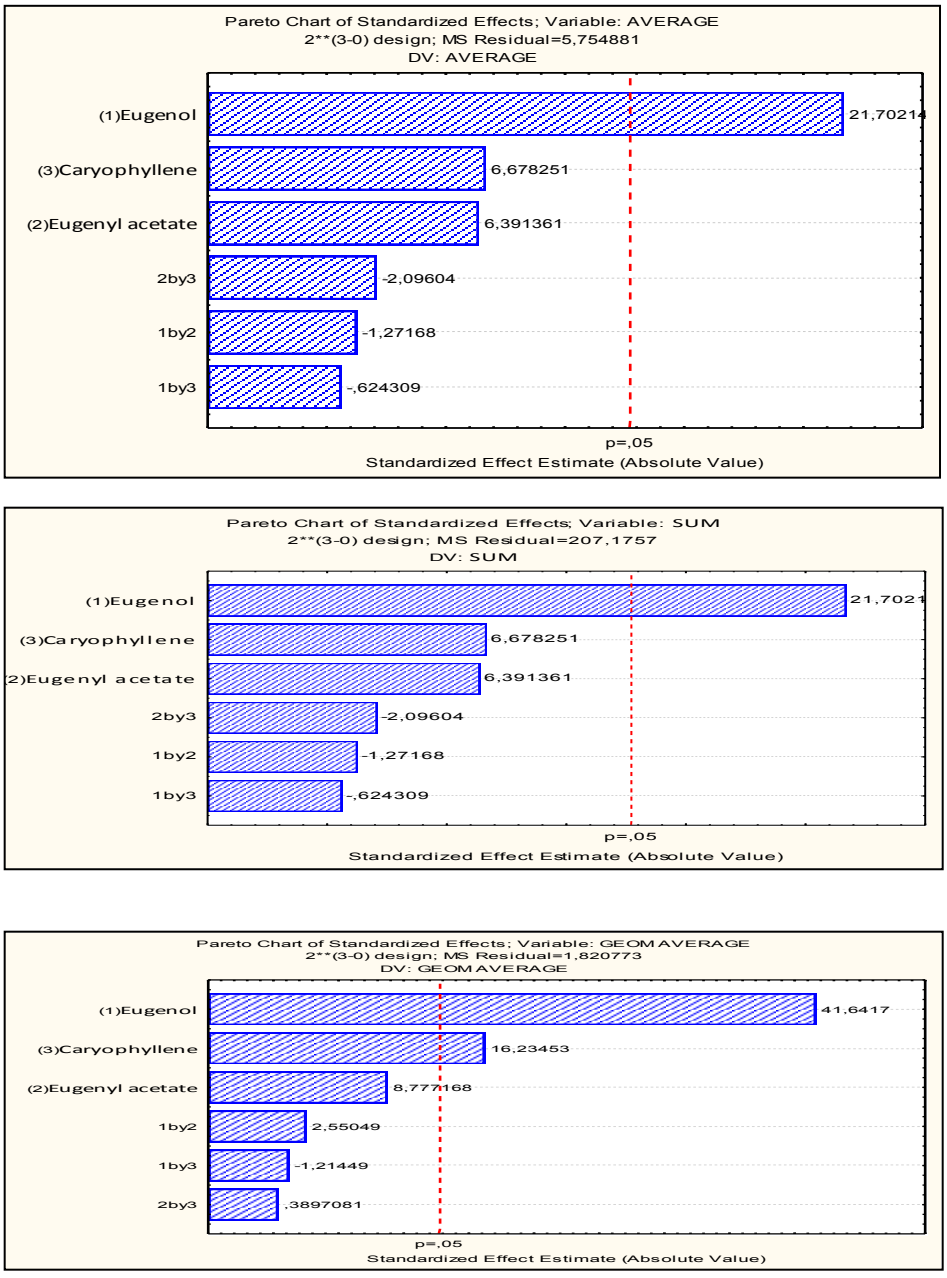

Figure 5.3 Pareto chart plots based on average, geomean, and sum of peak areas obtained from 96-blade SPME coupled to LC-MS related to metabolites whose peak areas were increased by addition of antibacterial agents.

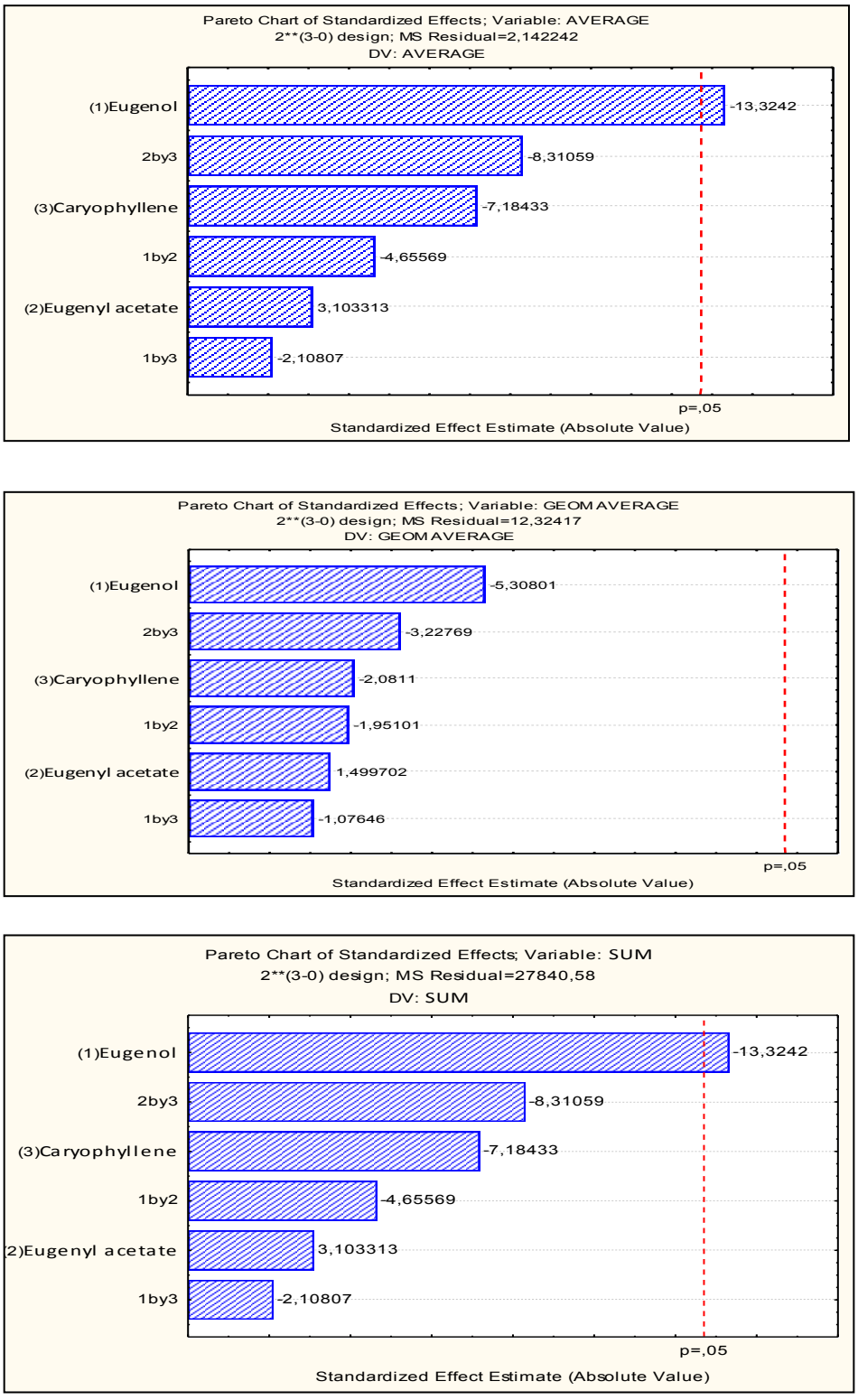

Figure 5.3 Pareto chart plots based on average, geomean, and sum of peak areas obtained from 96-blade SPME coupled to LC-MS related to metabolites whose peak areas were decreased by addition of antibacterial agents.

carried out. Table 5.3 shows the number of different possible conditions in this full factorial design experiment. The effect of any two factors was evaluated separately, as well as the effects of all three factors. Another experiment (experiment 9) was conducted by adding 10 μL clove oil. All experiments were done in triplicate. Metabolic profiling for each set of experiments was provided; the variable effects and interactions are summarized in the Pareto charts illustrated in Figure 5.3 and Figure 5.4. Metabolites were classified into two groups: Group A (Figure 5.3), comprised of metabolites whose peak areas were increased by addition of antibacterial agents, demonstrated as up-regulated metabolites in Table 5.4, and Group B (Figure 5.4), comprised of metabolites whose peak areas were reduced with the addition of antibacterial agents, demonstrated as down-regulated metabolites in Table 5.4. The plots were accomplished by integrating and evaluating the obtained peak areas, corresponding to about 300 extracted metabolites from growing *E.coli* treated by the naturally-occurring antibacterial agents under study. These metabolites had various retention times and polarity characteristics selected from the LC chromatogram. The responses were evaluated based on the sum, average, and geomean of peak areas. The obtained Pareto chart showed the response of the bacteria system to each clove oil constituent and their combinations; an evaluation of results showed that addition of antibacterial agents result in an increase (Group A) or decrease (Group B) in analytical signal. Of these constituents, eugenol, the major compound of clove bud oil, was found to possess the strongest antibacterial activity at the 95% confidence level, while other individually applied constituents (in the same volume ratio) did not indicate an antibacterial effect on *E.coli* growth at the 95% confidence level. The Pareto charts demonstrated no significant interactions between the constituents (at the 0.05 level).

5.3.3 Metabolic profiling of E.coli under different clove oil constituents as antibacterial agents

In this part of the study, the effects of clove oil and its constituents on the *E.coli* bacteria metabolic profile were investigated. Considering that clove oil is a mixture of different active agent components, the effects of each component as well as their interactions were evaluated in the context of nine batches of experiments designed by full factorial design. PCA score plots (Figures 5.4 and 5.5) demonstrate separation of clusters related to each set of experiments in positive and negative electrospray ionization modes, respectively. There is no variation between clusters related to experiments #1, #3, #5, and #7 in PC1, while for experiments #2, #4, #5, #6, #8, and #9, in which eugenol is present, the related clusters were separated in PC1. Results obtained from the Pareto chart plotting demonstrated that eugenol is the most effective antibacterial component of clove bud oil when these constituents are analyzed comparatively while maintaining the weight ratio in which they occur in this essential oil (76.8%/9.5%/6%) for eugenol, eugenyl acetate, and caryophellene, respectively.

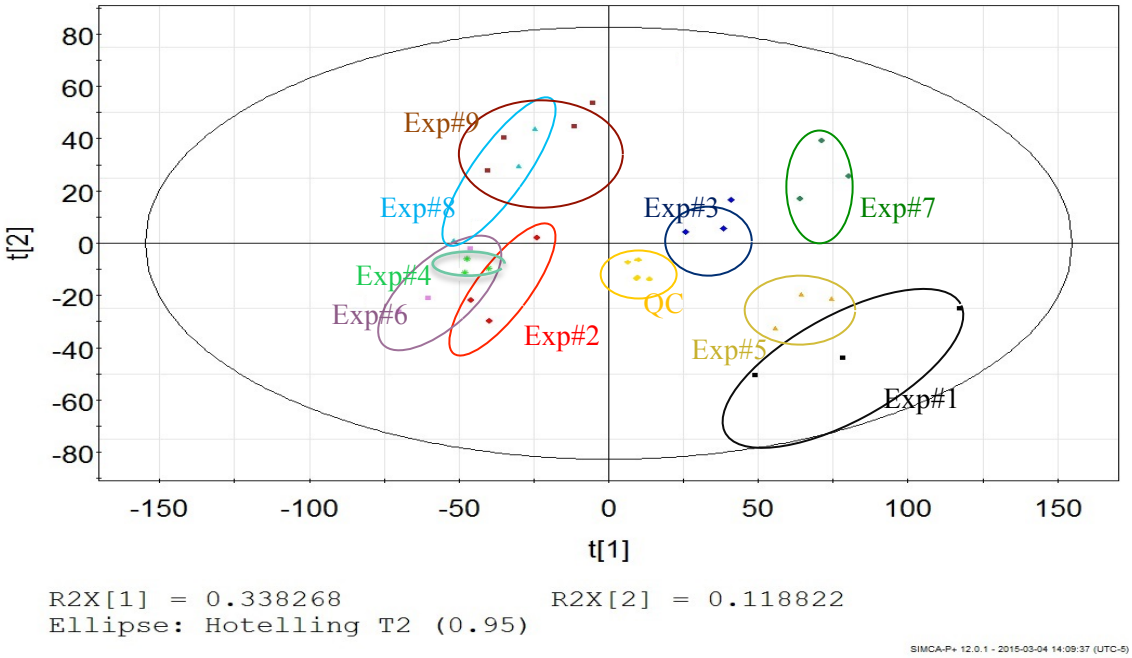

Figure 5.4 PCA score plot obtained from full factorial design for different types of treatments by various clove oil constituents (based on Table 5.3, exp 9 is clove oil treated bacteria)-positive ESI mode.

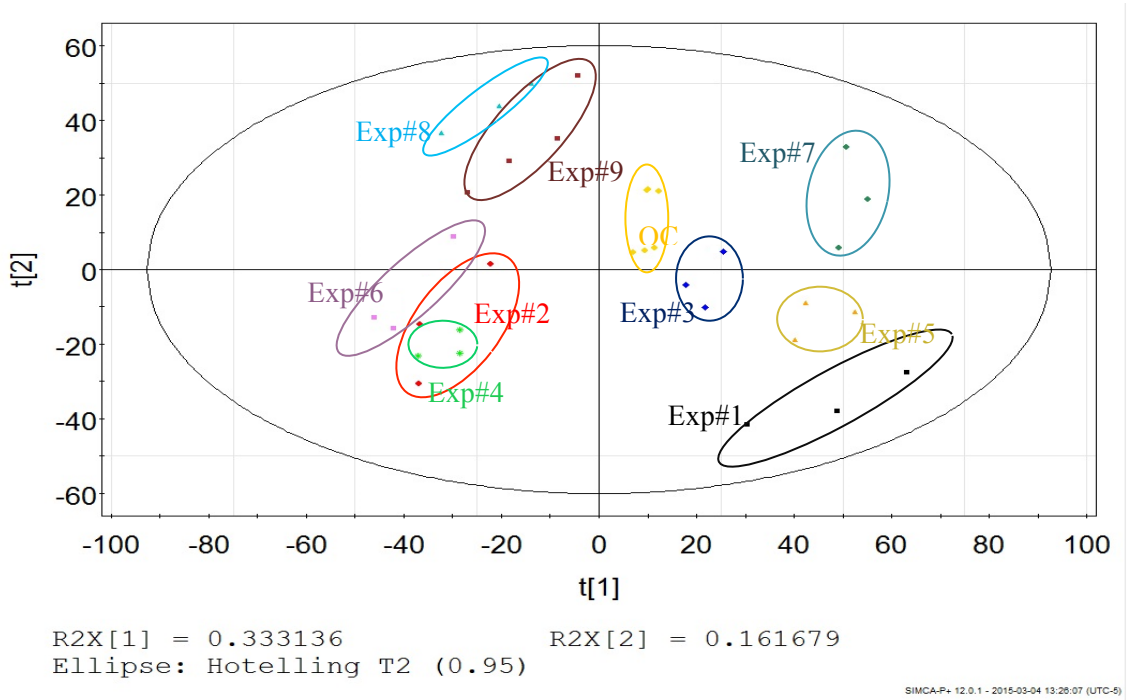

Figure 5.5 PCA score plot obtained from full factorial design for different types of treatments by various clove oil constituents (based on Table 5.3, exp 9 is clove oil treated bacteria)-negative ESI mode.

Results demonstrated a variation in the identified metabolites (a decrease or increase in relative

chromatographic areas) depending on the application of different compositions of antibacterial agents. Figure 5.6 and Figure 5.7 show the chromatogram related to *E.coli* extract in both positive and negative ionization modes, respectively. Figures 5.8 and 5.9 demonstrate chromatograms of *E.coli* treated by clove oil in both positive and negative ionization modes, respectively. The output of XCMS Online provides an overview of experimental results that can be assessed as a quality control mechanism (Figure 5.10). Nonlinear methods were used by XCMS Online to compensate for retention time drifts between samples (Figure 5.10). Figures 5.10-A and 5.10-B indicate an overlay of all total ion chromatograms (TICs) before and after retention time correction, respectively. Figure 5.10-C indicates the retention time deviation versus retention time in different analyzed samples. After retention time correction, all TICs should be in alignment. Figure 5.10-D is a cloud plot demonstrating dysregulated features to represent ions whose intensities are varied between sample groups according to statistical thresholds. Down-regulated features in these treated samples are the circles on the bottom of the plot (red bulbs), while up-regulated ones are circles on the top (green bulbs). Feature size demonstrates the fold change of features, and the color intensity represents the p-value. The program provides a feature table revealing detailed information for each individual feature, including statistics and extracted ion chromatograms, spectrum details and putative METLIN assignments.

About 10,000 features were detected in this study in both electrospray ionization modes, of which almost 60% of the peaks show a significant change of area size due to treatment with antibacterial agents (clove oil and eugenol).

This discrimination in the metabolic profile of *E.coli* was not observed when eugenyl acetate and caryophellene were applied as antibacterial agents. Based on the results, different compounds produced unique metabolic profiles on the bacteria profiles. In this study, a lethal concentration of clove oil was applied for 10^7 CFU mL^{-1} of bacteria. The amount of eugenol in clove oil for this amount of bacteria based on the composition of eugenol in clove oil prohibited bacteria growth. However, the amounts of eugenyl acetate and caryophyllene present in clove oil were shown to be insufficient to stop bacteria metabolism. Thus, the hydroxyl group present in eugenol has an effective role in the prevention of bacterial growth. Table 5.4 demonstrates the dysregulated metabolites in clove oil and eugenol treatment samples using XCMS software. Eugenol and eugenyl acetate belong to the phenylpropenes, as they have a six-carbon aromatic phenol group and a three-carbon propene tail from cinnamic acid produced during the first step of phenylpropanoid biosynthesis. Most antibacterial activity of phenylpropenes is related to the free hydroxyl group in the structure of this class [306,307]. The type and number of substitutions on the aromatic ring are important in the antibacterial activity of phenylpropenes [306,308]. These compounds in plants can disrupt the metabolism of bacterial cells by forming hydrogen bonds through interaction with proteins [309]. Caryophyllene is a natural bicyclic sesquiterpene ($C_{15}H_{24}$) from the

terpenes family, produced from a combination of several isoprene units (C_5H_8).

In eugenol, the presence of a phenolic group is responsible for its antibacterial phenomenon. Sakaguchi et al. reported amine formation interruption by *E. aerogenes* via enzyme inhibition [310,269]. The antibacterial activity showed that clove oil and eugenol exhibited stronger activities than β-caryophyllene on tested oral bacteria. The antibacterial activity of eugenyl acetate is less than that of eugenol, as there is no free hydroxyl group in its structure. Moreover, the clove oil and eugenol showed strong activity against *periodontopathogenic* bacteria [311]. Koutsoudaki et al. reported low or absent antibacterial activity for a group of terpenses as well as for caryophyllene against *E.coli* [312].

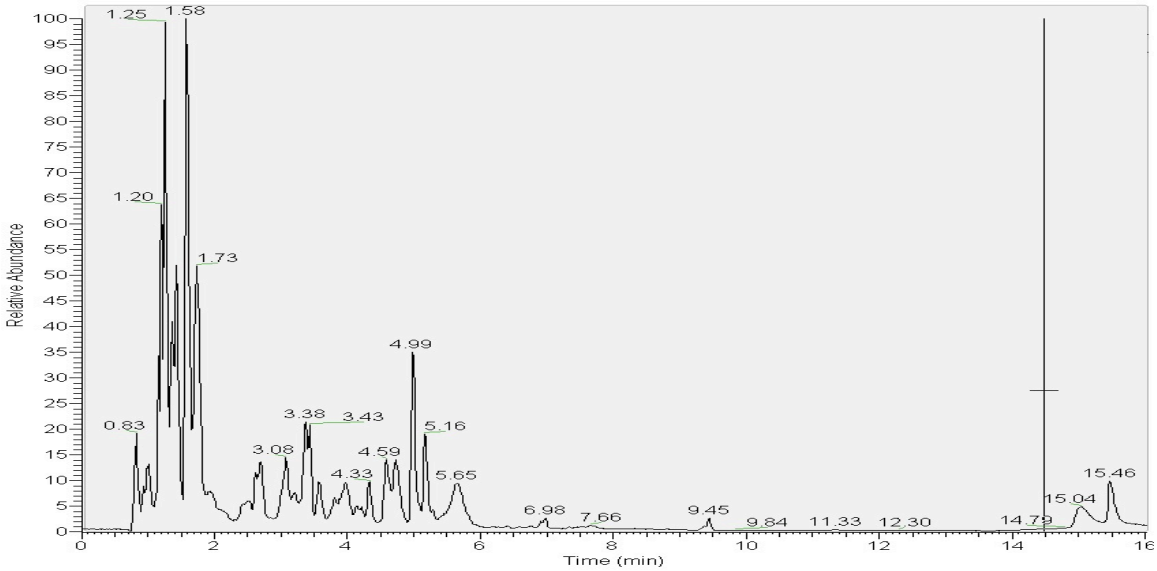

Figure 5.6 Chromatogram of *E.coli* extract by PS-DVB-WAX:HLB 50:50 (w:w) – positive ESI mode.

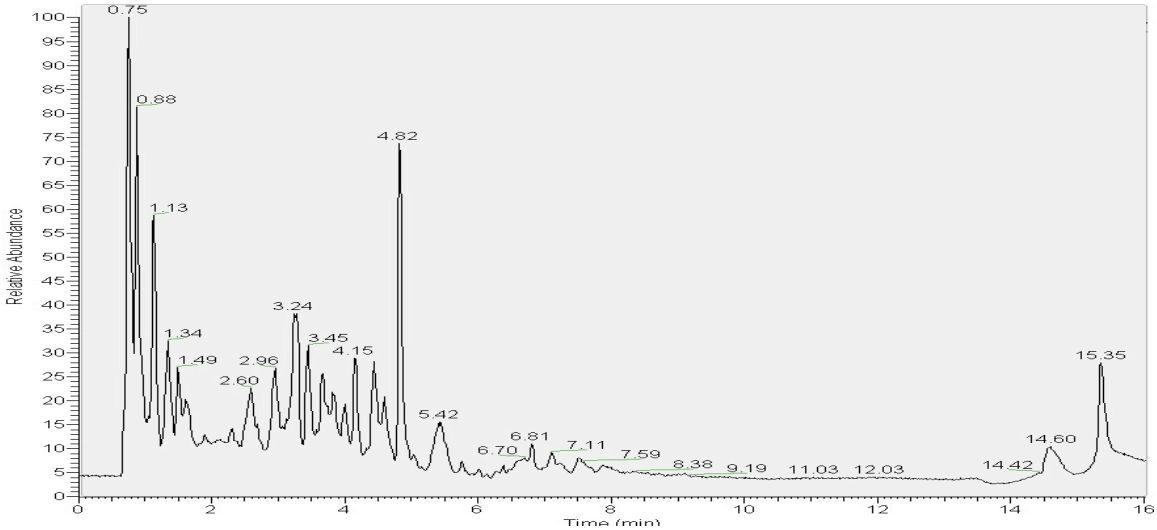

Figure 5.7 Chromatogram of *E.coli* extract by PS-DVB-WAX:HLB 50:50 (w:w) – negative ESI mode.

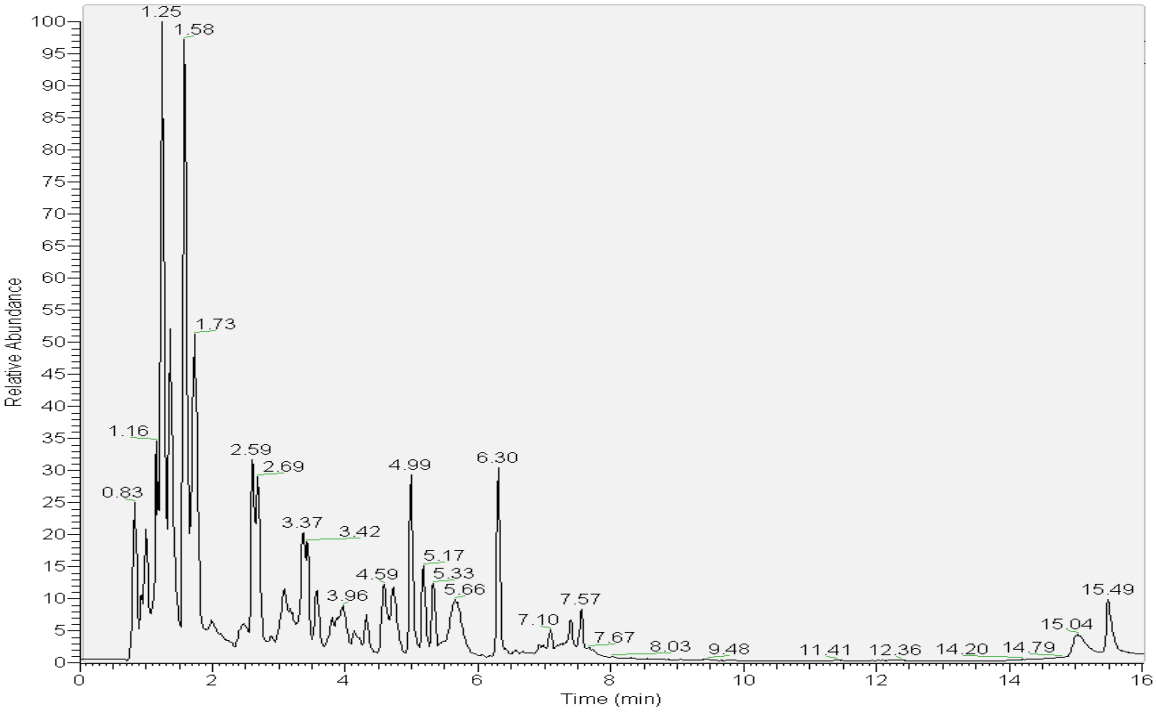

Figure 5.8 Chromatogram of extract from *E.coli* treated by clove oil by PS-DVB-WAX:HLB 50:50 (w:w) – positive ESI mode.

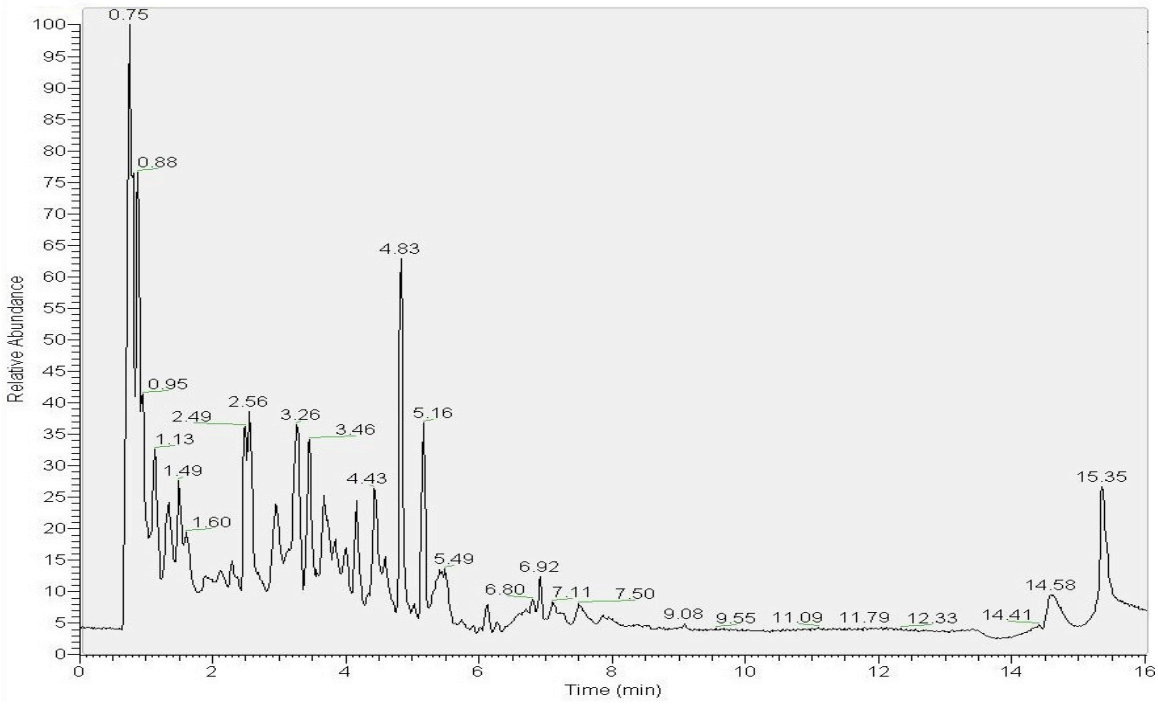

Figure 5.9 Chromatogram of extract from *E.coli* treated by clove oil by PS-DVB-WAX:HLB 50:50 (w:w) – negative ESI mode.

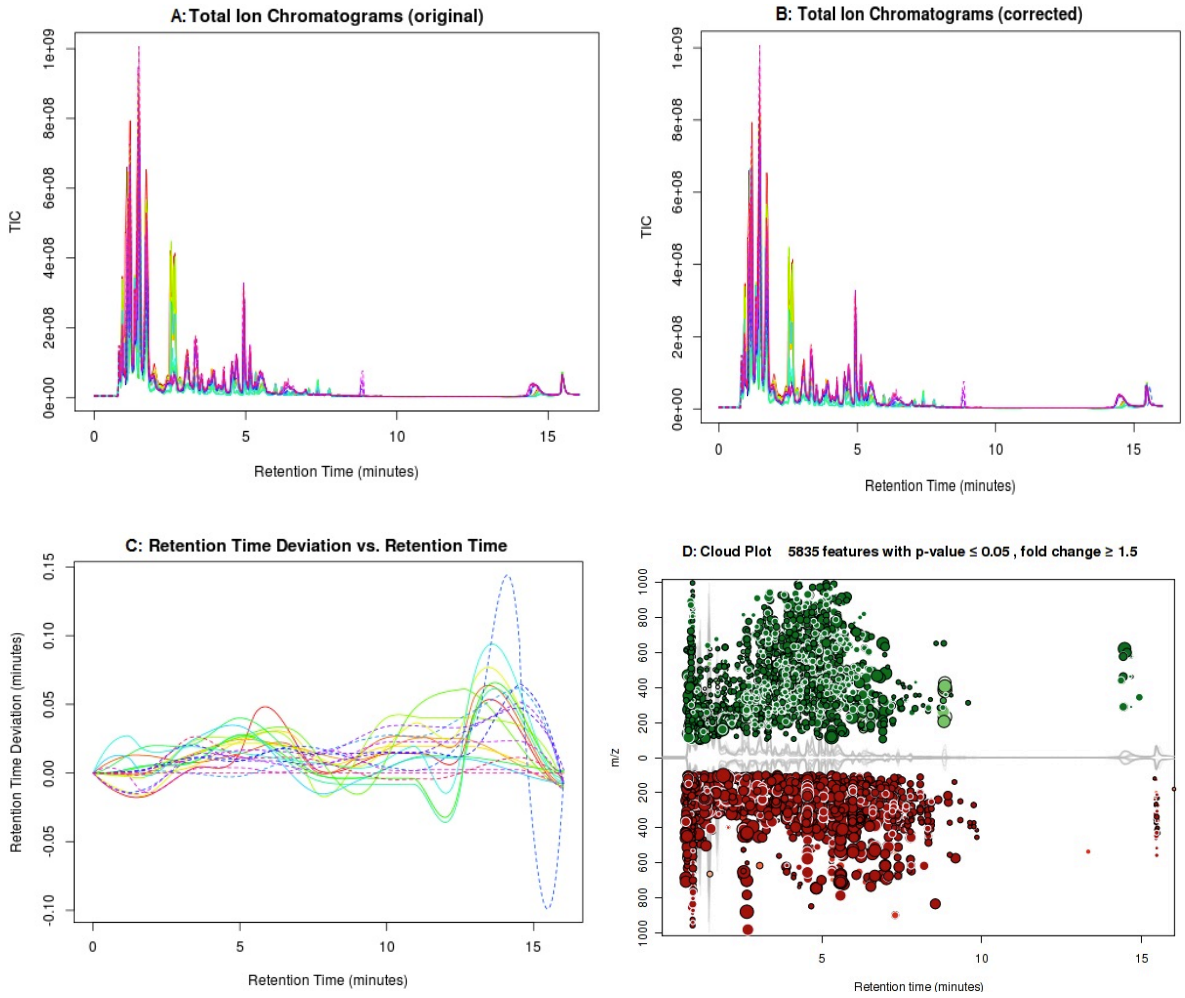

Figure 5.10 XCMS online output. A: total ion chromatograms (TICs) before (Figure 5.10-A) and after (Figure 5.10-B) retention time correction. Figure 5.10-C: the retention time deviation versus retention time in different analyzed samples. Figure 5.10-D: cloud plot: down-regulated (red bulbs) and up-regulated (green bulbs) features in *E.coli* sample treated by eugenol.

5.3.3.1 Effect on the fatty acid Profile of the *E.coli* cell membrane

Cellular responses to stress include adjustments of the membrane system, modifications of the membrane architecture, and changes in cell cycles and cell division. The cell membrane is the first target of antibacterial agents in this study, as these compounds can change its permeability and the functions of proteins embedded inside. Because of the hydrophobicity of these compounds, they can easily diffuse inside the cell from the membrane and disrupt the membrane via changes in the fatty acid balances. Cells adapt to the new environment in order to survive through changes in the ratio of iso and anteiso-branched fatty acids and unsaturated fatty acids to saturated fatty acids, and also by changing their fatty acid chain length [313]. The change in degree of saturation in fatty acids is applied by desaturase enzyme by adding

or removing two hydrogens to or from the acid's double bond [263].

In this current research, when antibacterial agents such as carryophellene and eugenyl acetate were applied under minimum inhibitory concentration, the percentage of unsaturated fatty acids increased to enhance cell membrane fluidity, whereas in experiments where the antibacterial agents were applied above the MIC (clove oil and eugenol), an increase in the amount of saturated fatty acids caused loss of membrane fluidity and enhancement in its rigidity. As demonstrated in Table 5.3, the levels of the unsaturated fatty acids octadecadienoic acid, 9-hydroperoxy-10E,12-octadecadienoic acid, dodecadienoic acid, tridecadienoic acid, 2Z-dodecenedioic acid, decatetraenedioic acid, tridecadienoic acid, nonadienoic acid, and 4,7,10-hexadecatrienoic acid were observed to decrease, while the level of myristic acid alkyne, as a saturated fatty acid, was observed to increase. Short and medium length levels of organic acids such as adipic and pimelic acids also increased.

On the other hand, in the case of caryophyllene and eugenyl acetate, the levels of unsaturated fatty acids such as 2-methyl-dodecanedioic acid, 12S-hydroxy-5Z,8E,10E-heptadecatrienoic acid, myristoleic acid, tetradecadienoic acid, tridecadienoic acid, and 9-oxo-2,4,5,7-decatetraenoic acid, increased.

Di Pasque et al. perceived that treatment of *E. coli O157:H7 ATCC 43888* with sub-lethal concentrations of thymol, lomonene, eugenol, carvacrol, and cinnamaldehyde increased the levels of saturated fatty acids such as myristic (C14), palmitic (C16), and stearic (C18) acids, while levels of unsaturated acids such as unsaturated oleic (C18:1 cis), linoleaidic (C18:2 trans), and linolenic (C18:3 cis) acids were observed to decrease as a result of treatment [262].

5.3.3.2 Action on proteins

Another target of eugenol and clove oil is the proteins that the hydroxyl group in eugenol binds to and prevents from functioning as enzymes [310]. Up-regulation or down-regulation of various metabolites involved in specific metabolic pathways in the treated sample demonstrated the change in the microorganism's metabolism in antibacterial environments caused by the change in enzymatic functions. For example, down regulation of cadaverine, one of the amines produced by biodegredative decarboxylases [314], accompanied by up-regulation of lysine in a sample treated with clove oil and eugenol, demonstrated the inhibition of lysine decarboxylase [315]. Wendakoon et al. observed that eugenol and cinnamaldehyde, as the most-effective species with inhibitory action towards the activity of the amino acid decarboxylase of a crude extract of *Enterobacter aerogenes,* prevented production of poisonous metabolites such as cadaverine, histamine, putescine, and tryamine [269]. In addition, the down-regulation of the glucose level in treated samples represents amylase down-regulation. This enzyme catalyzes the hydrolysis of long chain carbohydrates into simple sugars such as glucose. Thoroski et al. observed that the production of enzymes such as alpha-amylase and protease was inhibited or reduced in *Bacillus subtilis* when the concentration of eugenol was increased from 0.0 to 0.04% v/v [316]. This

phenomenon may delay glucose utilization in the glycolysis pathway, and consequently, clove oil has been suggested as a cancer care drug. Based on the Warburg effect, glycolysis is enhanced in most cancer cells to generate ATP as a main source of energy production. Consequently, targeting the glycolytic pathway may kill malignant cells and have a broad therapeutic effect [274]. Another pathway of interest is that for dGTP synthesis. Increased guanosine levels accompanied by decreased guanine levels could stop the salvage of guanine and guanosine, the metabolites at the beginning of the dGTP synthesis pathway, which could be attributed to inhibition of guanosine phosphorylase function.

5.3.3.3 Anti-quorum sensing activity

When the number of bacteria reaches a particular threshold during growth, intercellular communication, called quorum sensing (QS), will organize the interaction among bacteria. QS controls virulence factor expression, bioluminescence, sporulation, biofilm formation, and mating. Genes involved in the expression of QS produce the prompt of chemical-signaling molecules called autoinducers. Autoinducers are produced until the number of bacteria reaches their maximum threshold [317]. Researchers have introduced essential oils as nontoxic inhibitors of QS without strain resistance [318]. Various mechanisms are involved in QS inhibition, such as the inhibition of acyl homoserine lactones as autoinducers, inhibition of acyl homoserine lactone transport, and inhibition of targets downstream of the acyl homoserine lactone receptor binding [319]. In the present study, the level of homoserine lactone decreased in the clove oil- and eugenol-treated samples, demonstrating that these compounds are potential QC inhibitors that prevent biofilm formation. Previously, Khan et al. observed the QS inhibitory effect of clove oil [320].

Further interpretation of the observed changes will require a more comprehensive investigation and interpretation of biochemical pathways of *E.coli* growing under clove oil treatment.

Chromatograms and corresponding mass spectra indicating masses assigned as adducts of some important metabolites are shown in Figure 5.11.

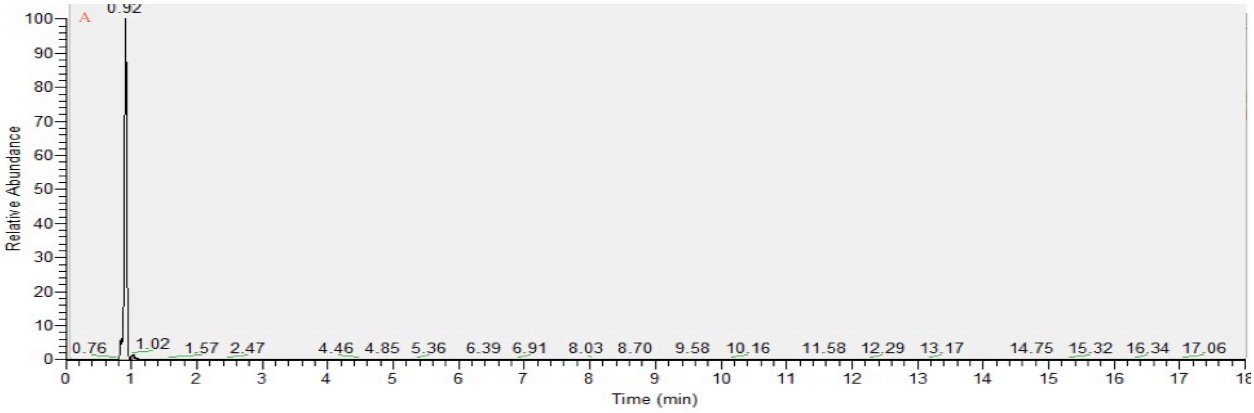
A
0.92
Relative Abundance
Time (min)
0.76
1.02
1.57
2.47
4.46
4.85
5.36
6.39
6.91
8.03
8.70
9.58
10.16
11.58
12.29
13.17
14.75
15.32
16.34
17.06

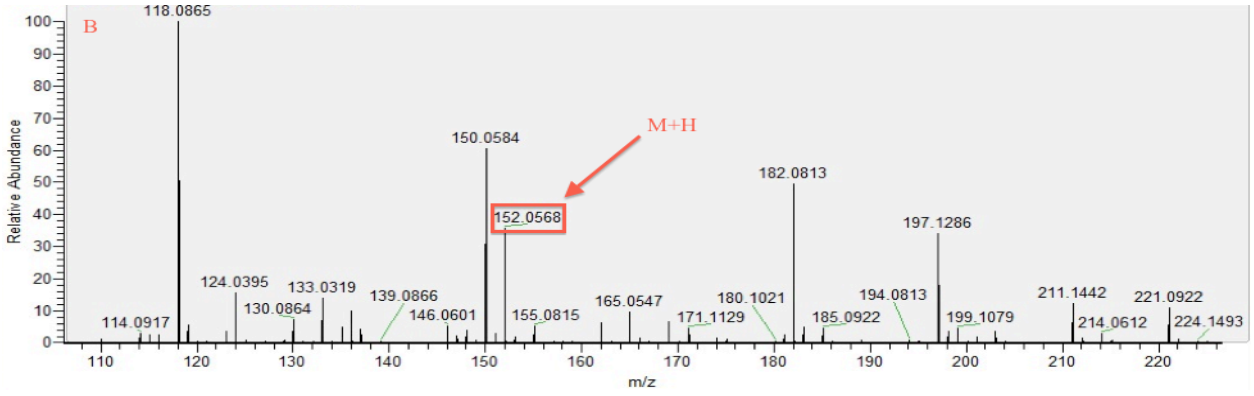
B
118.0865
150.0584
M+H
152.0568
182.0813
197.1286
124.0395
133.0319
139.0866
130.0864
146.0601
114.0917
155.0815
165.0547
171.1129
180.1021
185.0922
194.0813
199.1079
211.1442
221.0922
214.0612
224.1493
Relative Abundance
m/z

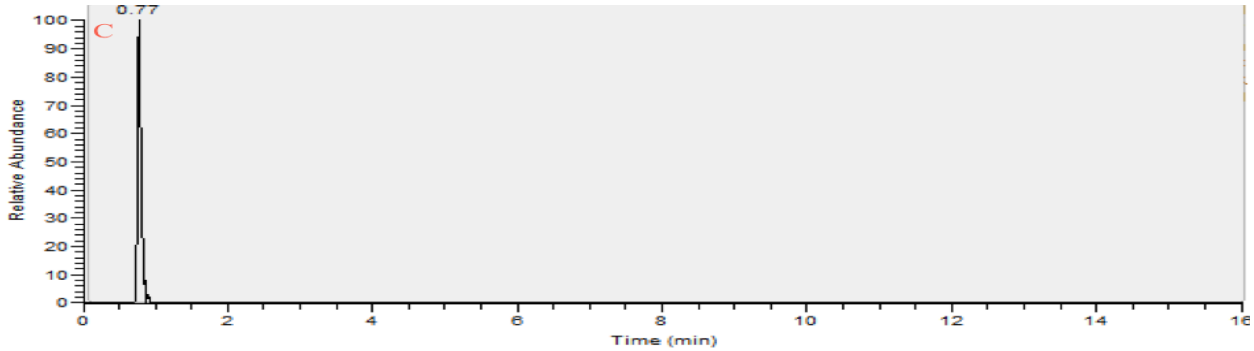
C
0.77
Relative Abundance
Time (min)

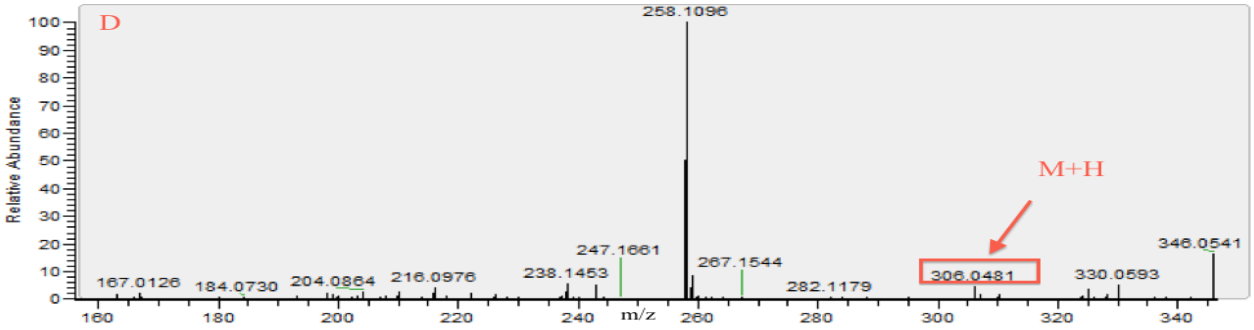
D
258.1096
M+H
247.1661
267.1544
306.0481
346.0541
167.0126
184.0730
204.0864
216.0976
238.1453
282.1179
330.0593
Relative Abundance
m/z

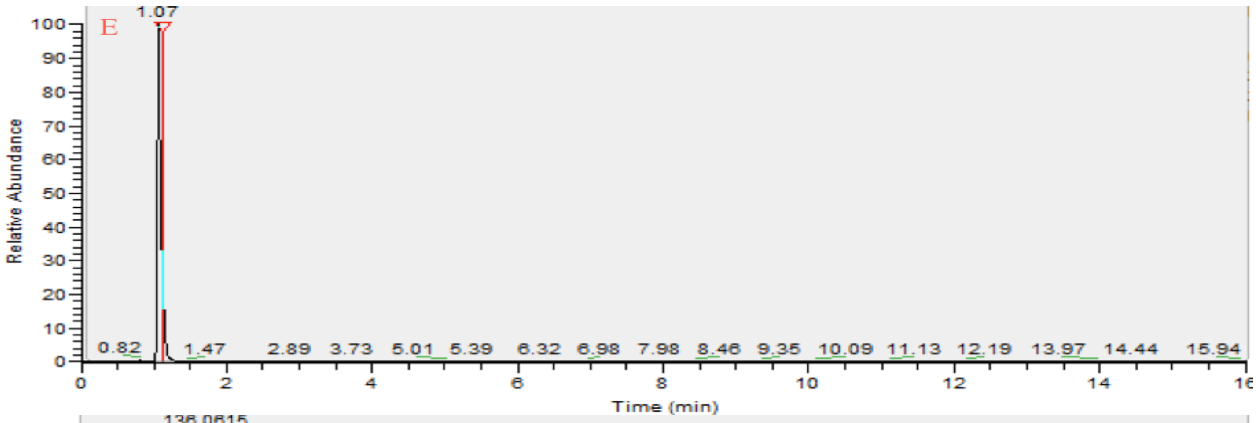
E
1.07
Relative Abundance
Time (min)
0.82
1.47
2.89
3.73
5.01
5.39
6.32
6.98
7.98
8.46
9.35
10.09
11.13
12.19
13.97
14.44
15.94

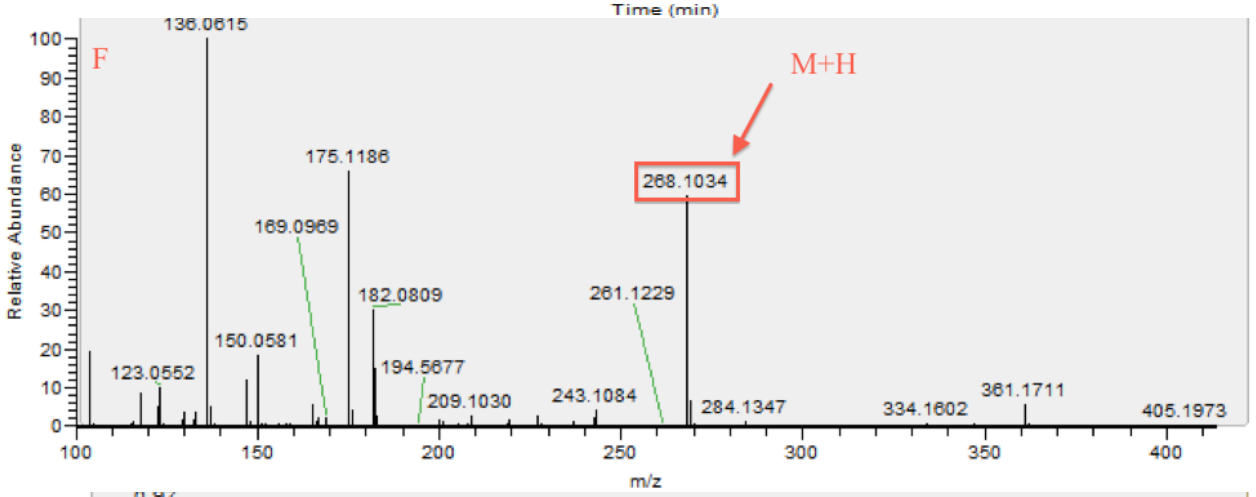
F
M+H
136.0615
175.1186
268.1034
169.0969
182.0809
261.1229
150.0581
123.0552
194.5677
209.1030
243.1084
284.1347
334.1602
361.1711
405.1973
Relative Abundance
m/z

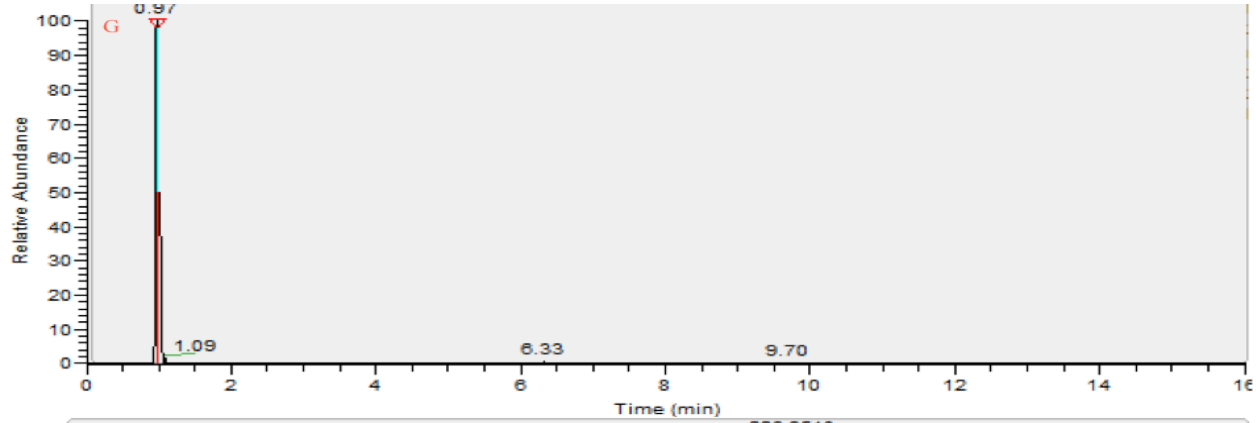
G
0.97
1.09
6.33
9.70
Relative Abundance
Time (min)

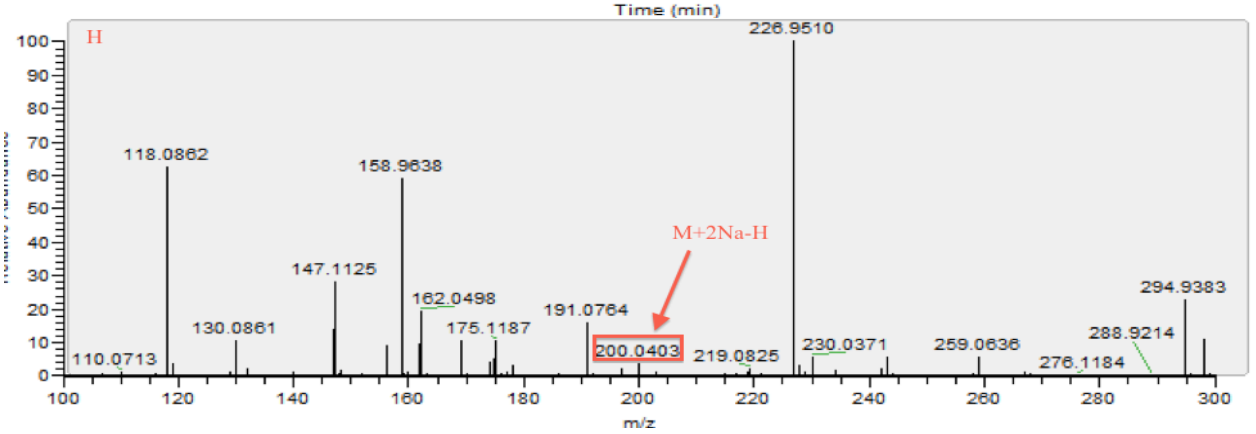
H
226.9510
118.0862
158.9638
M+2Na-H
147.1125
162.0498
191.0764
294.9383
130.0861
175.1187
200.0403
110.0713
219.0825
230.0371
259.0636
288.9214
276.1184
m/z

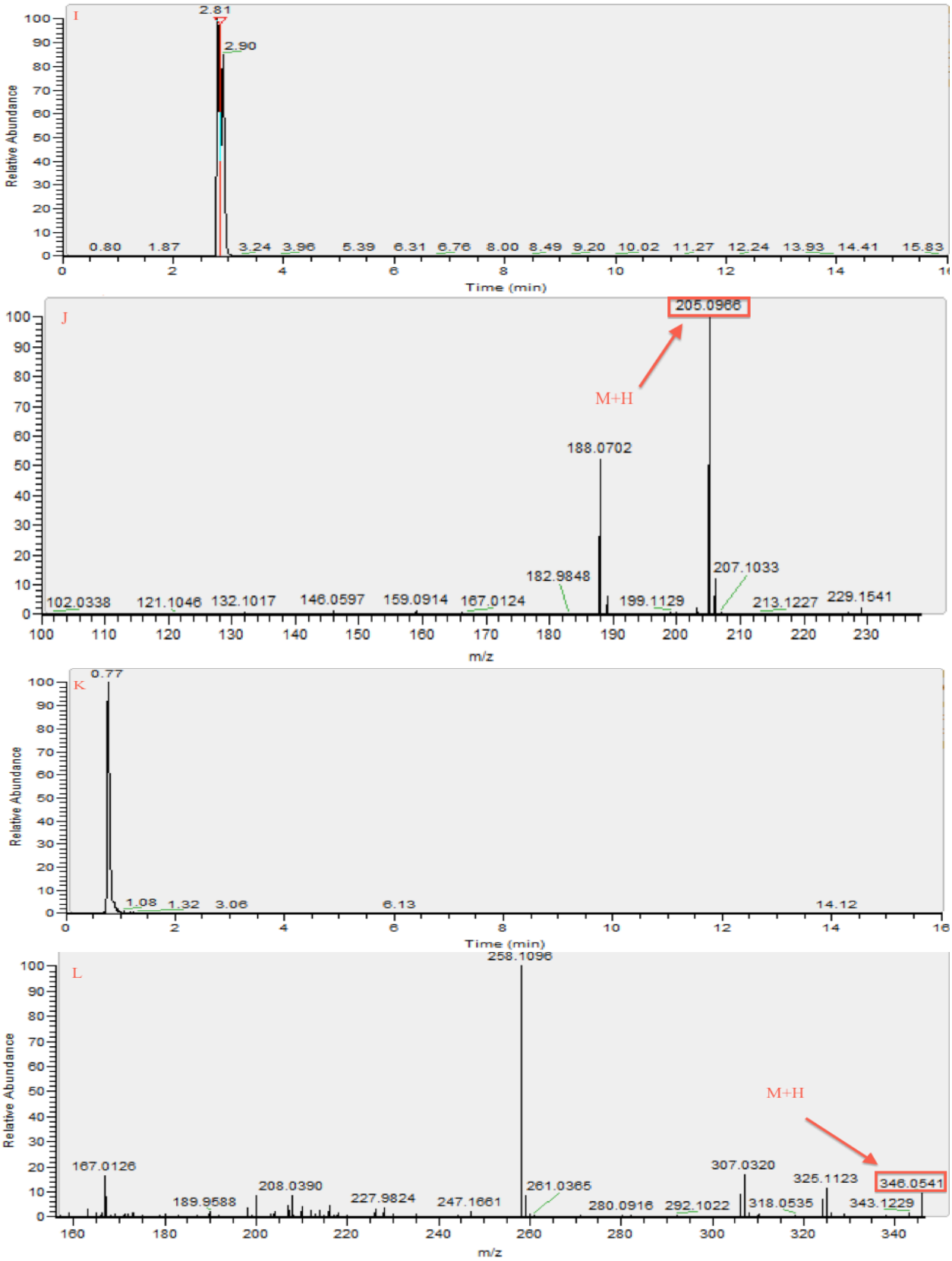

Figure 5. 11 Chromatograms and corresponding mass spectra indicating masses assigned as adducts of Guanine (A, B); 2',3' cyclic CMP (C, D); Adenosine (E, F); Histidine (G, H); Tryptophan (I, J), cGMP (K, L).

Table 5.4 Dysregulated metabolites in *E.coli* samples treated by clove oil and eugenol obtained from XCMS online and full factorial design.

Metabolite	Adduct	mz	METLIN ID	ppm	Chemical Formula	Regulation p-value
Amino Acids and Derivatives						
Proline	$[M+H]^+$	116.0707	58150	0.8	$C_5H_9NO_2$	Up 6.64574e-6
Asparagine	$[M+H]^+$	133.0608	65674	0	$C_4H_8N_2O_3$	Up 7.37334e-6
Tryptophan	$[M+H]^+$	205.0966	33	2	$C_{11}H_{12}N_2O_2$	Up 0.00345
N-Hydroxy-L-tryptophan	$[M+H]^+$	221.0920	73314	0	$C_{11}H_{12}N_2O_3$	Up 9.57623e-6
Glutamate	$[M+2Na-H]^+$	148.0604	3761	0	$C_5H_9NO_4$	Up 6.45342e-5
Valine	$[M+H]^+$	118.0864	71199	0.8	$C_5H_{11}NO_2$	Up 0.00008
Tyrosine	$[M+NH4]^+$	199.1078	58353	0	$C_9H_{11}NO_3$	Down 0.00019
Homoarginine	$[M+H]^+$	189.1343	5640	-1.6	$C_7H_{16}N_4O_2$	Down 0.00019
Homoglutamine	$[M+H]^+$	161.0920	3281	0	$C_6H_{12}N_2O_3$	Up 0.00021
Serine	$[M+H]^+$	106.0501	63419	2.8	$C_3H_7NO_3$	Up 0.00001
Glutamate	$[M+H]^+$	148.0604	3761	0	$C_5H_9NO_4$	Up 0.00014
Citrulline Nα-Acetyl-L-arginine	$[M+ACN+H]^+$ $[M+H]^+$	217.1295	16	0	$C_6H_{13}N_3O_3$	Down 0.00014
Tyrosine	$[M+NH4]^+$	199.1078	58353	4.6	$C_9H_{11}NO_3$	Up 0.00002
Histidine	$[M+2Na-H]^+$	200.0403	65529	-1.5	$C_6H_9N_3O_2$	Down 0.00005
Aspartic acid	$[M+H]^+$	134.0448	63097	0	$C_4H_7NO_4$	Up 0.00003
N6-Acetyl-N6-hydroxy-L-lysine	$[M+H]^+$	205.1182	63465	0	$C_8H_{16}N_2O_4$	Up 0.00007
N-Hydroxy-L-tryptophan	$[M+H]^+$	221.0921	73314	0	$C_{11}H_{12}N_2O_3$	Up 0.00007
Threonine	$[M+H]^+$	120.0656	32	0	$C_4H_9NO_3$	Up 0.00007
Azolines						
Creatinine	$[M+ACN+H]^+$	155.0927	8	0	$C_4H_7N_3O$	Up 9.74675e-6
Benzene and Substituted Derivatives						
Phoxim	$[M+2Na-H]^+$	343.0254	72530	1.6	$C_{12}H_{15}N_2O_3PS$	Up 0.00227
Carbohydrates and carbohydrate conjugates						
Acetylmannosamine	$[M+H]^+$	222.0973	3357	0.5	$C_8H_{15}NO_6$	Up 0.00002
Glucose	$[M+Na]^+$	203.0527	63118	0.5	$C_6H_{12}O6$	Down

						0.00004
Sucrose	$[M+H-H2O]^+$	325.1129	137	-1.5	$C_{12}H_{22}O_{11}$	Up 1.17474e-6
Glucosaminide	$[M+H-2H2O]^+$	466.2041	7043	1.1	$C_{18}H_{35}N_3O_{13}$	Down 0.00003
Carboxylic Acids and Derivatives						
N-Acetylcystathionine	$[M+H-H2O]^+$	247.0748	6656	1.6	$C_9H_{16}N_2O_5S$	Down 1.48854e-6
Lysopine	$[M+H]^+$	219.1340	89468	0	$C_9H_{18}N_2O_4$	Up 0.00368
Adipic acid	$[M+Na]^+$	169.0468	115	-1.7	$C_6H_{10}O_4$	Down 0.00055
Cystine	$[M+H]^+$	241.0310	63635	0.4	$C_6H_{12}N_2O_4S_2$	Up 0.00153
Glutathione	$[M+H]^+$	308.0909	44	0.3	$C_{10}H_{17}N_3O_6S$	Down 0.00033
N-Acetylcadaverine	$[M+H]^+$	145.1336	6592	0.7	$C_7H_{16}N_2O$	Down 0.00026
γ-Glutamyl-γ-aminobutyraldehyde	$[M+H]^+$	217.1183	63481	0	$C_9H_{16}N_2O_4$	Up 0.00119
Diaminopimelic acid	$[M+H]^+$	191.1027	352	0.5	$C_7H_{14}N_2O_4$	Up 0.00342
Homocitrulline	$[M]^+$	189.1116	46	1.5	$C_7H_{15}N_3O_3$	Down 3.84520e-6
Glutathione	$[M+H]^+$	308.0909	44	-0.3	$C_{10}H_{17}N_3O_6S$	Down
Diazines						
Cytosine	$[M+H]^+$	112.0507	283	1.7	$C_4H_5N_3O$	Up 0.00016
Fatty Acids and Conjugates						
tridecadienoic acid	$[M+H-H2O]^+$	193.1589	34909	-1.5	$C_{13}H_{22}O_2$	Down 0.00001
2-keto valeric acid	$[M+ACN+H]^+$	158.0811	3243	0	$C_5H_8O_3$	Down 0.00245
2E,4E-dodecadienoic acid (unsaturated)	$[M+H]^+$	197.1538	34895	-1.0	$C_{12}H_{20}O_2$	Down 0.00011
4,7,10-hexadecatrienoic acid (unsaturated)	$[M+H]^+$	251.2007	34809	0.8	$C_{16}H_{26}O_2$	Down 0.00010
dihydroxy-stearic acid (saturated)	$[M+Na]^+$	339.2509	45832	1.2	$C_{18}H_{36}O_4$	Up 0.00001
nonadienoic acid (unsaturated)	$[M+NH4]^+$	172.1332	35103	0	$C_9H_{14}O_2$	Down 0.00024
hydroxypalmitic acid (saturated)	$[M-H]^-$	271.2265	45829	-4.7	C16H32O3	Up 0.0001
Isodecenoic acid (unsaturated)	$[M+H]^+$	171.1380	34722	0	$C_{10}H_{18}O_2$	Up 0.00015
tridecadienoic acid (unsaturated)	$[M+H-H2O]^+$	193.1588	34909	2.1	$C_{13}H_{22}O_2$	Down 193.1588
dodecadienoic acid (unsaturated)	$[M+H]^+$	197.1538	34895	-1.3	$C_{12}H_{20}O_2$	Down 0.00004

Myristoleic acid (unsaturated)	$[M+H]^+$	227.2007	6424	0.8	$C_{14}H_{26}O_2$	Down 0.00496
Myristic Acid Alkyne	$[M+H-H2O]^+$	207.1745	35248	-1.9	$C_{14}H_{24}O_2$	Up 0.00190
Decatetraenedioic acid	$[M+NH4]^+$	212.0918	74898	0.5	$C_{10}H_{10}O_4$	Down 0.00168
Fatty acyls						
Octyl acetate	$[M+K]^+$	211.1095	46196	0	$C_{10}H_{20}O_2$	Down 0.00001
Caproic acid	$[M+K]^+$	155.0469	111	0	$C_6H_{12}O_2$	Down 7.38651e-6
2-Tridecene-4,6,8-triyn-1-ol	$[M+H]^+$	187.1119	87296	1.1	$C_{13}H_{14}O$	Up 0.00306
Fatty aldehydes						
2,4,7-tridecatrienal	$[M+H]^+$	193.1589	75353	1.5	$C_{13}H_{20}O$	Up
Tetradecadienal	$[M+H]^+$	209.1902	46461	1.4	$C_{14}H_{24}O$	Down 0.00007
Glycerols						
Glycyrol	$[M+ACN+H]^+$	408.1434	71470	-1.6	$C_{21}H_{18}O_6$	Up 0.00085
Glycerolipids						
1-Octylglycerol	$[M+K]^+$	243.1357	46620	0	$C_{11}H_{24}O_3$	Down
Glyceryl 5-hydroxydecanoate	$[M+Na]^+$	285.1669	88341	-1.1	$C_{13}H_{26}O_5$	Down 0.00301
Glycerophosphoglycerols						
PE(P-18:0/22:6(4Z,7Z,10Z,13Z,16Z,19Z))	$[M+H-H2O]^+$	758.5489	46708	0	$C_{45}H_{78}NO_7P$	Down 0.00220
PA(13:0/20:5(5Z,8Z,11Z,14Z,17Z))	[M+]	652.4114	81251	-1.5	$C_{36}H_{61}O_8P$	Up 0.00001
PE(O-20:0/0:0)	M+2Na-H	540.3392	77700	-1.5	$C_{25}H_{54}NO_6P$	Down 0.00219
Imidazopyrimidines						
Adenine	$[M+H]^+$	136.0618	85	0	$C_5H_5N_5$	Up 0.00005
Guanine	$[M+H]^+$	152.0568	315	1.3	$C_5H_5N_5O$	Down 4.68891e-6
6-Thiouric acid	$[M+NH4]^+$	202.0393	718	0	$C_5H_4N_4O_2S$	Up 0.00197
Hypoxanthine	$[M+H]^+$	137.0458	83	0	$C_5H_4N_4O$	Down 0.00110
Indoles and Derivatives						
3-Methylindole	$[M+H]^+$	132.0809	5453	1.5	C_9H_9N	Up 8.91649e-7
Indole	$[M+H]^+$	118.0653	286	1.6	C_8H_7N	Up 0.00145
Lactams						
Homoserine lactone	$[M+K]^+$	140.0108	65863	0	$C_4H_7NO_2$	Down 8.96060e-6
Lineolic acid and derivatives						

octadecadienoic acid	$[M]^+$	312.2300	35348	0	$C_{18}H_{32}O_4$	Down 0.00002
9-hydroperoxy-10E,12-octadecadienoic acid	$[M]^+$	312.2300	35348	0	$C_{18}H_{32}O_4$	Down 0.0000054
Prenol lipids						
2-Hexaprenyl-3-methyl-6-methoxy-1,4-benzoquinol	$[M]^+$	562.4379	62813	-1.2	$C_{38}H_{58}O_3$	Down 0.00028
Purine Nucleosides and Analogues						
Adenosine	$[M+H]^+$	268.1039	86	-0.4	$C_{10}H_{13}N_5O_4$	Up 0.00029
Guanosine	$[M+H]^+$	284.0988	87	-0.4	$C_{10}H_{13}N_5O_5$	Up 0.00006
Deoxyguanosine Adenosine	$[M+ACN+H]^+$	309.1304	3395	-0.6	$C_{10}H_{13}N_5O_4$	Up 0.00241
cGMP	$[M+H]^+$	346.0541	3485	1.7	$C_{10}H_{12}N_5O_7P$	Up 0.00106
Isopentenyl adenosine	$[M+H]^+$	336.1666	64086	0	$C_{15}H_{21}N_5O_4$	Up 0.00103
Xanthine	$[M+H]^+$	153.0407	82	0	$C_5H_4N_4O_2$	Down 0.0000053
1-Methyladenosine	$[M+H]^+$	282.1196	6888	0	$C_{11}H_{15}N_5O_4$	Up 0.00027
Pyrenes						
Pyrene	$[M+ACN+H]^+$	244.1121	69974	0	$C_{16}H_{10}$	Up 0.00048
Pyridines and Derivatives						
Nicotinic acid (Niacin)	$[M+H]^+$	124.0394	240	0.7	$C_6H_5NO_2$	Down 2.46054e-6
Pyridoxamine	$[M+ACN+H]^+$	210.1238	238	0.4	$C_8H_{12}N_2O_2$	Down 0.00210
Pyridoxal (Vitamin B6)	$[M+ACN+H]^+$	209.0921	2203	0	$C_8H_9NO_3$	Down 0.00266
Pyrimidine Nucleosides and Analogues						
Cytidine diphosphate choline	$[M+H]^+$	489.1142	3581	-0.8	$C_{14}H_{26}N_4O_{11}P_2$	Up 0.00004
2',3'-Cyclic UMP	$[M+H]^+$	307.0325	3438	0	$C_9H_{11}N_2O_8P$	Up 1.55770e-8
2',3' cyclic CMP	$[M+H]^+$	306.0481	62429	1.3	$C_9H_{12}N_3O_7P$	Down 1.92863e-7
Quaternary ammonium salts						
Choline	$[M+ACN+H]^+$	145.1336	56	0.6	$C_5H_{13}NO$	Down 0.00026

5.4 Conclusions and future directions

In this study, a 96-blade SPME-LC/MS method was developed using multivariate design, and applied to evaluate the synergistic effect of different major components of clove oil as antibacterial agents against *E.coli*. In contrast to traditional univariate optimization methodology applied in previous studies, multivariate experimental design assists in the optimization of important parameters affecting extraction recovery, taking into account their interactions as well. SPME provided clear separation between *E.coli* samples treated by clove oil major components, and the mechanism of antibacterial action of the naturally

occurring compounds suggested different metabolic pathways for samples treated with the active agents. Based on the obtained results, eugenol, as the major component of clove oil, clearly confirmed its characterization as an antimicrobial agent, while no synergistic effect was observed between the constituents of clove oil in the actual weight percent in which they appear in this oil. This study can be applied towards the utilization of antibacterial agents and reduce the antibacterial agent consumption in order to access to a particular antibacterial effect and health purposes. This study provided a better understanding of the metabolic responses of *E.coli* to clove oil and its major components, while demonstrating the SPME-LC-MS-based metabolomics platform as a superior technique for the study of complex biosystems, using *E.coli* as a model organism. Evaluation of the discriminatant metabolites in treated samples confirmed that eugenol is a lead candidate for further development as an active agent in anti-cancer treatments due to its ability to cause glycolysis inhibition of *E.coli* as a model organism. An investigation of metabolic profiles between treated and control *E.coli* samples demonstrated that this compound can stop *E.coli* metabolism by binding to proteins as well as through membrane disruption.

Chapter 6

Targeted and untargeted apple metabolomics with SPME-LC/MS

6.1 Introduction

The apple is an important fruit source for human consumption. The quality of apples is defined based on their appearance, sweetness, acidity, firmness, color, and potential health benefits [321]. Sweetness is related to their sugar and sugar alcohol content. Organic acids and complex cell wall polymers determine the fruit acidity and firmness, respectively. Fruit color is related to the composition of carotenoids and anthocynins in the peel, while polyphenolic metabolites and triterpenes provide potential health benefits [322-328]. Commercially, apples are kept at temperatures of -1 to 4°C without suffering abrupt damage, but after weeks or months of storage in such temperatures, chilling stress related to coldness can cause browning disorders or superficial scalds attributed to damage happening in the upper hypodermal layers associated with changes in fruit metabolism [329-331]. Ethylene, a naturally occurring plant hormone, assists in the maturation process of fruits through enzyme production, which breaks down starches and cell walls, causing fruit softness and sweetness. Physiological disorders such as superficial scald, soft scald, core flush, and greasiness develop during storage and are linked to fruit maturity. The shelf life of apples may be enhanced by controlling ethylene production, as considerable evidence indicates that ethylene leads to scald progress [332]. Better insight into the processes involved in this phenomenon will help suppliers better predict the maximum shelf life of apple products, achieve nutritional stability, and enhance market value.

Various methods are applied to chemically control ethylene biosynthesis; for instance, in the horticulture industry, ethylene inhibitors such as diazocyclopentadiene, 1-methylcyclopropane (1-MCP), and aminoethoxyvinylglycine (AVG) are widely used to reduce physiological apple disorders such as superficial scald and soft scald, which may result from storage and other types of stress that induce ethylene production by influencing ethylene biosynthesis, as well as other metabolic pathways [333,334].

Apple ripening involves complicated biological processes characterized by conversions in the transcriptome, proteome, and metabolome. Untargeted metabolomics is able to differentiate metabolites altered by ecological conditions or genotypes [335]. Metabolomic analyses consist of a sequence of steps, including sample preparation, metabolite extraction, separation, detection, and data treatment. As the nature of compounds of interest is mostly unknown, a reliable method is needed to extract as many metabolites as possible from apple samples [336].

Various studies have reported on the metabolic pathways involved in superficial scald or browning disorders that affect apple samples during storage; however, providing a comprehensive picture of

metabolism alteration requires a reproducible technique that is indiscriminating towards metabolites extraction, fast enough to inhibit metabolite degradation or loss, accompanied by a metabolism quenching stage, and that provides identification of a wide variety of metabolites [337-345]. Sampling and sample preparation should provide a good representative of the sample under study. Various chemical and physical properties of metabolites, as well as their high turnover rates, make metabolite extraction a challenging undertaking. Matrix complexity and metabolite loss are the most important issues faced in metabolomics performance. A powerful extraction technique should provide extraction of metabolites from interferences, and bring the metabolome concentration up to detectable levels for instrumental techniques. A number of metabolite extraction techniques are used in plant metabolomics, such as LLE, solid–liquid extraction (SLE), SPE, and accelerated solvent extraction. In the case of LLE and SLE, the type of solvent being used can cause metabolite discrimination as well as metabolite modification and degradation [336].

SPE, another technique used to remove the matrix of samples such as proteins and salts, provides efficient sample clean up and metabolite enrichment. SPE is widely used in plant and food metabolomics; however, cartridge clogging is probable during extraction. Also, due to the large volumes of solvent that are used in this technique, non-adsorbent analytes are retained in the void volume. In contrast, according to the guidelines related to green chemistry goals, the latest trend favors miniaturized sample preparation techniques, and decreases or eliminates solvent consumption [346,347]. Thin film SPME, using an open bed device, provides several benefits over other techniques, making it a powerful candidate for metabolomics research: it is easily automated, uses small sample volumes, consumes small amounts of organic solvent, is a fast sample preparation technique, and, depending on the choice of coating, SPME is capable of extracting a wide polarity range of metabolites [346,348]. MS and NMR are two analytical platforms extensively used in plant metabolomics. NMR has low sensitivity and lower resolving power in comparison to MS, allowing for the detection of low abundance metabolites. MS provides more complex spectra, especially in the case of complex matrices [348]. Efficient sample preparation and chromatographic techniques reduce the enhancement of matrix effects in MS-based metabolomics [346] SPME coupled to GC/MS has been successfully utilized as a sample preparation technique for plant metabolomics, especially in the identification of volatiles and semi-volatiles, although the technique is unsuitable for nonvolatile determinations without derivatization, which is associated with numerous difficulties and artifacts in chromatograms [349-361]. SPME-LC/MS can be applied to cover the identification of metabolites unidentifiable by SPME-GC/MS. In the literature, to the best of this author's knowledge, no reports are available on applications of SPME-LC/MS for plant and food metabolomics. The objective of the presently introduced work was the development of a high-throughput 96-blade SPME-LC/MS technique for the extraction of a broad range of metabolites from apple samples that could

be applied without the need of laborious sample pretreatment steps. Once developed, the 96-blade SPME-LC/MS was applied for untargeted metabolic profiling of "Honeycrisp" apples subjected to cold storage. PLS has been used to characterize changes in the metabolic profiles of apples during storage under a controlled atmosphere, applying AVG, and disorder development. Primary and secondary metabolic pathway alterations in apple samples were investigated, as were the metabolite variations following various time points of cold storage (4 and 8 months). The results demonstrate extensive changes in the metabolism of samples involving multiple pathways as a function of the stress generated by cold storage.

6.2 Experimental part

6.2.1 Metabolite standard mixture preparation

Standard mixtures of metabolites covering a wide range of polarities such as amino acids, sugars, nucleosides, and flavonoids, listed in Table 6.1, were prepared for SPME method development. Stock standard solutions were prepared in water/methanol, kept frozen (-30°C), and protected from light. Extractions were conducted from spiked standards prepared from 1 μg/mL of stock solution into a citrate buffer (pH=3.5), while keeping the organic solvent content of all extraction standards at 1% (v/v). The citrate buffer was prepared using the proper molar ratios of sodium citrate and citric acid in 1 L of water, and the pH levels of the buffers were adjusted to 3.5 based on the acidity of the Honeycrisp apple samples analyzed in this study. For instrument calibration, working standard solutions with known concentrations of metabolites were prepared by dilution of the stock standard with desorption solvent.

Table 6.1 Physicochemical properties of metabolites included in standard metabolite mixture.

Analyte	**Formula**	**Molecular Weight (MW)**	**Log P**
Glucose	$C_6H_{12}O_6$	180.1559	-2.9
Mannitol	$C_6H_{14}O_6$	182.1718	-3.7
Sucrose	$C_{12}H_{22}O_{11}$	342.2965	-4.5
Caffeic acid	$C_9H_8O_4$	180.1574	1.5
Catechin hydrate	$C_{15}H_{14}O_6$	290.2681	1.8
Naringenin	$C_{15}H_{12}O_5$	272.2528	2.8
t-resveratrol	$C_{14}H_{12}O_3$	228.2433	3.4
Taxifolin	$C_{15}H_{12}O_7$	304.25	1.8
Aspartic acid	$C_4H_7NO_4$	133.1027	-3.5
Glutamic acid	$C_5H_9NO_4$	147.1293	-3.2
Isoleucine	$C_6H_{13}NO_2$	131.1729	-1.5
Leucine	$C_6H_{13}NO_2$	131.1729	-1.6
Methionine	$C_5H_{11}NO_2S$	149.211	-2.2
Phenylalanine	$C_9H_{11}NO_2$	165.1891	-1.2
Proline	$C_5H_9NO_2$	115.1305	-2.9
Serine	$C_3H_7NO_3$	105.0926	-3.9
Tryptophan	$C_{11}H_{12}N_2O_2$	204.2252	-1.1
Tyrosine	$C_9H_{11}NO_3$	181.1885	-1.5

6.2.2 Sampling and sample preparation for metabolomics study

'Honeycrisp' apples (with a diameter of approximately 6-7 cm), were harvested on September 14, 2010, at 20°C, from a mature commercial orchard in Simcoe (Norfolk County), Ontario, Canada. Post-harvest conditions differed for apple samples. The first group refers to time point zero; for instance, HC-0 represents apples collected and brought to the lab, and kept on ice until preparation without storage. Time point one refers to apples kept at 3°C air storage conditions until January. This group, subdivided, experienced four types of conditions: HC-1 samples did not have any disorder, while HC-1-SC-D, HC-1-SC-D-R, and HC-1-SC-S samples demonstrated soft scalding. The HC-1-SC-D-R samples were air stored at 3°C, with AVG applied to inhibit ethylene production. HC-2 represents time point two, for apple samples air-stored at 3°C for 8 months after harvesting. Table 6.2 reviews the sample conditions.

The sampling process is summarized as follows. Immediately after harvesting, a metabolism-quenching step was performed by soaking the fruit in liquid nitrogen; the apples were then stored in dry ice (-70°C) during transportation to the laboratory. In the laboratory, individual fruits were rinsed with distilled water and dried with Kim Wipes, followed by apple core removal and slicing of the frozen fruit randomly from all possible sides of the fruit cortex. One hundred grams of disrupted frozen apple tissue was submitted to 250 mL of saturated sodium chloride solution (providing an additional metabolism-quenching step, terminating enzymatic activity, and decreasing aqueous solubility, leading to potential enhancement of SPME enrichment factors for selected compounds), followed by 1.5 min homogenization. Subsequently, an additional 250 mL aliquot of nanopure water was added to the homogenate, followed by introduction of an additional 1 min homogenization period. This last step was performed to enhance the release of metabolites during extraction and decrease matrix effects. The final homogenate was transferred into 20 mL vials (protected from light) and stored in a freezer at –30°C until the time of analysis, upon which they were thawed individually in a temperature-controlled water bath maintained at 30°C for 20 min.

Table 6.2 Apple samples under study at different treatment conditions.

# of samples	Treatment	Disorder	Sample code	Comments
5	None	No	HC-0	Harvest and brought to lab
2	Air storage 3°C	yes, soft scalding	HC-1-SC-D	Kept in storage for 4 months
4	Air storage 3°C Applied AVG to inhibit ethylene	Extensive soft scalding	HC-1-SC-D-R	Kept in storage for 4 months
1	Air storage 3°C	yes, soft scalding	HC-1-SC-S	Kept in storage for 4 months
9	Air storage 3°C	No	HC-1	Kept in storage for 4months
11	Air storage 3°C	No	HC-2	Kept in storage for 8 months

6.2.3 Automated SPME procedure for high throughput analysis

1.5 mL portions of thawed homogenate were transferred into 96-well plates, and a concept 96-autosampler was used for extraction. The Concept 96-blade SPME device and autosampler were provided by Professional Analytical System (PAS) Technology (Magdala, Germany). The Concept 96 autosampler includes three integrated arms to hold, move, and place the 96-blade SPME device into the 96-well plates, as well as four orbital agitators, which are allocated to agitate the 96-well plates at a defined speed. All arms and agitators are fully controlled by the Concept software, which enables automatic performance of preconditioning, extraction, wash, and desorption steps. The time of extraction was set at equilibrium for all compounds. The extraction was performed for 2 h (1000 rpm agitation speed, 2.5 mm amplitude). A 1.5 mL sample was used for the extraction, and this volume was precisely controlled throughout the entire study. A fast 20 s wash step in water +0.1% formic acid was carried out after extraction from apple samples in order to remove any particulates and macromolecules from the surface of the coating. Afterwards, desorption was performed for 120 min in 1.5 mL of methanol: acetonitrile: water 40:40:20 (v/v/v) with + 0.1% formic acid as the optimized desorption solvent (1500 rpm agitation speed, 1 mm amplitude).

6.2.4 Preparation of the coating for 96-blade SPME system

C18, PS-DVB-WAX, HLB, PBA, Si-RP-WCX, Strata X, as well as the lab made Si-IL, HILIC, and Diol, in addition to the mixed coatings PS-DVB-WAX: HLB 50:50 [w/w], PS-DVB-WAX: HLB 80:20 [w/w], and PS-DVB-WAX: Si-IL 80:20 [w/w)] were prepared and used in the currently presented study. Instructions regarding the coating preparation procedure have already been reported in Chapter 2 and Chapter 3 [137,222]. In brief, different SPE particles and synthesized lab-made particles were immobilized on the surface of stainless steel blades, using a spraying technique to affix a polyacrilonitile solution as a binder, at approximately the same thickness (80µL).

6.2.5 LC-MS analysis by a benchtop Orbitrap instrument for targeted and untargeted analysis

Separation was carried out on a Kinetex PFP column [100×2.1mm, 1.7µm] (Phenomenex, Torrance, CA, USA) with a guard filter (SecurityGuard ULTRA Cartridges UHPLC PFP for 2.1 mm). The column temperature was maintained at 25°C, and the gradient mobile phase conditions consisted of phase A (water containing 0.1% formic acid) and phase B (acetonitrile with 0.1% formic acid) set to the following conditions: 0-1 min 90% A; 1-9 min 90-10% A; 9-12 min 10% A; 12-16 min 10-90% A. Injection of each apple sample was followed by injection of control samples. Blank samples and QC samples were injected after every set of 15 sample injections so as to avoid cross contamination and verify instrument

performance. This QC sample was prepared by mixing a 10µL part of each sample into one sample. The injection volume for all methods was 10 µL. Samples were stored and refrigerated (4°C) on the autosampler while waiting for injection.

The MS system was operated using an accurate mass Exactive benchtop Orbitrap system (Thermo, San Jose, California, USA) in both negative and positive electrospray ionization (ESI) modes and a 100-1000 m/z mass range. The optimum values for sheath gas (arbitrary units), auxiliary gas (arbitrary units), ESI voltage (kV), capillary voltage (V), capillary temperature (°C), and tube lens voltage (V) were set at 40, 25, 4.0, 27.5, 275, and 100 for positive ESI mode, and 50, 25, -2.7, -67.5, 325, and -85 for negative ESI mode respectively. External instrument mass calibrations were performed every 24 h, and found to be within 2 ppm for all ions. Separated metabolites were analyzed using Xcalibur software, version 2.1 (Thermo) by isolating the extracted ion chromatograms (XIC), using a 5 ppm window around the accurate mass.

6.2.6 Metabolite identification, data mining, and statistical analysis

The raw data obtained with Xcalibur software (.raw) was converted to (mzXML) with the MS conversion software. The converted data was then processed with the XCMS R-package (Scripps Center for Metabolomics, California, USA). The resulting output is a table containing retention times, m/z, and intensity of features [142]. Mass spectral peak deconvolution, alignment, and peak picking (feature detection) were done by R software. The CAMERA R-package (Bioconductor Version 2.10) was applied to provide ion annotation on the list of features so as to identify detected isotopes, adducts, and in-source fragments ions. An Exactive Orbitrap detector was used in this study, providing high mass resolution and sensitivity. Multivariate data analysis was used by the SIMCA-P+ software (Umetrics, NJ, USA) for statistical analyses. Log transformation and pareto scaling prior to PLS were done to identify the differentiation between control and treated samples. OPLS-DA was performed on obtained data, and the resulting S-plots were applied towards further modeling to investigate markers with statistical relevance of variation ($p < 0.05$) related to storage stress and soft scald evidence. Metabolite identities were specified based on their accurate mass, retention time, comparison of fragmentation data with authentic standards, and METLIN databases within 5 ppm. In order to assign metabolites to metabolic pathways, the KEGG database (http://www.genome.jp/kegg) and the Plant Metabolic Network (http://www.plantcyc.org) were used.

6.3 Results and discussion

6.3.1 Targeted analysis for development of SPME-LC-MS analysis

6.3.1.1 Optimization of SPME parameters

Twelve different types of stationary phases with different polarities and functional groups (C18, PS-DVB-WAX, HLB, PBA, Si-RP-WCX, Strata X, Si-IL, HILIC, Diol, PS-DVB-WAX: HLB 50:50 [w/w], PS-DVB-WAX: HLB 80:20 [w/w], and PS-DVB-WAX: Si-IL 80:20 [w/w]) were evaluated as the stationary phase for the 96-blade SPME system with thin film geometry for the extraction of targeted metabolites ranging $-4.5 < \text{Log P} < 3.4$ from the citrate buffer and apple matrices. PS-DVB-WAX, HLB, IL, and the coating prepared with a mixture of these particles provided the highest absolute extraction recoveries. In all cases, RSD% was below 15%, except for Diol and Strata X, whose coatings stripped off from the stainless steel blades in the case of real samples due to the complexity of the matrix (RSD up to 40%). Detailed descriptions of the chemical characteristics and properties of these coatings are provided in Chapter 3.

6.3.1.2 Preconditioning

The preconditioning step was optimized for each set of coatings, with data obtained for polar coatings indicating that longer preconditioning times were needed in comparison to nonpolar coatings as metabolites were extracted from the aqueous phase. A 2-hour extraction time was determined for preconditioning in methanol/water 50:50 (v/v), with agitation set by the concept software chosen to prepare the surface coatings for extraction.

6.3.1.2 Extraction

The extraction time profiles of targeted metabolites in the citrate buffer (pH=3.5) and apple samples (pH=3.5) were evaluated for all coatings. Polar metabolites reach equilibrium more slowly on blades with nonpolar coatings than nonpolar metabolites, whereas for polar coatings, equilibrium is reached earlier. An evaluation of extraction time profiles indicated higher equilibrium extraction times for real samples. All metabolites in the apple matrices reached equilibrium in 2 hours. Therefore, 2-hours extraction times were used for the entire study, with 1000 rpm agitation.

6.3.1.3 Wash

To reduce the transfer of macromolecules, salts, and particulates from the apple matrix, a wash step was applied after extraction; however, this step needed to be optimized, as it is possible to lose polar metabolites during this step. After optimization, results indicated that a 20 s wash in 1 mL water + 0.1% formic acid helped decrease possible matrix effects while reducing metabolite loss for the most polar targeted metabolites to less than 10%.

6.3.1.4 Desorption

To increase the desorption of extracted metabolites from the surface of coatings, as well as decrease carryover, two parameters were optimized for desorption solvent: the type of desorption solvent, and desorption time. Results demonstrated that for different coatings, different types of optimized desorption solvent and the desorption time were needed for optimization, although a 1.5 mL methanol: acetonitrile: water 40:40:20 (v/v/v) at 1500 rpm agitation speed (1 mm amplitude) for 2 hours provided a high extraction efficiency for HLB with the least percent of carryover (less than 1%). Analysis of a second desorption was not needed for this coating in the case of real samples. While the PS-DVB-WAX coating provided the highest extraction efficiency, under optimized desorption conditions, it showed high carryover, and this phenomenon was observed as well for the coating prepared with a mixture of particles in the presence of PS-DVB-WAX for metabolomics studies. Considering the large number of samples to be processed and the advantages associated with reusing the coatings without sacrificing time and cost, the HLB coating was chosen for the metabolomics part of this study. Figure 6.1 demonstrates a comparison of 96-blade SPME coatings in terms of extraction efficiency and selectivity for representative targeted metabolites extracted from apple samples.

6.3.2 Metabolite identification

Approximately 8000 features were detected using XCMS R-package and CAMERA R-package for both negative and positive ionization modes. Figure 6.2 and Figure 6.3 show chromatograms of metabolites extracted using the HLB coating in positive and negative ionization modes, respectively. The METLIN database was used to match the obtained m/z values with a mass tolerance window of 5 ppm, resulting in a database of about 500 metabolites. The application of HLB 96-blade SPME covered extraction of a broad range of metabolites from apple matrices in a single experiment run, while UPLC/MS provided analysis of the extracted metabolites, including sugars, fatty acids, amino acids and peptides, sugar alcohols, organic acids, prenol lipids, glycerophospholipid, flavonoid, sphingolipids, ethers, proanthocyanidins, hydrolyzable tannins, steroids and steroid derivatives, thiamines, glycosyl compounds, fatty acids and conjugates, cinnamic acid derivatives, phenols and derivatives, fatty amides, cyclic alcohols and derivatives, alkyl glycosides, isoindoles and derivatives, pyrrolidines, fatty adehydes, furans, pyrans, indols, pyridines and derivatives, and acetals. Table 6.3 demonstrates the metabolites extracted from apple samples using the HLB coating. Traditionally, metabolomics focuses on individual metabolites or a specific class of metabolites; however, in this study, comprehensive metabolite analysis was possible with a single SPME coating, without further sample pretreatment. The SPME-LC/MS method was used for characterization of different apple samples based on quality attributes. PLS score plots as statistical tools were employed for classification purposes. OPLS plots showed good differentiation between different clusters of apple samples and QC. PLS-DA analyses and S-plots were

applied to distinguish components of interest and potential markers for storage conditions of apple samples. Results showed metabolic divergence in response to storage duration after 4 and 8 months, in comparison to apple samples without storage. There were also differences in the metabolic profiles of apple samples with evidence of scald.

Figures 6.4 and 6.5 demonstrate PCA score plots related to different apple samples. SPME demonstrated a correlation between different stored apple samples with scald evidence as well. Clear separation of clusters of each set of apple samples demonstrated that specific metabolites correlate directly with apple quality traits; their growth during storage as well as scald development is produced by changes in different classes of metabolites such as phenolics, anthocyanines, amino acids, lipids, and carbohydrates. Variability in apple samples is most likely attributable to environmental stresses, genetic variation, and virus expression [362]. Figure 6.6 demonstrates the metabolic changes of extracted metabolites in different evaluated apple samples. Plants alter their metabolism in various ways, including in the production of compatible solutes that are able to stabilize proteins and cellular structures and to preserve cell turgor by osmotic adjustment, and by altering the redox metabolism to remove excess levels of reactive oxygen species and re-establish the cellular redox balance. The most observed dysregulations in various classes of metabolites are summarized next.

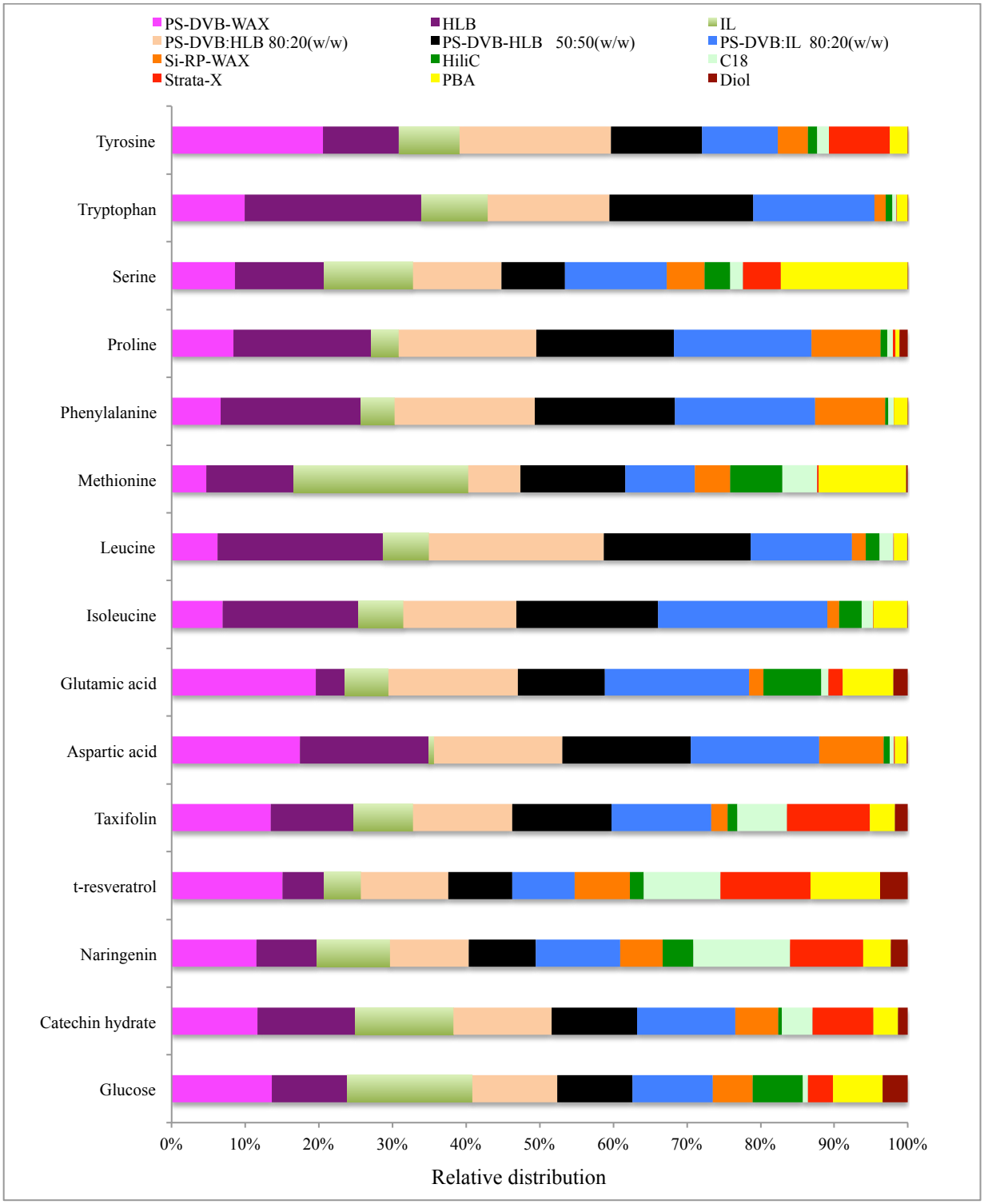

Figure 6.1 The comparison of 96-blade SPME coatings in terms of extraction efficiency and selectivity for representative targeted metabolites extracted from apple samples.

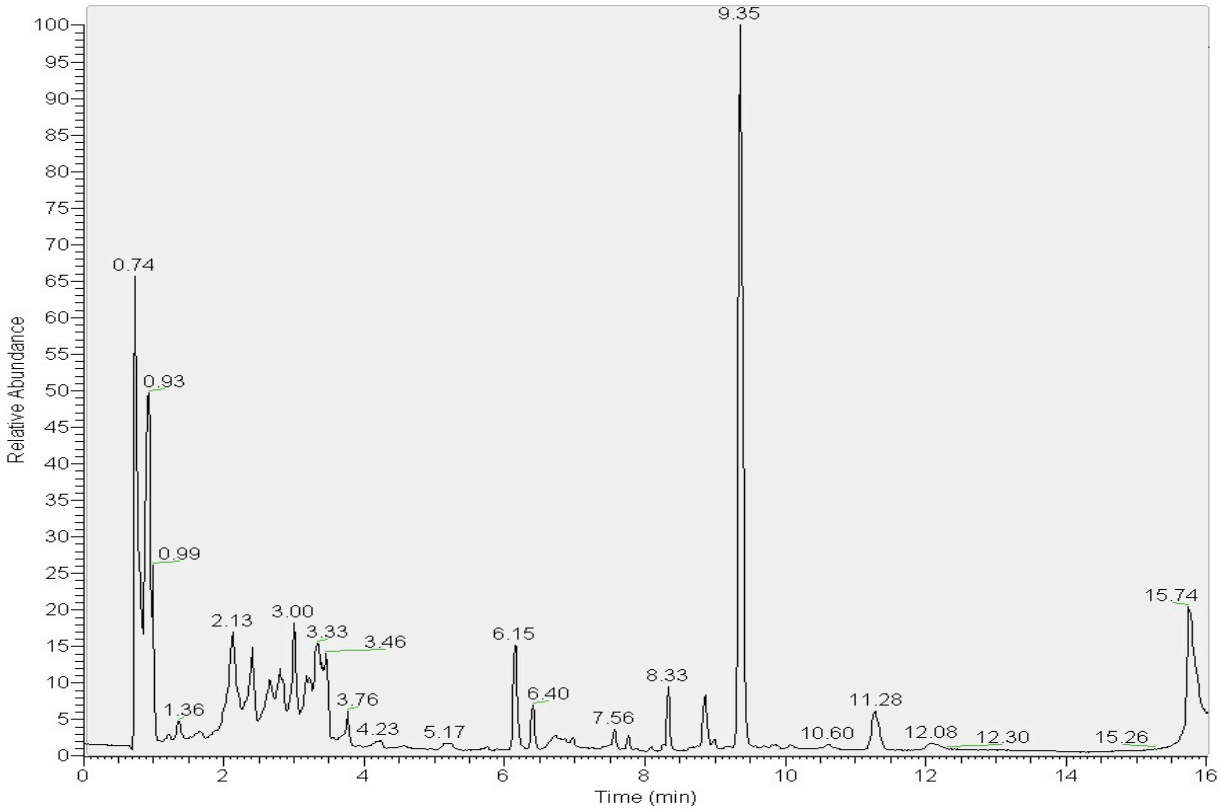

Figure 6.2 Chromatogram of extracted metabolites from apple samples (HC-0) using 96-blade HLB SPME-LC/MS, positive ESI mode.

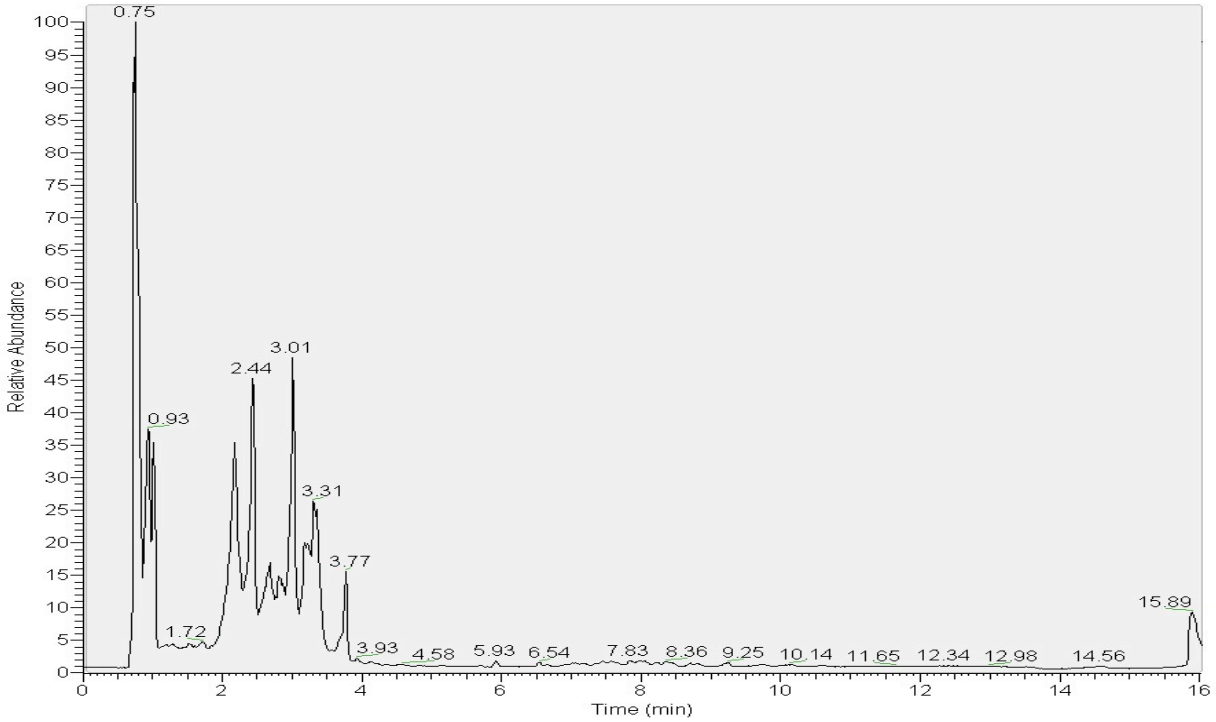

Figure 6.3 Chromatogram of extracted metabolites from apple samples (HC-0) using 96-blade HLB SPME-LC/MS, positive ESI mode.

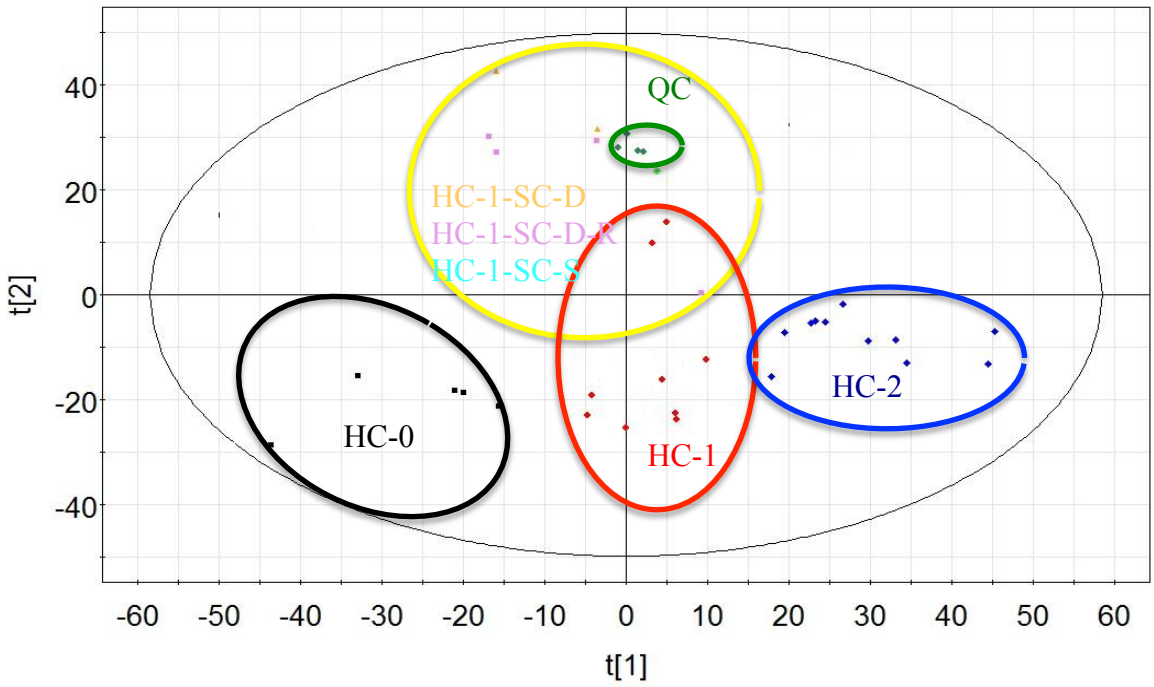

Figure 6.4 PCA score plot showing clustering of the apple samples collected under different storage conditions (positive ESI mode).

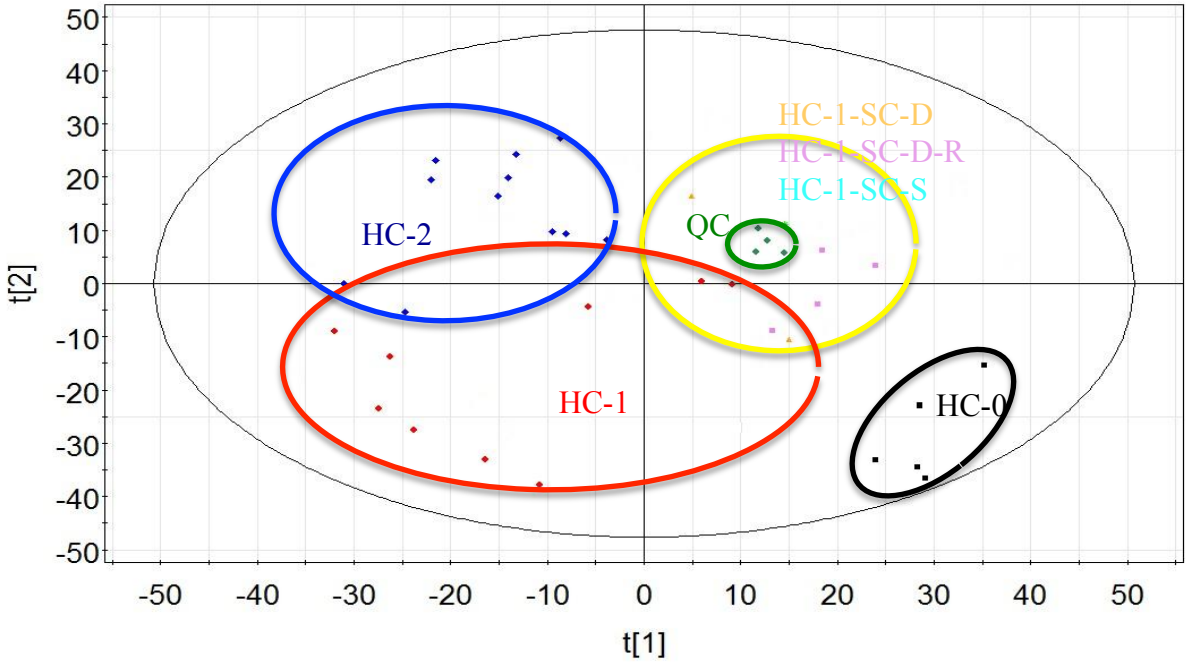

Figure 6.5 PCA score plot showing clustering of the apple samples collected under different storage conditions (negative ESI mode).

6.3.2.1 Changes in amino acids and peptides

Stored apple samples had higher levels of amino acids and peptides such as proline, leucine, tyrosine, beta-hydroxyarginine, N-formyl-L-glutamate, tryptophan, homomethionine, homoserine, homoglutamine, phenylalanine, galactosyl 4-hydroxyproline, and cinnamoylglycine, as well as a large number of peptides (Figure 6.6). This increase could be related to enhanced amino acid production or decreased protein synthesis due to a lower amino acid consumption rate, which consequently enhances amino acid accumulation, or to protein breakdown causing cell damage.

Accumulation of amino acids in plants exposed to abiotic stress has been reported previously [363-369]. Amino acids are building blocks of proteins, and important in many metabolic networks that control growth and adaptation to environmental stresses. Their biosynthesis is regulated by a complex network involving both nitrogen and carbon metabolic pathways, such as nitrate reduction occurring beside carbon oxidation. The enhancement of amino acid levels in stored apple samples has been thought to reflect an increase in nitrogen recycling processes, with amino acids being involved as a carbon source in TCA cycles [370,371]. One of the amino acids upregulated in apple samples during storage condition is proline. This metabolite has been reported to be a reactive oxygen species scavenger and osmolyte stabilizer that protects cells from stress damages [372-375]; its levels rise in response to different environmental stresses such as drought, high salinity, and exposure to heavy metals [376-379].

6.3.2.2 Changes in organic acids

Results demonstrated decreased levels of citric acid, malic acid, and glyoxylic acid, and increases in succinic acid levels during storage. Previous studies reported upregulation of TCA intermediates in response to temperature or drought stress [380-382]. Malic acid is the major organic acid in apples and one of the TCA intermediates, tasked with controlling respiration and flavor component during cold storage. Levels of malic acid were observed to decrease in relation to increased storage time after 4 and 8 months of storage. Ackermann et al. observed a decrease in levels of malic acid and citric acid during ripening and storage of apple samples [383]. In addition, the level of glyoxylic acid was also observed to decrease during storage as well as in the case of apple samples with evidence of scald. This compound is an intermediate of the glyoxylate cycle that enables plants to convert fatty acids into carbohydrates, which are osmoprotectant metabolites [384].

6.3.2.3 Changes in secondary metabolism

Significantly higher levels of polyphenols were noted for stored samples, and may be associated with the release of polyphenol oxidase from chloroplast [385]. However, as scald proceeds, both simple phenol and flavonoid concentrations decrease; in this study, flavonoid levels, such as those of coumaric acid, catechine, quercetin 3-sambubioside-3'-glucoside, catechin 7-O-alpha-L-rhamnopyranoside, quercetin 3'-

xyloside, myricitrin, quercetin 7-galactoside, quercetin 3-rhamnoside-7-glucoside, 5,7,2',4'-Tetrahydroxy-3,6,5'-trimethoxyflavone, 7,8-dimethoxyflavanone, (±)-catechin, quercetin, 8-methy caffeine, epigallocatechin 3-O-caffeate, kaempferol 3-p-coumarate, epiafzelechin 3-O-beta-D-allopyranoside, were observed to decrease in samples with scald evidence. Browning reactions in the apple surface attributed to scald are associated with polyphenols attached to proteins. Previous studies observed a correlation between high-levels of phenolic compounds in apple peel and less scald development after storage [386,387].

6.3.2.4 Changes in sugar metabolism

Stored carbohydrates such as starch are metabolized to soluble sugars under stress conditions to protect the apple membrane's cell structure and proteins from stress damage. Adjustment of sugar contents has also been recognized using the OPLS model. Levels of pentose sugars such as glucose increased with increased storage time, while sucrose was observed to decrease due to hydrolysis of sucrose to glucose during storage. Previous studies introduced the release of hexose sugars from fructans, which achieved osmotic adjustment and membrane stabilization in freezing and dehydration conditions [388]. The level of sorbitol, as a sugar alcohol, increased in stored apple samples over time; sorbitols, as major sugar alcohol constituents in apples, cause fruit sweetness enhancement. Stoop et al. distinguished a correlation between the accumulation of straight chain polyols, including mannitol and sorbitol, and stress tolerance in several plant species [389]. Fidler et al. observed a relation between increase in sorbitol and browning in scald apple samples [390]. Evidence of level increases in other alkyl glycosides such as (R)-1-O-b-D-glucopyranosyl-1,3-octanediol, heptanol glucoside, (R)-1-O-b-D-glucopyranosyl-1,3-octanediol, citrusin E, (R)-1-O-b-D-glucopyranosyl-1,3-octanediol, 1-(beta-D-glucopyranosyloxy)-3-octanone, and (R)-1-O-[b-D-glucopyranosyl-(1->6)-b-D-glucopyranoside]-1,3-octanediol was also demonstrated in the current study. Lee et al. reported that an enhanced concentration of disaccharides such as galactose-beta-1,4-xylose is associated with cell wall breakdown, as xylose is the major component of xyloglucan [391,392].

6.3.2.5 Changes in lipid metabolism

Up-regulation of glycerophospholipids was observed in the stored apple samples; however, their levels were noted to decrease in apple samples with scald evidence. On the other hand, in most cases, the level of fatty acids and conjugates in all samples increased. Enhancement in the levels of acylated steryl glucosides and steryl esters indicated membrane integrity alteration. Conversion of unsaturated fatty acids to saturated fatty acyl functional groups of alkyl glycosides due to the transfer of apple samples from low temperature storage conditions to ambient temperature has been noted in the case of apple samples with scald. Brackmann et al. observed increased amounts of fatty acids in air-stored apple samples [393]. Inositol, which is the precursor for phosphatidylinositol, was noted to increase in stored apple samples,

indicating alterations in cell metabolism. Loewus et al. reported elevation of this metabolite in response to cell membrane alteration and lipid membrane modification, as a result of chilling or oxidative stress [394]. Concentrations of phytosterol metabolites such as provitamin D6 and stigmasterol (6S,9R-dihydroxy-4,7E-megastigmadien-3-one 9-[apiosyl-(1->6)-glucoside]) conjugated in peel tissue were found to increase in scald apple samples. Phytosterols are integral units of plant membrane, modifying membrane fluidity and permeability [395]. Rudell et al. observed that the degree of phytosterol conjugation is correlated with ripening and chilling stress [396]. Picchioni et al. reported the constant level of conjugation in stigmasterols during ripening in cold storage [397]. Moreover, the level of abscisic acid increased during storage and decreased in apple samples with scald evidence. Abscisic acid is an isoprenoid plant hormone classified as a prenol lipid. It quickly accumulates in plants due to environmental stress [398-400].

The metabolic pathways of apples in cold storage conditions changed through the activation of free radicals, antioxidant enzymes, ethylene production, and α-farnesene synthesis. As in storage conditions, as fruits continue ripening, the level of metabolites changes. For example, esters with various functional groups are produced by glycolysis or β-oxidation of fatty acids [401]. An evaluation of the obtained results revealed an association between ripening and scald produced by chilling stress. Based on previous reports, AVG [402] delays ethylene production, so α-farnesene and its products will be reduced initially; however, their levels increase during storage. In the current study, batches of apple samples treated with AVG were noted to demonstrate signs of scald development after 4 months of storage.

Storage stress activates many processes in which free radicals, antioxidants, ethylene, farnesal, and α-conjugated trienols are involved. Our study demonstrated that the concentration of α-conjugated trienols such as 3Z,6E,8E-Dodecatrien-1-ol in scald samples increased in stored apple samples. Moreover, 6-methyl-5-hepten-2-one, as the byproduct of free radicals, which produces cell damage resulting from the reaction of conjugated trienols, was noted to increase in the same samples as well. These metabolites are directly associated with scald symptoms; however, the evidence of their enhancement was observed even in the case of stored samples without scald symptoms. Meigh et al. observed increases in α-farnesene early in storage and subsequent decreases during further storage time [403]. On the other hand, Huelin et al. reported enhancement in conjugated trienes during storage [404]. They observed a correlation between conjugated triene levels and scald development that was confirmed by the present study.

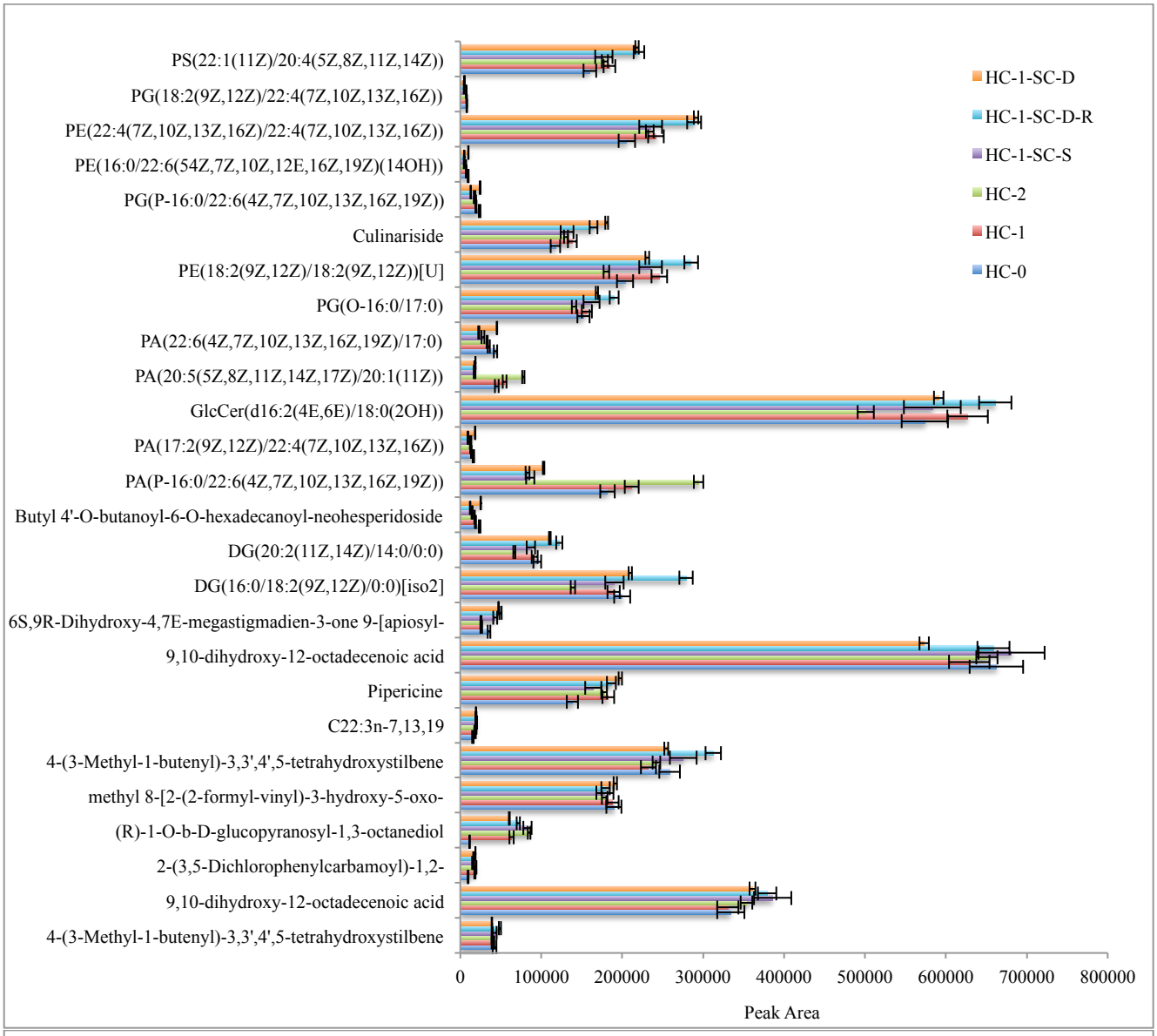
PS(22:1(11Z)/20:4(5Z,8Z,11Z,14Z))
PG(18:2(9Z,12Z)/22:4(7Z,10Z,13Z,16Z))
PE(22:4(7Z,10Z,13Z,16Z)/22:4(7Z,10Z,13Z,16Z))
PE(16:0/22:6(54Z,7Z,10Z,12E,16Z,19Z)(14OH))
PG(P-16:0/22:6(4Z,7Z,10Z,13Z,16Z,19Z))
Culinariside
PE(18:2(9Z,12Z)/18:2(9Z,12Z))[U]
PG(O-16:0/17:0)
PA(22:6(4Z,7Z,10Z,13Z,16Z,19Z)/17:0)
PA(20:5(5Z,8Z,11Z,14Z,17Z)/20:1(11Z))
GlcCer(d16:2(4E,6E)/18:0(2OH))
PA(17:2(9Z,12Z)/22:4(7Z,10Z,13Z,16Z))
PA(P-16:0/22:6(4Z,7Z,10Z,13Z,16Z,19Z))
Butyl 4'-O-butanoyl-6-O-hexadecanoyl-neohesperidoside
DG(20:2(11Z,14Z)/14:0/0:0)
DG(16:0/18:2(9Z,12Z)/0:0)[iso2]
6S,9R-Dihydroxy-4,7E-megastigmadien-3-one 9-[apiosyl-
9,10-dihydroxy-12-octadecenoic acid
Pipericine
C22:3n-7,13,19
4-(3-Methyl-1-butenyl)-3,3',4',5-tetrahydroxystilbene
methyl 8-[2-(2-formyl-vinyl)-3-hydroxy-5-oxo-
(R)-1-O-b-D-glucopyranosyl-1,3-octanediol
2-(3,5-Dichlorophenylcarbamoyl)-1,2-
9,10-dihydroxy-12-octadecenoic acid
4-(3-Methyl-1-butenyl)-3,3',4',5-tetrahydroxystilbene
HC-1-SC-D
HC-1-SC-D-R
HC-1-SC-S
HC-2
HC-1
HC-0
0
100000
200000
300000
400000
500000
600000
700000
800000
Peak Area
Myricitrin
E-Docosenamide
myo-Inositol
HC-1-SC-D
HC-1-SC-D-R
HC-1-SC-S
HC-2
HC-1
HC-0
0
50000000
100000000
150000000
200000000
250000000
300000000
350000000
Peak area

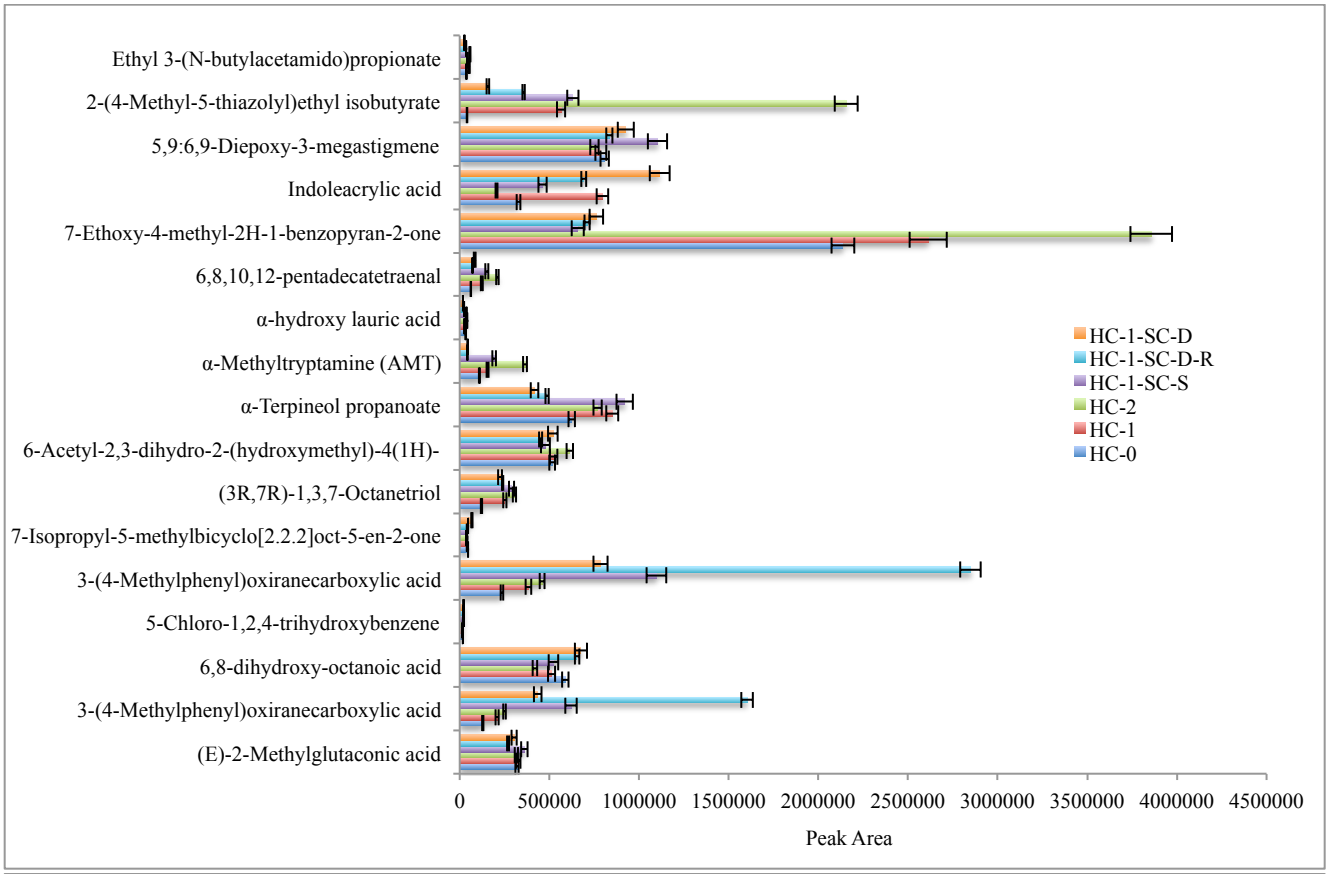
Ethyl 3-(N-butylacetamido)propionate
2-(4-Methyl-5-thiazolyl)ethyl isobutyrate
5,9:6,9-Diepoxy-3-megastigmene
Indoleacrylic acid
7-Ethoxy-4-methyl-2H-1-benzopyran-2-one
6,8,10,12-pentadecatetraenal
α-hydroxy lauric acid
α-Methyltryptamine (AMT)
α-Terpineol propanoate
6-Acetyl-2,3-dihydro-2-(hydroxymethyl)-4(1H)-
(3R,7R)-1,3,7-Octanetriol
7-Isopropyl-5-methylbicyclo[2.2.2]oct-5-en-2-one
3-(4-Methylphenyl)oxiranecarboxylic acid
5-Chloro-1,2,4-trihydroxybenzene
6,8-dihydroxy-octanoic acid
3-(4-Methylphenyl)oxiranecarboxylic acid
(E)-2-Methylglutaconic acid
HC-1-SC-D
HC-1-SC-D-R
HC-1-SC-S
HC-2
HC-1
HC-0
0
500000
1000000
1500000
2000000
2500000
3000000
3500000
4000000
4500000
Peak Area

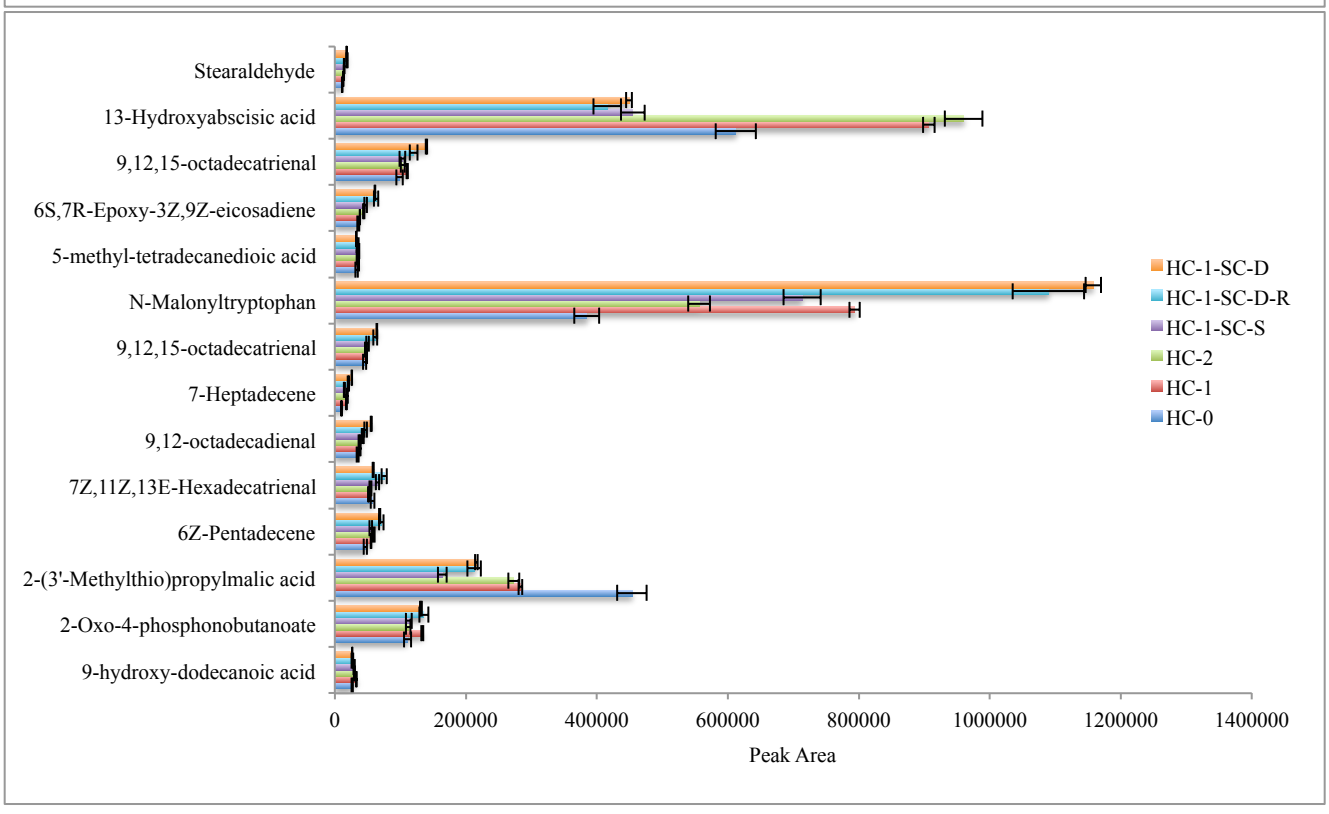
Stearaldehyde
13-Hydroxyabscisic acid
9,12,15-octadecatrienal
6S,7R-Epoxy-3Z,9Z-eicosadiene
5-methyl-tetradecanedioic acid
N-Malonyltryptophan
9,12,15-octadecatrienal
7-Heptadecene
9,12-octadecadienal
7Z,11Z,13E-Hexadecatrienal
6Z-Pentadecene
2-(3'-Methylthio)propylmalic acid
2-Oxo-4-phosphonobutanoate
9-hydroxy-dodecanoic acid
HC-1-SC-D
HC-1-SC-D-R
HC-1-SC-S
HC-2
HC-1
HC-0
0
200000
400000
600000
800000
1000000
1200000
1400000
Peak Area

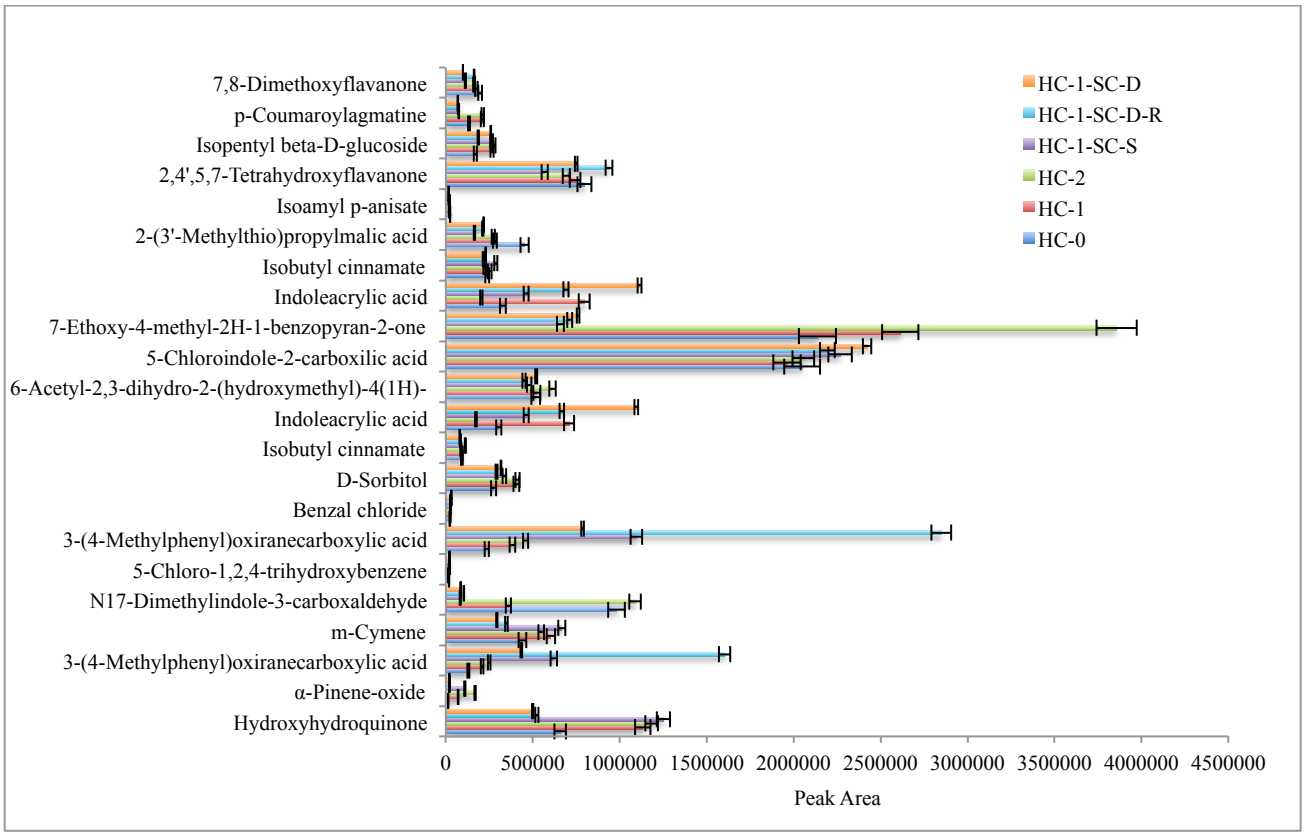
7,8-Dimethoxyflavanone
p-Coumaroylagmatine
Isopentyl beta-D-glucoside
2,4',5,7-Tetrahydroxyflavanone
Isoamyl p-anisate
2-(3'-Methylthio)propylmalic acid
Isobutyl cinnamate
Indoleacrylic acid
7-Ethoxy-4-methyl-2H-1-benzopyran-2-one
5-Chloroindole-2-carboxilic acid
6-Acetyl-2,3-dihydro-2-(hydroxymethyl)-4(1H)-
Indoleacrylic acid
Isobutyl cinnamate
D-Sorbitol
Benzal chloride
3-(4-Methylphenyl)oxiranecarboxylic acid
5-Chloro-1,2,4-trihydroxybenzene
N17-Dimethylindole-3-carboxaldehyde
m-Cymene
3-(4-Methylphenyl)oxiranecarboxylic acid
α-Pinene-oxide
Hydroxyhydroquinone
HC-1-SC-D
HC-1-SC-D-R
HC-1-SC-S
HC-2
HC-1
HC-0
0
500000
1000000
1500000
2000000
2500000
3000000
3500000
4000000
4500000
Peak Area

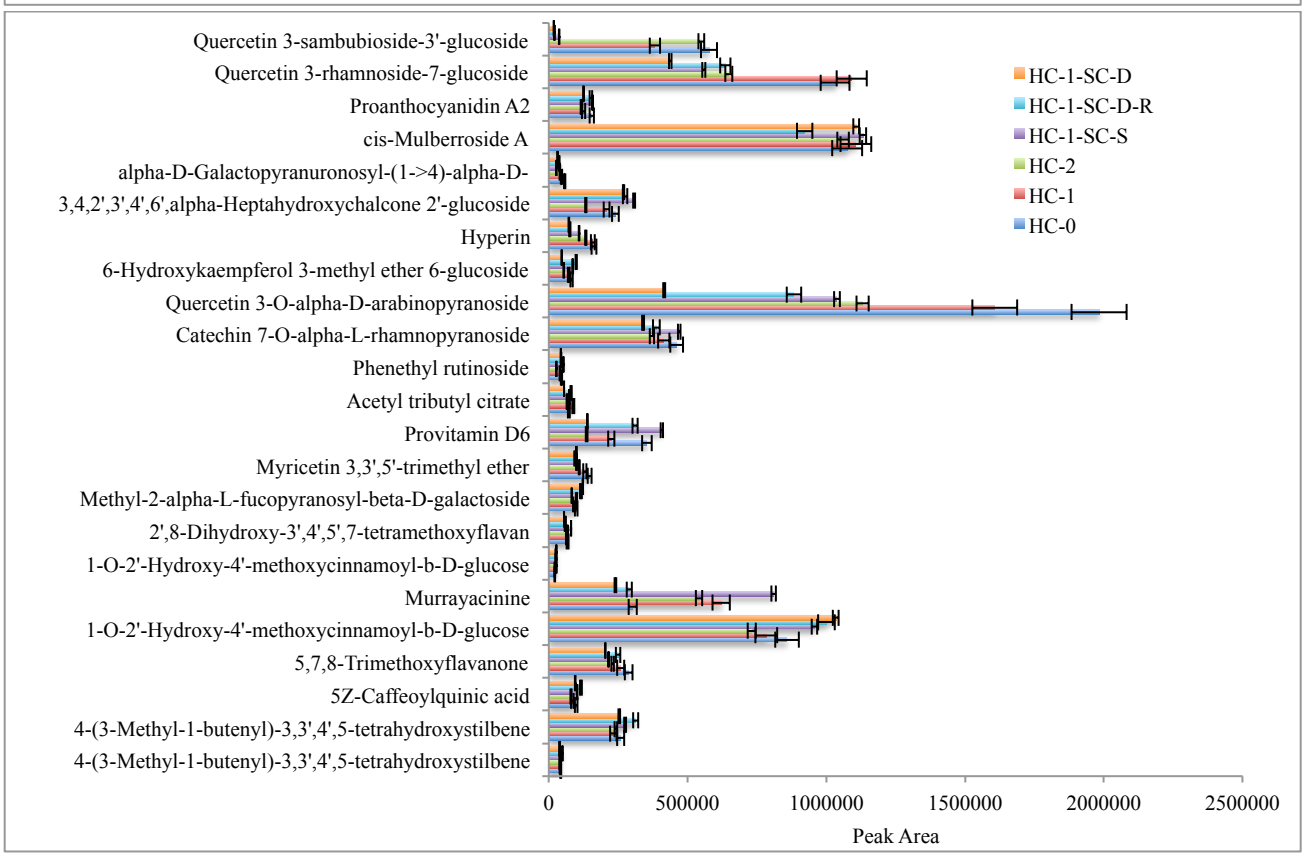
Quercetin 3-sambubioside-3'-glucoside
Quercetin 3-rhamnoside-7-glucoside
Proanthocyanidin A2
cis-Mulberroside A
alpha-D-Galactopyranuronosyl-(1->4)-alpha-D-
3,4,2',3',4',6',alpha-Heptahydroxychalcone 2'-glucoside
Hyperin
6-Hydroxykaempferol 3-methyl ether 6-glucoside
Quercetin 3-O-alpha-D-arabinopyranoside
Catechin 7-O-alpha-L-rhamnopyranoside
Phenethyl rutinoside
Acetyl tributyl citrate
Provitamin D6
Myricetin 3,3',5'-trimethyl ether
Methyl-2-alpha-L-fucopyranosyl-beta-D-galactoside
2',8-Dihydroxy-3',4',5',7-tetramethoxyflavan
1-O-2'-Hydroxy-4'-methoxycinnamoyl-b-D-glucose
Murrayacinine
1-O-2'-Hydroxy-4'-methoxycinnamoyl-b-D-glucose
5,7,8-Trimethoxyflavanone
5Z-Caffeoylquinic acid
4-(3-Methyl-1-butenyl)-3,3',4',5-tetrahydroxystilbene
4-(3-Methyl-1-butenyl)-3,3',4',5-tetrahydroxystilbene
HC-1-SC-D
HC-1-SC-D-R
HC-1-SC-S
HC-2
HC-1
HC-0
0
500000
1000000
1500000
2000000
2500000
Peak Area

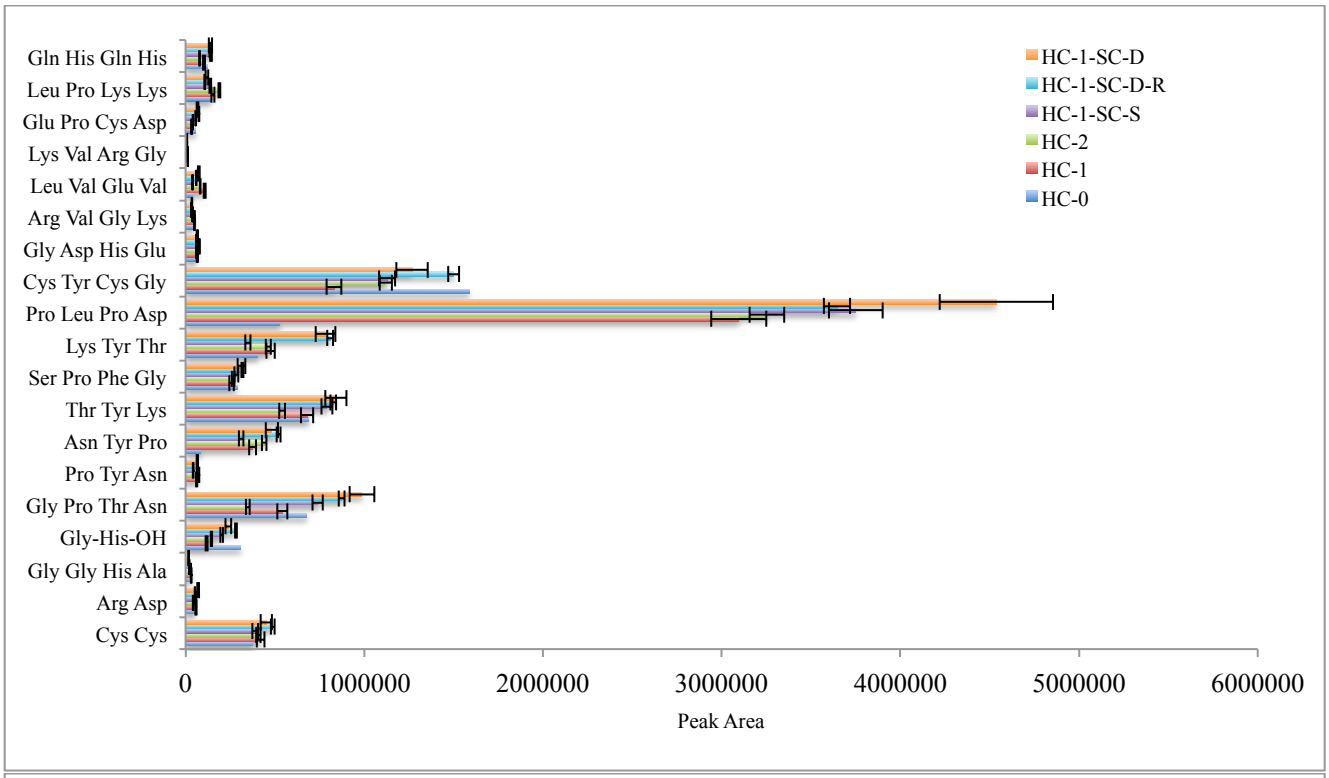
Gln His Gln His
Leu Pro Lys Lys
Glu Pro Cys Asp
Lys Val Arg Gly
Leu Val Glu Val
Arg Val Gly Lys
Gly Asp His Glu
Cys Tyr Cys Gly
Pro Leu Pro Asp
Lys Tyr Thr
Ser Pro Phe Gly
Thr Tyr Lys
Asn Tyr Pro
Pro Tyr Asn
Gly Pro Thr Asn
Gly-His-OH
Gly Gly His Ala
Arg Asp
Cys Cys
HC-1-SC-D
HC-1-SC-D-R
HC-1-SC-S
HC-2
HC-1
HC-0
0
1000000
2000000
3000000
4000000
5000000
6000000
Peak Area

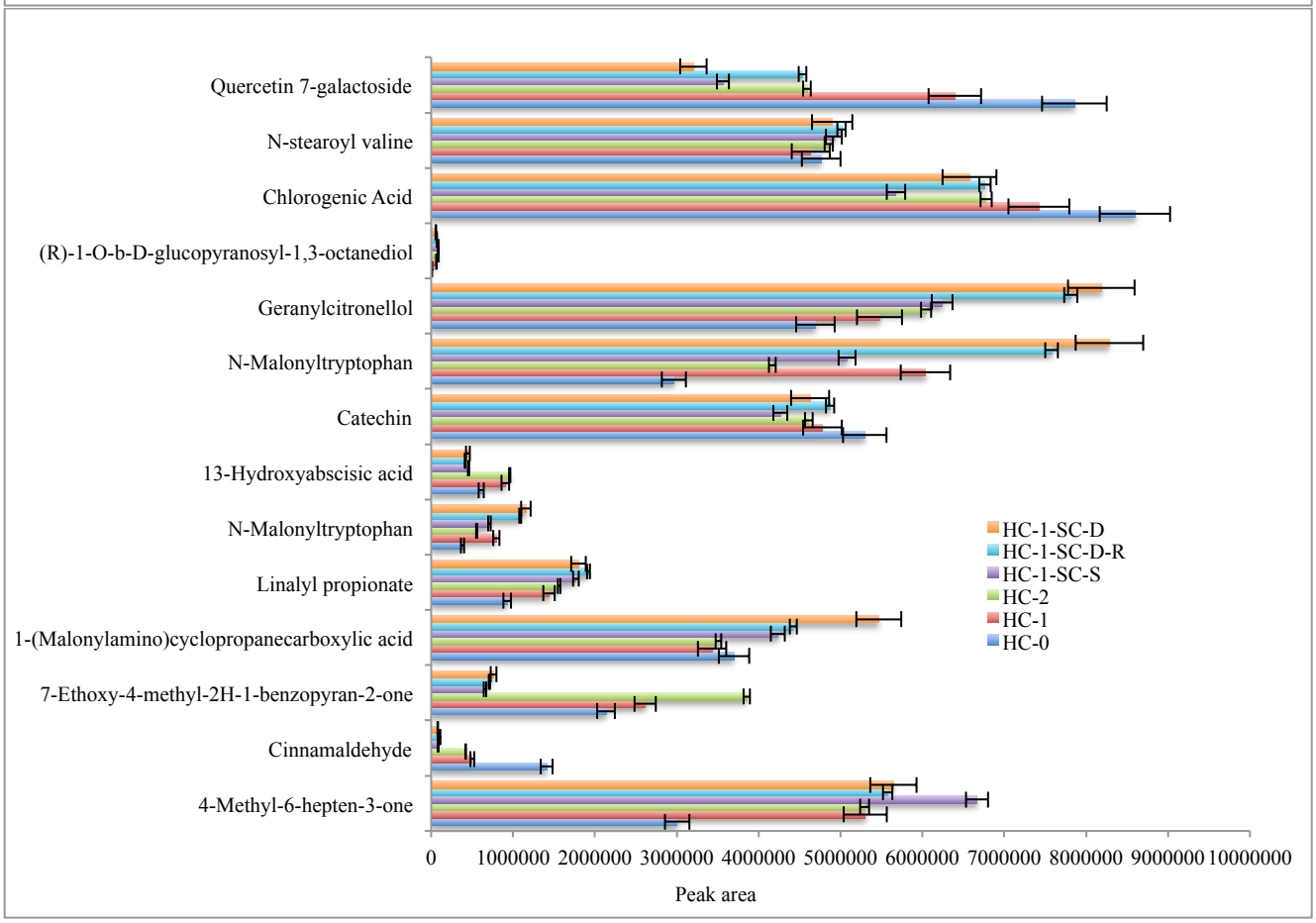
Quercetin 7-galactoside
N-stearoyl valine
Chlorogenic Acid
(R)-1-O-b-D-glucopyranosyl-1,3-octanediol
Geranylcitronellol
N-Malonyltryptophan
Catechin
13-Hydroxyabscisic acid
N-Malonyltryptophan
Linalyl propionate
1-(Malonylamino)cyclopropanecarboxylic acid
7-Ethoxy-4-methyl-2H-1-benzopyran-2-one
Cinnamaldehyde
4-Methyl-6-hepten-3-one
HC-1-SC-D
HC-1-SC-D-R
HC-1-SC-S
HC-2
HC-1
HC-0
0
1000000
2000000
3000000
4000000
5000000
6000000
7000000
8000000
9000000
10000000
Peak area

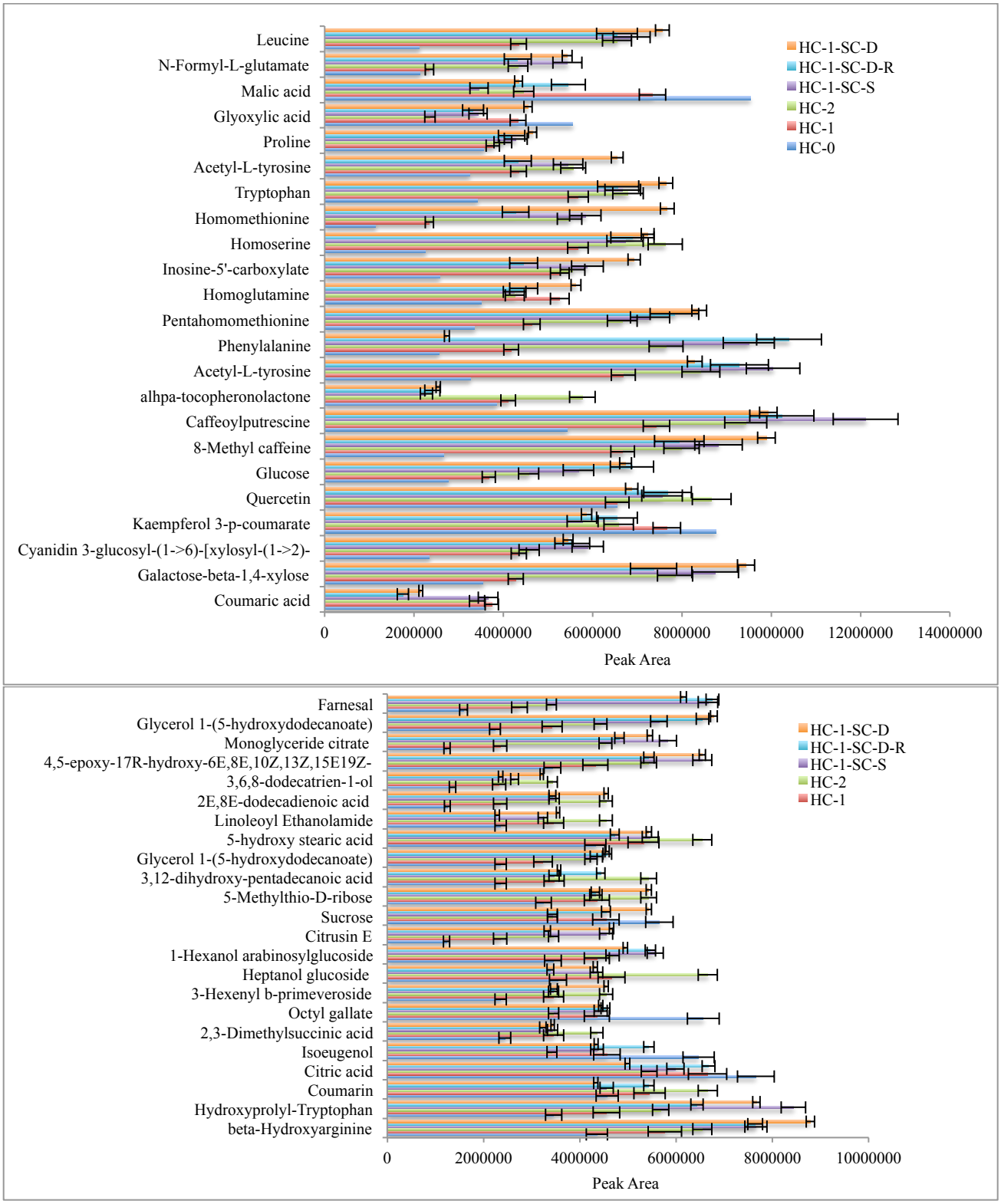

Figure 6.6 Metabolic profile of extracted metabolites from apple samples using 96-blade HLB SPME-LC/MS at different storage conditions.

Table 6. 3 Metabolite extracted from apple samples using 96-blade HLB SPME-LC/MS.

Metabolite	Exact Mass	Chemical formula	Adduct	METLIN ID	ppm
Alkyl Glycosides					
(R)-1-O-b-D-glucopyranosyl-1,3-octanediol	331.1727	$C_{14}H_{28}O_7$	$[M+Na]^+$	86223	0
(R)-1-O-b-D-glucopyranosyl-1,3-octanediol	309.1909	$C_{14}H_{28}O_7$	$[M+H]^+$	86223	0.6
Citrusin E	373.1489	$C_{17}H_{24}O_9$	$[M+H]^+$	93825	-1.1
(R)-1-O-b-D-glucopyranosyl-1,3-octanediol	309.1907	$C_{14}H_{28}O_7$	$[M+H]^+$	86223	0
1-(beta-D-Glucopyranosyloxy)-3-octanone	329.1576	$C_{14}H_{26}O_7$	$[M+Na]^+$	87578	1.8
(R)-1-O-[b-D-Glucopyranosyl-(1->6)-b-D-glucopyranoside]-1,3-octanediol	471.2441	$C_{20}H_{38}O_{12}$	$[M+H]^+$	88721	-1.1
Acetals					
Acetal R	209.1536	$C_{13}H_{20}O_2$	$[M+H]^+$	91838	0
Amino acids and conjugates					
Acetyl-L-tyrosine	223.0844	$C_{11}H_{13}NO_4$	$[M]^+$	5827	0
beta-Hydroxyarginine	235.0783	$C_6H_{14}N_4O_3$	$[M+2Na-H]^+$	72279	2.5
Leucine	173.1284	$C_6H_{13}NO_2$	$[M+ACN+H]^+$	64934	0
N-Formyl-L-glutamate	220.0192	$C_6H_9NO_5$	$[M+2Na-H]^+$	3769	0
Tryptophan	249.0615	$C_{11}H_{12}N_2O_2$	$[M+2Na-H]^+$	65364	2.0
Homomethionine	227.0829	$C_6H_{13}NO_2S$	$[M+ACN+Na]^+$	64484	2.2
Pentahomomethionine	220.1364	$C_{10}H_{21}NO_2S$	$[M+H]^+$	64511	-0.5
1-(Malonylamino)cyclopropanecarboxylic acid	226.0112	$C_7H_9NO_5$	$[M+K]^+$	87876	0
N-Malonyltryptophan	313.0795	$C_{14}H_{14}N_2O_5$	$[M+Na]^+$	94069	0
Proline	116.0710	$C_5H_9NO_2$	$[M+H]^+$	29	3.4
Benzopyrans					
Coumarin	147.0441	$C_9H_6O_2$	$[M+H]^+$	3525	0
Benzopyridines					
Isoquinoline	130.0652	C_9H_7N	$[M+H]^+$	44763	0.7
Carbonyl Compounds					
6-Nonenal	158.1539	$C_9H_{16}O$	$[M+NH4]^+$	87316	0
Octanal	129.1275	$C_8H_{16}O$	$[M+H]^+$	6033	-1.5
Carboxylic Acids and Derivatives					
Glyoxylic acid	118.9716	$C_2H_2O_3$	$[M+2Na-H]^+$	64613	0
Malic acid	178.9920	$C_4H_6O_5$	$[M+2Na-H]^+$	118	-3.3

Acetylputrescine	131.1185	$C_6H_{14}N_2O$	$[M+H]^+$	3252	5.3
Procaine hydrochloride	295.1184	$C_{13}H_{21}ClN_2O_2$	$[M+Na]^+$	66759	0.3
Citric acid	236.9981	$C_6H_8O_7$	$[M+2Na-H]^+$	124	0
Cinnamic acid and derivatives					
Methyl 3,4,5-trimethoxycinnamate	275.0890	$C_{13}H_{16}O_5$	$[M+Na]^+$	93223	0
Coumaric acid	147.0449	$C_9H_8O_3$	$[M+H-H2O]^+$	305	-2.0
Cinnamaldehydes					
Cinnamaldehyde	133.0648	C_9H_8O	$[M+H]^+$	6931	0
Cyclic Alcohols and Derivatives					
Chlorogenic Acid	377.0843	$C_{16}H_{18}O_9$	$[M+Na]^+$	3498	0
5Z-Caffeoylquinic acid	355.1031	$C_{16}H_{18}O_9$	$[M+H]^+$	95165	2.2
Disaccharides					
Galactose-beta-1,4-xylose	295.1023	$C_{11}H_{20}O_{10}$	$[M+H-H2O]^+$	62416	-2.0
cis-Mulberroside A	591.1684	$C_{26}H_{32}O_{14}$	$[M+Na]^+$	87898	0
3-Hexenyl b-primeveroside	417.1730	$C_{17}H_{30}O_{10}$	$[M+Na]^+$	87866	-0.2
Sucrose	381.0791	$C_{12}H_{22}O_{11}$	$[M+K]^+$	137	-0.5
1-Hexanol arabinosylglucoside	419.1888	$C_{17}H_{32}O_{10}$	$[M+Na]^+$	87865	0
3-Hexenyl b-primeveroside	395.1912	$C_{17}H_{30}O_{10}$	$[M+H]^+$	87866	0
Docosanoids					
4,5-epoxy-17R-hydroxy-6E,8E,10Z,13Z,15E19Z-docosahexaenoic acid	421.2349	$C_{25}H_{34}O_4$	$[M+Na]^+$	75237	0
Eicosanoids					
10-F2-dihomo-IsoP	419.2768	$C_{23}H_{40}O_5$	$[M+Na]^+$	96931	0
Fatty Acids and Conjugates					
2-hydroxy capric acid	211.1304	$C_{10}H_{20}O_3$	$[M+Na]^+$	35411	0
Pentadecanedioic acid	273.2059	$C_{15}H_{28}O_4$	$[M+H]^+$	35977	-1.5
3,12-dihydroxy-pentadecanoic acid	297.2035	$C_{15}H_{30}O_4$	$[M+Na]^+$	74562	-0.3
6,8-dihydroxy-octanoic acid	177.1121	$C_8H_{16}O_4$	$[M+H]^+$	74602	0
2E,8E-dodecadienoic acid	214.1802	$C_{12}H_{20}O_2$	$[M+NH4]^+$	34897	0
14-keto pentadecanoic acid	239.2014	$C_{15}H_{28}O_3$	$[M+H-H2O]^+$	35743	1.2
6,8-dihydroxy-octanoic acid	159.1021	$C_8H_{16}O_4$	$[M+H-H2O]^+$	74602	0

4-keto pentadecanoic acid	239.2014	$C_{15}H_{28}O_3$	$[M+H-H2O]^+$	35741	1
Fatty Aldehydes					
Stearaldehyde	291.2682	$C_{18}H_{36}O$	$[M+Na]^+$	6658	8.2
Fatty Acid Esters					
9-oxo-2,4,5,7-decatetraenoic acid	179.0703	$C_{10}H_{10}O_3$	$[M+H]^+$	74724	0
Propionyl-CoA	823.1384	$C_{24}H_{40}N_7O_{17}P_3S$	[M+]	442	-3.6
2-methylene dodecanoic acid	213.1848	$C_{13}H_{24}O_2$	$[M+H]^+$	34573	-0.5
Fatty esters					
Tridecatrienyl acetate	237.1849	$C_{15}H_{24}O_2$	$[M+H]^+$	46270	0
Fatty Acyls					
Octane-1,2-diol	147.1384	$C_8H_{18}O_2$	$[M+H]^+$	46044	3.3
10-amino-decanoic acid	188.1645	$C_{10}H_{21}NO_2$	$[M+H]^+$	74855	0
4-oxo-9Z,11Z,13E,15E-octadecatetraenoic acid	291.1952	$C_{18}H_{26}O_3$	$[M+H]^+$	74765	-0.2
Octyl acetate	173.1536	$C_{10}H_{20}O_2$	$[M+H]^+$	46196	0
6,8-dihydroxy-octanoic acid	159.1021	$C_8H_{16}O_4$	$[M+H-H2O]^+$	74602	0
Fatty Alcohols					
Decen-1-ol	198.1852	$C_{10}H_{20}O$	$[M+ACN+H]^+$	46092	0
Octane-1,2-diol	147.1385	$C_8H_{18}O_2$	$[M+H]^+$	46044	4.1
(3R,7R)-1,3,7-Octanetriol	185.1148	$C_8H_{18}O_3$	$[M+Na]^+$	89425	0
1,3,7-Octanetriol	163.1327	$C_8H_{18}O_3$	$[M+H]^+$	89425	-0.6
2,5-Octadien-1-ol	109.1017	$C_8H_{14}O$	$[M+H-H2O]^+$	94689	3
Sorbitol	183.0863	$C_6H_{14}O_6$	$[M+H]^+$	143	0
Dioctyl hexanedioate	371.3164	$C_{22}H_{42}O_4$	$[M+H]^+$	95990	-2.4
Fatty Amides					
Linoleoyl Ethanolamide	362.2468	$C_{20}H_{37}NO_2$	$[M+K]^+$	3718	3.5
(Z)-6-Tetradecene-1,3-diyne-5,8-diol	259.1109	$C_{14}H_{20}O_2$	$[M+K]^+$	93602	5.8
13E-Docosenamide	338.3417	$C_{22}H_{43}NO$	$[M+H]^+$	85041	0
N-stearoyl valine	384.3472	$C_{23}H_{45}NO_3$	$[M+H]^+$	75504	0
Flavonoids					
Quercetin 3-sambubioside-3'-glucoside	781.1798	$C_{32}H_{38}O_{21}$	$[M+Na]^+$	50545	0

Catechin 7-O-alpha-L-rhamnopyranoside	459.1262	$C_{21}H_{24}O_{10}$	$[M+Na]^+$	47244	0
Quercetin 3'-xyloside	457.0741	$C_{20}H_{18}O_{11}$	$[M+Na]^+$	50598	0
Myricitrin	465.1028	$C_{21}H_{20}O_{12}$	$[M+H]^+$	50852	0
Quercetin 7-galactoside	487.0847	$C_{21}H_{20}O_{12}$	$[M+Na]^+$	50594	0
Quercetin 3-rhamnoside-7-glucoside	611.1606	$C_{27}H_{30}O_{16}$	$[M+H]^+$	50615	0
5,7,2',4'-Tetrahydroxy-3,6,5'-trimethoxyflavone	399.0693	$C_{18}H_{16}O_9$	$[M+Na]^+$	51465	1.8
7,8-Dimethoxyflavanone	307.0941	$C_{17}H_{16}O_4$	$[M+Na]^+$	52580	0
(±)-Catechin	291.0868	$C_{15}H_{14}O_6$	$[M+H]^+$	3419	1.7
Quercetin	303.0504	$C_{15}H_{10}O_7$	$[M+H]^+$	409	1.6
8-Methy caffeine	247.0590	$C_9H_{12}N_4O_2$	$[M+K]^+$	84980	-0.4
Cyanidin 3-glucosyl-(1->6)-[xylosyl-(1->2)-galactoside]	765.1818	$C_{32}H_{38}O_{20}$	$[M+Na]^+$	46866	-4.0
Kaempferol 3-p-coumarate	433.0932	$C_{24}H_{16}O_8$	$[M+H]^+$	50408	3.4
Kaempferol 3-p-coumarate	433.0923	$C_{24}H_{16}O_8$	$[M+H]^+$	50408	1.4
Epiafzelechin 3-O-beta-D-allopyranoside	475.1001	$C_{21}H_{24}O_{10}$	$[M+K]^+$	47242	0
Glycerolipids					
DG(20:2(11Z,14Z)/14:0/0:0)	575.5039	$C_{37}H_{68}O_5$	$[M+H-H2O]^+$	88644	0
Glycerol 1-(5-hydroxydodecanoate)	273.2059	$C_{15}H_{30}O_5$	$[M+H-H2O]^+$	94704	-2.1
Glycerophospholipids					
PA(21:0/22:4(7Z,10Z,13Z,16Z))	794.5833	$C_{46}H_{83}O_8P$	$[M]^+$	81866	1.0
PC(O-16:0/O-16:0)	728.5931	$C_{40}H_{84}NO_6P$	$[M+Na]^+$	40207	4.1
PC(0:0/7:0)	411.2254	$C_{15}H_{32}NO_7P$	$[M+ACN+H]^+$	40361	0
PE(20:4(5Z,8Z,11Z,14Z)/16:0)	740.5225	$C_{41}H_{74}NO_8P$	$[M+H]^+$	60781	0
Indoles					
N-Methyltryptamine	197.1049	$C_{11}H_{14}N_2$	$[M+Na]^+$	63558	0
Methylindolepyruvate	259.1082	$C_{12}H_{11}NO_3$	$[M+ACN+H]^+$	86813	1.9
Neutral glycosphingolipids					
GlcCer(d16:2(4E,6E)/18:0(2OH))	714.5514	$C_{40}H_{75}NO_9$	$[M+H]^+$	103318	0
Monosaccharides					
5-Methylthio-D-ribose	181.0529	$C_6H_{12}O_4S$	$[M+H]^+$	63429	0

Glucose	203.0526	$C_6H_{12}O_6$	$[M+Na]^+$	3755	0
Isoprenoids					
Cymene	163.1481	$C_{12}H_{18}$	$[M+H]^+$	85265	0
Peptides					
Gly-His-OH	338.1095	$C_{13}H_{12}N_4O_6$	$[M+NH4]^+$	65205	0
Gln Gly Pro Ser	388.1827	$C_{15}H_{25}N_5O_7$	$[M+H]^+$	209734	0.2
Tyr Lys Thr	428.2504	$C_{19}H_{30}N_4O_6$	$[M+NH4]^+$	19980	0.2
Ser Gly Phe Pro	429.1745	$C_{19}H_{26}N_4O_6$	$[M+Na]^+$	225571	0
Pro Leu Pro Asp	463.2163	$C_{20}H_{32}N_4O_7$	$[M+Na]^+$	203321	0
Pro Lys Lys Ser	476.3191	$C_{20}H_{38}N_6O_6$	$[M+NH4]^+$	202854	0
Phe Ile Trp	503.2055	$C_{26}H_{32}N_4O_4$	$[M+K]^+$	18310	0
Met Tyr Cys Cys	541.1220	$C_{20}H_{30}N_4O_6S_3$	$[M+Na]^+$	191100	0.2
Pro Arg	296.2225	$C_{15}H_{26}O_3$	$[M+ACN+H]^+$	85909	1.6
Hydroxyprolyl-Tryptophan	359.1709	$C_{16}H_{19}N_3O_4$	$[M+ACN+H]^+$	85780	-1.1
Phenylpropenes					
4-Hydroxycinnamoylagmatine	299.1478	$C_{14}H_{20}N_4O_2$	$[M+Na]^+$	66195	0
Prenol Lipids					
Limonene	137.1324	$C_{10}H_{16}$	$[M+H]^+$	41063	0
6-Methyl-5-hepten-2-ol	129.1274	$C_8H_{16}O$	$[M+H]^+$	44731	-0.8
Farnesal	203.1794	$C_{15}H_{24}O$	$[M+H-H2O]^+$	44756	-1.5
7-Drimene-11,12,14-triol	255.1950	$C_{15}H_{26}O_3$	$[M+H]^+$	91869	-1.6
6S,9R-Dihydroxy-4,7E-megastigmadien-3-one 9-[apiosyl-(1->6)-glucoside]	541.2255	$C_{24}H_{38}O_{12}$	$[M+Na]^+$	86480	0
Geranylcitronellol	310.3104	$C_{20}H_{36}O$	$[M+NH4]^+$	46161	0
Eriojaposide A	503.2487	$C_{24}H_{38}O_{11}$	$[M+H]^+$	92803	0.2
Linalyl propionate	228.1958	$C_{13}H_{22}O_2$	$[M+NH4]^+$	86966	0
alhpa-tocopheronolactone	301.1410	$C_{16}H_{22}O_4$	$[M+Na]^+$	53844	0
Carvyl propionate	209.1536	$C_{13}H_{20}O_2$	$[M+H]^+$	92819	0
3,6,8-dodecatrien-1-ol	198.1852	$C_{12}H_{20}O$	$[M+NH4]^+$	36515	0
Cyclocitral	153.1274	$C_{10}H_{16}O$	$[M+H]^+$	95447	0.7
Proanthocyanidins					

Procyanidin B5	579.1497	$C_{30}H_{26}O_{12}$	$[M+H]^+$	71836	0
Proanthocyanidin A2	591.1504	$C_{31}H_{26}O_{12}$	$[M+H]^+$	68190	1.1
Purine Nucleotides					
Guanosine monophosphate	427.0751	$C_{10}H_{14}N_5O_8P$	$[M+ACN+Na]^+$	98	3.2
Inosine-5'-carboxylate	313.0793	$C_{11}H_{12}N_4O_7$	$[M+H]^+$	65946	4.7
Pyridines and Derivatives					
Pyridoxine (Vitamin B6)	192.0631	$C_8H_{11}NO_3$	$[M+Na]^+$	6307	0
Sphingolipids					
GlcCer(d18:2/16:0)	697.5481	$C_{40}H_{75}NO_8$	$[M]^+$	83808	-1.5
N-(2R-Hydroxytricosanoyl)-2S-amino-1,3S,4R-octadecanetriol	670.6345	$C_{41}H_{83}NO_5$	$[M+H]^+$	90755	0.1
Styrenes					
Caffeoylputrescine	295.1022	$C_{13}H_{18}N_2O_3$	$[M+2Na-H]^+$	3380	-2.3
(3xi,6E)-1,7-Diphenyl-6-hepten-3-ol	266.1670	$C_{19}H_{22}O$	$[M]^+$	86754	0
Stilbenes					
4-(3-Methyl-1-butenyl)-3,3',4',5-tetrahydroxystilbene	313.1439	$C_{19}H_{20}O_4$	$[M+H]^+$	87088	-1.5

6.4 Conclusions and future directions

This is the first application of the 96-blade SPME in direct extraction mode coupled to LC-MS for all small molecular weight species in apple samples for determinations of the dynamic processes occurring in apple samples under storage. The objective of the current research was the successful application of the solvent-free and environmentally-friendly SPME sample preparation technique for global metabolomics analyses of complex food matrices. In comparison to traditional sample preparation techniques, SPME offers a solvent-free procedure, lower sample preparation times, use of small sample sizes, high-throughput capability, and matrix effect reduction. SPME method development for apple metabolomics demonstrated that the type of SPME coating can affect the metabolic profile of apple samples. Sample preparation for global metabolite discovery was shown to be performed efficiently, with hundreds of features profiled using R software. The developed HLB coating as the stationary phase for the 96-blade system provided simultaneous extraction of both polar and hydrophobic compounds in a single run, accompanied by high-throughput analysis, while use of the open-bed thin film microextraction afforded an increase in sensitivity and reduced extraction time, without any need for further sample pretreatment. Chromatographic conditions employed a short gradient, resulting in peak widths < 0.3 min; such conditions were useful for both metabolite profiling and for metabolite identification experiments. SPME showed good separation between various groups of apple samples in different conditions, and some of the most important markers related to browning reactions produced by scald in apple samples were

determined. The optimized method can be applied to find changes in metabolite levels due to storage disorders of apples. The proposed method not only shows metabolic profiling to be an efficient tool for mapping biochemical pathway analysis, but could also be helpful in achieving information regarding markers related to chemical phenotypes as well as storage and marketing decisions. Direct immersion SPME coupled to LC-MS provides sample characterization for a broad range of metabolites, and in order to obtain more a comprehensive metabolic picture of apple samples and potential biomarkers regarding storage effect, in future studies, the present results with the results obtained from SPME-GCxGC-TOFMS for the same apple samples will provide comprehensive metabolic profile for wide range of metabolite comparing both techniques.

Chapter 7

Summary and future perspectives

7.1 Summary

Global metabolomics focuses on the analysis of all metabolites in biological systems; it is applied to investigate the metabolic differences between case studies and control samples. Consequently, metabolomics can be utilized in biomarker discoveries related to diseases, toxicant exposure, evaluation of nutritional status, and drug discovery and development. Among the various analytical chemistry techniques, the most comprehensive high-resolution analysis of non-volatiles and semi-volatiles is provided by LC-MS. Recent research in this area has shown that many factors, such as sample preparation, quantification, column type, and detection technique, as well as peak identification, are important factors in determining the quality of metabolomics data. As such, further improvement of metabolomics techniques for quantification and qualification need to involve consideration of these variables. However, there currently exists a need for sample preparation techniques prior to LC-MS analysis that are capable of increasing sensitivity and reducing matrix effects caused by co-elution of highly abundant metabolites, salts, and proteins as low abundance metabolites need more sample clean-up and preconcentration to be detected.

The main objective of this study was the development of a high-throughput SPME-LC/MS technique that involves a solventless, green, and environmentally-friendly sample preparation methodology for targeted and non-targeted metabolome profiling of complex sample matrices. In this work, both polar and apolar metabolites from *E.coli* as a model sample were separated by the UPLC PFP LC column. Exactive Orbitrap facilitated high-resolution detection (<5ppm) of mass ions, providing differentiation between isobaric compounds with the same nominal mass. Optimization of coating characteristics for extraction of metabolites produced by *E.coli* bacteria as a model organism demonstrated the tested coatings possess selectivity to provide extraction of different classes of metabolites with high extraction recoveries. The results indicated a relationship exists between the chemistries of the tested coatings, resulting in different extraction profiles demonstrating that coatings with various chemical structures extract metabolite with different functional groups. For example, the PBA coating, which contains a diol-hydroxyl group in its phenylboronic acid structure, can covalently bind with alcohols, nucleotides, and carbohydrates. PS-DVB-WAX can provide various types of extraction capabilities such as van der waals and π- π interactions, as well as hydrogen binding and ionic interactions due to the weak ionic exchange group available in its polymer structure, which function to balance the characteristics of this coating for extraction of both polar and nonpolar metabolites. Consequently, a large number of classes of metabolites can be extracted with this coating. The HLB coating demonstrated similar characteristics; however, this

coating was shown to extract a class of lipids with higher extraction recovery. As such, the commercially available HLB coating with ionic exchange groups possesses different coating characteristics towards a different class of metabolites. It is worth mentioning that pH, ionic strength, and the type of sample matrix under study were factors that were shown to potentially influence the final metabolomics results. Coatings with alkaline long chains such as C18 were shown to provide high extraction recovery for lipid classes, which are nonpolar metabolites that do not contain polar functional groups in their structure. The presented results demonstrated that ion exchange phases such as Si-RP-WCX or polar functional groups embedded in the chemistry of a coating like Si-IL can change the coating characteristics towards extraction of metabolites with higher polarity. In Chapter 3, the use of Heatmap illustrated optimum coating characteristics towards the extraction of different classes of metabolites. The results demonstrated that each type of coating is specific for extraction of particular classes of metabolites that influence metabolic profile. Application of various extractive phases for the 96-blade system utilized for metabolomics indicates that the obtained metabolome profile differs depending on the selected coating type, an effect similar to the use of different solvents in LLE. Therefore, this study shows that based on the type of metabolite classes that are being investigated in a metabolomics study, appropriate coatings must be selected.

In contrast to LLE and SPE, SPME is a non-exhaustive extraction method that eliminates the need for metabolism quenching and produces lower MS signal intensities. Therefore SPME is less susceptible to matrix effect due to lower extraction recovery and lower intensity of highly intense ions reducing ion suppression or enhancement in comparison to traditional technique. In addition, the small amounts of extracted metabolites are generally sufficient for quantitative analysis. Clean extract obtained from SPME has less problem of obscuring low intensities ions by ion suppression phenomenon. The SPME coatings developed in this research have long-term reusability and allow for the extraction of a wide polarity range of metabolites. For biocompatible SPME coatings, the addition of a wash step can eliminate particulates, salt, and protein retardation on the surface of the coating, allowing the desorption solvent to be free of suppressing salt, proteins, and other interferences. In this work, the obtained results demonstrated the higher reproducibility of SPME in comparison to LLE for non-biological replicates extraction from the same bacteria growth culture (Figure 7.1). This particular set of experiments allowed for a comparison of variability within sample preparation and analysis techniques in terms of experimental errors to set confidence limits for the significant data. The observed findings can be explained by the ability of the SPME method to only extract the free portion of metabolites present in the sample, which allows reduction in matrix effects and contributes to lower chromatographic backgrounds. Data nalaysis related to statistically siginificant-differentiated metabolites between two clusters in Figure 7.1 between two metods demonstrates extraction of phospholipids with high ion abundance in LLE experiment in

comparison to SPME. Conversely, during the solvent extraction step of the LLE method, dissolved phospholipids and other cellular components can interfere or co-elute with the metabolites of interested that are separated at the same retention time, which in turn causes ion suppression. In addition, SPME was shown to have higher metobite coverage due to lower ion suppression as well as extract unstable and short-lived metabolites (Chapter 3). In short, SPME was shown to be a more sustainable and reproducible method by extracting lower amounts of metabolites due to its non-exhaustive characteristics, and extraction of free portion of metabolites resulting in producing smaller matrix effects than LLE.

SPME provides separate clusters for each experiment (Chapter 4, Chapter 5, Chapter 6) as well as good instrument performance after a large number of extractions, thus confirming the superior repeatability and precision of the method, as well as its ability to provide cleaner extracts, which consequently lead to sound analytical results. The obtained results shows that SPME has the potential to act as a one-step sample preparation and sample clean-up technique with high method precision for various areas of research, including biological, clinical, pharmaceutical, environmental, food, and metabolomics studies.

In this work, high-throughput instantaneous preparation of up to 96 samples was attained with an average of ~1-2 min per sample for equilibrium extraction. However, with the application of an automated, highly sensitive 96-blade SPME system, this analysis time can be considerably decreased via pre-equilibrium extraction, without sacrificing precision or limiting sensitivity. Performing experiment at lower extraction times using the automation technique helps diminish possibility of metabolite transformation or degradation happening in longer extraction times. Thin film microextraction, as an open bed extraction technique, results in significant enhancement in extraction efficiency, providing faster extractions than methods involving commercial SPME fibers, in addition to eliminating common issues experienced in the workflow of traditional methods such as SPE, for instance the clogging of packed bed systems.

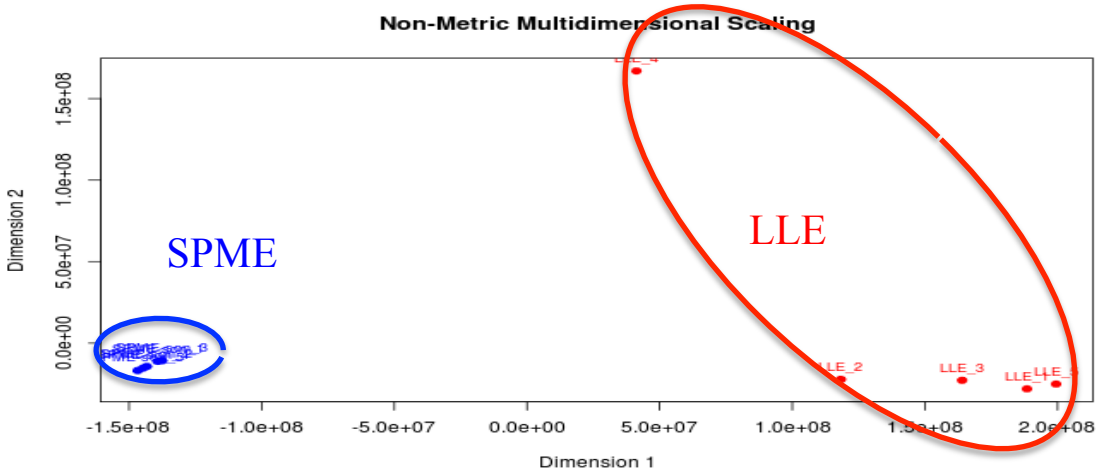

Figure 7.1 Cluster separation and reproducibility of extraction results by SPME and LLE from *E.coli* bacteria (10^{-5} CFU mL^{-1}) for 5 non-biological replicates.

Another dimension of the currently reviewed work involved the application of the developed analytical technique towards a novel procedure for acquiring semi-quantitative metabolic information from under-stressed biological systems (Chpater 4, Chapter 5, Chapter6). First, the developed method was applied for in vivo DI-SPME sampling of bacteria growing in media, with minimum perturbation and the elimination of metabolism-quenching steps and manipulative sample preparation. The global SPME metabolic profiles of bacteria treated with different naturally-occurring antibacterial agents indicates that widely differing SPME-LC/MS profiles can be obtained depending on the type and amount of antibacterial agent added, as well as the time point of the growth phase during which sampling is conducted. The SPME method showed good cluster separation between two different antibacterial agents (Figure 7.2) and provided metabolite differentiation, demonstrating that the tested essential oils have differing modes of action in regards to microorganism metabolism interruption, through interruption of various metabolic pathways. To this purpose, different types of experiments were designed in order to evaluate results in terms of different errors (biological or nonbiological) and explain significant biological differences with higher confidence. Biological replicates were obtained to differentiate between random results and statistically significant differences between two groups of samples exposed to different treatments, so as to ascertain whether the observed differences represent a true biological difference induced due to treatment with the naturally-occurring antibacterial agents. For this series of experiments, the obtained SPME profiles were composed of potential biomarkers, which can potentially help in determinations of biosynthetic pathways and biological roles of antibacterial agents on *E.coli* bacteria. However, the obtained results are still exploratory in nature; further investigations are needed to properly identify and characterize these biomarkers. Cinnamaldehyde and clove oil have likely to be used as active anticancer agents based on their potential effect to stop the glycolysis pathway. The obtained results indicate that the state-of-the-art 96-blade SPME coupled to LC/MS has the potential to provide metabolic profiling of uni- and multicellular living systems under the induction of various environmental stresses.

The second application of the developed method involved investigations to provide and compare metabolic snapshots of stored apple samples (with and without superficial scald) versus healthy apple samples. SPME demonstrated good differentiation between sample types and different time points, in addition to allowing for identification of potential biomarkers related to disturbed apple metabolism under storage conditions. The change in metabolic pathway of apple samples under stress in comparison to the control samples help increase the shelflife utilizing particular agent to inhibit the scald progress.

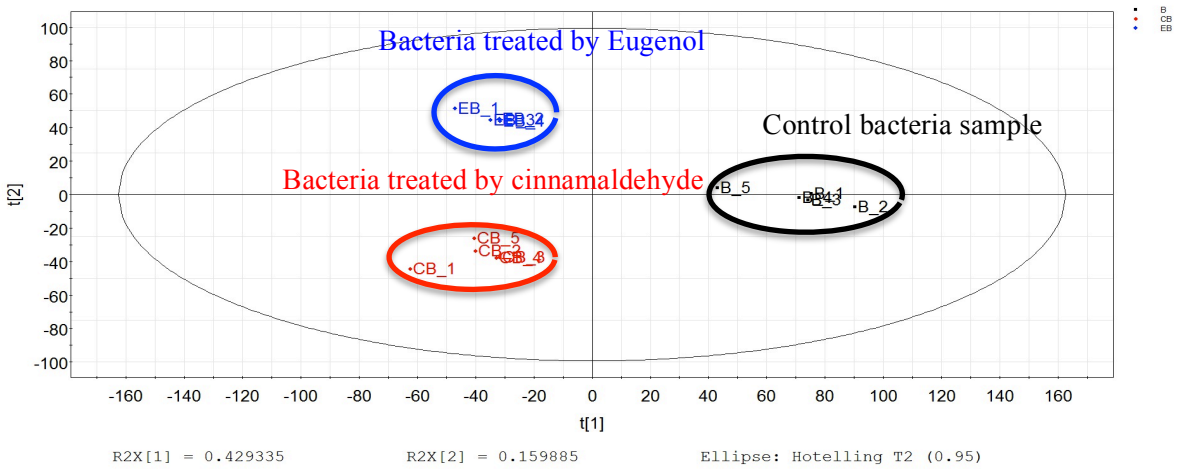

Figure 7.2 Cluster differentiation between bacteria treated with clove oil and cinnamaldehyde, with the matched control samples.

7.2 Future perspective

A future step of this thesis, currently in progress in our laboratory, involves the development and evaluation of the full potential of SPME in the field of global metabolite analysis through hyphenation of this technique with high-resolution instrumentation, such as HS-SPME GCxGC-ToFMS and 96-blade SPME-LC/MS. The goal of these applications is to provide comprehensive metabolic profiles of both bacteria and apple samples under environmental stress conditions. Results so far have demonstrated that a coupling of the DI-SPME technique to multidimensional LCxLC-MS techniques will result in the provision of comprehensive complex sample characterization, high-resolution metabolite separation, and single-run profiles of living systems. Miniaturized SPME-LC/MS may also be applied in single cell metabolomics studies, allowing for a less invasive technique and providing spatial resolution enhancement. Essential oils, which are small molecules of plant origin, are suggested as potential leads towards drug design; in-depth investigations of metabolic pathway transformation using comparisons between control bacteria and matched treated bacteria samples can assist in the characterization of the modes of action of essential oils against pathogens, as well as aid in the discovery of the targets of these antibacterial agents. This can in turn allow for the use of these naturally occurring compounds as drugs in place of conventional chemicals that increase microorganism resistance. Additionally, the application of SPME-LC-MS metabolomics techniques imparts new information into the physiological processes controlling superficial scald and ripening processes that affect fruit flavor, appearance, and overall quality. Deregulation of different metabolite levels connected with ripening and browning disorders suggest changes in various metabolic pathways and biochemical mechanisms taking place in stored apple samples. The results introduced to date confirm the currently introduced method as a promising technique for the evaluation of adverse growth conditions such as drought, salinity, chilling, freezing, and high

temperature, which can cause delayed growth and reduce productivity, or, in extreme cases, even plant death. Capturing metabolites with a wide variety of polarities assists in the creation of snapshots of the biosynthesis and degradation pathways of the main metabolites associated with stress tolerance, which in turn helps to explain the role of metabolites in adapting to severe environments. Finally, SPME-LC-MS based metabolomics could provide the data for study of biological systems alongside with proteomics and genomics in order to provide a full map of living organism.

Copyright permission for the materials of Chapter 2

Copyright Clearance Center RightsLink®

Home | Account Info | Help

Title: Silica-based ionic liquid coating for 96-blade system for extraction of aminoacids from complex matrixes

Author: Fatemeh Mousavi,Janusz Pawliszyn

Publication: Analytica Chimica Acta

Publisher: Elsevier

Date: 25 November 2013

Logged in as: Fatemeh Mousavi

LOGOUT

Order Completed

Thank you very much for your order.

This is a License Agreement between Fatemeh Mousavi ("You") and Elsevier ("Elsevier"). The license consists of your order details, the terms and conditions provided by Elsevier, and the payment terms and conditions.

Get the printable license.

License Number	3707930989468
License date	Sep 14, 2015
Licensed content publisher	Elsevier
Licensed content publication	Analytica Chimica Acta
Licensed content title	Silica-based ionic liquid coating for 96-blade system for extraction of aminoacids from complex matrixes
Licensed content author	Fatemeh Mousavi,Janusz Pawliszyn
Licensed content date	25 November 2013
Licensed content volume number	803
Licensed content issue number	n/a
Number of pages	9
Type of Use	reuse in a thesis/dissertation
Portion	full article
Format	both print and electronic
Are you the author of this Elsevier article?	Yes
Will you be translating?	No
Title of your thesis/dissertation	Optimization of SPME coating characteristics for metabolomics and targeted analysis with LC/MS
Expected completion date	Sep 2015
Estimated size (number of pages)	20
Elsevier VAT number	GB 494 6272 12
Customer Tax ID	CACanada
Permissions price	0.00 CAD
VAT/Local Sales Tax	0.00 CAD / 0.00 GBP
Total	0.00 CAD

Copyright permission for the materials of Chapter 3

Copyright Clearance Center RightsLink®

Home | Account Info | Help

Title: Development of high throughput 96-blade solid phase microextraction-liquid chromatrography-mass spectrometry protocol for metabolomics

Author: Fatemeh Mousavi,Barbara Bojko,Janusz Pawliszyn

Publication: Analytica Chimica Acta

Publisher: Elsevier

Date: Available online 22 August 2015

Logged in as: Fatemeh Mousavi

LOGOUT

Permission Request Submitted

Your request is now under review.
You will be notified of the decision via email.
Please print this request for your records.

Get the printable order details.

Order Number	501047994
Order Date	Sep 14, 2015
Licensed content publisher	Elsevier
Licensed content publication	Analytica Chimica Acta
Licensed content title	Development of high throughput 96-blade solid phase microextraction-liquid chromatrography-mass spectrometry protocol for metabolomics
Licensed content author	Fatemeh Mousavi,Barbara Bojko,Janusz Pawliszyn
Licensed content date	Available online 22 August 2015
Licensed content volume number	n/a
Licensed content issue number	n/a
Number of pages	1
Type of Use	reuse in a thesis/dissertation
Portion	full article
Format	both print and electronic
Are you the author of this Elsevier article?	Yes
Will you be translating?	No
Title of your thesis/dissertation	Optimization of SPME coating characteristics for metabolomics and targeted analysis with LC/MS
Expected completion date	Sep 2015
Elsevier VAT number	GB 494 6272 12
Customer Tax ID	CACanada
Permissions price	Not Available
VAT/Local Sales Tax	Not Available
Total	Not Available

References

[1] U. Ceglarek, A. Leichtle, M. Brügel, L. Kortz, R. Brauer, K. Bresler, J. Thiery, G.M. Fiedler, Mol. Cell. Endocrinol. 301 (2009) 266-271.

[2] D. Ryan, K. Robards, Anal. Chem. 78 (2006) 7954-7958.

[3] S.J. Bruce, I. Tavazzi, V. Parisod, S. Rezzi, S. Kochhar, P. Guy, Anal. Chem. 81 (2009) 3285-3296.

[4] S.L. Robinette, E. Holmes, J.K. Nicholson, M.E. Dumas, Genome Med. 4 (2012) 30-40.

[5] J. Tang, C.Y. Tan, M. Oresic, A. Vidal-Puig, Genome Med. 1 (2009) 35.

[6] J. L. Griffin, C.D. Rosiers, Genome Med. 1 (2009) 32.

[7] S. G. Oliver, M. K. Winson, D. B. Kell, F, Baganz, Trends Biotechnol. 16 (1998) 373-378.

[8] R. J. Williams, Individual metabolic patterns and human disease: an exploratory study utilizing predominantly paper chromatographic methods. Austin: Univ. Texas, 1951.

[9] R. J. Williams, Biochemical individuality. John Wiley & Sons; 1956.

[10] E. C. Horning, M. G. Horning, Clin. Chem. 17 (1971) 802-809.

[11] E. C. Horning, M. G. Horning, J. Chromatogr. Sci. 9 (1971) 129-140.

[12] L. Pauling , A.B. Robinson, R. Teranishi, P. Cary, Proc Nat Acad Sci. 68 (1971) 2374-2376

[13] D.S. Wishart, Brief Bioinform. 8 (2007) 279-293.

[14] A. Nordström, G. O'Maille, C. Qin, G. Siuzdak, Anal. Chem. 78 (2006) 3289-3295.

[15] N. R. Pace, Proc. Natl. Acad. Sci. 98 (2001) 805–808.

[16] K. Dettmer, P. A. Aronov, B. D. Hammock, Mass Spectrom Rev. 26 (2007) 51-78.

[17] J. Nielsen, S. Oliver, Trends Biotechnol. 23 (2005) 544-546.

[18] D. B. Kell, Microbiol. 7 (2004) 296–307.

[19] W. J. Griffiths, Y. Wang, Chem. Soc. Rev. 38 (2009) 1882-1896.

[20] G. Theodoridis, H. G. Gika, I. D. Wilson, TrAC Trends. Anal. Chem. 27 (2008) 251-260.

[21] T. O. Metz, Metabolic Profiling: Methods and Protocols Methodsin Molecular Biology, Springer Protocols, Humana Press, Heidelberg, 2011.

[22] S. Vaidyabnathan, G. G. Harrigan, R. Goodacre, Metabolome Analyses: Strategies for Systems Biology, Springer, New York, 2005.

[23] R. L. Last, A. D. Jones, Y. Shachar-Hill, Nat. Rev.Mol. Cell Biol. 8 (2007) 167-174.

[24] B. Cavaliere, A. De Nino, F. Hayet, A. Lazez, B. Macchione, C. Moncef, J. Agric. Food Chem. 55 (2007) 1454-1462.

[25] Y. Wu, L. Li, Anal. Chem. 85 (2013) 5755-5763

[26] J. M. Cevallos-Cevallosa, J.I. Reyes-De-Corcueraa, E. Etxeberriaa, M.D. Danyluka, G.E. Rodrick, Trends in Food Science & Technology 20 (2009) 557-566

[27] E. M. Lenz, I. D. Wilson, J. Proteome Res. 6 (2007) 443-458.

[28] I. D. Wilson, K. E. Wade, J. K. Nicholson, TrAC Trends Anal. Chem. 8 (1989) 368-374.
[29] H. C. Keun, O. Beckonert, J. L. Griffin, C. Richter, D. Moskau, J. C. Lindon, J. K. Nicholson, Anal. Chem. 74 (2002) 4588-4593.
[30] M. Coen, E. Holmes, J.C. Lindon, J. K. Nicholson, Chem. Res. Toxicol. 21 (2008) 9-27.
[31] M. Beckmann, D. Parker, D. P. Enot, E. Duval, J. Draper, Nat. Protoc. 3 (2008) 486-504.
[32] R. Shroff, L. Rulisek, J. Doubsky, A. Svatos, Proc. Natl. Acad. Sci. 106 (2009) 10092-10096.
[33] Y. Li, B. Shrestha, A. Vertes, Anal. Chem. 80 (2008) 407-420.
[34] T. R. Northen, O. Yanes, M. T. Northen, D. Marrinucci, W. Uritboonthai, J. Apon, S.L. Golledge, A. Nordstrom, G. Siuzdak, Nature 449 (2007) 1033-1036.
[35] S. Cha, E. S. Yeung, Anal. Chem. 79 (2007) 2373-2385.
[36] A. U. Jackson, S. R. Werner, N. Talaty, Y. Song, K. Campbell, R. G. Cooks, J. A. Morgan, Anal. Biochem. 375 (2008) 272-281.
[37] H. Chen, Z. Pan, N. Talaty, D. Raftery, R.G. Cooks, Rapid Commun. Mass Spectrom. 20 (2006) 1577–1584.
[38] M. Zhou, J. F. McDonald, F. M. Fernández, J. Am. Soc. Mass Spectrom. 21 (2010) 68-75.
[39] C. Brunelli, C. Bicchi, A. Di Stilo, A. Salomone, M. Vincenti, J. Sep. Sci. 29 (2006) 2765-2771.
[40] S. D. Brown, D. J. Rhodes, B. Pritchard, J. Forensic Sci. Int. 171 (2007) 142-150.
[41] M. R. Meyer, F. T. Peters, H. H. Maurer, Clin. Chem. 56 (2010) 575-584.
[42] D. Hori, Y. Hasegawa, M. Kimura, Y. Yang, I.C. Verma, S. Yamaguchi, Brain Dev. 27 (2005) 39-45.
[43] H. R. Yoon, Arch. Pharm. Res. 30 (2007) 387-395.
[44] A. Zhang, H. Sun, P. Wang, Y. Han, X. Wang, Analyst 137 (2012) 293-300.
[45] J. G. Dorsey, K. A. Dill, Chem. Rev. 89 (1989) 331-346.
[46] M. Shortreed, S. Lamos, B. Frey, M. Phillips, M. Patel, P. Belshaw, L. Smith, Anal. Chem. 78 (2006) 6398-6404.
[47] T. Santa, Biomed. Chromatogr. A. 25 (2011) 1-10.
[48] C. Horvath, W. Melander, I. Molnar, P. Molnar, Anal. Chem. 49 (1997) 2295-2298.
[49] P. Jandera, J. Sep. Sci. 31 (2008) 1421-1437.
[50] B. A. Rappold, R. P. Grant, J. Sep. Sci. 34 (2011) 3527-3537.
[51] H. P. Nguyen, S. H. Yang, J. G. Wigginton, J. W. Simpkins, K. A. Schug, J. Sep. Sci. 33 (2010) 793-802.
[52] S. Yang, M. Sadilek, M. E. Lidstrom, J. Chromatogr. A. 1217 (2010) 7401-7410.
[53] R. Lee, A. S. Ptolemy, L. Niewczas, P. Britz-McKibbin, Anal. Chem. 79 (2007) 403-415.
[54] J. Pawliszyn (Ed.), Handbook of Solid Phase Microextraction, Chemical Industry Press, Beijing,

2009.
[55] K. Ridgway, S. P. D. Lalljie, R. M. Smith, J. Chromatogr. A. 1153 (2007) 36-53.
[56] S.G. Villas-Boˆas, J. Højer-Pedersen, M. A. kesson, J. Smedsgaard, J. Nielsen, Yeast 22 (2005) 1155-1169.
[57] S.G. Villas-Boˆas, J. Højer-Pedersen, M. A. kesson, J. Smedsgaard, J. Nielsen, Mass Spectrometry Reviews 24 (2005) 613-646
[58] W. B. Dunn, D. I. Ellis, TrAC, Trends Anal. Chem. 24 (2005) 285-294.
[59] G. Sun, K. Yang, Z. Zhao, S. Guan, X. Han, R.W. Gross, Anal. Chem. 79 (2007) 6629-6640.
[60] R. E. Rammouz, F. Létisse, S. Durand, J. Portais, Z.W. Moussa, X. Fernandez, Anal. Biochem. 398 (2010) 169-177.
(61) C. J. Bolten, P. Kiefer, F. Letisse, J. Portais, C. Wittmann, Anal. Chem. 79 (2007) 3843-3849.
[62] R. A. Dixon, D. R. Gang, A. J. Charlton, O. Fiehn, H. A. Kuiper, T. L. Reynolds, J. Agric. Food Chem. 54 (2006) 8984-8994.
[63] J. L. Wolfender, S. Rudaz, Y. H. Choi and H. K. Kim, Curr. Med. Chem., 20 (20113)1056-1090.
[64] H. K. Kim and R. Verpoorte, Phytochem. Anal. 21 (2010) 4-13.
[65] J. W. Allwood and R. Goodacre, Phytochem. Anal. 21 (2010) 33-47.
[66] M. C. Hennion, J. Chromatogr. A. 856 (1999) 3-54.
[67] D. Vuckovic, Anal. Bioanal. Chem. 403 (2012) 1523-1548.
[68] S. G. Villas-Bôas, U. Roessner, M. A. E. Hansen, J. Smedsgaard, J. Nielsen, metabolome analysis, an introduction, 2007, New Zealand, Wiley-Interscience Series in Mass Spectrometry
[69] W. de Koning, K. van Dam, Anal. Biochem. 204 (1992) 118-123.
[70] B. Gonzalez, J. Francois, M. Renaud, Yeast 13 (1997) 1347-1355.
[71] M. Ganzera, P. Vrabl, E. Worle, W. Burgstaller, H. Stuppner, Anal. Biochem. 359 (2006) 132-140.
[72] N. Tomiya, E. Ailor, S.M. Lawrence, M.J. Betenbaugh, Y. C. Lee, Anal. Biochem. 293 (2001) 129-137.
[73] T. Ryll, R. Wagner, J. Chromatogr. 570 (1991) 77-88.
[74] M. Imamura, T. Kumagai, N. Sugihara, K. Furuno, J. Health Sci. 49 (2003) 395-400.
[75] J. C. Shryock, R. Rubio, R. M. Berne, Anal. Biochem. 159 (1986) 73-81.
[76] R. P. Maharjan, T. Ferenci, Anal. Biochem. 313 (2003) 145-154.
[77] M. K. Grob, K. O'Brien, J. J. Chu, D. D. Y. Chen, J. Chromatogr. B 788 (2003) 103-111.
[78] C. J. Bolten, P. Kiefer, F. Letisse, J. C. Portais, C. Wittmann, Anal. Chem. 79 (2007) 3843-3849.
[79] C. Y. Lin, H. F. Wu, R. S. Tjeerdema, M. R. Viant, Metabolomics 3 (2007) 55-67.
[80] D. Josic, S. Kovac, J. Biotechnol. 3 (2008) 496-509.
[81] T. Hartung, H. Koeter, Altex 25 (2008) 259-264.

[82] A. R. Joyce, B. Ø. Palsson, Nature Rev. Mol. Cell Biol. 7 (2006) 198-210.

[83] V. García-Canas, C. Simó, M. Herrero, E. Ibáñez, A. Cifuentes, Anal. Chem. 84 (2012) 10150-10159.

[84] D. Gaso-Sokac, S. Kovac, D. Josic, Food Technol. Biotechnol. 48 (2010) 284-295.

[85] M. Srajer Gajdosik, D. Gaso-Sokac, H. Pavlovic, J. Clifton, L. Breen, L. Cao, J. Giacometti, Food Res. Int. 51 (2013) 46-52.

[86] M. Severgnini, P. Creminesi, C. Consolandi, G. De Bellis, B. Castiglioni, Adv. Bioprocess Technol. 4 (2011) 936-953.

[87] J. M. Cevallos-Cevallos, M. D. Danyluk, J. I. Reyes-De-Corcuera, J. Food Sci. 76 (2011) M238-M246.

[88] A. Alvarez-Ordóñez, A. Fernández, M. López, R. Arenas, A. Bernardo, Int. J. Food Microbiol, 123, (2008) 212-219.

[89] J. Giacometti, D. Josic, Microbial proteomics for food safety, in: F. Toldra, L.M.L. Nollet (Eds.), Proteomics in Foods Principles and Applications, Springer, New York, 2013.

[90] M. Ceragioli, M. Mols, R. Moezelaar, E. Ghelardi, S. Senesi, T. Abee, Appl. Environ. Microbiol. 76 (2010) 3352-3360.

[91] A. Zhang, H. Sun, H. Xu, S. Qiu, X. Wang, OMICS A Journal of Integrative Biology 17 (2013) 495-501.

[92] M. Nomura, J. Biol. Chem. 284 (2009) 9625-9635

[93] M. J. van der Werf, K. M. Overkamp, B. Muilwijk, L. Coulier, T. Hankemeier, Anal. Biochem. 370 (2007) 17–25.

[94] I. Bertini, X. Hu, C. Luchinat, Metabolomics 10 (2014) 241-249.

[95] W. De Koning, K. van Dam, Anal. Biochem. 204 (1992) 118-123.

[96] R. P. Maharjan, T. Ferenci, Anal. Biochem. 313 (2003) 145-154.

[97] M. Jos´e Nunes de Paiva, H. Costa Menezes, Z. de Lourdes Cardeal, Analyst, 139 (2014) 3683-3694

[98] S.H. Zeisel, Am. J. Clin. Nutr. 86 (2007) 542-548.

[99] H. Sauter, M. Lauer, H. Fritsch, Metabolic profiling of plants—a new diagnostic technique. In D. R. Baker, J. G. Fenyes, & M. K. Moberg, Synthesis and chemistry of Agrochemicals II. ACS Symposium Series 443 (288–299). Washington, DC: American Chemical Society, 1991.

[100] E. von Roepenack-Lahaye, T. Degenkolb, M. Zerjeski, M. Franz, U. Roth, L. Wessjohann, J. Schmidt, D. Scheel, S. Clemens, Plant Physiol. 134 (2004) 548-559

[101] A. Aharoni, C.H.R. de Vos, H.A. Verhoeven, C.A. Maliepaard, G. Kruppa, R. Bino, OMICS 6 (2002) 217-234.

[102] S. Sato, T. Soga, T. Nishioka, M. Tomita, Plant J. 40 (2004) 151-163.

[103] M. Ernst, D. Brentan Silva, R. Roberto Silva, R. Z. N. Vêncio, N. Peporine Lopes, Nat. Prod. Rep. 31 (2014) 784-806

[104] U. Roessner, F. Pettolino, in Metabolomics A Powerful Tool in Systems Biology, ed. J. Nielsen, M.C. Jewett, Springer-Verlag, Berlin Heidelberg, 2007.

[105] T. Moritz, A. I. Johansson, in Metabolomics, Metabonomics and Metabolite Profling, ed. W. J. Griffiths, RSC Publishing, Cambridge, 2008.

[106] R. Verpoorte, Y. H. Choi, N. R. Mustafa and H. K. Kim, Phytochem. Rev. 7 (2008) 525-537.

[106] S. G. Villas-Bˆoas, A. Koulman, G. A. Lane, in Metabolomics A Powerful Tool in Systems Biology, ed. J. Nielsen, M. C. Jewett, Springer-Verlag, Berlin Heidelberg, 2007.

[107] A. Oikawa and K. Saito, J. Plant 70 (2012) 30-38.

[108] J. L. Wolfender, S. Rudaz, Y. H. Choi and H. K. Kim, Curr. Med. Chem. 20 (2013) 1056-1090.

[109] H. K. Kim and R. Verpoorte, Phytochem. Anal. 21 (2010) 4-13.

[110] E. A. Schmelz, J. Engelberth, J. H. Tumlinson, A. Block, H. T. Alborn, J. Plant 39 (2004) 790-808.

[111] C. Deng, N. Liu, M. Gao and X. Zhang, J. Chromatogr. A 1153 (2007) 90-96.

[112] N. D. Yuliana, M. Jahangir, R. Verpoorte and H. Y. Choi, Phytochem. Rev. 12 (2013) 293-304.

[113] E. Urbanczyk, C. Baxter, A. Kolbe, J. Kopka, L. J. Sweetlove, A. R. Fernie, Planta 221 (2005) 891-901.

[114] E. Martino, I. Ramaiola, M. Urbano, F. Bracco and S. Collina, J. Chromatogr. A 1125 (2006) 147-151.

[115] A. Mustafa, C. Turner, Anal. Chim. Acta, 703 (2011) 8-18.

[116] Y. Liu, T. Chen, Y. Qiu, Y. Cheng, Y. Cao, A. Zhao and W. Jia, Anal. Bioanal. Chem. 400 (2011) 1405-1417.

[117] J. W. Allwood and R. Goodacre, Phytochem. Anal. 21 (2010) 33-47.

[118] G. Romanik, E. Gilgenast, A. Przyjazny and M. Kami´nski, J. Biochem. Biophys. Methods. 70 (2007) 253-261.

[119] B. Kleidus, D. Vitamv´asov´a and V. Kub´a&ncaron, J. Chromatogr. A 839 (1999) 261-263.

[120] C. W. Huie, Anal. Bioanal. Chem. 373 (2002) 23-30.

[121] K. Hoyerová, A. Gaudinová, J. Malbeck, P. I. Dobrev, T. Kocábek, B. Solcová, A. Trávnicková, M. Kam´ınek, Phytochemistry. 67 (2006) 1151-1159.

[122] M. C. Hennion, J. Chromatogr. A 856 (1999) 3-54.

[123] A. Zwir-Ferenc, M. Biziuk, Polish. J. Environ. Stud.15 (2006) 677-690.

[124] D. Vuckovic, Anal. Bioanal. Chem. 403 (2012) 1523-1548.

[125] V. Shulaev, D. Cortes, G. Miller, R. Mittler, Physiologia Plantarum 132 (2008) 199-208.

[126] J. O'Reilly, Q. Wang, L. Setkova, J.P. Hutchinson, Y. Chen, H.L. Lord, C.N. Linton, J. Pawliszyn,

J. Sep. Sci. 28 (2005) 2010-2022.
(127) Chen, J.; Pawliszyn, J. B. Anal. Chem. 67 (1995) 2530-2533.
[128] Eisert, R.; Pawliszyn, J. Anal. Chem. 69 (1997) 3140-3147.
[129] W. Xie, J. Pawliszyn, W.M. Mullett, B.K. Matuszewski, J. Pharm. Biomed. Anal. 45 (2007) 599-608.
[130] D. Vuckovic, E. Cudjoe, D. Hein, J. Pawliszyn, Anal. Chem. 80 (2008) 6870-6880.
[131] E. Cudjoe, D. Vuckovic, D. Hein, J. Pawliszyn, Anal. Chem. 81 (2009) 4226-4232.
[132] X. Zhang, K. D. Oakes, D. Luong, J.Z. Wen, C.D. Metcalfe, J. Pawliszyn, M. Servos, Anal. Chem. 82 (2010) 9492-9499.
[133] E. Cudjoe, J. Pawliszyn, J. Pharm. Biomed. Anal 50 (2009) 556-562.
[134] R. Vatinno, D. Vuckovic, C. G. Zambonin, J. Pawliszyn, J. Chromatogr. A. 1201 (2008) 215-221.
[135] D. Vuckovic, X. Zhang, E. Cudjoe, J. Pawliszyn, J. Chromatogr. A. 1217 (2010) 4041-4060.
[136] I. Bruheim, X. Liu, J. Pawliszyn, J. Anal. Chem. 75 (2003) 1002-1010.
[137] F. S. Mirnaghi, Y. Chen, L.M. Sidisky, J. Pawliszyn, Anal. Chem. 83 (2011) 6018-6025.
[138] F. S. Mirnaghi, M.R.N. Monton, J. Pawliszyn, J. Chromatogr. A. 1246 (2012) 2-8.
[139] F.S. Mirnaghi, J. Pawliszyn, J. Chromatogr. A. 1261 (2012) 91-98.
[140] B. Bojko, M.Wąsowicz, J. Pawliszyn, J. Pharmaceutical Analysis. 4 (2014) 6-13.
[141] E. Boyaci, K. Gorynski, A. Rodriguez-Laufuente, B. Bojko, J. Pawliszyn, Anal. Chim. Acta. 809 (2014) 69-81.
[142] V. Bessonneau, B. Bojko, J. Pawliszyn, Bioanalysis. 5 (2013) 783-792.
[143] D. Vuckovic, I. Lannoy, B. Gien, R.E. Shirey, L. M. Sidisky, S. Dutta, J. Pawliszyn, Angew. Chem. 123 (2011) 5456-5460.
[144] J. Guo, T. Yue, Y. Yuan, J. Food Sci. 77 (2012) C1090-C1096
[144] E. Dixon, C. Clubb, S. Pittman, L. Ammann, Z. Rasheed, N. Kazmi, PLoS ONE 6 (2011) e18471.
[146] S. Zhang, L. Liu, D. Steffen, T. Ye, D. Raftery, Metabolomics. 8 (2012) 323-334
[147] P. M. Eggink, C. Maliepaard, Y. Tikunov, J. P. W. Haanstra, A. G. Bovy, R. G. F. Visser, Food Chem. 132 (2012) 301-310.
[148] J. Rodriguez-Campos, H. B. Escalona-Buend.a, S. M. Contreras-Ramos, I. Orozco-Avila, E. Jaramillo-Flores, E. Lugo-Cervantes, Food Chem. 132 (2012) 277-288.
[149] E.M. Humston, J.D. Knowles, A. McShea, R.E. Synovec, J. Chromatogr. A, 1217 (2010) 1963-1970.
[150] T. Abaffy, R. Duncan, D.D. Riemer, O. Tietje, G. Elgart, C. Milikowski, R.A. DeFazio, PLoS ONE 5 (2010) e13813.
[151] T. Abaffy, M.G. M.ller, D.D. Riemer, C. Milikowski, R.A. Defazio, Metabolomics 9 (2013) 998-

1008.
[152] E. A. Souza Silva, J. Pawliszyn, Anal. Chem. 84 (2012) 6938-6988.
[153] D. Vuckovic, S. Risticevic, J. Pawliszyn, Angew. Chem. Int. Ed. 50 (2011) 5618-5628.
[154] B. Bojko, N. Reyes-Garces, V. Bessonneau, K. GorynÅLski, F. Mousavi, E. A. Souza Silva, J. Pawliszyn, TrCA, Trends in Anal.Chem. 61 (2014) 168-180.
[155] S. Risticevic, Y. Chen, L. Kudlejova, R. Vatinno, B. Baltensperger, J. R. Stuff, D. Hein, J. Pawliszyn, Nat. Protoc. 5 (2010) 162-176.
[156] E. Aprea, H. Gika, S. Carlin, G. Theodoridis, U. Vrhovsek, F. Mattivi, J Chromatogr. A 1218 (2011) 4517-4524.
[157] T. Abaffy, R. Duncan, D. D. Riemer, O. Tietje, G. Elgart, C. Milikowski, R. A. DeFazio, PLoS ONE 5 e13813 (2010) e13813.
[158] C. L. Silva, M. Passos, J.S. Câmara, Br. J. Cancer 105 (2011) 1894-1904.
[159] B. Bojko, K. Gorynski, G. Augusto Gomez-Rios, J. Matthias Knaak, T. Machuca, V. Nikolaus Spetzler, E. Cudjoe, M. Hsin, M. Cypel, M. Selzner, M. Liu, S. Keshavjee, J. Pawliszyn, Anal. Chim. Acta. 803 (2013) 75–81
[160] E. Cudjoe, B. Bojko, I. de Lannoy, V. Saldivia, J. Pawliszyn, Angew. Chem. Int 53 (2013) 12124-12126.
[161] A. N. Thomas, S. Riazanskaia,W. Cheung, Y. Xu, R. Goodacre, C. L. P. Thomas, Wound Repair Regen. 18 (2010) 391-400.
[162] M. Hartmann, D. Zimmermann, J. Nolte, In Vitro Cell. Dev. Biol. Anim. 44 (2008) 458-463.
[163] B. Buszewski, A. Ulanowska, T. Ligor, M. Jackowski, E. KłodzinÅL ska, J. Szeliga, J. Chromatogr. B 868 (2008) 88-94.
[164] U. Siripatrawan, B.R. Harte, Anal. Chim. Acta. 581 (2007) 63-70.
[165] H.D. Bean, J.M.D. Dimandja, J.E. Hill, J. Chromatogr. B. 901 (2012) 41–46.
[166] S.M.Z. Hossain, B. Bojko, J. Pawliszyn, Anal. Chim. Acta. 776 (2013) 41-49.
[167] D. Mecerreyes, Progress in Polymer Science 36 (2011) 1629-1782.
[168] L. He, W. Zhang, L. Zhao, X. Liu, S. Jiang, J. Chromatogr. A. 1007 (2003) 39-45.
[169] S. Pandey, Anal. Chim. Acta. 556 (2006) 38-45.
[170] M.J. Ruiz-Angel, S. Cardá-Broch, A. Berthod, J. Chromatogr. A. 1119 (2006) 202-208.
[171] A. Martín-Calero, V. Pino, J.H. Ayala, V. González, A.M. Afonso, Talanta. 79 (2009) 590-597.
[172] A. Martín-Calero, J.H. Ayala, V. González, A.M. Afonso, Anal. Bioanal. Chem. 394 (2009) 937-946.
[173] Y. Wang, M. Tian, W. Bi, K.H. Row, Int. J. Mol. Sci. 10 (2009) 2591-2610.
[174] H. Qiu, X. Liang, M. Sun, S. Jiang, Anal. Bioanal. Chem. 399 (2011) 3307-3322.

[175] M. Koel (Ed.), Ionic Liquids in Chemical Analysis, CRC Press, 2009.
[176] Y. Sun, B. Cabovsk, C.E. Evans, T.H. Ridgway, A.M. Stalcup, Anal. Bioanal. Chem. 382 (2005) 728-734.
[177] Y. Sun, A.M. Stalcup, J. Chromatogr. A 1126 (2006) 276-282.
[178] D. S. Van Meter, Y. Sun, K.M. Parker, A. M. Stalcup, Anal. Bioanal. Chem. 390 (2008) 897-905.
[179] D. S. Van Meter, O. D. Stuart, A. B. Carle, A. M. Stalcup, J. Chromatogr. A. 1191 (2008) 67-71.
[180] K. R. Chitta, D. S. Van Meter, A. M. Stalcup, Anal. Bioanal. Chem. 396 (2010) 775-781.
[181] D. S. Van Meter, N. J. Oliver, A. B. Carle, S. Dehm, T. H. Ridgway, A. M. Stalcup, Anal. Bioanal. Chem. 393 (2009) 283-288.
[182] P. R. Fields, Y. Sun, A. M. Stalcup, J. Chromatogr. A 1218 (2011) 467-475.
[183] S. J. Liu, F. Zhou, X. H. Xiao, L. Zhao, X. Liu, S. X. Jiang, Chem. Lett. 15 (2004)1060-1062.
[184] H. Qiu, Q. Jiang, X. Liu, S. Jiang, Chromatographia 68 (2008) 167-171.
[185] H. Qiu, M. Takafuji, X. Liu, S. Jiang, H. Ihara, J. Chromatogr. A 1217 (2010) 5190-5196.
[186] H. Qiu, M. Takafuji, T. Sawada, X. Liu, S. Jiang, H. Ihara, Chem. Commun. 46 (2010) 8740-8742.
[186] H. Qiu, S. Jiang, X. Liu, J. Chromatogr. A 1103 (2006) 265-270.
[187] H. Qiu, S. Jiang, X. Liu, L. Zhao, J. Chromatogr. A 1116 (2006) 46-50.
[188] H. Qiu, Q. Jiang, Z. Wei, X. Wang, X. Liu, S. Jiang, J. Chromatogr. A 1163 (2007) 63-69.
[189] X. Liang, Q. Chen, X. Liu, S. Jiang, J. Chromatogr. A 1182 (2008) 197-204.
[190] H. Qiu, L. Wang, X. Liu, S. Jiang, Analyst 134 (2009) 460-465.
[191] L. Auler, C. R. Silva, K. E. Collins, C. H. Collins, J. Chromatogr. A. 1073 (2005) 147-153.
[192] W. Bi, K.H. Row, Chromatographia 71 (2010) 25-30.
[193] W. Bi, J. Zhou, K. H. Row, Anal. Chim. Acta. 677 (2010) 162-168.
[194] Q. Wang, G.A. Baker, S.N. Baker, L.A. Colón, Analyst 131 (2006) 1000-1005.
[195] C. L. Arthur, J. Pawliszyn, Anal. Chem. 62 (1990) 2145-2148.
[196] C. L. Arthur, L. M. Killam, S. Motlagh, M. Lim, D.W. Potter, J. Pawliszyn, Env. Sci. Technol. 26 (1992) 979-983.
[197] H. Prosen,S.L. Zupancic–Kralj, Trends Anal. Chem. 18 (1999) 272-282.
[198] D. Vuckovic, E. Cudjoe, D. Hein, J. Pawliszyn, Anal. Chem. 80 (2008) 6870-6880.
[199] E. G. Yanes, S. R. Gratz, M. J. Baldwin, S. E. Robison, A. M. Stalcup, Anal. Chem. 73 (2001) 3838-3844.
[200] J. L. Anderson, T. Welton, J. Ding, D.W. Armstrong, J. Am. Chem. Soc. 124 (2002) 14247-14254.
[201] W. Z. Zhang, L. J. He, X. Liu, S. X. Jiang, Chin. J. Chem. 22 (2004) 549-552.
[202] S. Özcan, H. Z. Şenyuva, J. Chromatogr A, 1135 (2006) 179-185.
[203] R. M. Callejón, A. M. Troncoso, M. L. Morales, Talanta 81 (2010) 1143-1152.

[204] D. Guzmάn-Lucero, O. Olivares-Xometl, R. Martìnez-Palou, N. V. Likhanova, M. A. Dominguez-Aguilar, V. Garibay-Febles, Ind. Eng. Chem. Res. 50 (2011) 7129-7140.

[205] H. Qiu, A.K. Mallika, M. Takafujia, X. Liu, S. Jiang, H. Ihara, J. Chromatogr A. 1232 (2012) 116-122.

[206] B.K. Matuszewski, M.L. Constanzer, C.M. Chavez-Eng, Anal. Chem. 75 (2003) 3019-3030.

[207] J. Ivanisevic, Z.J. Zhu, R. Tautenhahn, S. Chen, P.J. Ó Brien, C.H. Marletta, G.J. Patti, G. Siuzdak, Anal. Chem. 85 (2013) 6876-6884.

[208] J.D. Rabinowitz, Expert Rev. Proteomics 4 (2007) 187-198.

[209] Y. Wu, L. Li, Anal. Chem. 85 (2013) 5755-5763.

[210] S.U. Bajad, W. Lua, E.H. Kimball, J. Yuan, C. Peterson, J.D. Rabinowitz, J. Chromatogr. A. 1125 (2006) 76-88.

[211] O. Yanes, R. Tautenhahn, G.J. Patti, G. Siuzdak, Anal. Chem. 83 (2011) 2152-2161.

[212] J. L, Edwards, R. L. Edwards, K. R, Reid, R.T, Kennedy, J. Chromatogr. A 1172 (2007) 127-134.

[213] N. L. Kuehnbaum, P. Britz-McKibbin, Chem. Rev. 113 (2013) 2437-2468.

[214] S. Carneiro, S. G. Villas-Bôas, E. C. Ferreira, I. Rocha, Mol Biosyst. 7 (2011) 899-910.

[215] M. Faijes, A.E. Mars, E. Smid, J. Microb. Cell Fact. 6 (2007) 27-34.

[216] B. Alvarez-Sanchez, F. Priego-Capote, M.D. Luque de Castro, TrAC, Trends Anal. Chem. 29 (2010) 120-127.

[217] C. L. Winder, W. B. Dunn, S. Schuler, D. Broadhurst, R. Jarvis, G. M. Stephens, R. Goodacre, Anal. Chem. 80 (2008) 2939-2948.

[218] H. Wu, A.D. Southam, A. Hines, M.R. Viant, Anal. Biochem. 372 (2008) 204-212.

[219] M. R. Mashego, K. Rumbold, M. De Mey, E. Vandamme, W. Soetaert, J. J. Heijnen, Biotechnol. Lett. 29 (2007) 1-16.

[220] M. Hye Shin, Y. Do, K. W. Lee, O. Liu, K. Fiehn, K. Heon, Anal. Chem, 82 (2010) 6660-6666.

[221] H. D. Bean, J. M. D. Dimand, E. Hill, J. Chromatogr. B 901 (2012) 41-46.

[222] F. Mousavi, J. Pawliszyn, Anal. Chim. Acta. 803 (2013) 66-74.

[223] G. J. Patti, R. Tautenhahn, G. Siuzdak, Nat. Protoc. 7 (2012) 508-516.

[224] F. S. Mirnaghi, K. Gorynski, A. Rodriguez-Lafuente, E. Boyaci, B. Bojko, J. Pawliszyn, J. Chromatogr. A 1316 (2013) 37-43.

[225] S. Colazza, G. Aquila, C. De Pasquale, E. Peri, J. G. Millar, J. Chem. Ecol. 33 (2007) 1405-1420.

[226] A. Halasz, J. Hawari, J. Chromatogr. Sci. 44 (2006) 379-386.

[227] A. Halasz, C. Groom, E. Zhou, L. Paquet, C. Beaulieu, S. Deschamps, A. Corriveau, S. Thiboutot, G. Ampleman, C. Dubois, J. Hawari, J. Chromatogr. A 963 (2002) 411-418.

[228] T. MacPherson, C. W. Greer, E. Zhou, A. M. Jones, G. Wisse, P. C. K. Lau B. Sankey, M. J. Grossman, J. Hawari, J. Env. Sci. Tech. 32 (1998) 421-426.

[229] L. G. Whyte, J. Hawari, E. Zhou, L. Bourbonniere, W. E. Inniss, C. W. Greer, Appl. Environ. Microbiol. 64 (1998) 2578-2584.

[230] M. A. Mirata, M. Wüst. A. Mosandl, J. Schrader, J. Agric. Food Chem. 56 (2008) 3287-3296.

[231] J. L. Griffin, R. A. Kauppinen, J. Proteome Res. 6 (2007) 498-505.

[232] S. Ma, N. Grinberg, N. Haddad, S. Rodriguez, C.A. Busacca, K. Fandrick, H. Lee, J.J. Song, N.Yee, D. Krishnamurthy, C.H. Senanayake, J. Wang, J. Trenck, S. Mendonsa, P.R. Claise, R.J. Gilman, T.H. Evers, Org. Process Res. Dev. 17 (2013) 806-810.

[233] X. Yang, Y. Levin, H. Rahmoune, D. Ma, S. Schffmann, Y. Umrania, P. C. Guest, S. Bahn, Proteomics. 11 (2011) 501-505.

[234] F.S. Mirnaghi, F. Mousavi, S.M. Rocha, J. Pawliszyn, J. Chromatogr. A 1276 (2013) 12-19.

[235] E. A. Decker, R. J. Elias, D. J. McClements, Oxidation in foods and beverages and antioxidant application, Vol 2: Management in different industry sectors, Woodhead Publishing Limited, 2010.

[236] L. N. Bell, Peptide Stability in Solids and Solutions, Biotechnol. Prog. 13 (1997) 342-346.

[237] M. M. Koek, B. Muilwijk, M. J. Van der Werf, T. Hankemeier, Anal. Chem. 78 (2006) 1272-1281.

[238] R. Tautenhahn, G. J. Patti, E. Kalisiak, T. Miyamoto, M. Schmidt, F.Y. Lo, J. McBee, N.S. Baliga, G. Siuzdak, Anal. Chem. 83 (2011) 696=700.

[239] A. H. Zhang, H. Sun, Y. Han, G. Yan, Y. Yuan, G.C. Song, X. Yuan, N. Xie, X. Wang, Anal. Chem. 84 (2012) 8442-8447.

[240] W. B. Dunn, D. Broadhurst, P. Begley, E. Zelena, S. Francis-McIntyre, N. Anderson, M. Brown, J.D. Knowles, A. Halsall, J.N. Haselden, A.W. Nicholls, I.D. Wilson, D.B. Kell, R. Goodacre, Nature protocols. 6 (2011) 1060-1083.

[241] B. A. Annous, P. M. Fratamico, J. L. Smith, J. Food science. 74 (2009) R24-R37.

[242] C. Marcus, E. P. Lichtenstein, J. Agric. Food Chem. 27 (1979) 1217-1223.

[243] R. Bruni, A. Medici, E. Andreotti, C. Fantin, M. Muzzoli, M. Dehesa, Food Chem. 85 (2003) 415-421.

[244] G. Sacchetti, S. Maietti, M. Muzzoli, M. Scaglianti, S. Manfredini, M. Radice, R. Bruni, Food Chem. 91 (2005) 621-632.

[245] F. Bakkali, S. Averbeck, D. Averbeck, M. Idaomar, Food and Chemical Toxicology 46 (2008) 446-475.

[246] M. Hyldgaard, T. Mygind, R.L. Meyer, Frontiers in Microbiology, 3 (2012) 1-24.

[247] S. Jozefczuk, S. Klie, G. Catchpole, J. Szyanski, A. Cuadros-Inostroza, D. Steinhauser, J. Selbig, L. Willmitzer, Mol. Sys. Biol. 6 (2010) 1-16.

[248] P. Suresh, V.K. Ingle, V.J. Vijaya Lakshmi, Food Sci Technol, 29 (1992) 254-256.

[249] K. S. Bilgrami, K. K. Sinha, A. K. Sinha, Indian J Med Res. 96 (1992) 171-175

[250] P. Pacheco, J. Sierra, G. Schmeda-Hirschmann, C. W. Potter, B. M. Jones, M. Moshref, Phytother Res. 7 (1993) 415-418.

[251] F. Nazzaro, F. Fratianni, L.D. Martino, R. Coppola, V. De Feo, Pharmaceuticals. 6 (2013) 1451-1474.

[252] D. Vuckovic, Doctoral thesis, University of Waterloo, Chapter 1, 2010.

[166] S. M. Z. Hossain, B. Bojko, J. Pawliszyn, Anal. Chim. Acta. 776 (2013) 41-49.

[253] O. Yanes, R. Tautenhahn, G. J. Patti, G. Siuzdak, Anal. Chem. 83 (2011) 2152-2161.

[142] V. Bessonneau, B. Bojko, J. Pawliszyn, Bioanalysis. 5 (2013) 783-792.

[254] M. Kates. Bacterial lipids. Adv. Lipid Res. 2 (1964) 17-90.

[255] J. R. J. E. Cronan, J. Bacteriol. 95 (1968) 2054-2061

[256] J. Karkas, H. Türler, E. Chargaff, Biochim. Biophys. Acta. 111 (1965) 96-109.

[257] V. Knivett, J. Cullen, J. Biochem. 96 (1965) 771-776.

[258] A. G. Marr, J. L. Ingraham. J. Bacteriol. 84 (1962) 1260-1267.

[259] D. Le Rudulier, A.R. Strϕm, A.M. Dandekar, L. T. Smith, R. Valentine, Science. 224 (1984) 1064-1068.

[260] R. J. W. Lambert, P.N. Skandamis, P.J. Coote, G.J.E. Nychas, J. Appl. Microbiol. 91 (2001) 453-462.

[261] S.A. Burt, R. van der Zee, A. P. Koets, A. M. de Graaff, F. van Knapen, W. Gaastra, H. P. Haagsman, E. J. A. Veldhuizen, Appl. Environ. Microbiol. 73 (2007) 4484-4490.

[262] R. Di PasquaI, N. Hoskins, G. Betts, G. Mauriello, J. Agric. Food Chem. 54 (2006) 2745-2749.

[263] N. J. Russell, Trends Biochem. Sci. 9 (1984) 108-112.

[264] R. Di Pasqua, G. Betts, N. Hoskins, M. Edwards, D. Ercolini, G. Mauriello, J. Agric. Food Chem. 55 (2007) 4863-4870.

[265] J. E. Gustafson, Y. C. Liew, S. Chew, J. L. Markham, H. C. Bell, S. G. Wyllie, J. R. Warmington, Lett. Appl. Microbiol. 26 (1998) 194-198.

[266] M. Oussalah, S. Gaillet, M. Lacroix, J. Food Prot. 69 (2006) 1046-1055.

[267] A. S. Bayer, R. Presad, J. Chandra, A.M. Smirti, A. Varma, R.A. Skurray, N. Firth, M.H. Brown, S. P. Koo, M. R. Yeaman, Infect. Immun. 68 (2000) 3548-3553.

[268] N. J. Russell, Comp. Biochem.Physiol. 118 (1997) 489-493.

[269] C. N. Wendakoon, M. J. Sakaguchi, Food Protection. 58 (1995) 280-283.

[270] E. A. Auger, K. E. Redding, T. Plumb, L.C. Childs, S.Y. Meng, G.N. Bennett, Mol. Microbiol. 3 (1989) 609-620.

[271] A.O. Gill, R.A. Holley, Int. J. Food Microbiol, 108 (2006a) 1-9.

[272] A.O. Gill, R.A. Holley, Int. J. Food Microbiol. 111 (2006b) 170-174.

[273] G. Picone, L. Laghi, F. Gardini, R. Lanciotti, L. Siroli, F. Capozzi, Food Chem. 141 (2013) 4367-4374.

[274] H. Pelicano, D.S. Martin, R.H. Xu, P. Huang, Oncogene 25 (2006) 4633-4646.

[275] A. R. Strϕm, J. Biosci. 23 (1998) 437-445.

[276] E.J. Mullaney, C.B. Daly, A.H. Ullah, Adv Appl Microbiol. 47 (2000) 157-199.

[277] E.J. Mullaney, A.H. Ullah, Biochem Biophys Res Commun. 312 (2003) 179-184.

[278] T. Kanai, K. Takahashi, H. Inoue, J. Biochem. 140 (2006) 703-711.

[279] C. Niu, S. Afre, E.S. Gilbert, 43 (2006) 489-494.

[280] M. L. Urbanowski, C.P. Lostroh, E.P. Greenderg, J. Bacteriol. 186 (2004) 631-637.

[281] S. Burt, Int.J. Food Microbiol. 94 (2004) 223-253.

[282] S.G. Deans, G. Ritchie, Int.J. Food Microbiol. 5 (1987) 165-180.

[283] S.I, Kim, J.Y. Roh, D.H. Kim, H.S. Lee, Y.J. Ahn, J. Stored Prod Res. 39 (2003) 293-303.

[284] A. Astani, J. Reichling, P. Schnitzler, Evid.Based Complement. Alternat. Med. (2011) 253643-253650.

[285] D. Kalemba, A. Kunicka, Curr.Med. Chem, 10 (2003) 813-829.

[286] A. Brenes, E. Roura, Anim. Feed Sci. Technol. 158 (2010) 1-14.

[287] N.G. Chorianopoulos, E.D. Giaouris, P.N. Skandamis, S. A. Haroutounian, G. J. E. Nychas, J. Appl. Microbiol. 104 (2008) 1568-1599.

[288] S.A. Burt, R.D. Reinders, Lett. Appl. Microbiol. 36 (2003)162-167.

[289] L. De Martino, V. de Feo, F. Nazzaro, Molecules 14 (2009) 4213-4230.

[290] A. Koroch, H.R. Juliani, J.A. Zygadlo, Falvours and Fragrances, 94 (2007) 87-115.

[291] P.J. Delaquis, K. Stanich, B. Girard, G. Mazza, Int. J. Food Microbiol. 74 (2002) 101-109.

[292] A. Smith-Palmer, J. Stewart, L. Fyfe, Letters in applied microbiology. 26 (1998) 118-122.

[293] X. W. Huanga, Y. C. Fenga, Y. Huanga, H.L. Lia, The Journal of Essential Oil Research, 25 (2013) 315-323.

[294] P.M. Davidson, M. E. Parish, Food Technol. 43 (1989) 148155.

[295] A. O. Gill, P. Delaquis, P. Russo, R. A Holley, Int. J. Food Microbiol. 3 (2002) 8392.

[296] A. Santiesteban-Lopez, E. Palou, A. López-Malo, A. J. Appl. Microbiol. 102 (2007) 486-497.

[297] J. Gutierrez, C. Barry-Ryan, P. Bourke, Int. J. Food Microbiol. 124 (2008) 91-97.

[298] B. Delgado, P. S. Fernández, A. Palop, P. M. Periago, Food Microbiol. 21 (2004) 327-334.

[299] G. J. E. Nychas, New Methods of Food Preservation; Gould, G.W., Ed.; Blackie Academic and Professional: London, UK, (1995) 58-89.

[300] R. S. Pei, F. Zhou, B. P. Ji, J. Xu, J. Food Sci. 74 (2009) 379-383.
[301] S. Jozefczuk, S. Klie, G. Catchpole, J. Szymanski, A. Cuadros-Inostroza, D. Steinhauser, J. Selbig, L. Willmitzer, Mol. Syst. Biol. 6 (2010) 364-381.
[302] K. Dettmer, P. A. Aronov, B. D. Hammock, Mass Spectrom. Rev. 26 (2007) 51-78.
[231] J. L. Griffin, R. A. Kauppinen, J. Proteome Res. 6 (2007) 498-505.
[303] G. Theodoridis, H.G. Gika, I. D. Wilson, TrAC Trends. Anal. Chem. 27 (2008) 251-260.
[304] F. Pellati, S. Benvenuti, F. Yoshizaki, D. Bertelli, M.C. Rossi, J. Chromatogr. A 1087 (2005) 265-273.
[305] E.T. Sousa, F.M. Rodrigues, C.C. Martins, F.S. Oliviera, P.A.P. Pereira, J.B. Andrade, J. Microchem. 82 (2006) 142-149.
[306] M. Hyldgaard, T. Mygind, L.M Rikke, Microbiol. 3 (2012) 1-24.
[307] A. O. Gill, R. A. Holley, Appl. Environ. Microbiol. 70 (2004) 5750-5755.
[308] A. Pauli, K.H. Kubeczka, Nat. Prod. Commun. 5 (2010) 1387-1394.
[309] G. M. Laekeman, L. VanHoof, A. Haemers, A. A. V. Berghe, A. G. Herman, A. J. Vlietinck, Phytother. Res. 4 (1990) 90-96.
[310] C. N. Wendakoon, M. Sakaguchi, Effects of spices on growth and biogenic amine formation by bacteria in fish muscle. Amsterdam: Elsevier Science Publishers; 1992.
[311] S. E. Moon, H.Y. Kim, J. D. Cha, Arch Oral Biol. 56 (2011) 907-916.
[312] C. Koutsoudaki, M. Krsek, A. Rodger, J. Agric.Food Chem. 53 (2005) 7681-7685.
[313] S. Roller, In Natural Antimicrobials for the Minimal Processing of Food; Roller, S., Ed.; Woodhead Publishing Ltd.: Cambridge, England, 2003.
[314] D. R. Morris, R. H. Fillingame. Ann. Rev. Biochem. 43 (1974) 303-325.
[315] S. L. Taylor, S. S. Sumner, D.E. Kramer, J. Liston (eds.). Sea Food Quality Determination. Elsevier Science Publishers, Amsterdam (1986) 235-245.
[316] J. Thoroski, G. Blank, C. Biladeris, J. Food Protection. 52 (1989) 399-403.
[317] B.L. Bassler, Cell. 109 (2002) 421-424.
[318] M. Hentzer, M. Givskov, J. Clin. Invest. 112 (2003) 1300-1307.
[319] F. Nazzaro, F. Fratianni, R. Coppola, Int. J. Mol. Sci. 14 (2013) 12607-12619.
[320] M.S. Khan, M. Zahin, S. Hasan, F.M. Husain, I. Ahmad, Lett. Appl. Microbiol. 49 (2009) 354-360.
[321] S. Péneau, Doctoral thesis, freshness of fruits and vegetebles: Concept and perception, swiss federal institute of technology Zurich. 2005.
[322] F. R. Harker, F. A. Gunson, S. R. Jaeger, Postharvest Biol Technol. 28 (2003) 333-347.
[323] F. R. Harker, K. B. Marsh, H. Young, S. H. Murray, F. A. Gunson, S. B. Walker, Postharvest Biol Technol. 24 (2002) 241-250.

[324] M. N. Merzlyak, T. B. Melø, K. R. Naqvi, J. Exp Bot. 59 (2008) 349-359.
[325] J. Wu, H. Gao, L. Zhao, X. Liao, F. Chen, Z. Wang, X. Hu, Food Chem. 103 (2007) 88-93.
[326] N. Oraguzie, P. Alspach, R. Volz, C. Whitworth, C. Ranatunga, R. Weskett, R. Harker, Postharvest Biol Technol. 52 (2009) 279-287.
[327] F. Cost, C.P. Peace, S. Stella, S. Serra, S. Musacchi, M. Bazzani, S. Sansavini, J Exp Bot. 61 (2010) 3029-3039.
[328] K. Amaki, E. Saito, K. Taniguchi, K. Joshita, M. Murata. Biosci, Biotechnol Biochem. 75 (2001) 829-832.
[329] C. B. Watkins, E. Kupferman, D.A. Rosenberger, D. A. Gross, K., Ed.; USDA-ARS Handbook 66; U.S. GPO: Washington, DC, 2004.
[330] C. B. Watkins, W. J. Bramlage, B. A. Cregoe, J. Am. Soc. Hortic. Sci. 12 (1995) 88-94.
[331] J. M. A. Bain, J. Hortic. Sci. 31 (1956) 234-238.
[332] H. Hayama, M. Tatsuki, Y. Nakamura, Biology and technology, 50 (2008) 228-230.
[333] X. Fan, J. P. Mattheis, J. Agric. Food Chem. 47 (1999) 3063-3068.
[334] H. Halder-Doll, F. Bangerth, Sci. Hortic. 33 (1987) 87-96.
[335] D. R. Rudell, J. P. Mattheis, E.A. Curry, J. Agric. Food Chem. 56 (2008) 1138-1147.
[336] B. Zhou, J. F. Xiao, L. Tuli, H. W. Ressom, Mol. Bio Syst. 8 (2012) 470-481.
[337] J. Ackermann, M. Fischer, R. Amadò, J. Agric. Food Chem. 40 (1992) 1131-1134.
[338] T. Fuleki, E. Pelayo, R.B. Palabay, J. Agric. Food. Chem. 42 (1994) 1266-1275.
[339] S. Tisza, P. Sass, I. Molnár-Perl, J. Chromatogr. A. 676 (1994) 461-468.
[340] D. Hatouma, C. Annaratonea, M.L.A.T.M. Hertoga, A.H. Geeraerda, B.M. Nicolaia, Postharvest Biology and Technology. 96 (2014) 33-41.
[341] D. Cuthbertson, P. K. Andrews, J. P. Reganold, N. M. Davies, B. M. Lange, J. Agric. Food Chem. 60 (2012) 8552-8560.
[342] S. Burda, W. Oleszek, C. Y. Lee, J. Agric. Food Chem. 38 (1990) 945-948.
[343] M. Suni, M. Nyman, N.A. Eriksson, L. Björk, I. Björck, J. Sci. Food Agric. 80 (2000) 1538-1544.
[344] A. Brackmann1, J. Streif, F. Bangerth, J. Amer. Soc. Hort. Sci. 118 (1993) 243-247.
[345] B. D. Whitaker, J. Agric. Food Chem. 55 (2007) 3708-3712.
[346] E. Boyaci, A. Rodriguez-Lafuente, K. Gorynski, F. Mirnaghi, E. A. Souza-Silva, D. Hein, J. Pawliszyn, Anal. Chim. Acta. Article in press.
[347] J. G. Miller, S. C. Fry, Res.332 (2001) 389-403.
[348] S. Risticevic, J. R. DeEll, J. Pawliszyna J.Chromatogr. A, 1251 (2012) 208-218.
[349] V. Shulaeva, D. Cortesa, G. Millerb, R. Mittler, Physiologia Plantarum 132 (2008) 199-208.
[350] J. Guo, T. Yue, Y. Yuan, J. Food Sci. 77 (2012) C1090–C1096.

[351] E. Liberto, M.R. Ruosi, C. Cordero, P. Rubiolo, C. Bicchi, B. Sgorbini, J. Agric. Food Chem. 61 (2013) 1652-1660.
[352] J. Gon.alves, J. Figueira, F. Rodrigues, J.S. C.mara, J. Sep. Sci. 35 (2012) 2282-2296.
[353] U. Siripatrawan, B.R. Harte, Anal. Chim. Acta. 581 (2007) 63-70.
[354] G. S.nchez, C. Besada, M.L. Badenes, A.J. Monforte, A. Granell, PLoS ONE, 7 (2012) e38992.
[355] C. Cagliero, C. Bicchi, C. Cordero, P. Rubiolo, B. Sgorbini, E. Liberto, Food Chem. 132 (2012) 1071-1079.
[356] S.M. Rocha, E. Coelho, J. Zrostl.kov., I. Delgadillo, M.A. Coimbra, J. Chromatogr. A. 1161 (2007) 292-299.
[357] F. Bianchi, M. Careri, C. Conti, M. Musci, R. Vreuls, J. Sep. Sci. 30 (2007) 527-533.
[358] J. Rodriguez-Campos, H.B. Escalona-Buend.a, S.M. Contreras-Ramos, I. Orozco-Avila, E. Jaramillo-Flores, E. Lugo-Cervantes, Food Chem. 132 (2012) 277-288.
[359] P.M. Eggink, C. Maliepaard, Y. Tikunov, J.P.W. Haanstra, A.G. Bovy, R.G.F. Visser, Food. Chem. 132 (2012) 301-310.
[360] S. Ducki, J. Miralles-Garcia, A. Zumb., A. Tornero, D.M. Talanta. 74 (2008) 1166-1174.
[361] J. Figueira, H. C.mara, J. Pereira, J.S. C.mara, Food Chem. 145 (2014) 653-663.
[362] J. Cline, J. Gardner, OMAFRA Horticulture News (2009).
[363] D. Bartels, R. Sunkar, Critical Reviews in Plant Sciences 24 (2005) 23-58.
[364] S. R. Draper, Phytochemistry 11 (1972) 639–641.
[365] S. Handa, R. A. Bressan, A. K. Handa, N. C. Carpita, P. M. Hasegawa, Plant Physiology. 73 (1983) 834-843.
[366] R. Lugan, M. F. Niogret, L. Leport, J. P. Guegan, F. R. Larher, A. Savoure, J. Kopka, A. Bouchereau, Plant J. 64 (2010) 215-229.
[367] B. Usadel, O. E. Blasing, Y. Gibon, F. Poree, M. Hohne, M. Gunter, R. Trethewey, B. Kamlage, H. Poorter, M. Stitt, Plant Cell and Environment. 31 (2008) 518-547.
[368] D.H. Sanchez, M.R. Siahpoosh, U. Roessner, M. Udvardi, J. Kopka, Physiologia Plantarum. 132 (2008) 209-219.
[369] S. Kempa, W. Rozhon, J. Samaj, Plant J. 49 (2007) 1076-1090.
[370] S. Galili, R. Amir, G. Galili, Adv. Plant Biochem. Mol. Biol. 1 (2008) 49-80.
[371] O. Owen, S. Kalhan, R. Hanson, J. Biol. Chem. 277 (2002) 30409-30412.
[372] P. D. Hare, W.A. Cress, Plant Growth Regulation. 21 (1997) 79-102.
[373] D. Rhodes, A.D. Hanson, Annual Review of Plant Physiology and Plant Molecular Biology 44 (1993) 357–384.
[374] N. Verbruggen, C. Hermans, Amino Acids 35 (2008) 753-759.

[375] L. Szabados, A. Savoure, Trends in Plant Science 15 (2010) 89-97.
[376] L. Rizhsky, H.J. Liang, J. Shuman, V. Shulaev, S. Davletova, R. Mittler, Plant Physiology. 134 (2004) 1683-1696.
[377] J. Dobra, V. Motyka, P. Dobrev, J. Malbeck, I. T. Prasil, D. Haisel, A. Gaudinova, M. Havlona, J. Gubis, R. Vankova, J. Plant Physiol. 167 (2010) 1360-1370.
[378] A. Gaudinova, M. Havlova, J. Gubis, R. Vankova, J. Plant Physiology. 167 (2010) 1360-1370.
[379] W. T. L, B. Lin, M. Zhang, X. J. Hua, Plant Physiology 156 (2011) 1921-1933.
[380] F. Kaplan, J. Kopka, D.W. Haskell, W. Zhao, K.C. Schiller, N. Gatzke, D.Y. Sung, C.L. Guy, Plant Physiology. 136 (2004) 4159-4168.
[381] B. Usadel, O.E. Blasing, Y. Gibon, F. Poree, M. Hohne, M. Gunter, R. Trethewey, B. Kamlage, H. Poorter, M. Stitt, Plant, Cell and Environment. 31 (2008) 518-547
[382] K. Urano, K. Maruyama, Y. Ogata, Plant J. 57 (2009) 1065-1078.
[383] J. Ackermann, M. Fischer, R. Amadb J. Agric. Food Chem. 40 (1992) 1131-1134
[384] C. L. Escher, F. Widmer, Biol. Chem. 378 (1997) 803–813.
[385] R. Leisso, D. Buchanan, J. Lee, J. Mattheis, D. Rudell J. Agric. Food. Chem. 61 (2013) 1373-1387.
[386] Z.G. Ju, Y.B. Yuan, C.L. Liu, S.M. Zhan, M.X. Wang, Postharvest Biol. Technol. 8 (1996) 83–93.
[387] Z. Ju, W. J. Bramlage, Postharvest Biol. Technol. 16 (1999) 107-118.
[388] W. G. Spollen, C. J. Nelson, Crop Science. 35 (1994) 496-502.
[389] J. H. M. Stoop, J. D. Williamson, D. M. Pharr, Trends in Plant Science. 1 (1996) 139-144.
[390] J.C. Fidler, C.J. North, J.Hort.Sci. 45 (1070) 197–204.
[391] J. Lee, D.R. Rudell, P.J. Davies, C.B. Watkins, Metabolomics. (2012a) 742-753.
[392] J. Lee, J. P. Mattheis, D. R. Rudell, Postharvest Biol. Technol. 68 (2012) 32-42.
[393] Brackmann, J. Streif, F. Bangerth, J. Amer. Soc. Hotr. Sci. 118 (1993) 243-247.
[394] F. A. Loewus, P. P. N. Murthy, Plant Sci. 150 (2000) 1-19.
[395] I. Schuler, G. Duportail, N. Glasser, P. Benveniste, M. A. Hartmann, Biochim. Biophys. Acta. 1028 (1990) 82-88.
[396] R. D. Rudell, D. A. Buchanan, R. S. Leisso, B. D. Whitaker, J. P. Mattheis, Y. Zhu, V. Varanasi, Phytochemistry, 72 (2011) 1328-1340
[397] G. A. Picchioni, A. E. Watada, W. S. Conway, B. D. Whitaker, C. E. Sams, Phytochemistry. 39 (1995) 763-769.
[398] S. R. Cutler, P. L. Rodriguez, P. R. Finkelstein, S. R. Abrams, Annual Review of Plant Biology. 61 (2010) 651-679.
[399] K. E. Hubbard, N. Nishimura, K. Hitomi, E. D. Getzoff, J. I. Schroeder, Genesand Development. 24 (2010) 1695-1708.

[400] A. S. Raghavendra, V. K. Gonugunta, A. Christmann, E. Grill, Trends in Plant Science 15 (2010) 395-401.

[401] J. Dixon, E. W. Hewett, Crop Hortic. 28 (2000) 155-173.

[402] N. A. Mir, R. Perez, P. Schwallier, R. Beaudry, J. Agric. Food Chem. 47 (1999b) 2653–2659.

[403] D. E. Meigh, A. A. E. Filmer, J. Sci. Food Agric. 18 (1969) 307-313.

[404] E. E. Huelin, I. M. Coggiola, J. Sci. Food Agric. 21 (1970b) 584-589.